

NO-A122 962

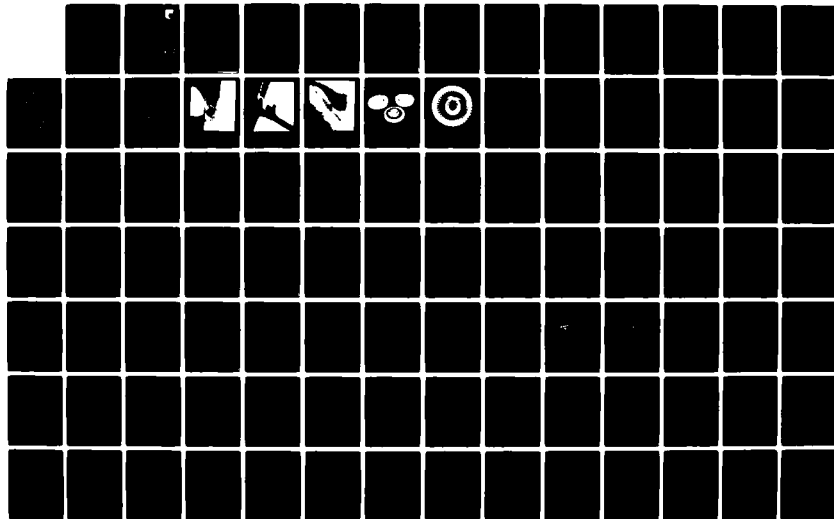
TPE331/T76 TURBOPROP PROPULSION ENGINE DURABILITY(U)
GARRETT TURBINE ENGINE CO PHOENIX AZ L P WYNN AUG 82
21-3640(22) AFWAL-TR-82-4069 F33615-81-C-5016

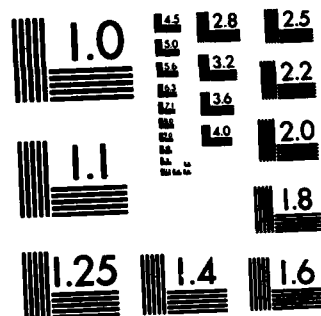
1/2

UNCLASSIFIED

F/G 21/5

NL

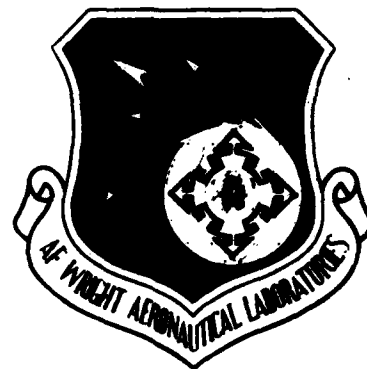




MICROCOPY RESOLUTION TEST CHART
NATIONAL BUREAU OF STANDARDS-1963-A

AC A 122962

AFWAL-TR-82-4069



TPE331/T76 TURBOPROP PROPULSION ENGINE DURABILITY

GARRETT TURBINE ENGINE COMPANY
111 S. 34TH ST., P.O. BOX 5217
PHOENIX, AZ 85010

AUGUST 1982

FINAL REPORT

DTIC
ELECTE
S JAN 4 1983 D
A

APPROVED FOR PUBLIC RELEASE: DISTRIBUTION UNLIMITED

MATERIALS LABORATORY
AIR FORCE WRIGHT AERONAUTICAL LABORATORIES
AIR FORCE SYSTEMS COMMAND
WRIGHT-PATTERSON AIR FORCE BASE, OHIO

DTIC FILE COPY

82 01 03 003

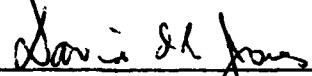
NOTICE

When Government drawings, specifications, or other data are used for any purpose other than in connection with a definitely related Government procurement operation, the United States Government thereby incurs no responsibility nor any obligation whatsoever; and the fact that the government may have formulated, furnished, or in any way supplied the said drawings, specifications, or other data, is not to be regarded by implication or otherwise as in any manner licensing the holder or any other person or corporation, or conveying any rights or permission to manufacture use, or sell any patented invention that may in any way be related there to.

This technical report has been reviewed and is approved for publication.

This report has been reviewed by the Office of Public Affairs (ASD/PA) and is releasable to the National Technical Information Service (NTIS). At NTIS, it will be available to the general public, including foreign nations.

FOR THE COMMANDER



DAVID I. G. JONES, Act'g Chief
AFWAL/MLLN



RONALD P. SINAVAGE, 2LT USAF
METALS Behavior Branch
Metals and Ceramics Division

"If your address has changed, if you wish to be removed from our mailing list, or if the addressee is no longer employed by your organization please notify AFWAL/MLLN, W-P AFB, OH 45433 to help us maintain a current mailing list".

Copies of this report should not be returned unless return is required by security considerations, contractual obligations, or notice on a specific document.

REPORT DOCUMENTATION PAGE		READ INSTRUCTIONS BEFORE COMPLETING FORM
1. REPORT NUMBER AFWAL-TR-82-4069	2. GOVT ACCESSION NO. AD-A122962	3. RECIPIENT'S CATALOG NUMBER
4. TITLE (and Subtitle) TPE331/T76 Turboprop Propulsion Engine Durability		5. TYPE OF REPORT & PERIOD COVERED Final Report
		6. PERFORMING ORG. REPORT NUMBER 21-3640(22)
7. AUTHOR(s) Larry P. Wynn		8. CONTRACT OR GRANT NUMBER(s) F33615-81-C-5016
9. PERFORMING ORGANIZATION NAME AND ADDRESS Garret Turbine Engine Company 111 S. 34 St., P.O. Box 5217 Phoenix, Arizona 85010		10. PROGRAM ELEMENT, PROJECT, TASK AREA & WORK UNIT NUMBERS P.E. 61102F Project 2303Q316
11. CONTROLLING OFFICE NAME AND ADDRESS Materials Laboratory (AFWAL/MLBP) AF Wright Aeronautical Laboratories Wright-Patterson AFB, OH 45433		12. REPORT DATE August 1982
14. MONITORING AGENCY NAME & ADDRESS (if different from Controlling Office)		13. NUMBER OF PAGES 186
		15. SECURITY CLASS. (of this report) Unclassified
15a. DECLASSIFICATION/DOWNGRADING SCHEDULE		
16. DISTRIBUTION STATEMENT (of this Report) Approved for public release; distribution unlimited.		
17. DISTRIBUTION STATEMENT (of the abstract entered in Block 20, if different from Report)		
18. SUPPLEMENTARY NOTES		
19. KEY WORDS (Continue on reverse side if necessary and identify by block number) aircraft propulsion engine durability		
20. ABSTRACT (Continue on reverse side if necessary and identify by block number) This report on retirement-for-cause is based on the Garrett TPE331/T76 turbo-prop engine second-stage turbine wheel. This second-stage turbine wheel is an integrally bladed wheel with continuous rim slots between each blade at the rim. The slot is ended with a circular hole. The slot and hole reduce thermal and centrifugal stresses existing at the heated outer rim and extend turbine low-cycle-fatigue life. This program was planned to develop criteria from examination and analysis of field service wheels that would allow the		

Air Force to define how much life remained in the wheel with an observed crack.

The investigated wheel displayed significant scatter in cycles to initiate a given crack size. This scatter was traceable to the large variation in grain size at the rim of these cast integrally bladed wheels. Crack propagation analysis was able to predict the observed crack-growth rate. However, no correlation between crack initiation and usage could be identified during this program that would aid implementation of retirement-for-cause.

Accession For	
NTIS GRA&I	<input checked="" type="checkbox"/>
DTIC TAB	<input type="checkbox"/>
Unannounced	<input type="checkbox"/>
Justification	
By	
Distribution/	
Availability Codes	
Dist	Avail and/or Special
A	



TABLE OF CONTENTS

	<u>Page</u>
1.0 INTRODUCTION	1-1
2.0 SUMMARY AND RECOMMENDATIONS	2-1
2.1 Summary	2-1
2.2 Recommendations	2-3
3.0 TECHNICAL DISCUSSION	3-1
3.1 Component Selection	3-1
3.2 Engine Start Information	3-2
3.2.1 Service Definition	3-2
3.2.2 Engine Start Peak Temperature Variations	3-5
3.2.3 Engine Start Transient Test Data	3-5
3.3 Engine Service Information	3-9
3.3.1 Commuter Survey Forms	3-9
3.3.2 Customer Survey Results	3-9
3.4 Thermal Analysis	3-9
3.4.1 Secondary Flow Analysis	3-14
3.4.2 Steady State Boundary Condition Analysis	3-24
3.4.3 Transient Boundary Condition Scaling	3-27
3.4.4 Transient Thermal Results	3-30
3.5 Stress Analysis	3-30
3.6 Material Mechanical Properties	3-43
3.6.1 LC Procedure for Material Properties	3-43
3.6.2 Results of Material Testing	3-56
3.6.2.1 Tensile Properties	3-56
3.6.2.2 LCF Properties	3-60
3.6.2.3 Cyclic Crack Growth Rate	3-60
3.6.2.3.1 Data Reduction	3-60
3.6.2.3.2 Discussion	3-70
3.6.3 Conclusions of Materials Testing	3-75
3.7 Analytical Life Prediction	3-75
3.7.1 Crack Propagation Analysis	3-75
3.7.2 Low-Cycle-Fatigue Prediction	3-76
3.8 Turbine Wheel Crack Characterization from Field Service Wheels	3-93

TABLE OF CONTENTS (Contd)

	<u>Page</u>
3.9 Correlation of Cracked Wheels with Analytical Prediction	3-107
3.9.1 Isolation of Problem Areas in Data Correlation	3-107
3.9.1.1 Crack Initiation Determination	3-107
3.10 Whirlpit Test	3-120

APPENDIX

A	Fluid Boundary Conditions	A-1
B	Secondary Flow Conditions	B-1
C	Summary of Heat Transfer Ratios	C-1
D	Crack Lengths from MA Numbers	D-1

LIST OF ILLUSTRATIONS

<u>Figure</u>	<u>Title</u>	<u>Page</u>
1-1	Model TPE331 Engine Cross-Section View	1-2
1-2	Model TPE331 Solid-Rim Turbine Wheel with Typical Rim-Check Locations	1-4
1-3	Model TPE331 Solid-Rim Turbine Wheel Rim Cracks	1-5
1-4	Model TPE331 Solid-Rim Turbine Wheel Rim Cracks	1-6
1-5	Model TPE331 Solid-Rim Turbine Wheel Rim Cracks	1-7
1-6	Model TPE331 Turbine Disks with and without Rim Holes/Slots	1-8
1-7	Forward Face of Model T76 Second-Stage Turbine Wheel P/N868272, S/N 7-13488-3673, Showing Location and Rework of Rivet-Hole Cracks (Arrows)	1-9
3-1	Typical Flight Spectrum	3-3
3-2	Start History on the Merlin IV Aircraft Starboard Engine, S/N 03001, January 1973 to January 1973 to January 1974.	3-4
3-3	Start-Up Transient ITT Temperatures for L/H Engine APU Starts	3-7
3-4	Start-Up Transient ITT Temperatures for R/H Engine APU Starts	3-8
3-5	Blade and Disk Geometry	3-25
3-6	Schematic Diagram of Disk	3-26
3-7	Normalized Temperature Versus Normalized Time for Hot and Cold Starts.	3-31
3-8	Percent Speed Versus Normalized Time for Hot and Cold Starts.	3-32
3-8a	Disk Temperatures During Light-Off Cold Start/Normal Spike	3-33
3-8b	Disk Temperatures During Light-Off Cold Start/Hot Spike	3-34
3-8c	Disk Temperatures During Light-Off Warm Start/Normal Spike	3-35
3-8d	Disk Temperature Take-Off at 180 Seconds to Landing Cold Start/Normal Spike	3-36
3-8e	Disk Temperatures Take-Off at 500 Seconds to Landing Cold Start/Normal Spike	3-37

LIST OF ILLUSTRATIONS (Contd)

<u>Figure</u>	<u>Title</u>	<u>Page</u>
3-8f	Disk Temperatures Take-Off at 180 Seconds to Landing Warm Start/Normal Spike	3-38
3-8g	Disk Temperatures Take-Off at 500 Seconds to Landing Warm Start/Normal Spike	3-39
3-9	Isometric View of Stress Model	3-40
3-10	Meridional View of Stress Model	3-41
3-11	Axial View of Stress Model	3-42
3-12	Peak Stress During Ignition (Cold Engine)	3-45
3-13	Peak Stress During Ignition (Cold Engine)	3-46
3-14	Peak Stress During Ignition (Warm Engine)	3-47
3-15	Peak Stress During Ignition (Warm Engine)	3-48
3-16	Peak Stress During Takeoff at 180 Seconds (Cold Engine)	3-49
3-17	Peak Stress During Takeoff at 180 Seconds (Cold Engine)	3-50
3-18	Peak Stress During Takeoff at 500 Seconds (Cold Engine)	3-51
3-19	Peak Stress During Takeoff at 500 Seconds (Cold Engine)	3-52
3-20	Peak Stress During Landing	3-53
3-21	Peak Stress During Landing	3-54
3-22	Sketch Showing Location of Test Specimens	3-57
3-23	Small Center Notched Specimen for Compressive CCGR Testing	3-58
3-24	Yield Strength of IN-100	3-62
3-25	Ultimate Tensile Strength	3-63
3-26	Percent Elongation of IN-100	3-64
3-27	Percent Reduction In Area of IN-100, of IN-100	3-65
3-28	Axial Strain Controlled LCF of IN-100	3-67
3-29	Axial Strain Controlled LCF of IN-100	3-68
3-30	Axial Strain Control LCF of IN-100 at 593°C (1100°F) Compared to Baseline at Various Temperatures	3-69

LIST OF ILLUSTRATIONS (Contd)

<u>Figure</u>	<u>Title</u>	<u>Page</u>
3-31	Crack Growth Rate Data for IN-100	3-71
3-32	Crack Growth Rate Data for IN-100	3-72
3-33	Crack Growth Rate Data for IN-100	3-73
3-34	Crack Growth Rate Data for IN-100	3-74
3-35	Cycles to Failure Versus Crack Length, Turbine Rim Durability, Forward Corner - Principle	3-77
3-36	Cycles to Failure Versus Crack Length, Turbine Rim Durability, Aft Corner - Principle	3-78
3-37	Cycles to Failure Versus Crack Length, Turbine Rim Durability, Rivet Retainer - Principle	3-79
3-38	Crack Length Versus Crack Depth, Turbine Rim Durability, Forward Corner - Principle	3-80
3-39	Crack Length Versus Crack Depth, Turbine Rim Durability Aft Corner - Principle	3-81
3-40	Crack Length Versus Crack Depth, Turbine Rim Durability Rivet Retainer - Principle	3-82
3-41	Stress Intensity Factor Versus Crack Depth, Turbine Durability, Forward Corner - Principle	3-83
3-42	Stress Intensity Factor Versus Crack Depth, Turbine Rim Durability, Aft Corner - Principle	3-84
3-43	Stress Intensity Factor Versus Crack Depth, Turbine Rim Durability, Rivet Retainer - Principle	3-85
3-44	Crack Face at A Versus Crack Length at B	3-87
3-45	Crack Face at A Versus Crack Face at C	3-88
3-46	Crack Face at A Versus Crack Length at D	3-89
3-47	Crack Face at A Versus Crack Face at E	3-90
3-48	Crack Face at A Versus Crack Length at F	3-91
3-49	Crack Face at A Versus Crack Face at G	3-92
3-50	Crack Locations and Dimensions	3-94
3-51	Crack Face at A Versus Crack Length at B.	3-95
3-52	Crack Face at A Versus Crack Face at C	3-96
3-53	Crack Face at A Versus Crack Length at D	3-97
3-54	Crack Face at A Versus Crack Face at E	3-98

LIST OF ILLUSTRATIONS (Contd)

<u>Figure</u>	<u>Title</u>	<u>Page</u>
3-55	Crack Face at A Versus Crack Length at F	3-99
3-56	Crack Face at A Versus Crack Face at G	3-100
3-57	Crack Length at A Versus Crack Depth at A	3-101
3-58	Crack Length at B Versus Crack Depth at B	3-102
3-59	Crack Length at C Versus Crack Depth at C	3-103
3-60	Crack Length at D Versus Crack Depth at D	3-104
3-61	Crack Length at E Versus Crack Depth at E	3-105
3-62	Crack Length at F Versus Crack Depth at F	3-106
3-63	Crack Locations and Directions	3-108
3-64	Cycles Versus Maximum Cracks Forward Corner - Equivalent	3-109
3-65	Cycles Versus Maximum Crack Aft Corner - Equivalent	3-110
3-66	Cycles Versus All Cracks Forward Corner - Equivalent	3-111
3-67	Cycles Versus All Cracks Aft Corner - Equivalent	3-112
3-68	Turbine Rim Durability - Aft Corner	3-113
3-69	Turbine Rim Durability - Forward Corner	3-115
3-70	Turbine Rim Durability - Rivet Retainer	3-116
3-71	Turbine Rim Durability - Rivet Retainer	3-117
3-72	Turbine Rim Durability - Forward Corner	3-118
3-73	Turbine Rim Durability - Aft Corner	3-119
3-74	Crack Growth Data from Whirlpit Test Wheel 2197	3-122
3-75	Crack Growth Data from Whirlpit Test Wheel 4275	3-123
3-76	Typical Stress Intensity Factor Range Versus Incremental Crack Growth Rate for IN-100 Castings at Room Temperature	3-124

LIST OF TABLES

<u>Table</u>	<u>Title</u>	<u>Page</u>
3-1	Peak Light-off Temperatures of Merlin and Metro Aircraft	3-6
3-2	Computer Airline Questionnaire for Turbine Wheel Durability Program	3-10
3-3	Platform Heat Transfer Coefficients	3-15
3-4	Blade Heat Transfer Coefficients	3-16
3-5	Blade Adiabatic Wall Temperatures	3-17
3-6	Second Stage Disk Heat Transfer Coefficients	3-18
3-7	Second Stage Adiabatic Wall Temperatures	3-19
3-8	Second Stage Disk Bore Heat Transfer Coefficients	3-20
3-9	Heat Transfer Coefficients in Rivet Hole	3-21
3-10	Heat Transfer - Coefficient Ratios - Cold Start	3-22
3-11	Heat Transfer Coefficient Ratios - Hot Start	3-22
3-12	Transient Heat Transfer Coefficient Ground Idle to Maximum Power Acceleration	3-23
3-13	Transient Temperature Ratios	3-23
3-14	Transient Stress Analysis Peak Stresses	3-44
3-15	Listing of Half Wheels	3-55
3-16	Room Temperature Tensile Properties	3-59
3-17	Tensile Test Results (Garrett)	3-61
3-18	LCF Data Summary	3-66
3-19	LCF Life Prediction Summary	3-86
3-20	Crack Sizes in Cyclic Whirlpit Test	3-121

1.0 INTRODUCTION

The U.S. Air Force Materials Laboratory, in its continuing effort to control support costs for engine replacement hardware, undertook the task to define the data base and technology necessary to implement a retirement-for-cause program. A major part of the initial objectives of retirement-for-cause was to define useful disk life remaining after a crack had been identified. This objective requires that a predictable and repeatable process be found to identify crack initiation and predict crack growth after initiation of the crack. Large economic returns are foreseen if identifiable disk life exists after discovery of a crack. Procedures needed to make retirement-for-cause a viable approach for the Air Force fleet indicate defining a crack analysis model and a switched data base to which the model can be applied.

To meet these objectives, the Garrett Turbine Engine Company (then called AiResearch) entered into this contract with the Materials Laboratory whereby the large data base existing from commuter airline use of the Garrett TPE331/T76 engine could be analyzed with widely available analytical models (including models the USAF contracted with Garrett to develop) to establish retirement-for-cause principles.

The Model TPE331/T76 turboprop propulsion engines have been in production for about 13 years. To date, over 6000 engines are in commercial flight service as power plants for commuter airlines, executive aircraft, crop dusters, and helicopters (TSE331). The military version, T76, is the power plant in the North American Rockwell OV10A, used by the Navy, Marine Corps, and Air Force.

The power section of this engine, shown in Figure 1-1, consists of two centrifugal compressor stages and three axial turbine stages. Early development testing with the conventional continuous rim turbine

wheels resulted in the identification of multiple rim cracks after numerous engine start-stop cycles. These rim cracks are shown in Figures 1-2 through 1-5. To minimize the high transient compressive stress at the rim, a continuous slot was introduced between the blades at the rim. The slot was terminated by a circular hole. Figure 1-6 shows three turbine stages, one of which has the slots and holes. A rivet was inserted into each hole to minimize bypass gas leakage. This concept was patented by Garrett and has proven to substantially increase the crack-free LCF life of the rim. Furthermore, crack-propagation life has been considerably extended.

Nonetheless, rim cracks still occur with these turbine wheels after moderate field usage. Figure 1-7 is the forward face of the second-stage turbine wheel with arrows pointing to cracks at the rim holes. The tolerance of disk structural integrity to these cracks has been demonstrated by their routinely observed presence when disks are retired from field service.

The rim-crack problem for the first two turbine stages is recognized to be the result of low-cycle-fatigue. Field service usage has substantiated that a portion of the usable disk life exists well after crack initiation. Analytical methods applied to this problem prior to this program predicted acceptable disk life to be beyond the service life limitations now imposed. The program described herein was to achieve the following objectives:

- o Rigorously quantify the local rim three-dimensional stress field, both transient and steady-state, resulting from the imposed centrifugal and thermal fields.
- o Analytically predict rim-crack initiation and propagation rates considering combined LCF and creep damage.

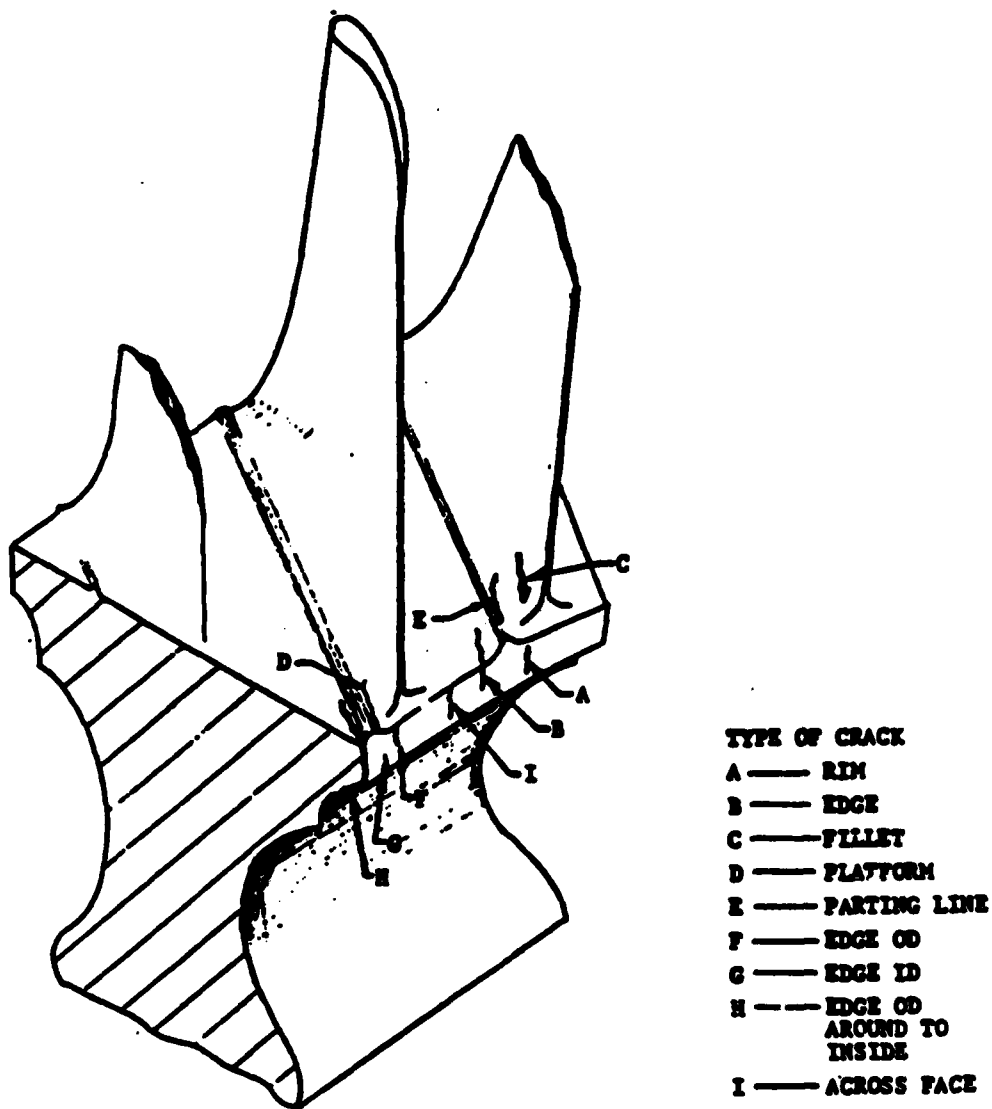


Figure 1-2. Model TPE331 Solid-Rim Turbine Wheel With Typical Rim-Crack Locations.



Figure 1-3. Model TPE331 Solid-Rim Turbine Wheel Rim Cracks.

21-3649(22)

1-5



Figure 1-4. Model TPE331 Solid-Rim Turbine Wheel Rim Cracks.

21-3640(22)

1-6



Figure 1-5. Model TPE331 Solid-Rim Turbine Wheel Rim Cracks.

21-3640 (22)

1-7

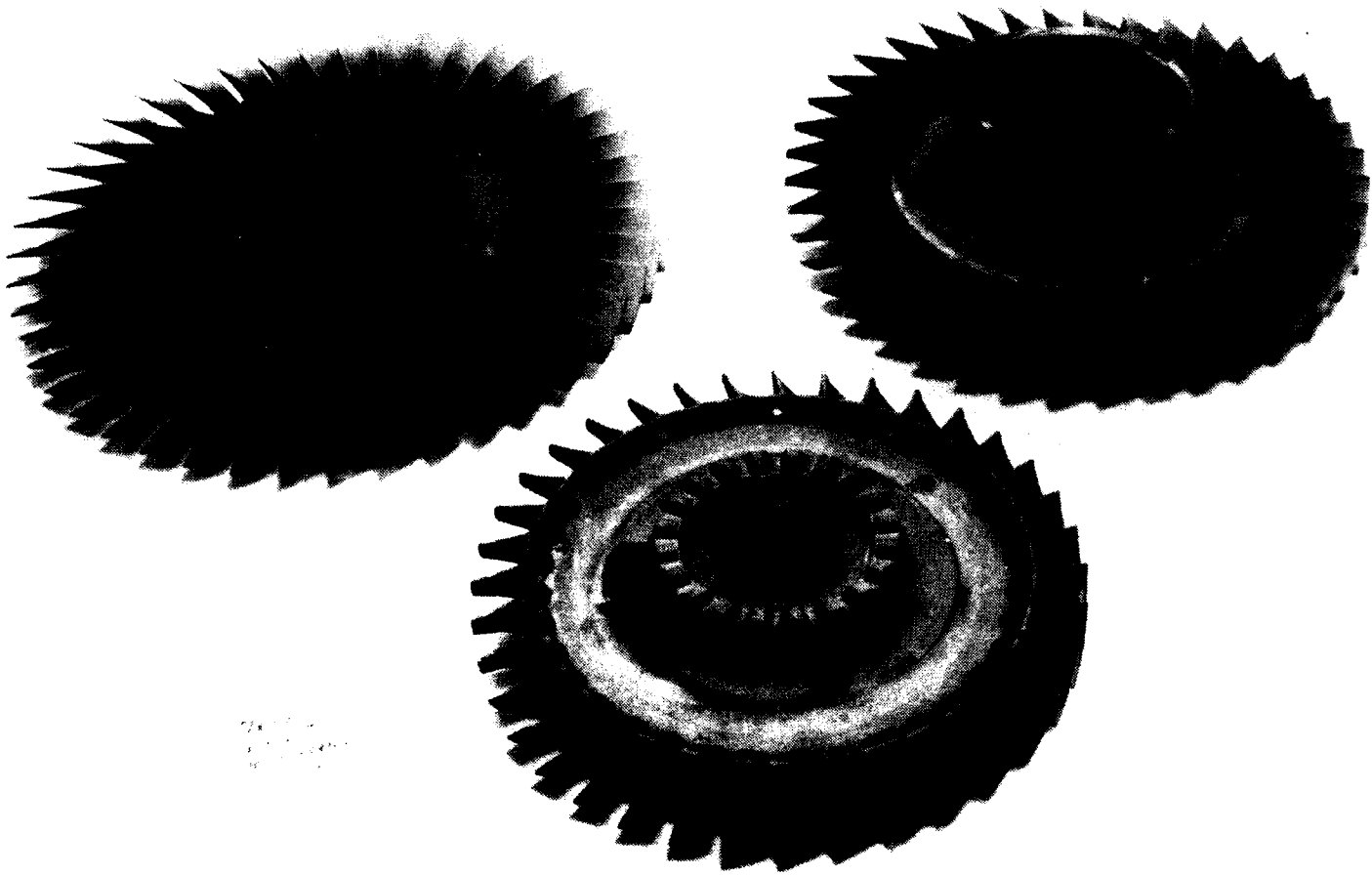


Figure 1-6. Model TPE331 Turbine Disks With and Without Rim Holes/Slots.



Figure 1-7. Forward Face of Model T76 Second-Stage Turbine Wheel
Part 868272, Serial No. 7-13488-3673, Showing Location
and Rework of Rivet-Hole Cracks (Arrows).

21-3640(22)

1-9

- o Verify analytical predictions with disks retired from field usage for which cycle, mission profile, and temperature histories are known.
- o Refine analytical correlations and establish a pragmatic design procedure.
- o As a future option, further verify analytical predictions of disk life by imposing additional cycles on selected disks beyond the maximum cycles to which disks have operated.

The generalized benefits to be achieved from this effort:

- o Quantified prediction of turbine disk usable-life potential for Model TPE331/T76 turboprop engines from which attendant service life increase and ancillary economic return can be realized.
- o Predictive design methodology that can be rigorously applied to future generation turbine disk designs and by which damage tolerance can be reliably predicted.

2.0 SUMMARY AND RECOMMENDATIONS

2.1 Summary

At the initiation of this program, it was believed that the variation of light-off temperature would have a major impact on the scatter of the fatigue crack initiation of the subject turbine wheel. For this reason, a great deal of effort was expended to determine the thermal boundary conditions to be used in this analysis. The result of this work concluded that light-off temperature variations had a minor effect on the actual variations in stress level. The primary stress variation driver was whether or not the engine was started for the first time of the day when the metal temperatures were ambient, or whether the engine was restarted after a delay of approximately 15 minutes.

A survey of commuter users determined how the damage from these two different starts accumulated to cause fatigue damage.

A test program was initiated to determine the low-cycle-fatigue and crack-propagation characteristics of the material for specimens taken from actual cast wheels. This test program consisted of smooth-bar-fatigue tests and center panel crack-propagation tests.

A three-dimensional stress and thermal analysis was made for the turbine for both steady-state and transient conditions. This analysis was the basis for all fatigue and crack-propagation calculations.

A crack-propagation analysis was made using a program called "BIGIF." The results of this analysis gave the life remaining in the wheel, given an initial crack size. However, definition of crack initiation became the major drawback in the correlation of crack data from field service wheels and analysis.

Garrett does utilize TPE331 turbine disks in the manner desired under retirement-for-cause. However, no intermediate inspection is scheduled between crack initiation and crack rework or wheel removal. Therefore, in order to verify the analytical crack-propagation results, a program measuring the sizes and location of cracks in wheels retired from field service was conducted. The program measured the cracks at designated locations around the rivet hole. This was accomplished by cracking open each slot of each wheel and recording the crack depth and length. This data provided information on crack sizes in wheels for which cyclic history was known.

Many cracks were measured on wheels destructively examined for this program. The key problem encountered was the inability to separate crack initiation from crack propagation. Ideally if the crack initiation point were known for the cracks examined, a correlation between actual and analytical results could be obtained. With this correlation, analytical procedures and limits could be refined to a point of increased confidence in crack-propagation prediction.

Lacking the qualitative information on crack initiation needed for a straightforward correlation of the crack propagation, a number of approaches were made to statistically determine the initiation cycles and crack size.

These approaches to determine crack initiation statistically are presented in this report, but the results are inconclusive. The field wheel cracks can be bounded by the analysis, so while the data does not dispute the analysis, the large scatter does not allow identification or removal of errors in analysis or basic assumptions. In this regard, Garrett was unable to define the procedures needed to establish retirement-for-cause (RFC).

Garrett attempted to experimentally define the critical crack size and to allow an extension of the allowable number of cycles on the TPE331/T76 wheel. A whirlpit test of two wheels was undertaken. One wheel failed in a region of no interest to this program, and the other ran for another 7500 cycles without breaking. These results lead Garrett to the following recommendations.

2.2 Recommendations

The USAF has been successful in developing RFC principles for extremely fine-grained materials. The course-grained materials used by Garrett for integrally bladed turbine wheels cannot apply these same principles. In order to establish RFC principles applicable with coarse-grained materials, Garrett recommends that the following steps be taken, singly or in groups:

- (a) Apply the existing models and methodology to an accelerated endurance test (or simulated engine cycle test) where both the crack initiation and propagation phases were covered by multiple inspections that included measurement of crack size.
- (b) Apply the existing models and methodology to a whirlpit test with multiple inspections covering crack initiation and propagation phases. The test specimens must be a specifically designed wheel to avoid unwanted failure at other locations.

Data from either, or both, of these steps could be used to establish RFC principles for other than fine-grained materials.

3.0 TECHNICAL DISCUSSION

3.1 Component Selection

The second-stage turbine wheel for the Model TPE331/T76 was selected as the component to study for this hot-section durability analysis for the following reasons:

- o This turbine wheel represents a component from an engine that has seen experience in both commercial and military service. To date, about 13-million fleet hours have been accrued in commercial service alone.
- o One of the life-limiting factors in restricting the life of these turbines to 4240 hours or 4900 cycles in commercial service has been the high-temperature, low-cycle-fatigue cracking in the holes at the rim of the disk. These holes were designed to reduce stresses due to thermal gradients encountered during engine start.
- o The turbine configuration is well defined with a long history of operation under several definable mission profiles for both commercial and military operations.
- o The uprated versions of the Model TPE331 are used on popular aircraft such as the Cessna Conquest. The present production rate is about 60 engines per month and is increasing to meet a projected delivery totaling 5500 engines by the end of 1982.
- o The selected turbine wheel is an integral one-piece vacuum investment casting of IN100. The one-piece casting has been developed to minimize turbine costs.

The time-dependent thermal analysis of the second-stage turbine disk was conducted for a representative service cycle, as shown in Figure 3-1, comprising engine light-off and acceleration to ground-idle, acceleration to maximum takeoff power, and the cycle duration from takeoff through landing, engine shutdown, and thermal soakback. The engine-start transient from a residually hot engine is known to be much more benign to the turbine disk rim than from an isothermally ambient temperature engine with respect to low-cycle fatigue. Hence, thermal analysis was conducted for the two initial temperature conditions, where the hot-engine start will correspond to disk temperatures resulting 15 minutes after the previous shutdown. These results were used for correlation of damage severity of hot and cold-engine starts with field engines.

Treatment of the variation in light-off peak temperature will use the spectral distribution of measured temperatures shown in Figure 3-2, as well as data obtained primarily for this program from flight tests.

3.2 Engine Start and Service Information

3.2.1 Engine Service Definition

In order to obtain as much data as possible on engine flight conditions and start histories, a two-fold program was pursued. The first step was to record the interstage turbine temperature and speed as a function of time on an in-service aircraft with TPE331 engines. The second step was to send questionnaires to the commercial users of this engine, asking such questions as:

- o Duration of flight
- o Which engine starts first
- o What power source is used to start the engine
- o Altitude spectrum

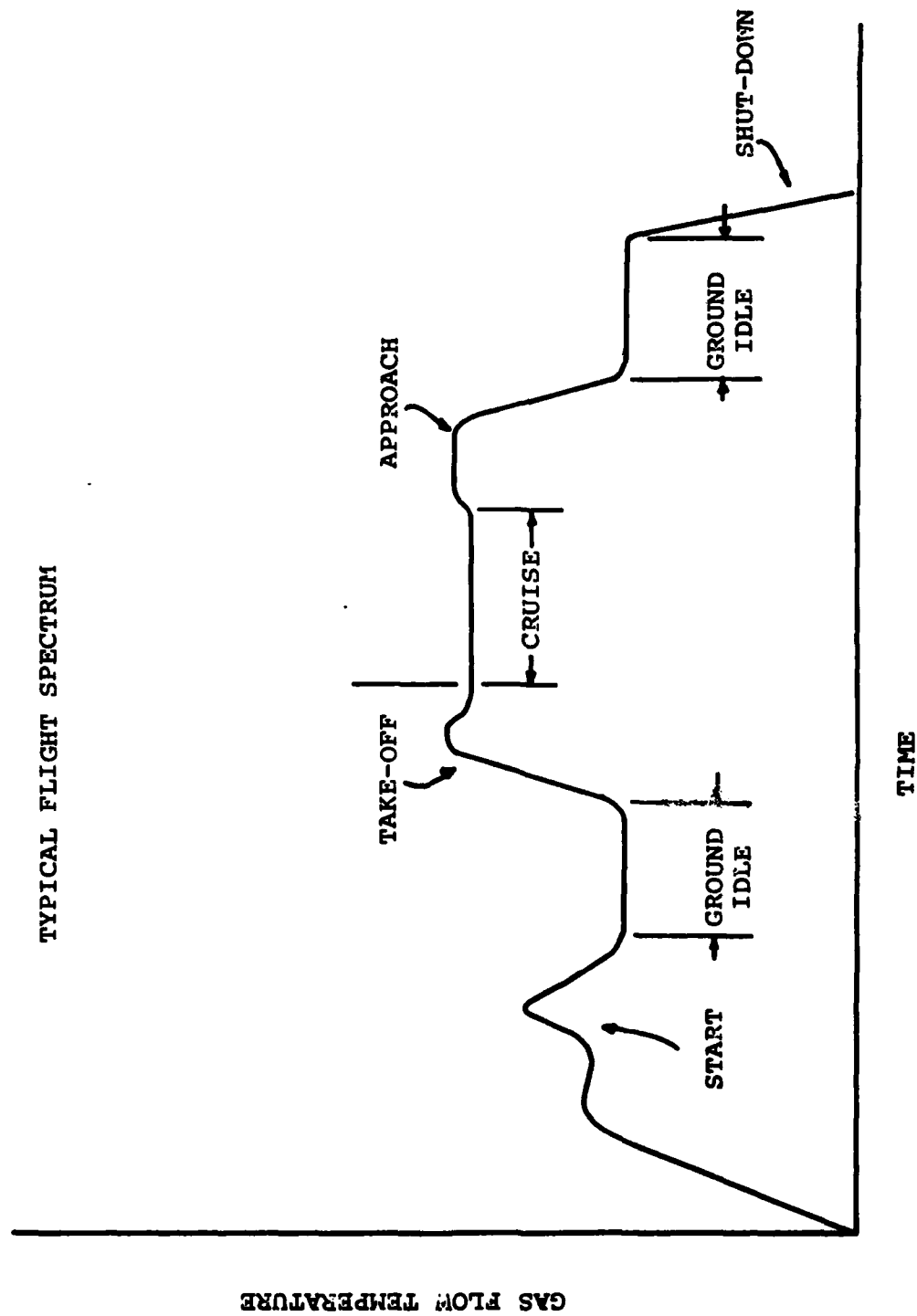


Figure 3-1. Typical Flight Spectrum.

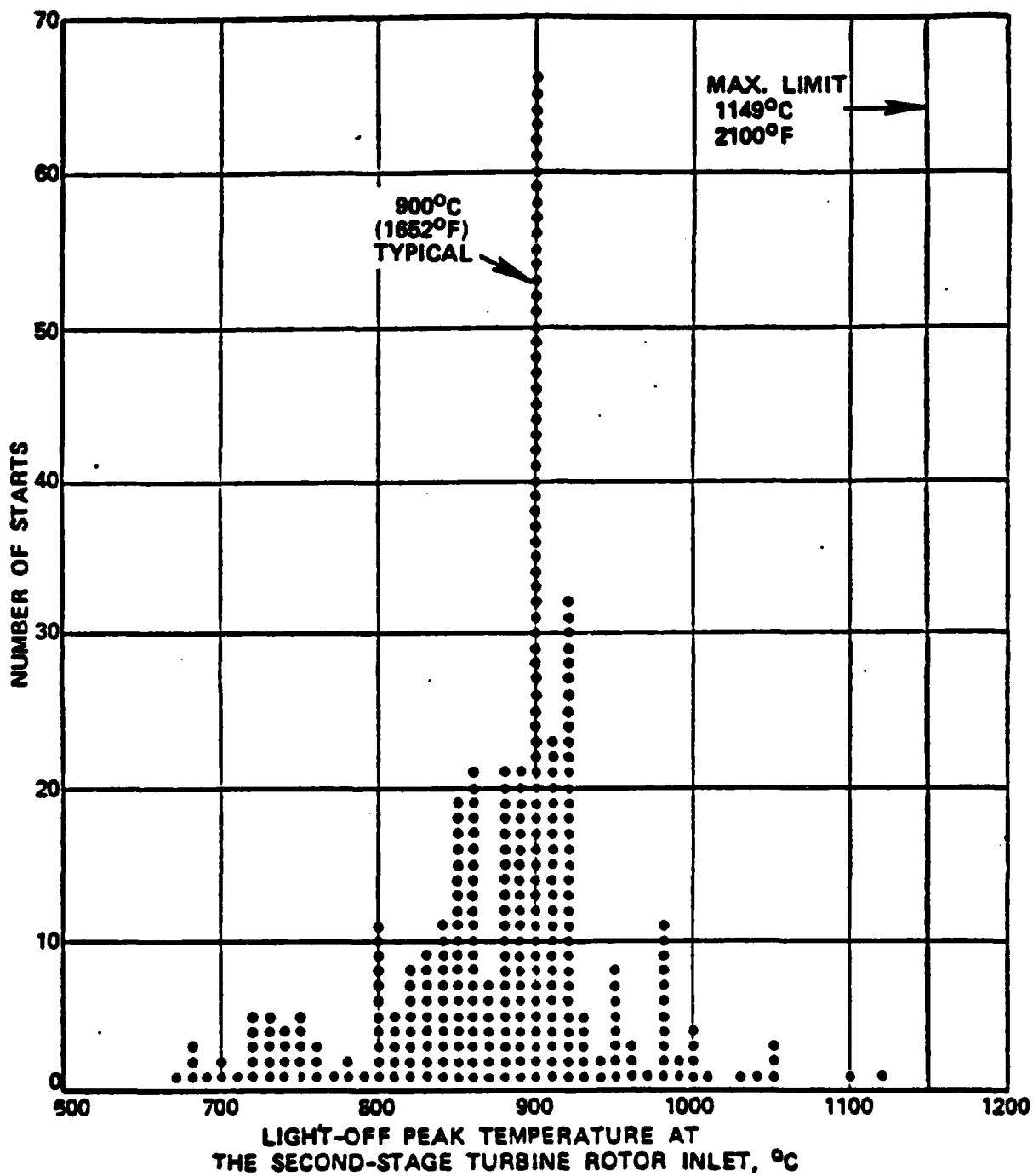


Figure 3-2. Start History on the Merlin IV Aircraft Starboard Engine, Serial No. 03001, January 1973 to January 1974.

- o Duration of taxi
- o Take-off and cruise
- o Outside ambient conditions.

3.2.2 Engine Start Peak Temperature Variations

To date, peak light-off temperatures for over 1000 engine starts have been recorded during a year of service on the Garrett Merlin and Metro aircraft. This data has been tabulated and is shown in Table 3-1. Some interesting and possible significant results that can be seen from this data are: the Merlin aircraft has a peak light-off temperature about 50°C (122°F) colder than the Metro aircraft; for both the Metro and Merlin, the left-hand engine is hotter by about 30° to 40°C (86° to 104°F) than the right-hand engine; and a battery start is generally about 60°C (140°F) hotter than an APU start. This information was used in establishing the correlation between predicted crack initiation and the actual crack history of an engine with known service histories.

3.2.3 Engine Start Transient Test Data

Another aspect of the data acquisition program is the recording of start temperatures for the Merlin and Metro aircraft as a function of time. This data provided the engine gas temperatures as a function of time and was input to the transient thermal analysis. Data from nine engine starts were recorded for both left and right engines. A sample of this data is shown in Figures 3-3 and 3-4. From this data, it is possible to obtain a range of times required for the engine to reach peak temperature. Comparing the peak temperature of these limited number of starts with the large number of starts (as described in the preceding paragraph) gave statistical significance to the data obtained for the transient study.

TABLE 3-1. PEAK LIGHT-OFF TEMPERATURES OF MERLIN AND METRO AIRCRAFT.

METRO II ONLY

Engine	Start	Average °C	Peak °C	Low °C	St. Dev.
L/H	APU	1018.7	1095.	905.	31.98
L/H	BATT	1048.2	1127.	990.	34.48
R/H	APU	976.3	1085.	910.	30.97
R/H	BATT	1046.6	1097.	991.	26.22
L&R (2)	APU	997.7	1095.	905.	37.94
L&R (2)	BATT	1047.7	1127.	990.	31.89
L/H	ALL	1025.9	1127.	905.	34.92
R/H	ALL	985.9	1097.	910.	38.77
ALL	ALL	1007.4	1127.	905.	41.79

MERLIN IV ONLY

Engine	Start	Average °C	Peak °C	Low °C	St. Dev.
L/H	APU	964.5	1085.	890.	28.06
L/H	BATT	1036.3	1090.	950.	32.65
R/H	APU	930.9	1050.	870.	30.07
R/H	BATT	1004.7	1060.	910	37.34
L&R (2)	APU	947.8	1085.	870.	33.56
L&R (2)	BATT	1021.3	1090.	910	38.19
L/H	ALL	976.2	1090.	890	39.20
R/H	ALL	942.1	1060.	870	40.96
ALL	ALL	959.4	1090.	870.	43.53

METRO II AND MERLIN IV

Engine	Start	Average °C	Peak °C	Low °C	St. Dev.
L&R (4)	APU	971.4	1095.	870.	43.53
L&R (4)	BATT	1035.4	1127.	910.	37.26
ALL	TOTAL	982.7	1127.	870.	48.96

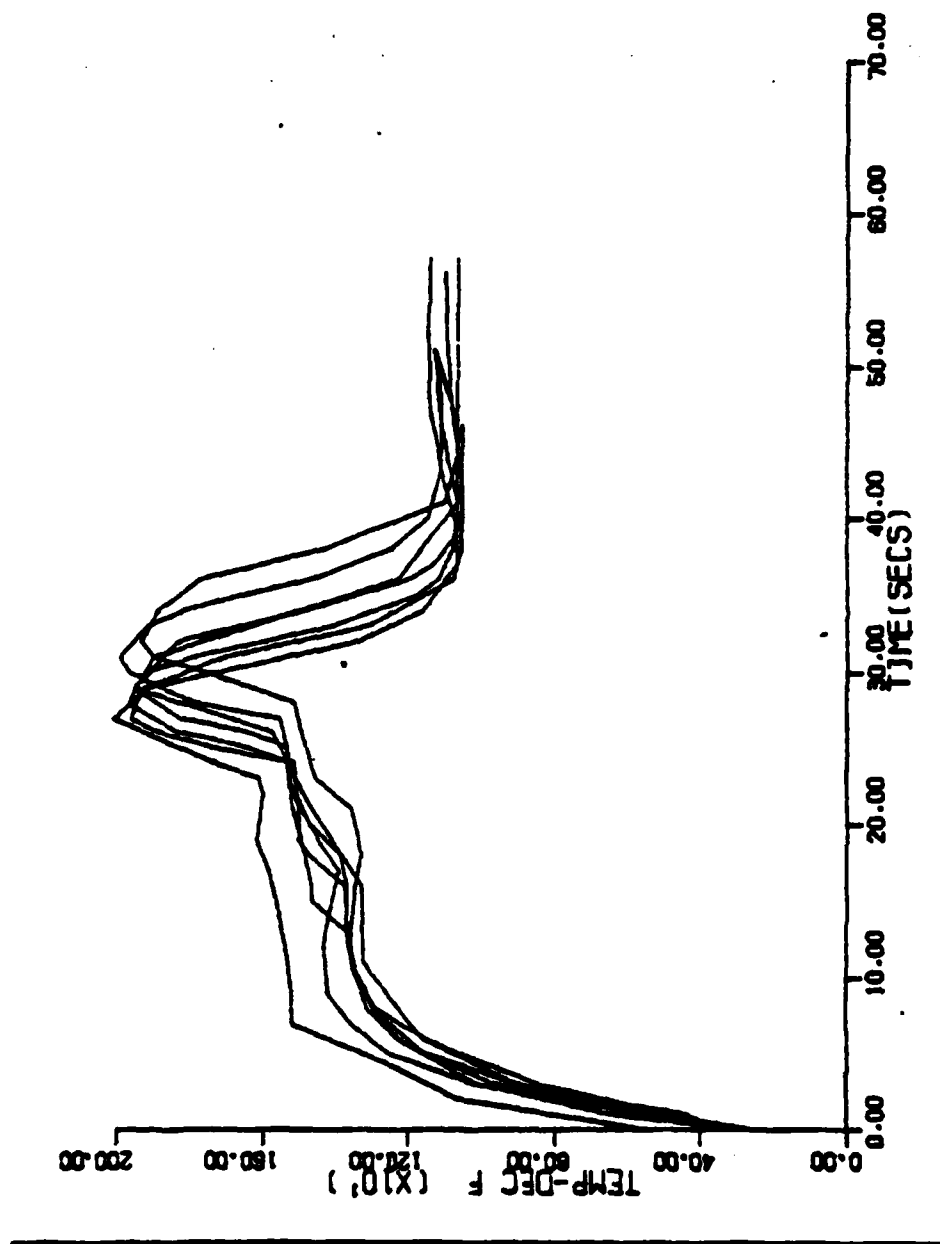


Figure 3-3. Start-Up Transient ITT Temperatures for L/H Engine APU Starts.

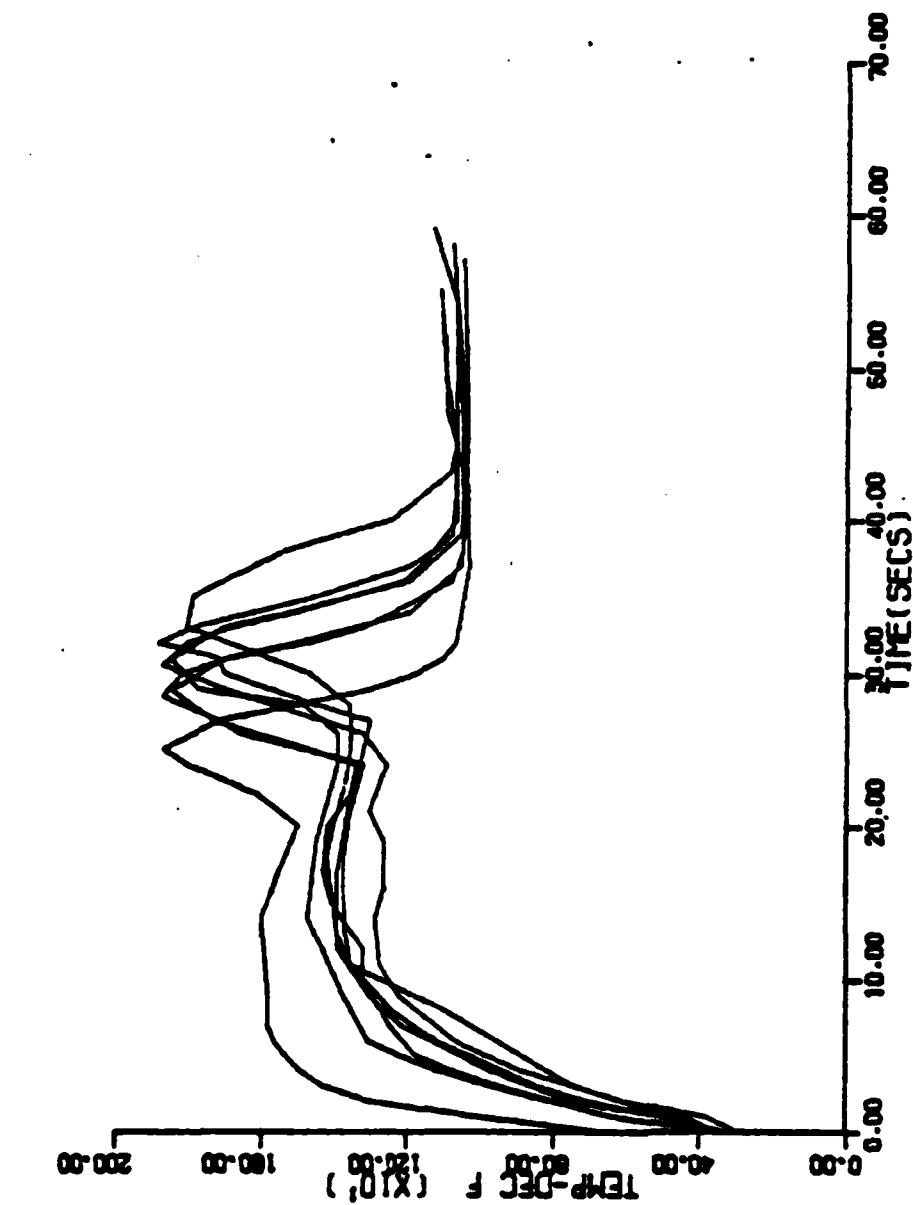


Figure 3-4. Start-Up Transient ITT Temperatures for R/H Engine APU Starts.

3.3 Engine Service Information

3.3.1 Commuter Survey Forms

A reproduction of the commuter survey that was sent to various airlines is shown in Table 3-2.

3.3.2 Customer Survey Results

Customer survey forms for three different airlines have been received. A total of six aircraft were monitored for one week. The significant results are summarized as follows:

- o Typical time at take-off is 2 to 3 minutes with a minimum of 1 minute and a maximum of 3 minutes.
- o All replies had a time at climb power of 10 minutes.
- o All altitudes at cruise were 3658 to 4572 m (12,000 to 15,000 feet).
- o Between 85 percent and 100 percent of the starts were made with APU's.
- o All airlines reported that at least 3 minutes of ground-idle power was held before take-off power was initiated.
- o A small number of times (0 to 8 percent), the left-hand engine was shutdown for loading passengers, while the right engine remained at idle.

3.4 Thermal Analysis

This section describes the analysis to develop thermal boundary conditions to be used in a three-dimensional thermal analysis of the second-stage turbine wheel for the TPE331-3U. Boundary conditions were calculated for three engine conditions - maximum power, cruise,

TABLE 3-2. COMMUTER AIRLINE QUESTIONNAIRE.

COMMUTER AIRLINE QUESTIONNAIRE
FOR
TURBINE WHEEL DURABILITY PROGRAM

- I Select a sample of aircraft from your fleet. (We would prefer data on all your aircraft but not wanting to impose more than absolutely necessary a sampling of your fleet can serve our purposes.)

<u>Fleet Size</u>	<u>Sample Size</u>
1 to 3 aircraft	1 aircraft
4 to 8 aircraft	2 aircraft
9 or more aircraft	3 aircraft

- II Choose, from operating records for each aircraft in the sample, a recent week during which the aircraft experienced a normal operating schedule. The same week need not be chosen for all aircraft.
- III Please answer the following 17 questions regarding aircraft and engine operation during the chosen week.

Aircraft data

1. Data is for week beginning _____ Date _____
2. Aircraft model _____
3. Aircraft serial no. _____
4. No. departures _____
5. No. aircraft hours logged _____

TABLE 3-2. COMMUTER AIRLINE QUESTIONNAIRE (COND).

	R.H.	L.H
6. Engine S/N	_____	_____
7. Engine hours at beginning of week	_____	_____
8. Engine hours logged during week	_____	_____
9. Engine cycles at beginning of week	_____	_____
10. Cycles logged during week	_____	_____
11. No. engine starts for ground checks, moving A/C, etc. not logged as cycles	_____	_____
12. No. engine starts, including (11) above which were made within 30 minutes of the previous shutdown	_____	_____
14. On approximately what percentage of landings L.H. engine was shut down and R.H. engine kept running during discharge and boarding of passengers	_____	
15. If only L.H. engine was shut down (question 14 above) what was typical number of minutes of each shutdown	_____	
16. On approximately what percentage of landings was one engine only (L.H./R.H.) used as an APU during ground operation (other than while discharging or boarding passengers per (14) above)	_____	
17. What was typical time of such operation (16) above:	_____ minutes.	

TABLE 3-2. COMMUTER AIRLINE QUESTIONNAIRE (COND).

IV Please answer the following 5 questions based on your normal operating procedures (not necessarily on the above sample weeks).

1. Which engine is normally started first R.H. L.H.
2. What power source is used for 1st engine starts indicated in (1) above)?
- Auxiliary power unit % of starts
- Aircraft batteries % of starts
- Auxiliary batteries % of starts
3. What power source is used for starting the second engine?
- Auxiliary power unit % of starts
- Aircraft batteries % of starts
- Auxiliary battereis % of starts
- Cross generator % of starts
4. On what percent of landings is "full" reverse used?
-
5. How are cycles counted?
1. By actual number of engine starts
2. By number of A/C flights
3. By number of A/C flights followed by engine shutdown
4. Other (describe)

TABLE 3-2. COMMUTER AIRLINE QUESTIONNAIRE (COND).

VI ROUTE STRUCTURE:

Please provide the following information for typical flights over your regularly scheduled routes. Use one sheet for each leg.

Route No. _____ Leg No. _____
From: _____ To: _____
(city) (city)

Number of times flown per week: _____

1. Engine ground operation prior to take-off:
(a) Is engine shutdown after previous landing?

L.H. _____ R.H. _____
yes or no yes or no

- (b) Time at ground idle:

L.H. min. R.H. min.

- (c) Taxi time:**

L.H. _____ min. R.H. _____ min.

- ## 2. Normal in-flight engine operation:

	ITT	RPM	TIME
(a) Take-off	_____ °C,	_____ %	_____ min.
(b) Climb	_____ °C	_____ %	_____ min.
(c) Cruise	_____ °C	_____ %	_____ min.
(d) Descent	_____ °C	_____ %	_____ min.
(e) Cruise Altitude			ft.

- ### 3. Normal engine operation after landing:

(a) Taxi time: L.H. _____ min. R.H. _____ min.

(b) Ground idle time: L.H. _____ min. R.H. _____ min.

and ground idle. The boundary conditions at these steady-state points, along with knowledge of engine operating characteristics, were used for transient scaling of the boundary conditions for engine starts, engine accels from ground idle to maximum power, etc.

Throughout the analysis, pressure and temperature boundary conditions as well as velocity distributions along the blade were used. This information was supplied by the Aero/Thermo Components Group for maximum power, cruise and idle conditions and is summarized in Appendix A. The analysis consisted of determining the engine secondary flows at steady-state, calculation of the corresponding steady-state thermal boundary conditions, and scaling of the steady-state values to find the transient thermal boundary conditions.

Transient scaling is usually done strictly from maximum power conditions. However, for this analysis, estimates of engine conditions (main gas flow path pressures and temperatures) at cruise and idle were also used. It should be emphasized that the engine conditions at cruise and idle were estimates and not the result of detailed calculations as were done at maximum power.

The steady-stage heat-transfer coefficients and gas temperatures are shown in Tables 3-3 through 3-9. The ratio of transient heat-transfer coefficients and gas temperatures to their appropriate steady-state values are listed in Tables 3-10 through 3-12.

3.4.1 Secondary Flow Analysis

The first step in the analysis was to develop a model of the engine to determine the secondary flows in the vicinity of the second-stage disk. A computer program was used to carry out the analysis. The program solves for steady-state pressures and flow distribution in a network of cavities connected by flow resistances. The cavities and resistances used in the analysis are given in Appendix B.

TABLE 3-3. PLATFORM HEAT TRANSFER COEFFICIENTS.

X cm/in.	82.5	84.6	86.8	88.9	91.1	93.2	95.4	97.5
-1.14/-0.45	746/365	795/389	634/310	685/335	736/360	785/384	836/409	674/330
-1.02/-0.40	681/333	726/355	581/284	626/306	673/329	718/351	763/373	617/302
-0.89/-0.35	615/301	656/321	525/257	566/277	607/290	648/317	689/337	558/273
-0.76/-0.30	605/296	649/311	484/237	540/264	593/290	648/317	701/343	527/258
-0.63/-0.25	609/298	653/313	468/229	532/260	597/292	660/323	715/343	519/254
-0.51/-0.20	613/300	657/315	466/218	521/255	597/292	673/329	728/343	507/248
-0.25/-0.10	597/292	641/308	452/221	517/253	583/285	648/317	701/343	503/246
+0.13/+0.05	552/270	607/303	429/210	484/237	540/264	597/292	648/317	474/232
+0.38/+0.15	513/251	568/300	413/202	458/224	505/247	550/269	597/292	450/220
+0.63/+0.25	472/231	505/247	403/197	435/213	466/228	499/244	529/259	429/210
+0.76/+0.30	462/226	482/236	421/206	440/215	458/224	478/234	497/243	517/253
+0.89/+0.35	462/226	470/230	480/235	450/220	460/225	468/229	478/234	489/239
+1.02/+0.40	470/230	472/231	472/232	476/233	470/230	472/231	474/232	476/233
+1.14/+0.45	489/239	482/236	476/233	470/230	489/239	482/236	476/233	470/230
+1.27/+0.50	452/221	452/221	452/221	452/221	452/221	452/221	452/221	452/221

MAXIMUM POWER		CRUISE	
-1.14/-0.45	527/258	560/274	458/224
-1.02/-0.40	478/234	509/249	413/202
-0.89/-0.35	429/210	458/224	368/180
-0.76/-0.30	423/207	301/147	339/166
-0.63/-0.25	427/209	288/141	331/162
-0.51/-0.20	429/210	258/126	311/152
-0.25/-0.10	415/203	266/130	313/153
+0.13/+0.05	384/188	262/128	301/147
+0.38/+0.15	366/179	253/124	288/141
+0.63/+0.25	329/161	352/172	276/135
+0.76/+0.30	317/155	335/164	278/136
+0.89/+0.35	313/153	323/158	333/163
+1.02/+0.40	321/157	321/157	327/160
+1.14/+0.45	333/163	331/162	329/161
+1.27/+0.50	352/172	343/168	335/164

-1.14/-0.45	527/258	560/274	458/224	489/239	521/255	554/271	587/287	482/236
-1.02/-0.40	478/234	509/249	413/202	442/216	472/231	503/246	534/261	435/213
-0.89/-0.35	429/210	458/224	368/180	395/193	423/207	452/221	480/235	390/191
-0.76/-0.30	423/207	301/147	339/166	376/184	415/203	454/222	491/240	368/181
-0.63/-0.25	427/209	288/141	331/162	376/184	419/205	462/226	503/246	366/179
-0.51/-0.20	429/210	258/126	311/152	364/178	417/204	470/230	503/246	354/173
-0.25/-0.10	415/203	266/130	313/153	360/176	405/198	452/221	503/246	350/171
+0.13/+0.05	384/188	262/128	301/147	337/165	378/185	415/203	452/221	331/162
+0.38/+0.15	366/179	253/124	288/141	323/158	358/175	395/193	429/210	317/155
+0.63/+0.25	329/161	352/172	276/135	301/147	323/158	348/170	372/182	296/145
+0.76/+0.30	317/155	335/164	278/136	296/145	313/153	331/162	348/170	366/179
+0.89/+0.35	313/153	323/158	333/163	301/147	311/152	321/157	331/162	341/167
+1.02/+0.40	321/157	321/157	327/160	331/162	319/156	323/158	327/160	331/162
+1.14/+0.45	333/163	331/162	329/161	325/159	335/164	331/162	329/161	327/160
+1.27/+0.50	352/172	343/168	335/164	329/161	323/158	345/169	337/165	331/162

-1.14/-0.45	368/180	429/210	233/114	294/144	356/174	417/204	478/234	282/138
-1.02/-0.40	307/150	360/176	192/94	245/120	296/145	350/171	401/196	235/115
-0.89/-0.35	247/121	290/142	151/74	196/96	239/117	282/138	325/159	186/91
-0.76/-0.30	251/123	121/59	161/79	202/99	239/117	284/139	325/159	194/95
-0.63/-0.25	253/124	127/62	168/82	206/101	245/120	284/139	325/159	198/97
-0.51/-0.20	256/125	133/65	172/84	211/103	247/121	286/140	325/159	202/99
-0.25/-0.10	239/117	135/66	168/82	200/98	233/114	266/130	325/159	194/95
+0.13/+0.05	245/102	139/68	161/79	182/89	204/100	225/110	325/159	178/87
+0.38/+0.15	196/96	135/66	153/75	174/85	192/94	211/103	325/159	170/83
+0.63/+0.25	174/85	190/93	145/71	159/78	174/85	188/92	325/159	157/77
+0.76/+0.30	170/83	180/88	149/73	159/78	168/82	178/87	325/159	198/97
+0.89/+0.35	168/82	174/85	180/88	161/79	168/82	174/85	325/159	184/90
+1.02/+0.40	182/89	176/86	176/86	176/86	174/85	176/86	325/159	178/87
+1.14/+0.45	182/89	180/88	178/87	176/86	182/89	180/88	325/159	176/86
+1.27/+0.50	190/93	186/91	182/89	178/87	174/85	186/91	325/159	178/87

TABLE 3-4. BLADE HEAT TRANSFER COEFFICIENTS, J/Hr $\text{cm}^2\text{C/Btu/Hr Ft}^2\text{-F}$.

X (cm/in.)	Radius = 2.963		3.263		3.563		3.863		4.163	
-1.14/-0.45	2745/1343	2745/1343	5920/2896	5920/2896	4479/2191	4479/2191	3389/1658	3389/1658	3551/1737	3551/1737
-1.02/-0.40	760/372	590/289	1002/500	920/450	971/475	613/300	1103/540	613/300	1329/650	1073/525
-0.89/-0.35	666/326	527/258	748/366	458/224	844/413	409/200	920/450	460/225	973/476	542/265
-0.76/-0.30	646/316	474/232	707/346	419/205	775/379	403/197	822/402	450/220	873/427	495/242
-0.63/-0.25	636/311	446/218	693/339	204/197	742/363	407/199	659/342	536/262	836/409	484/237
-0.51/-0.20	626/306	413/202	679/332	395/193	711/348	407/199	642/314	609/298	711/348	560/274
-0.25/-0.10	599/293	419/205	646/316	397/194	711/348	407/199	595/291	636/311	617/302	658/322
+0.13/+0.05	562/275	415/203	621/304	427/209	681/333	464/227	589/288	636/311	613/300	660/323
+0.38/+0.15	544/266	417/204	556/272	460/225	630/308	562/275	589/288	636/311	613/300	660/323
+0.63/+0.25	517/253	421/206	540/264	491/240	585/286	562/275	589/288	636/311	613/300	660/323
+0.76/+0.30	501/245	437/214	529/259	503/246	572/280	581/284	589/288	636/311	613/300	660/323
+0.89/+0.35	487/238	454/222	507/248	505/247	558/273	595/291	589/288	636/311	613/300	660/323
+1.02/+0.40	476/233	470/230	505/247	521/255	550/269	605/296	589/288	636/311	613/300	660/323
+1.14/+0.45	464/227	487/238	503/246	558/273	550/269	605/296	589/288	636/311	613/300	660/323
+1.27/+0.50	452/221	452/221	503/246	558/273	550/269	605/296	589/288	636/311	613/300	660/323

MAXIMUM POWER									
-1.14/-0.45	2175/1064	2175/1064	1997/977	1997/977	1907/933	1907/933	1962/960	1962/960	2104/1029
-1.02/-0.40	532/260	419/205	777/380	675/330	767/375	409/200	440/215	440/215	817/400
-0.89/-0.35	464/227	368/180	513/251	319/156	613/300	286/140	695/340	695/340	817/400
-0.76/-0.30	452/221	331/162	495/242	292/143	558/273	280/137	593/290	593/290	817/400
-0.63/-0.25	446/218	317/155	484/237	282/138	542/265	280/137	572/280	572/280	817/400
-0.51/-0.20	437/214	288/141	476/233	276/135	529/244	294/144	548/273	548/273	817/400
-0.25/-0.10	417/204	290/142	452/221	278/136	474/232	323/158	487/238	487/238	817/400
+0.13/+0.05	393/192	290/142	435/203	298/146	440/215	358/175	448/219	448/219	817/400
+0.38/+0.15	388/190	292/143	415/203	319/156	409/200	390/191	413/202	413/202	817/400
+0.63/+0.25	362/177	290/142	388/190	343/168	409/200	390/191	413/202	413/202	817/400
+0.76/+0.30	352/172	294/144	378/185	352/172	398/195	405/198	411/201	411/201	817/400
+0.89/+0.35	339/166	305/149	370/181	354/173	388/190	415/203	411/201	411/201	817/400
+1.02/+0.40	333/163	319/156	360/176	366/179	382/187	421/206	411/201	411/201	817/400
+1.14/+0.45	323/158	333/163	352/172	390/191	382/187	421/206	411/201	411/201	817/400
+1.27/+0.50	317/155	348/170	352/172	390/191	382/187	421/206	411/201	411/201	817/400

CRUISE									
-1.14/-0.45	1521/744	1521/744	1355/663	1355/663	1265/619	1265/619	1275/624	1275/624	1365/668
-1.02/-0.40	399/195	204/100	429/210	245/120	511/250	1204/100	164/80	164/80	307/150
-0.89/-0.35	301/147	153/75	358/175	164/80	409/200	94/46	1275/624	1275/624	1365/668
-0.76/-0.30	282/138	153/75	307/150	119/58	317/155	117/57	429/210	429/210	511/250
-0.63/-0.25	270/132	153/75	280/137	131/64	292/143	129/63	362/177	362/177	380/186
-0.51/-0.20	262/128	155/76	266/130	133/65	266/130	141/69	294/144	294/144	333/163
-0.25/-0.10	241/118	151/74	247/121	137/67	245/121	155/76	247/121	247/121	311/152
+0.13/+0.05	213/104	155/76	229/112	149/73	227/111	176/86	227/111	227/111	258/126
+0.38/+0.15	209/102	155/76	221/108	164/80	210/103	196/96	206/101	206/101	235/115
+0.63/+0.25	196/96	153/75	206/101	174/85	210/103	206/101	206/101	206/101	227/111
+0.76/+0.30	190/93	157/77	198/97	164/80	209/102	213/104	206/101	206/101	227/111
+0.89/+0.35	184/90	164/80	192/94	186/91	198/97	217/106	206/101	206/101	227/111
+1.02/+0.40	178/87	174/85	184/90	196/96	194/95	217/106	206/101	206/101	227/111
+1.14/+0.45	174/85	182/89	180/88	202/99	194/95	217/106	206/101	206/101	227/111
+1.27/+0.50	170/83	188/92	180/88	202/99	194/95	217/106	206/101	206/101	227/111

TABLE 3-5. BLADE ADIABATIC WALL TEMPERATURES (°C/°F).

X (cm/in)	Radius = 2.963	MAXIMUM POWER			
		3.263	3.563	3.863	4.163
-1.14/-0.45	774/1425	774/1425 784/1443 784/1443			
-1.02/-0.40		772/1422 781/1437	791/1455	801/1474 801/1474	813/1495 802/1495
-0.89/-0.35			788/1450	799/1470	
-0.76/-0.30					
-0.63/-0.25					
-0.51/-0.20				799/1471	802/1475
-0.25/-0.10		771/1420			
+0.13/+0.05			781/1437 788/1450	791/1456	809/1488
+0.38/+0.15	767/1412	776/1428			802/1475
+0.63/+0.25					802/1475
+0.76/+0.30				791/1456 791/1456	802/1475
+0.89/+0.35					
+1.02/+0.40			782/1439 782/1439		
+1.14/+0.45					
+1.27/+0.50	768/1414	768/1414 777/1430 777/1430			
CRUISE					
-1.14/-0.45	741/1365	741/1365 746/1375 746/1375			
-1.02/-0.40	735/1355	740/1364 741/1369	756/1393	767/1413 767/1413	774/1426 774/1426
-0.89/-0.35				766/1411	
-0.76/-0.30					
-0.63/-0.25					
-0.51/-0.20					
-0.25/-0.10					
+0.13/+0.05			747/1376	758/1396	763/1406
+0.38/+0.15	733/1352				
+0.63/+0.25					
+0.76/+0.30		742/1367		758/1396 758/1396	763/1406 763/1406
+0.89/+0.35			748/1378 748/1378		
+1.02/+0.40					
+1.14/+0.45	734/1354	740/1354 739/1362 739/1362			
IDLE					
+1.27/+0.50	573/1063	590/1094 575/1067 587/1088			
-1.14/-0.45		575/1067	578/1072 586/1087		
-1.02/-0.40		572/1062	577/1071 586/1087	580/1076 580/1091	581/1080 593/1100
-0.89/-0.35					
-0.76/-0.30				576/1069	
-0.63/-0.25					
-0.51/-0.20					
-0.25/-0.10					
+0.13/+0.05					
+0.38/+0.15					
+0.63/+0.25					
+0.76/+0.30					
+0.89/+0.35					
+1.02/+0.40					
+1.14/+0.45					
+1.27/+0.50	570/1058	588/1090 572/1062 584/1083	574/1066 583/1081		
	SUCT. SURF.	PRESS SURF.	SUCT. SURF.	PRESS SURF.	SUCT. SURF.
					PRESS SURF.

R = 7.526 cm (2.963 in.) AT THE HUB
 X = 0.0 AT THE BLADE STACKING AXIS
 LINEAR INTERPOLATION WAS USED TO FILL IN THE TABLE.

TABLE 3-6. SECOND-STAGE DISK HEAT TRANSFER COEFFICIENTS.
J/Hr CM² °C/(BTU/Hr Ft² °F)

FORWARD FACE

R cm./in.	<u>MAXIMUM POWER</u>	<u>CRUISE</u>	<u>IDLE</u>
4.06/1.60	217/106.	143/70.	
4.19/1.65	237/116.	155/76.	90/44.
4.45/1.75	258/126.	170/83.	98/48.
4.70/1.85	272/133.	180/88.	104/51.
4.95/1.95	288/141.	192/94.	110/54.
5.21/2.05	301/147.	200/98.	114/56.
5.46/2.15	321/157.	215/105.	125/61.
5.72/2.25	358/175.	237/116.	137/67.
5.97/2.35	382/187.	253/124.	145/71.
6.22/2.45	395/193.	260/127.	149/73.
6.48/2.55	401/196.	266/130.	151/74.
6.73/2.65	407/199.	268/131.	153/75.
6.99/2.75	411/201.	270/132.	155/76.
7.24/2.85	415/203.	272/133.	155/76.
7.49/2.95	419/205.	274/134.	

AFT FACE

4.06/1.60	70/34.	51/25.	39/19.
4.19/1.65	92/45.	65/32.	43/21.
4.45/1.75	144/56.	80/39.	47/23.
4.70/1.85	131/64.	90/44.	49/24.
4.95/1.95	147/72.	100/49.	51/25.
5.21/2.05	164/80.	112/55.	55/27.
5.46/2.15	180/88.	123/60.	57/28.
5.72/2.25	196/96.	131/64.	61/30.
5.97/2.35	213/104.	143/70.	63/31.
6.22/2.45	231/113.	155/76.	67/33.
6.48/2.55	253/124.	172/84.	74/36.
6.73/2.65	284/139.	190/93.	80/39.
6.99/2.75	319/156.	217/106.	92/45.
7.24/2.85	386/189.	264/129.	139/68.
7.49/2.95	421/206.	311/152.	186/91.

TABLE 3-7. SECOND STAGE DISK ADIABATIC WALL TEMPERATURES (°F).

R	<u>MAXIMUM POWER</u>		<u>CRUISE</u>		<u>IDLE</u>	
	FWD	AFT	FWD	AFT	FWD	AFT
1.6	1013.	1265.	909.	1213.		783.
1.7	1015.		909.		626.	
1.8	1018.		909.		620.	
1.9	1021.		910.		616.	
2.0	1024.		911.		613.	
2.1	1026.		913.		610.	
2.2	1029.		916.		606.	
2.3	1033.		927.		604.	
2.4	1038.		935.		604.	
2.5	1044.		942.		606.	
2.6	1051.		951.		609.	
2.7	1060.		962.		613.	
2.8	1070		974.		619.	
2.9	1082.		974.		625.	

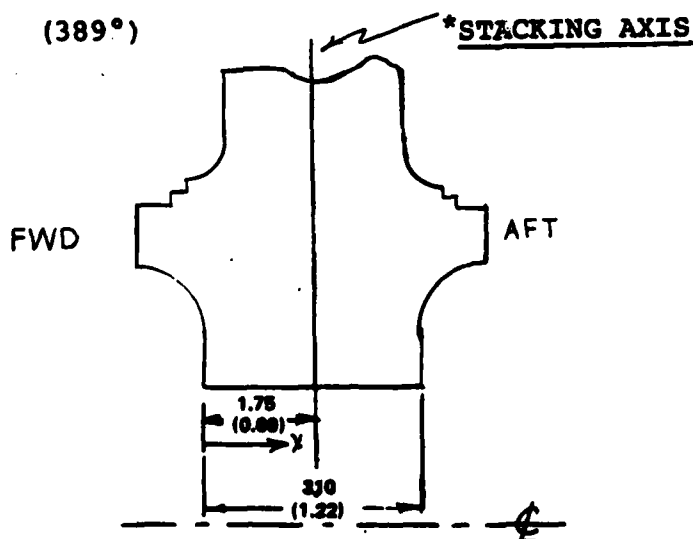
TABLE 3-8. SECOND STAGE DISK BORE HEAT TRANSFER
COEFFICIENTS J/HR, CM² °C (BTU/HR, FT² °F)

	<u>Maximum Power</u>		<u>Cruise</u>		<u>Idle</u>	
X						
0.1	253.5	(124.0)	179.9	(88.0)	101.4	(49.6)
0.2	122.9	(60.1)	87.3	(42.7)	49.1	(24.0)
0.3	80.1	(39.2)	56.8	(27.8)	32.1	(15.3)
0.5	46.8	(22.9)	33.3	(16.3)	18.9	(9.2)
0.7	32.8	(16.0)	23.3	(11.4)	13.1	(6.4)
1.0	22.5	(11.0)	15.9	(7.8)	9.0	(4.4)
1.2	18.6	(9.1)	13.3	(6.5)	7.4	(3.6)
1.4	15.7	(7.7)	11.2	(5.5)	6.3	(3.1)

X = 0.69 Corresponds to the Stacking Axis*

Gas Temperatures (°C (°F))

MP	372	(702°)
Cruise	326	(620°)
Idle	198	(389°)



21-3640 (22)
3-20

TABLE 3-9. HEAT TRANSFER COEFFICIENTS IN RIVET HOLE AND SLOT, $J/HR\text{ }cm^2\text{ }^{\circ}C/(BTU/HR\text{ }ft^2\text{ }^{\circ}F)$.

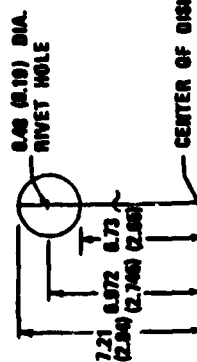
R	SLOT	X -.422	-.357	-.227	-.097	-.030	.030	.1035	.2505	.3850	.470
0.	0										
2.84	810/396.	810/396.	480/235.	405/198.	405/198.	405/198.	501/245.	501/245.	317/155.	243/119.	243/119.
2.745	691/338.	691/338.	409/200.	345/169.	345/169.	345/169.	437/214.	437/214.	276/135.	211/103.	211/103.
2.65	572/280.	572/280.	339/166.	286/140.	286/140.	286/140.	372/182.	372/182.	235/115.	180/88.	180/88.

MAXIMUM POWER

SLOT	0.	0.	660/323.	861/421.	861/421.	861/421.	850/413.	850/412.	921/451.	921/451.	921/451.
2.84	601/294.	601/294.	360/176.	290/142.	290/142.	290/142.	233/114.	233/114.	145/71.	119/58.	119/58.
2.745	515/252.	515/252.	309/151.	249/122.	249/122.	249/122.	213/104.	213/104.	108/64.	108/53.	108/53.
2.65	429/210.	429/210.	258/126.	209/102.	209/102.	209/102.	192/94.	192/94.	98/50.	98/48.	98/48.

CRUISE

SLOT	0.	0.	444/217.	609/298.	609/298.	609/298.	718/351.	718/351.	750/367.	750/367.	750/367.
2.84	286/140.	286/140.	182/89.	141/69.	141/69.	141/69.	164/80.	164/80.	96/47.	80/39.	80/39.
2.745	251/123.	251/123.	159/78.	123/60.	123/60.	123/60.	151/74.	151/74.	89/44.	74/36.	74/36.
2.65	217/106.	217/106.	139/68.	106/52.	106/52.	106/52.	139/68.	139/68.	82/40.	67/33.	67/33.

IDLE

MEASUREMENTS: CM (IN.)

GAS TEMPERATURE IN RIVET HOLE AND SLOT, $^{\circ}C\text{ }(^{\circ}F)$

	MAXIMUM POWER	CRUISE	IDLE
Forward	567 (1053)	512 (954.)	324 (615.)
Aft	768 (1415.)	735 (1355.)	579 (1075.)

TABLE 3-10. HEAT TRANSFER COEFFICIENT RATIOS.

COLD START

TIME (SEC)	PLATFORM & BLADES	SLOT FWD	SLOT AFT	RIVET HOLES		DISK FACE		BORE
				FWD	AFT	FWD	AFT	
0	0	0	0	0	0	0	0	0
3.2	.0056	.197	.210	.019	.032	.012	.005	.009
6.4	.026	.287	.315	.061	.089	.045	.026	.034
12.8	.049	.334	.420	.096	.134	.075	.044	.057
16.0	.064	.358	.498	.115	.160	.093	.054	.072
19.2	.081	.381	.551	.137	.186	.112	.066	.087
22.4	.099	.404	.584	.159	.213	.133	.081	.104
25.6	.13	.443	.612	.200	.259	.172	.113	.137
28.8	.16	.467	.643	.227	.289	.198	.133	.160
32.0	.25	.547	.760	.326	.396	.295	.212	.248
35.2	.35	.625	.758	.429	.492	.399	.324	.347
38.4	.33	.625	.665	.429	.483	.399	.349	.347

TABLE 3-11. HEAT TRANSFER COEFFICIENT RATIOS.

HOT START

0	0	.124	0	.004	0	0	0	.001
2.7	.000	.207	.209	.022	.036	.014	.006	.010
5.3	.021	.270	.320	.051	.077	.037	.019	.028
10.6	.055	.342	.482	.111	.144	.081	.045	.062
13.	.070	.365	.526	.122	.170	.099	.057	.077
16.	.093	.396	.575	.151	.204	.126	.076	.099
19.	.11	.419	.599	.175	.232	.148	.093	.117
21.	.14	.451	.631	.209	.269	.180	.119	.145
24.	.18	.490	.707	.255	.321	.225	.151	.184
27.	.35	.616	.848	.417	.490	.387	.291	.335
29.	.46	.706	.759	.545	.595	.518	.460	.465
32.	.35	.642	.666	.454	.505	.424	.380	.371

TABLE 3-12 . TRANSIENT HEAT TRANSFER COEFFICIENT GROUND IDLE TO MAXIMUM POWER ACCELERATION.

TIME (SEC)	PLATFORM & BLADES	SLOT FWD	SLOT AFT	RIVET HOLES		DISK FACE		BORE
				FWD	AFT	FWD	AFT	
0.	.367	.651	.666	.466	.552	.402	.396	.384
1.	.477	.715	.795	.558	.642	.501	.471	.479
2.	.641	.811	.878	.703	.816	.661	.632	.639
3.	.771	.840	.932	.812	.856	.785	.761	.765
3.5	.926	.849	.859	.922	.883	.939	.948	.933
6.	.927	.951	.795	.963	1.935	.980	1.09	.977
8.	.998	1.050	.954	1.012	1.027	1.02	1.07	1.022
10.5	1.017	1.050	1.021	1.012	1.036	1.02	1.03	1.022
14.	1.026	1.050	1.052	1.012	1.055	1.02	1.02	1.022

TABLE 3-13. TRANSIENT TEMPERATURE RATIOS (°F/°F).

<u>COLD START</u>			<u>HOT START</u>			<u>GROUND IDLE TO MAXIMUM POWER ACCELERATION</u>		
TIME (SEC)	T _{cd} RATIO	T _{t4} RATIO	TIME (SEC)	T _{cd} RATIO	T _{t4} RATIO	TIME (SEC)	T _{cd} RATIO	T _{t4} RATIO
0.	.147	.324	0.	.150	.494	0.	.559	.697
3.2	.165	.560	2.7	.170	.520	1.0	.637	.888
6.4	.205	.611	5.3	.195	.674	3.0	.848	.979
12.8	.235	.762	10.6	.240	.899	3.5	.957	.939
16.0	.250	.897	13.3	.260	.944	6.0	.986	.697
19.2	.270	.964	16.0	.285	.980	8.0	1.014	.854
22.4	.290	.981	18.6	.305	.980	10.5	1.014	.967
25.6	.325	.956	21.3	.335	.980	14.0	1.014	1.024
28.8	.350	.973	23.9	.380	1.061			
32.0	.440	1.065	26.6	.520	1.120			
35.2	.530	.947	29.3	.565	.862			
38.4	.530	.788	31.9	.550	.773			

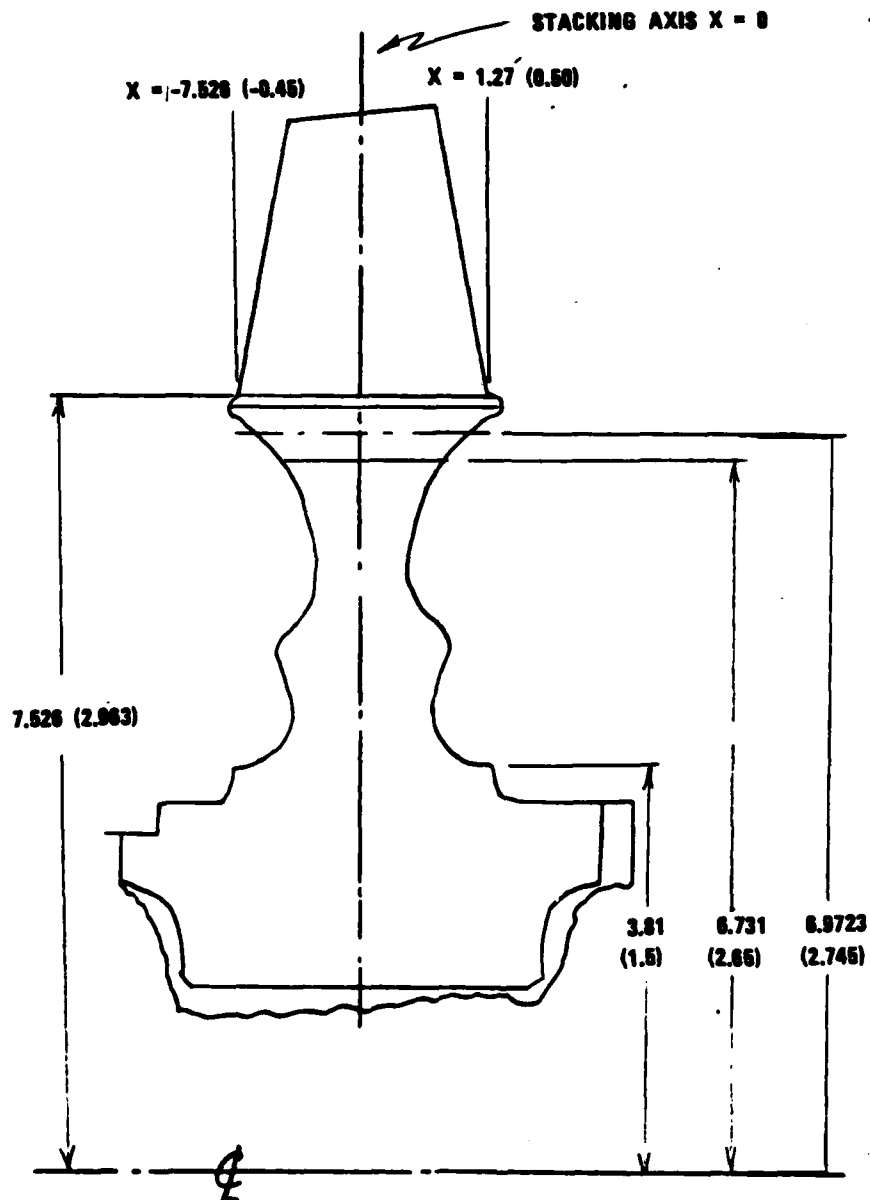
3.4.2 Steady State Boundary Condition Analysis

Heat-transfer coefficients and gas temperatures on the blades were calculated using a Garrett computer program. The program input consists of velocity distributions along the blade at several radial stations, as well as upstream pressure and temperature. The program calculates leading edge heat-transfer coefficients using a correlation for a cylinder in a cross flow. The remainder of the blade is treated as a flat plate in turbulent flow. Heat-transfer coefficients and gas temperatures on the platform were calculated by linearly interpolating the values at the hub from suction surface to pressure surface on adjacent blades. Since the adiabatic wall temperature on the platform showed so little variation, a constant value was used at each power setting in the thermal analysis. These values are given in Table 3-4. The platform heat-transfer coefficients and the blade heat-transfer coefficients and adiabatic wall temperatures are shown in Tables 3-3, 3-4, and 3-5 respectively. Figure 3-5 shows the wheel geometry.

The heat-transfer coefficients and gas temperatures on the disk faces were calculated using a program whose input consisted of disk geometry, wheel speed, estimated metal temperatures, and the pressure and temperatures of the gas where it first contacts the disk. Heat-transfer coefficients and adiabatic wall temperatures adjacent to the disk are given in Tables 3-6 and 3-7, respectively.

Heat-transfer coefficients in the disk bore were calculated by treating the bore as an annular tube. The flow rate through the bore was determined in the secondary flow analysis. The gas temperature in the bore was the compressor discharge temperature. The heat-transfer coefficients and gas temperatures are listed in Table 3-8.

The flow distribution in the region of the rim-rivet hole and slot was much more difficult to analyze than any other area on the wheel. This is due, in part, to the fact that pressures are known far away



DIMENSIONS IN CM (IN.)

Figure 3-5. Blade and Disk Geometry.

from the region (in the cavity adjacent to the disk and in the main gas flow path) but variations inside the rivet hole are unknown. The following procedure was used to estimate the flow distribution. Please refer to Figure 3-6 for a schematic diagram.

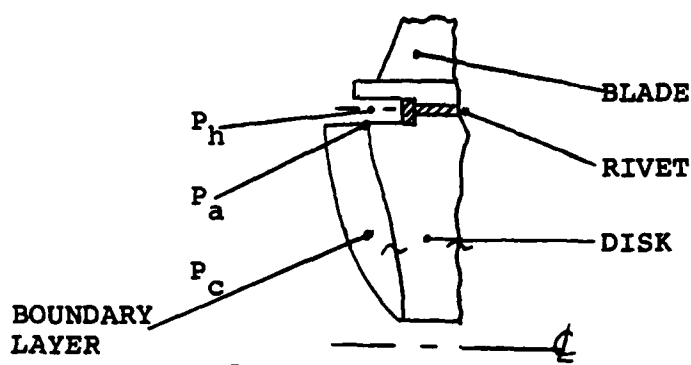


Figure 3-6. Schematic Diagram of Disk.

The pressure, P_c , in the cavity adjacent to the disk is known as a function of radius from the program DSKFLO. Since the boundary layer cannot support a pressure gradient normal to the wheel, P_c is approximately equal to P_a . The rivet hole is small enough that the pressure should not vary substantially across it. For this reason, the pressure, P_h , in the rivet hole was assumed to be the same as the cavity pressure, P_c , evaluated at the centerline of the rivet hole. The static pressure in the gas path at the blade hub is known as a function of axial position. The flow rate across the slot was calculated using the pressure ratio and treating the slot as an orifice. Heat-transfer

coefficients were calculated using Figure 6-24 of Reference 1. The mass flow rate through the rivet hole is the same as the mass flow rate in the slot. The rivet hole was treated as a tube with known through flow to calculate the heat-transfer coefficients. The values calculated in this manner assume a stationary tube. The augmentation of the heat-transfer coefficient due to rotation was accounted for using Reference 2. In the forward-rivet hole, the augmentation varied from approximately 225 percent at idle to 320 percent at maximum power. In the aft-rivet hole, the corresponding values were 150 percent and 245 percent. The gas temperatures in the rim-rivet hole and slots on the forward face of the disk were the adiabatic wall temperatures predicted earlier at the corresponding radius. The secondary flow analysis showed that air from the main gas flow path was ingested on the aft side of the disk so the gas temperature at the blade hub was used for the aft slot and rivet hole. Engine tests conducted in January and February of 1981 showed the original temperature predictions to be somewhat low. The final predictions were corrected to reflect the results of these tests. Heat-transfer coefficients and gas temperatures in the rivet hole and slot are shown in Table 3-9.

3.4.3 Transient Boundary Condition Scaling

The transient boundary was scaled from the steady-state values as described below. The basic heat-transfer coefficient correlation was used to express the ratio of the value at some time varying state 1 to a normalizing state 0. In this analysis, subscript 0 represents maximum power conditions. For example, on the blades away from the leading edge, the ratio of Nusselt numbers can be expressed as:

¹Kays, William, and London, A.L.; Compact Heat Exchangers, p 119; 2nd Edition.

²Metzger, D.E.; SA-8610-MR, March 27, 1972, "Literature Summary and Design Recommendations -- Friction and Heat-Transfer in Rotating Passages",

$$\frac{Nu_1}{Nu_0} = \frac{C Re_1^{.8} Pr_1^{.6}}{C Re_1^{.8} Pr_1^{.6}} \quad (1)$$

Fluid properties can be expressed as a function of absolute temperature as follows:

$$\begin{aligned} \text{Conductivity: } K &\propto T \\ \text{Viscosity: } \mu &\propto T^{.75} \\ \text{Density: } \rho &\propto P/T \end{aligned}$$

For the temperature range of interest, the Prandtl number can be considered to be a constant. The Reynolds number can be written

$$Re = \frac{\dot{m} L_C}{\mu A}$$

where \dot{m} is mass flow rate
 L_C is a characteristic length and is constant for a given geometry.
 A is a flow area which is constant for a given geometry.

Substituting this information in eq. (1) and solving for the ratio of heat transfer coefficient yields:

$$\left(\frac{h_1}{h_0} \right) = \left(\frac{\dot{m}_1}{\dot{m}_0} \right)^{.8} \left(\frac{T_1}{T_0} \right)^{.4} \quad (2)$$

Reference 5 shows that the flow rate is proportional to engine speed raised to a power. If the mass flow rate and speed are known at two different conditions, the exponent can be calculated from:

⁵Hale, Pat, 22-0101, March 24, 1977, "Transient Variation of Boundary Conditions in Thermal Analyses".

$$\frac{\dot{m}_a}{\dot{m}_b} = \left(\frac{N_a}{N_b} \right)^c \quad (3)$$

If "a" represents conditions at ground idle and "b" represents conditions at maximum power, the exponent, c , for this engine is approximated as 2.2 between these conditions only. The ratio of heat-transfer coefficients becomes:

$$\frac{h_1}{h_o} = \left(\frac{N_1}{N_o} \right)^{2.2} \left(\frac{T_1}{T_o} \right)^{.4} \quad (4)$$

This same procedure was followed at other positions on the wheel to obtain the expressions given in Appendix C. For those correlations which were presented in graphical form in the original reference, curve fits were developed so that the scaling could be done. Note that the temperature used for the scaling should be the compressor discharge temperature for the bore, the forward slot and rivet hole, and the forward face of the disk. The interstage turbine temperature (ITT) should be used for the platform, blades, aft rivet hole and slot, and the aft face of the disk.

In order to complete the scaling process, some information about engine operation is required. Engine speed and temperature were recorded as a function of time for several engine starts. This data was normalized by setting the maximum value of ITT equal to one and setting the time required to reach maximum temperature equal to one. Normalized curves were plotted and then divided into two groups, cold starts and hot starts. A cold start occurs when the engine metal temperatures are approximately the same as ambient air prior to the start. A hot start occurs when the engine metal temperatures are greater than ambient prior to the start. Definite trends could be observed from the normalized plots. The cold starts exhibit a gradual increase in ITT with a short plateau immediately preceeding a hot spike. The hot starts reach the plateau temperature sooner and have a longer plateau prior to the spike than the cold starts. After

comparing the data from several starts, the average hot- and cold-start cycles shown in Figure 3-7 and 3-8 were developed.

All engine data that was received was scaled and the resulting ratios of transient heat-transfer coefficients and gas temperatures divided by the corresponding values at maximum power are summarized in Tables 3-10 and 3-13.

3.4.4 Transient Thermal Results

The boundary conditions described previously were applied to a thermal model and the temperatures were calculated for the key transient conditions. These temperatures were used to predict transient thermal stresses later. The temperatures are shown in Figures 3-8a through 3-8g.

3.5 Stress Analysis

The stress analysis of the turbine wheel was accomplished using Garrett Program ISO3DQ. This is an isoparametric finite element, three-dimensional stress analysis program developed under a contract from the Air Force Propulsion Laboratory (Contract No. F33615-75-C-2012).

The three-dimensional, finite-element model of the turbine rotor is shown in Figures 3-9, 3-10, and 3-11. As may be seen in the model plots, the blade appears to overhang - hang over the edge of the platform. This is done to aid in the modeling and allow the blade to be input as a single unit. The stress program allows the blade to be tied to and restrained by the platform on the other side of the slot. The model is a wedge taken out of the wheel that is equal to 1/40th of a wheel with symmetrical boundary conditions on the side of the wedge. This is an acceptable mathematical representative of the actual wheel due to the symmetry of the thermal profile.

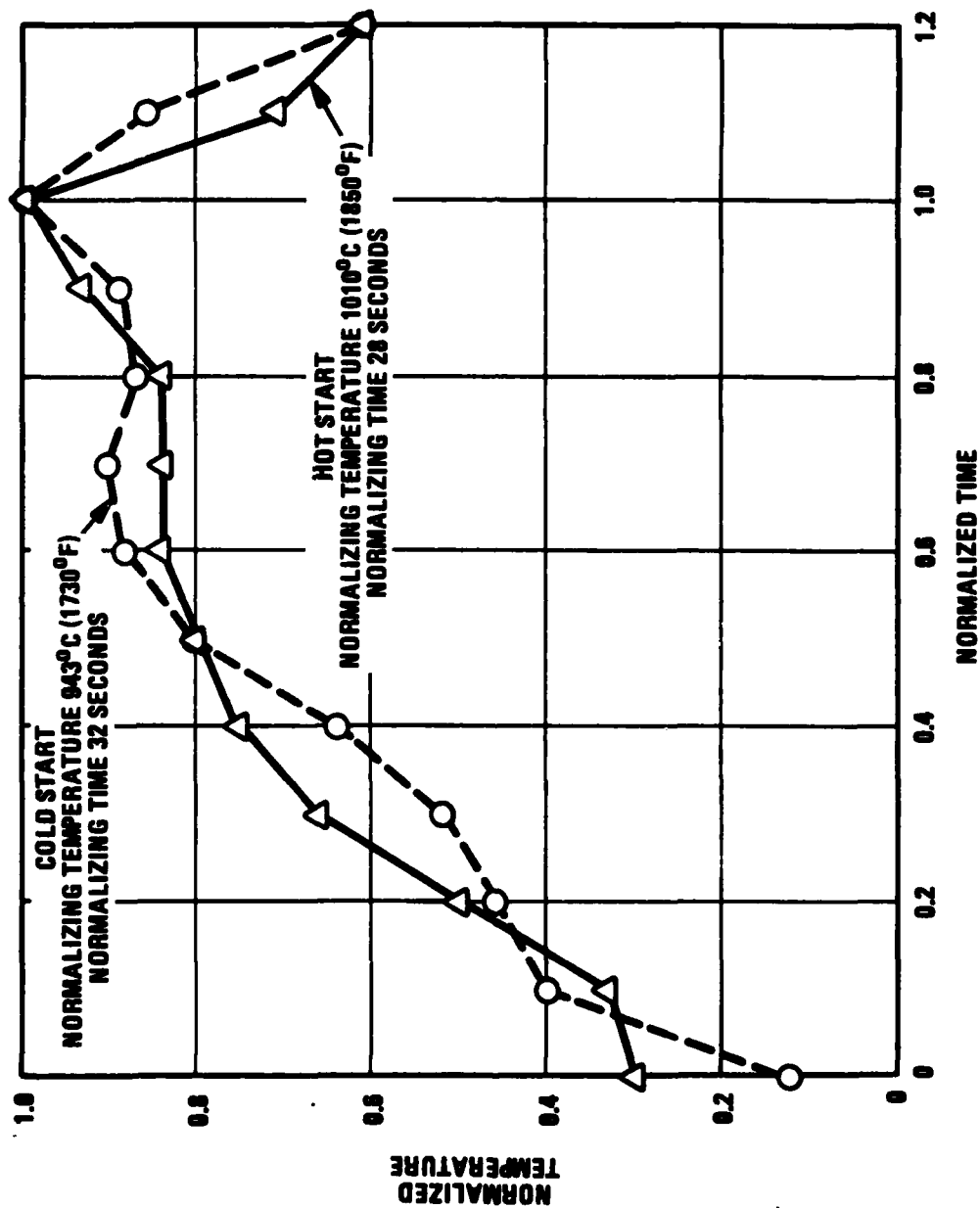


Figure 3-7. Normalized Temperature Versus Normalized Time for Hot and Cold Starts.

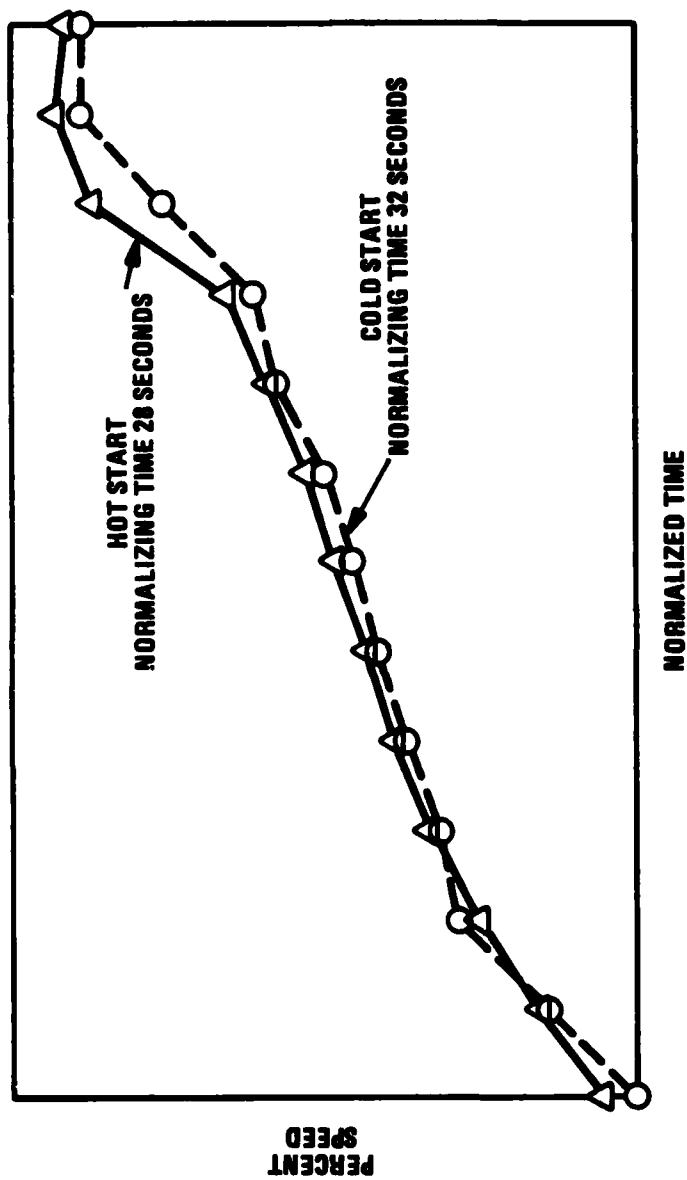


Figure 3-8. Percent Speed Versus Normalized Time for Hot and Cold Starts.

DISK TEMPERATURES DURING LIGHT-OFF COLD START / NORMAL SPIKE

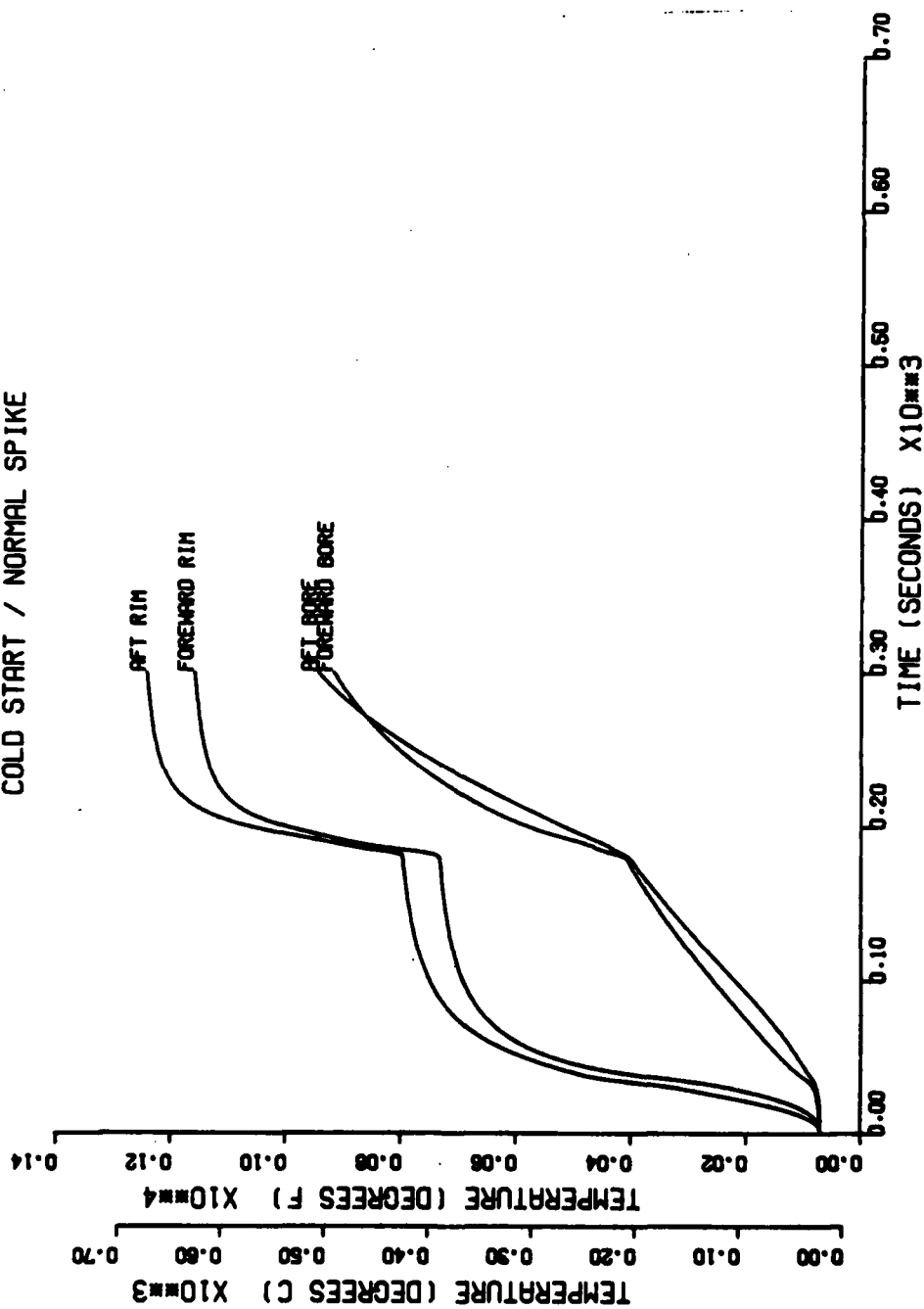


Figure 3-8a. Disk Temperatures During Light-Off Cold Start/Normal Spike.

DISK TEMPERATURES DURING LIGHT-OFF
COLD START / HOT SPIKE

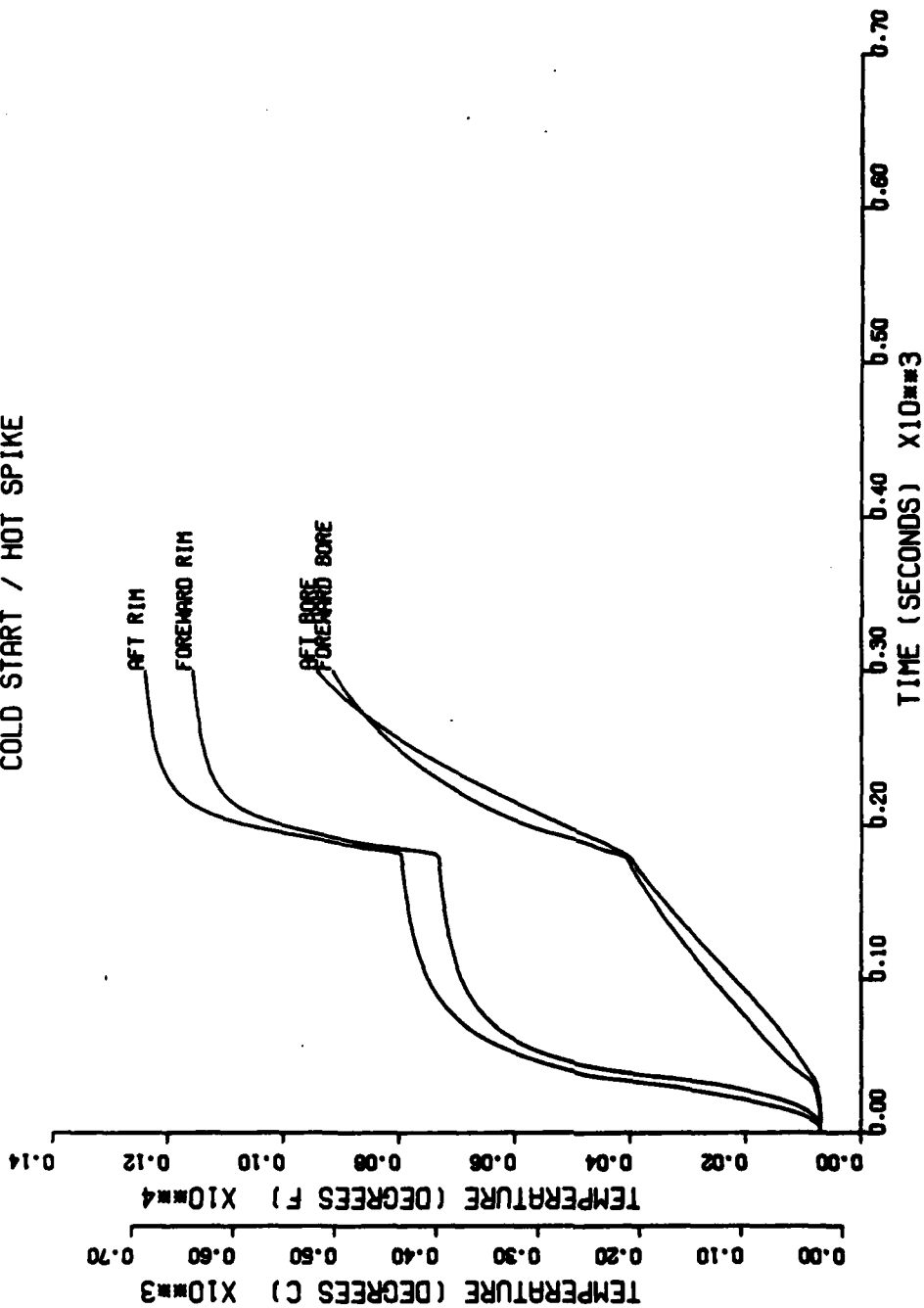


Figure 3-8b. Disk Temperatures During Light-Off Cold Start/Hot Spike.

DISK TEMPERATURES DURING LIGHT-OFF
WARM START / NORMAL SPIKE

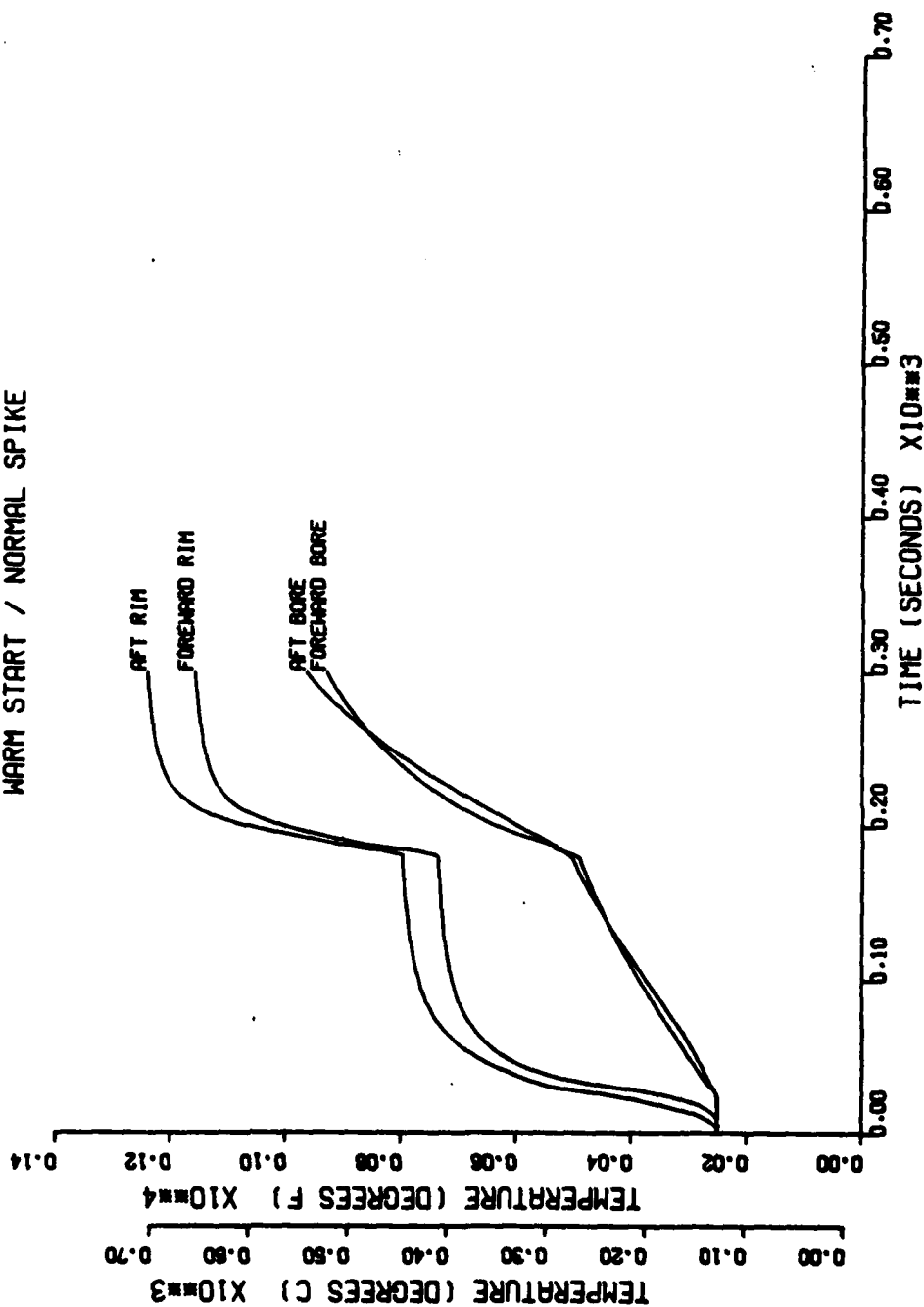


Figure 3-8c. Disk Temperatures During Light-Off Warm Start/Normal Spike.

DISK TEMPERATURES TAKE-OFF AT 180 SECONDS TO LANDING
COLD START / NORMAL SPIKE

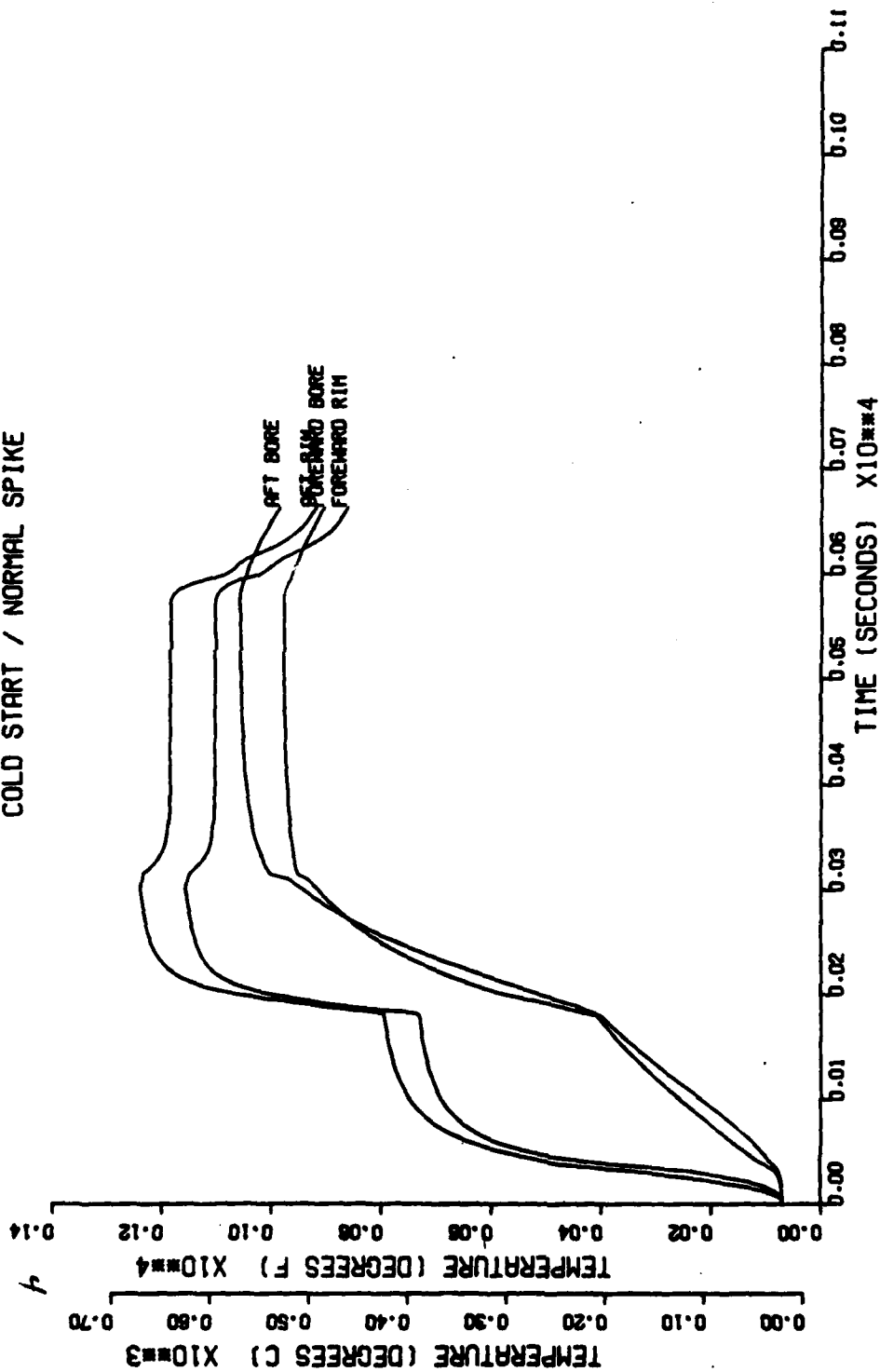


Figure 3-8d. Disk Temperatures Take-Off at 180 Seconds to Landing Cold Start/Normal Spike.

DISK TEMPERATURES TAKE-OFF AT 500 SECONDS TO LANDING
WARM START / NORMAL SPIKE

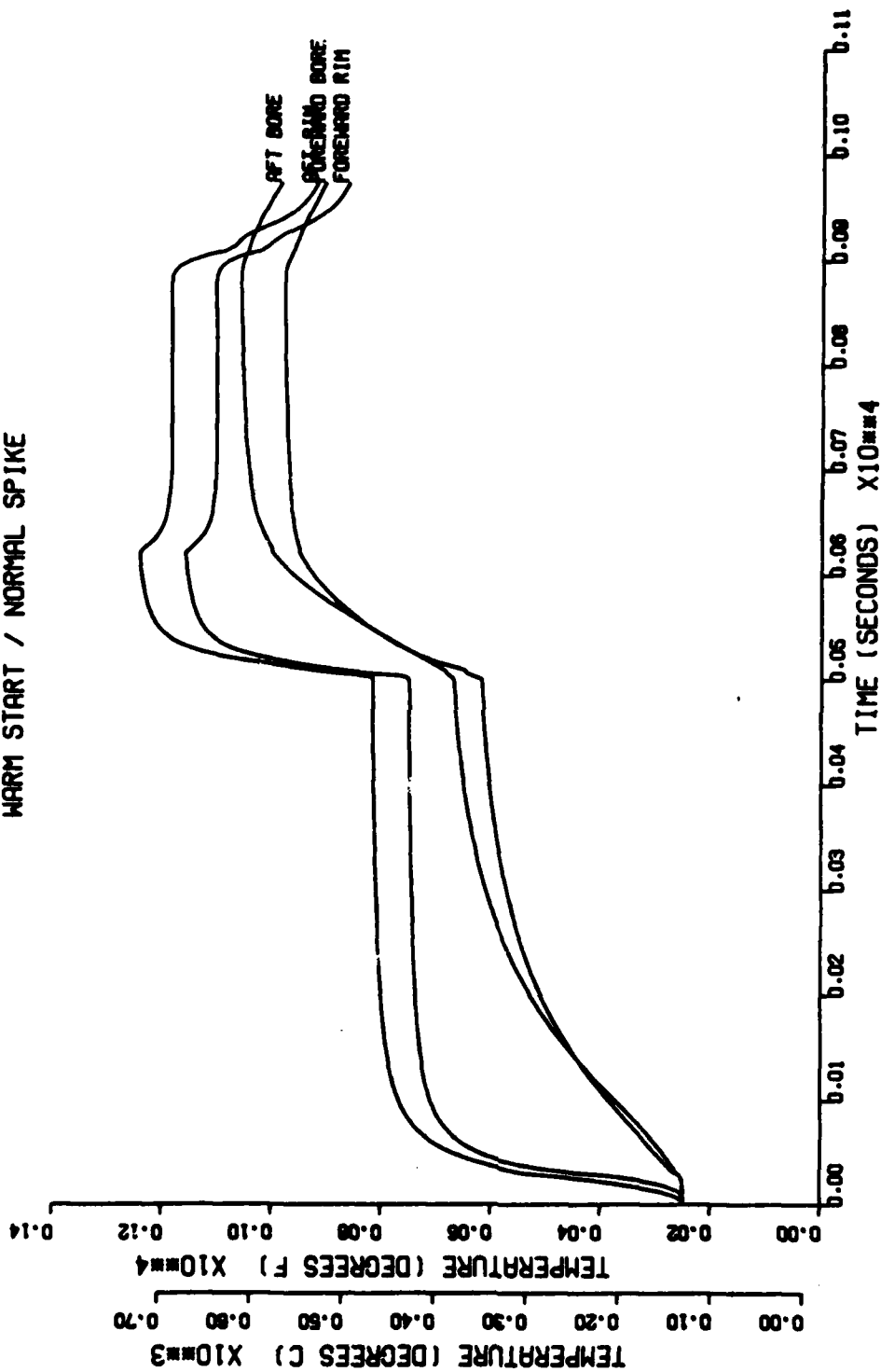


Figure 3-8e. Disk Temperatures Take-Off at 500 Seconds to Landing Cold Start/Normal Spike.

DISK TEMPERATURES TAKE-OFF AT 180 SECONDS TO LANDING WARM START / NORMAL SPIKE

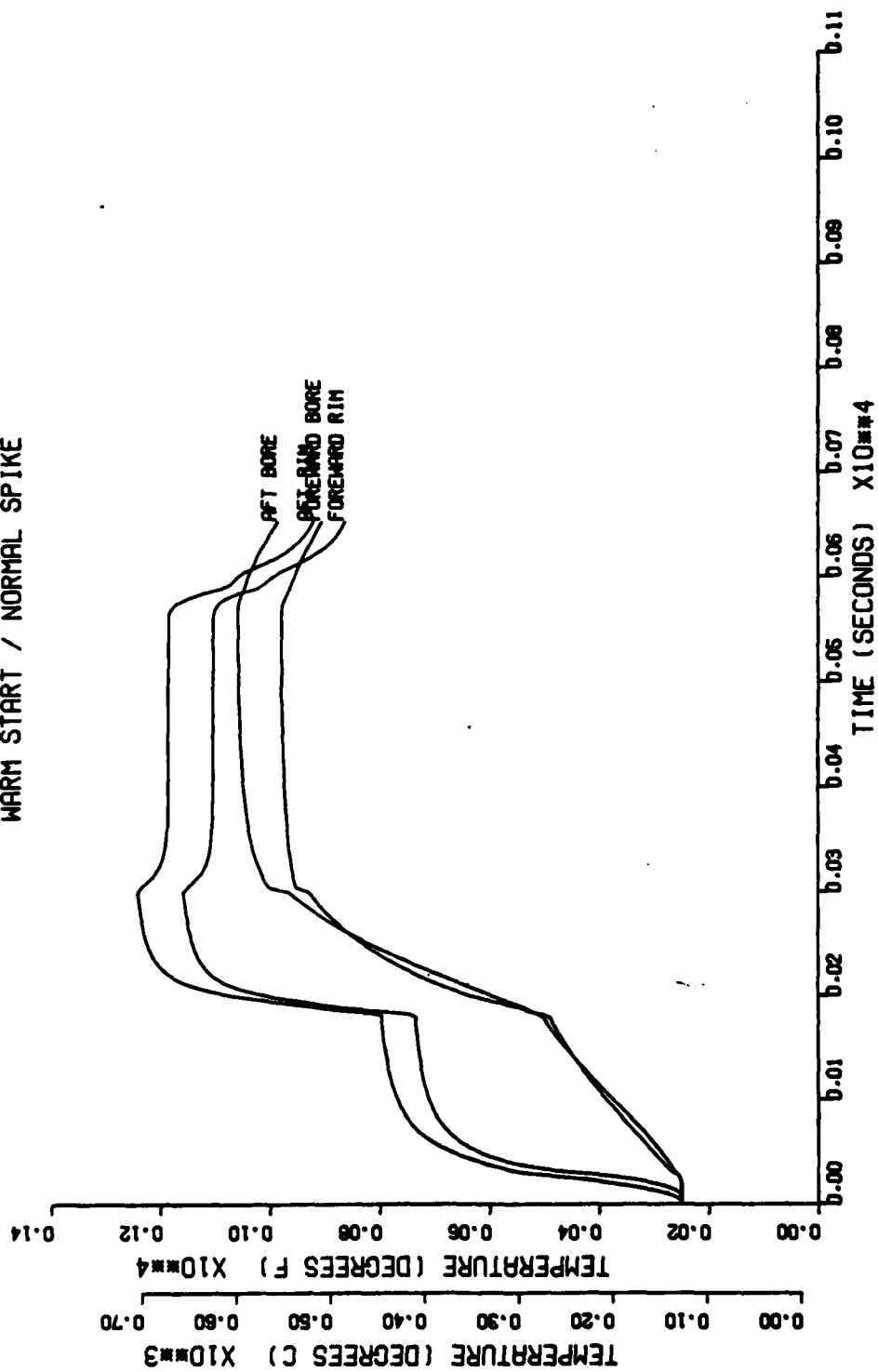


Figure 3-8f. Disk Temperatures Take-Off at 180 Seconds to Landing Warm Start/Normal Spike.

DISK TEMPERATURES TAKE-OFF AT 500 SECONDS TO LANDING COLD START / NORMAL SPIKE

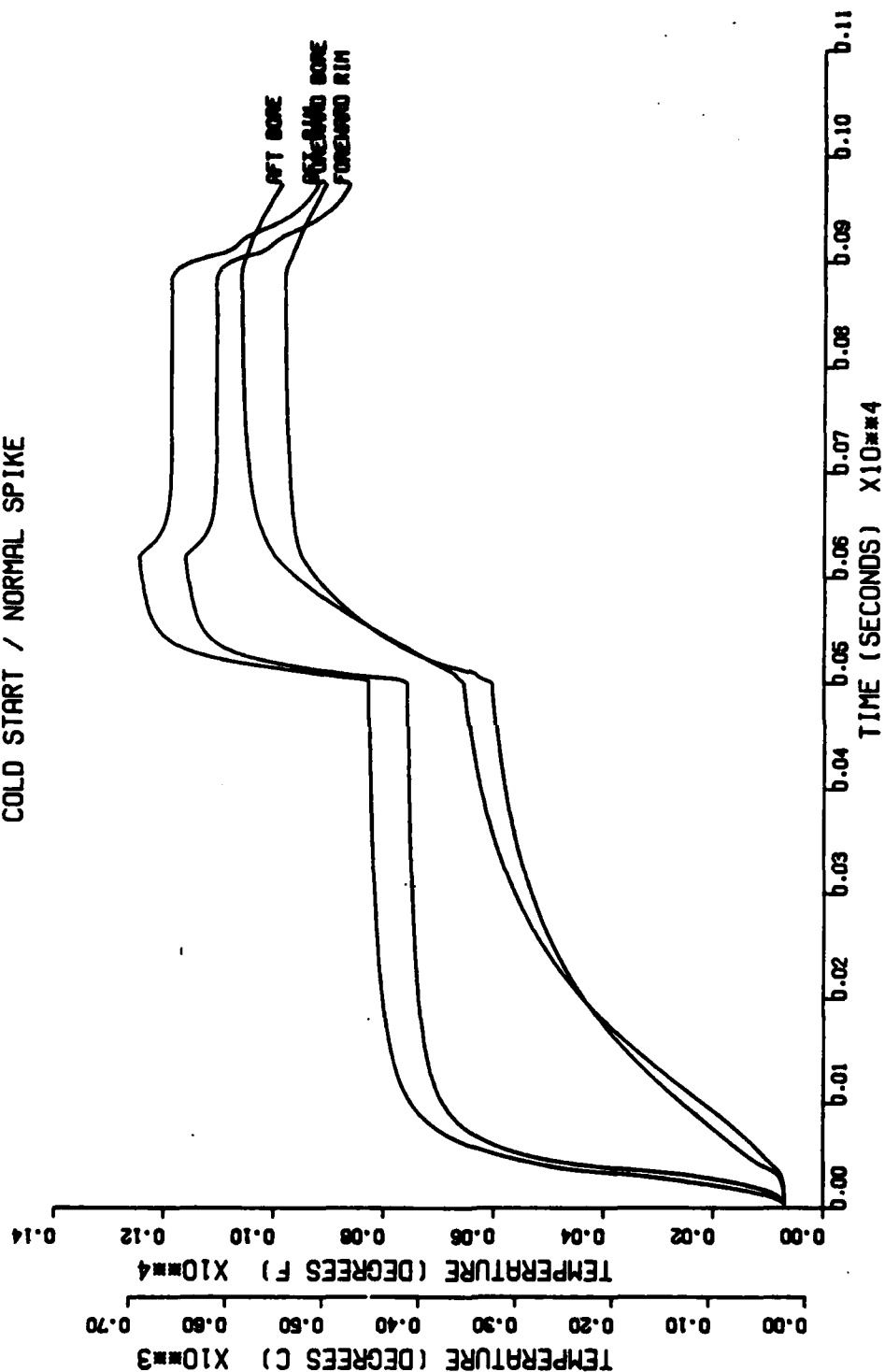


Figure 3-8g. Disk Temperatures Take-Off at 500 Seconds to Landing Warm Start/Normal Spike.

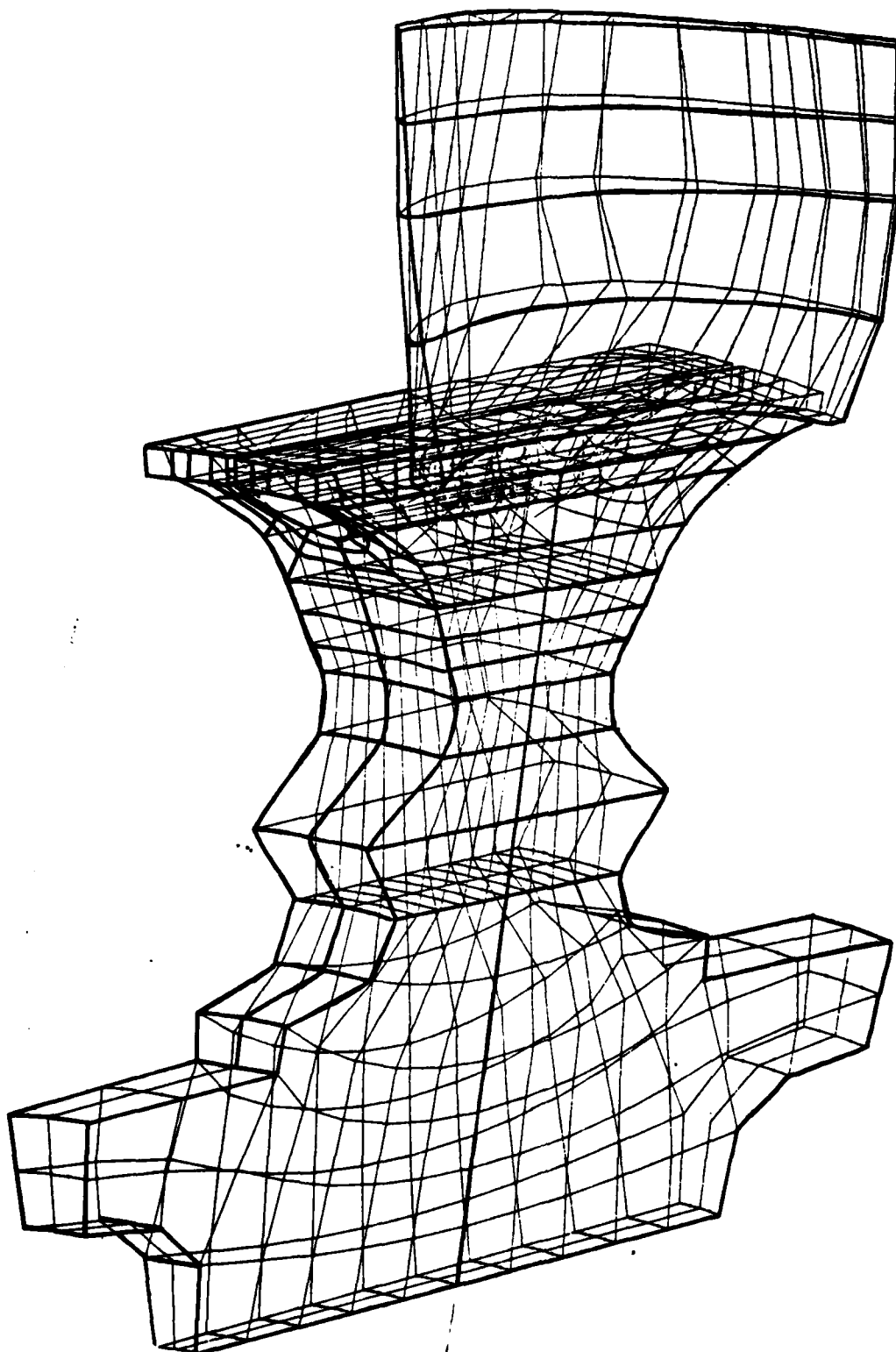


Figure 3-9. Isometric View of Stress Model.

21-3640(22)
3-40

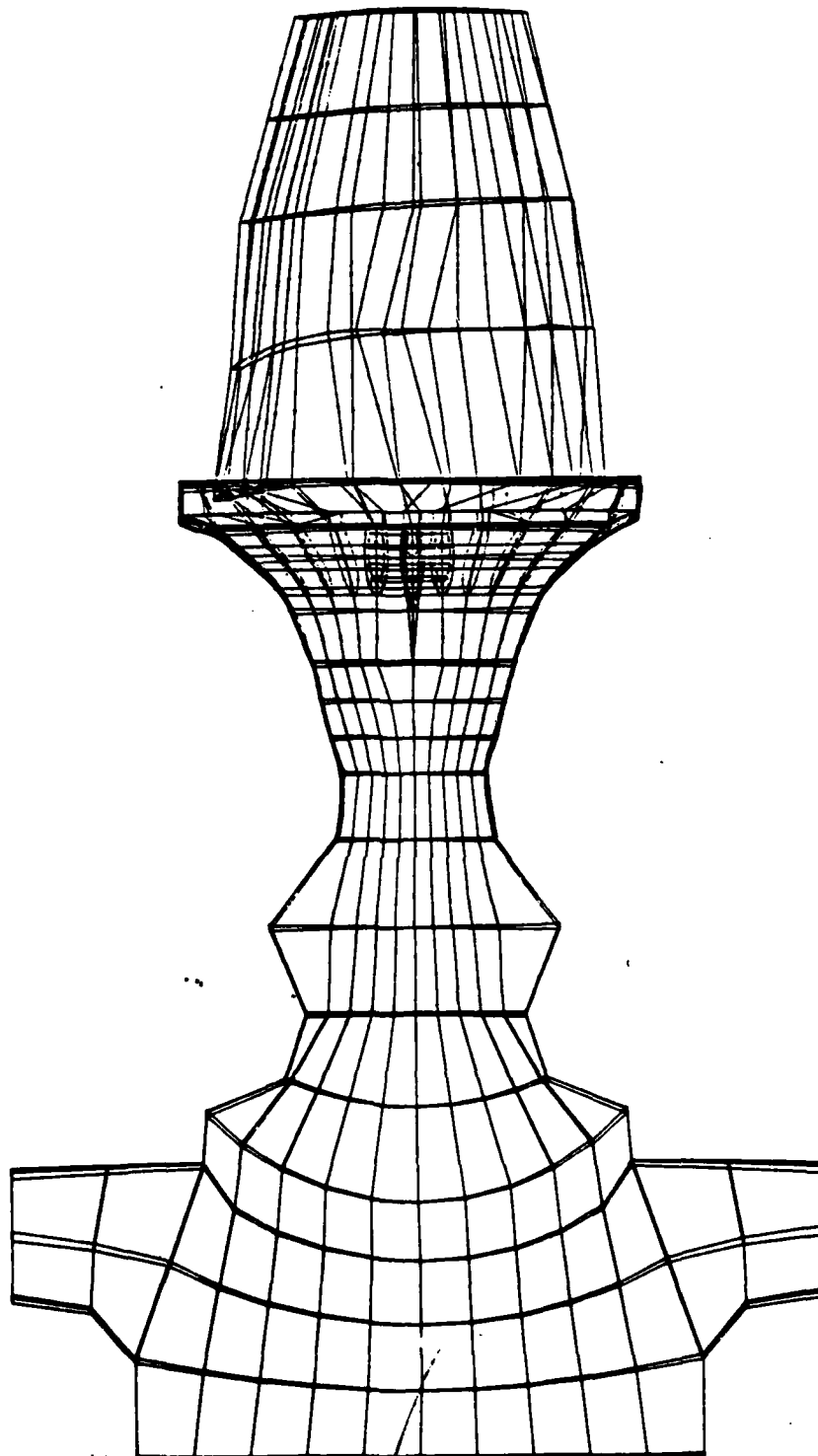


Figure 3-10. Meridional View of Stress Model.

21-3640(22)

3-41

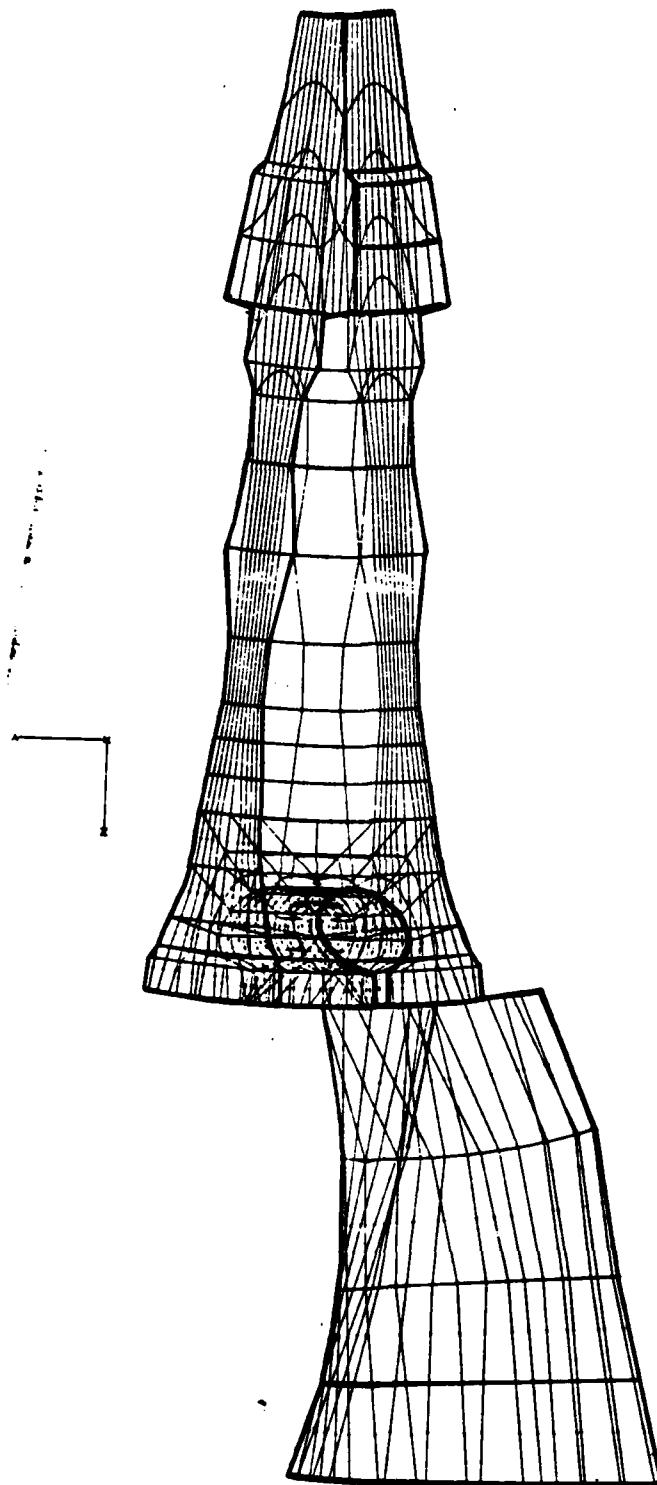


Figure 3-11. Axial View of Stress Model.

21-3640(22)

3-42

The first step in the stress analysis was to apply rotational loads to the model at room temperature and save the deflections and stresses. Then the thermal analyses were done at various key times in the transient cycle. These stresses were also saved and added to the mechanical stresses due to rotation. The key stress analyses presented were reduced to those times that had the highest compressive and tensile stresses and are summarized below:

- o Start with cold engine, 21°C (70°F)
- o Start with warm engine, 121°C (250°F)
- o Take-off power with cold start at 180 seconds
- o Take-off power with warm start at 180 seconds
- o Take-off power with cold start at 500 seconds
- o Take-off power with warm start at 500 seconds
- o Landing

The peak stresses for each of the above conditions are summarized in Table 3-14.

The isopleths for each of these cases are shown in Figures 3-12 through 3-21.

The results of these transient analyses are then used to predict the crack initiation and propagation for a typical commuter aircraft.

3.6 Material Mechanical Properties

3.6.1 LC Procedure for Material Properties

The specimens were taken from production wheels, P/N 868272-1, which represent several master heats and casting lots. Howmet (Austenal LaPorte), ships to Garrett a half wheel with each lot of castings. A group of these half-wheels were obtained for this program. Table 3-15 is a listing of the half-wheels used with their master heat numbers and casting dates.



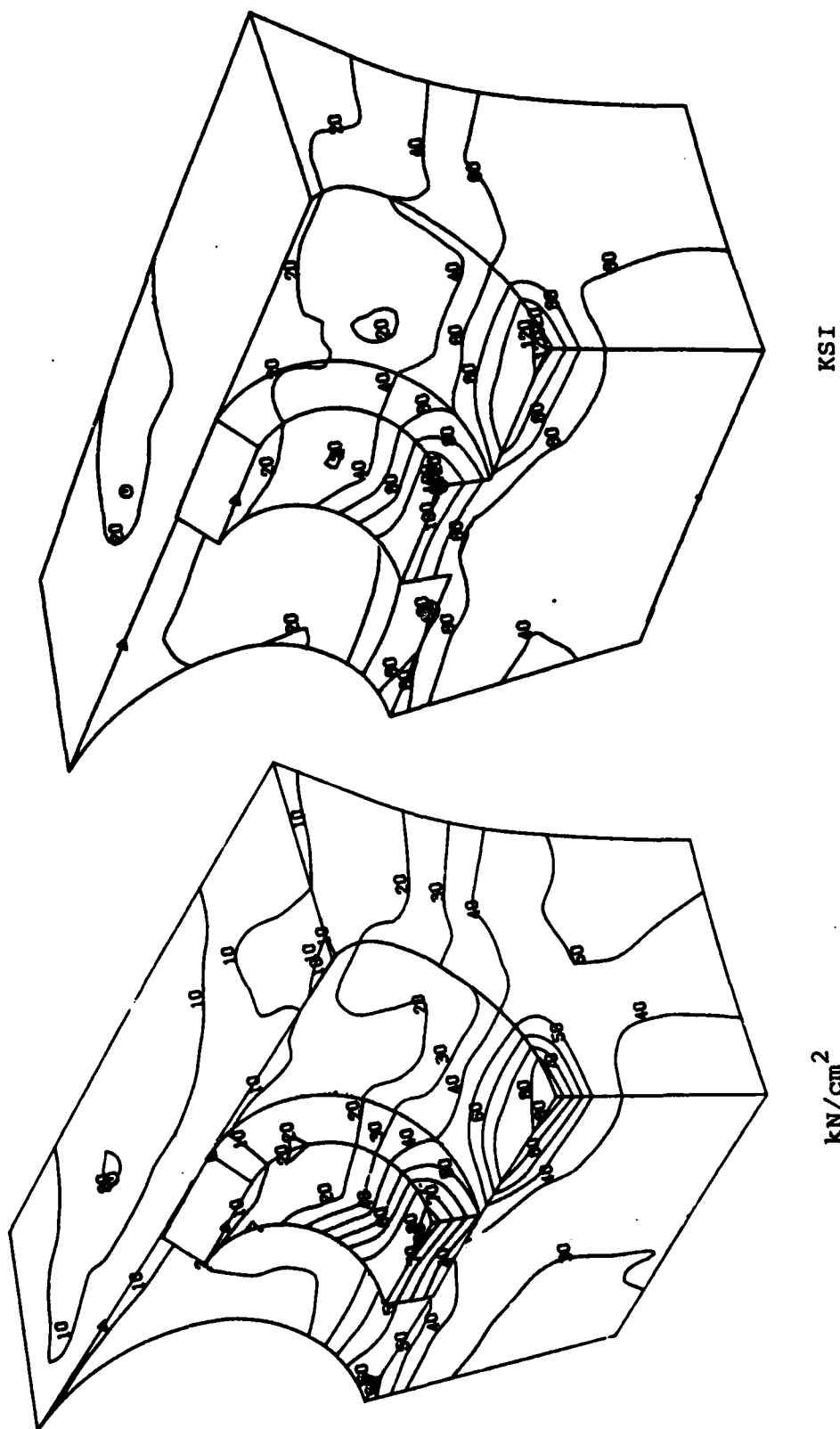
GARRETT TURBINE ENGINE COMPANY
A DIVISION OF THE GARRETT CORPORATION
PHOENIX, ARIZONA

TABLE 3-14. TRANSIENT STRESS ANALYSIS PEAK STRESSES.
(TOP NUMBER IN EACH CASE IS Pa. BOTTOM
NUMBER IS PSI)

Isopleth Figure	Case	Thermal Stress, Psi			Rotational Stress, Psi			Equiv- alent Stress* σ_e , Psi
		σ_{p1}	σ_{p2}	σ_{p3}	σ_{p1}	σ_{p2}	σ_{p3}	
1, 2	a.	-9,239	-134,466	-26,200	33,233	1338	5585	87,839
		-13,400	-195,027	-38,000	48,200	1940	8100	127,400
3, 4	b.	-7,977	-105,766	-21,235	33,302	1338	5585	62,072
		-11,570	-153,400	-30,800	48,300	1940	8100	90,028
5, 6	c.	-8,984	-146,720	-27,268	79,634	3199	13,376	58,659
		-13,030	-212,800	-39,550	115,500	4640	19,400	85,078
N/A	d.	-10,310	-137,081	-27,165	79,630	3199	13,376	48,434
		-14,953	-198,820	-39,400	115,500	4640	19,400	70,247
7, 8	e.	-10,396	-122,692	-25,331	79,630	3199	13,376	35,110
		-15,078	-177,950	-36,740	115,500	4640	19,400	50,924
N/A	f.	-11,004	-120,934	-25,635	79,634	3199	1338	32,957
		-15,960	-175,400	-37,180	115,500	4640	1940	47,800
9, 10	g.	117	-10,514	-1351	81,702	3378	13,790	63,858
		170	-15,250	-1960	118,500	4900	20,000	92,618

*Equivalent stress (Hincky-VonMises),

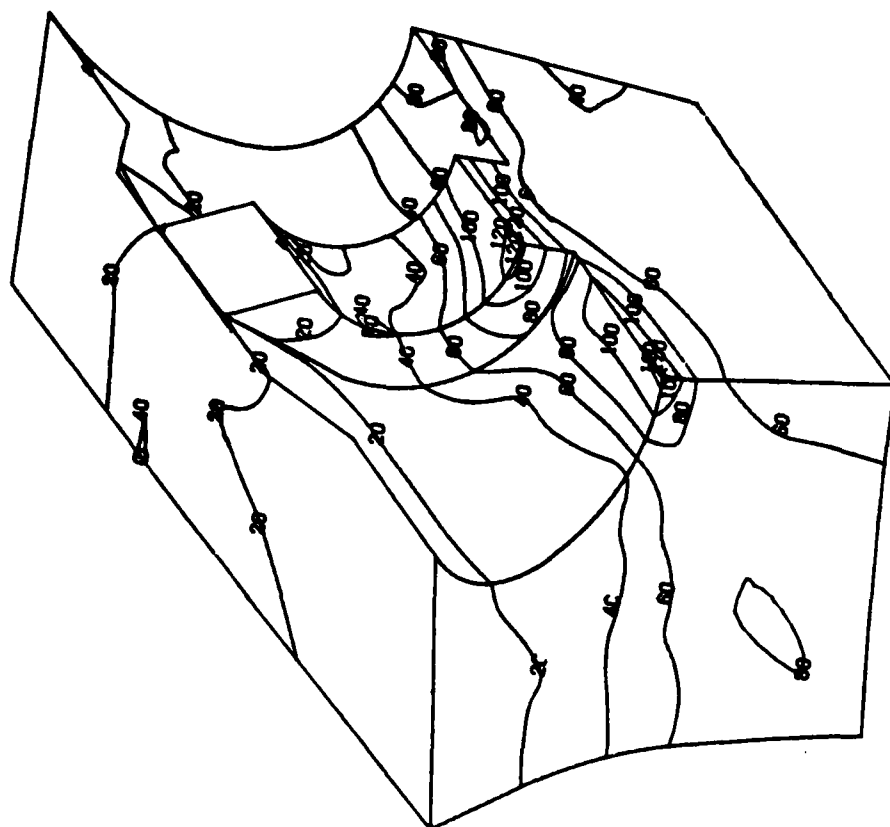
$$\sigma_e = \sqrt{(\sigma_{p1} - \sigma_{p3})^2 + (\sigma_{p2} - \sigma_{p3})^2 + (\sigma_{p1} - \sigma_{p2})^2}$$



EQUIVALENT STRESS

PRESSURE SIDE

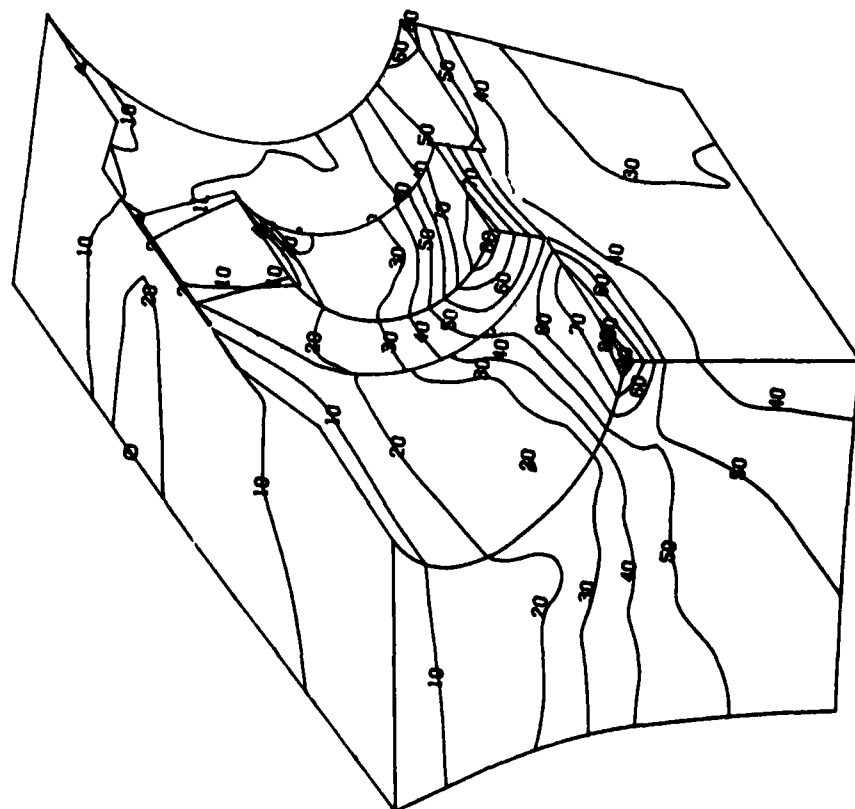
Figure 3-12. Peak Stress During Ignition (Cold Engine).



KSI

EQUIVALENT STRESS

SUCTION SIDE



kN/cm^2

21-3640(22)
3-46

Figure 3-13. Peak Stress During Ignition (Cold Engine).

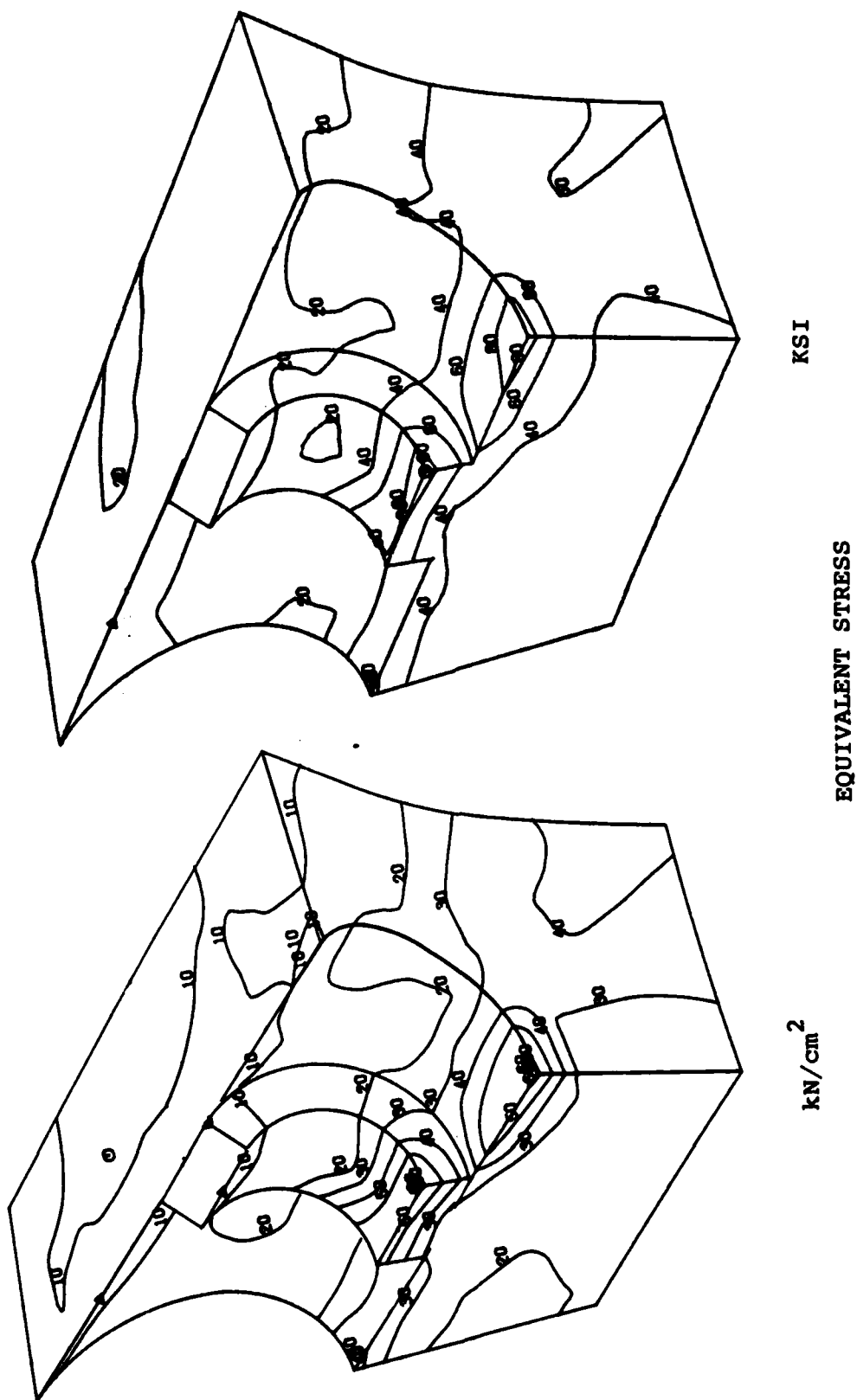
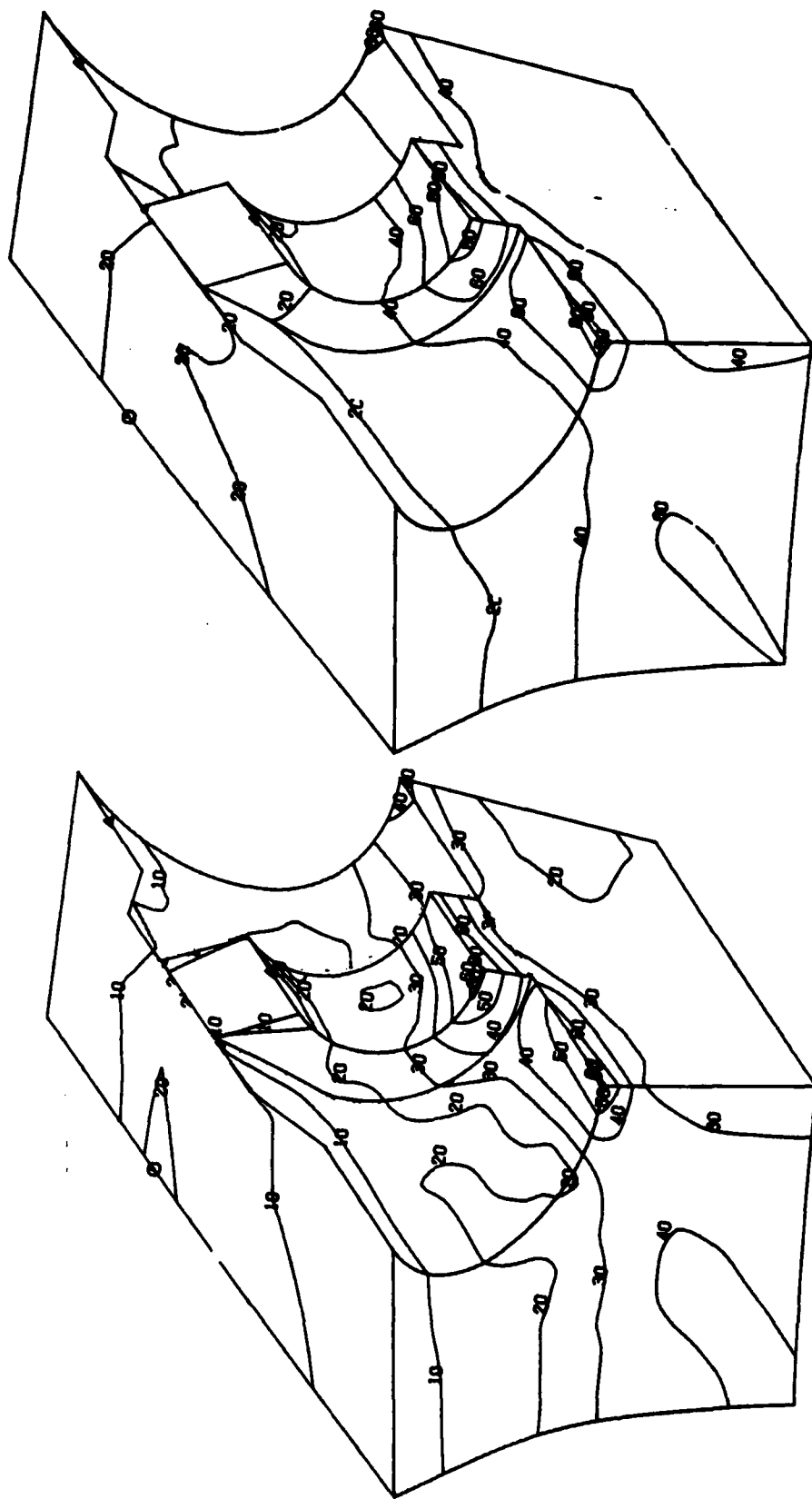


Figure 3-14. Peak Stress During Ignition (Warm Engine).



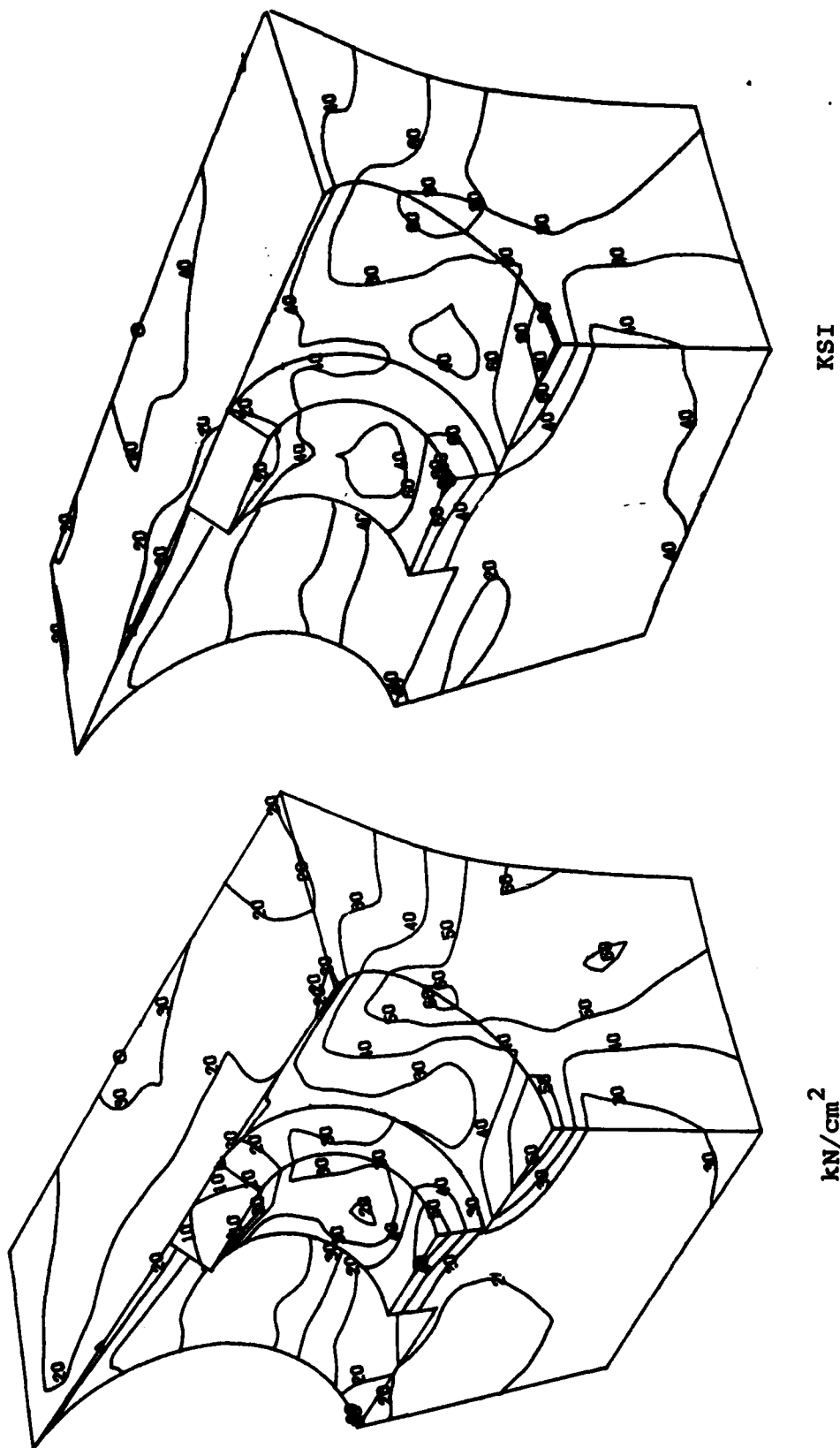
kN/cm²

KSI

EQUIVALENT STRESS

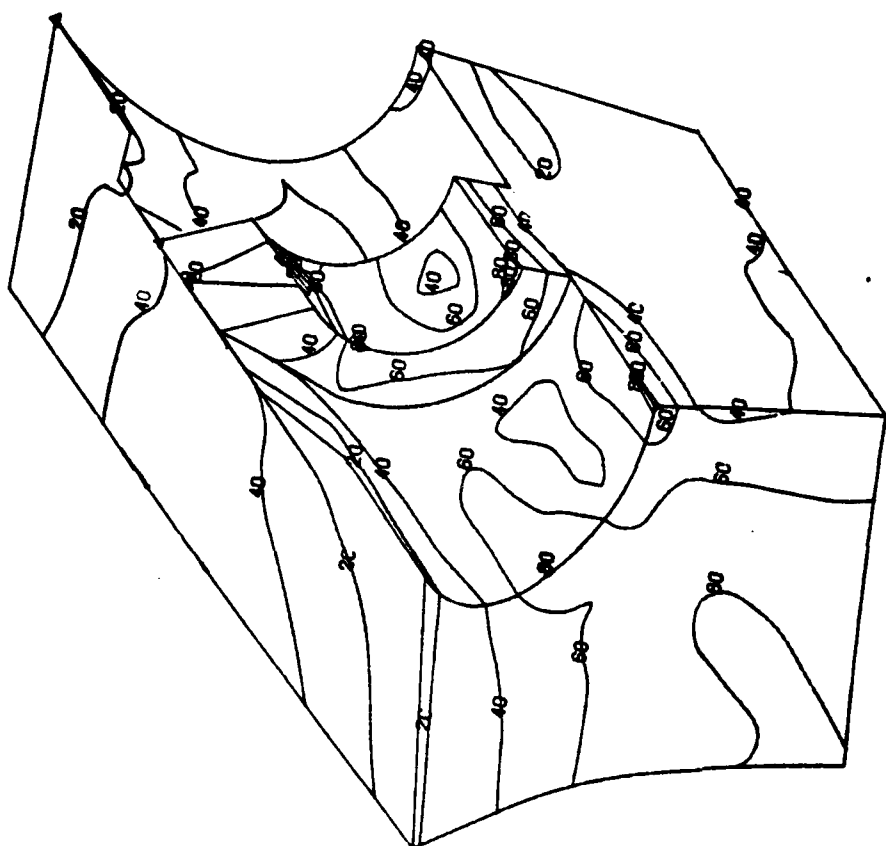
SUCTION SIDE

Figure 3-15. Peak Stress During Ignition (Warm Engine).



EQUIVALENT STRESS
PRESSURE SIDE

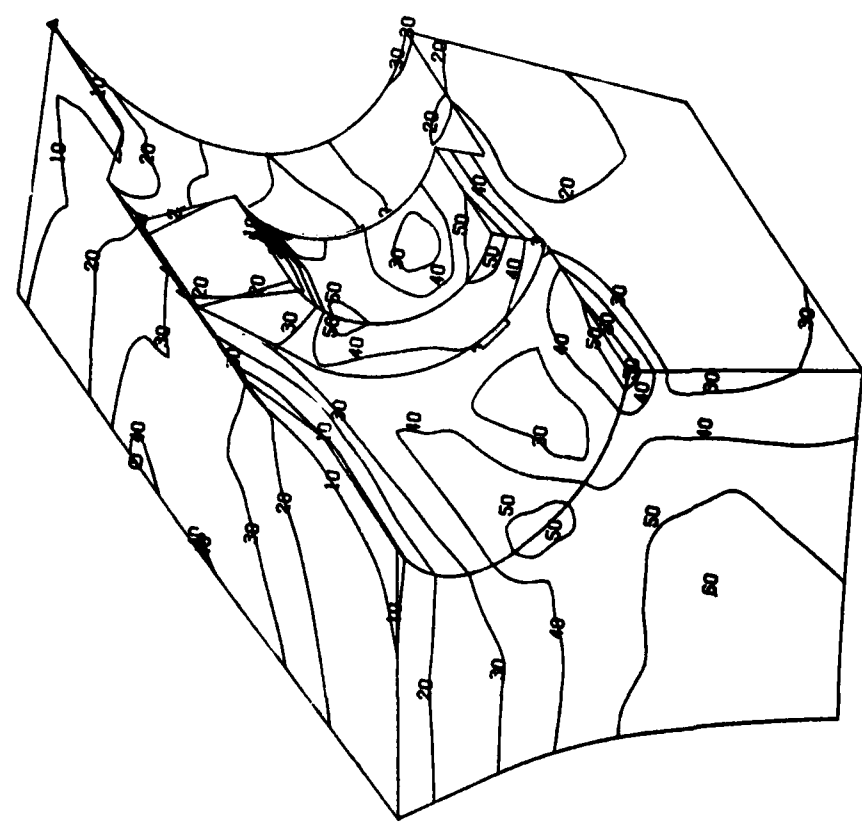
Figure 3-16. Peak Stress During Takeoff at 180 Seconds (Cold Engine).



KSI

EQUIVALENT STRESS

SUCTION SIDE



kN/cm²

Figure 3-17. Peak Stress During Takeoff at 180 Seconds (Cold Engine).

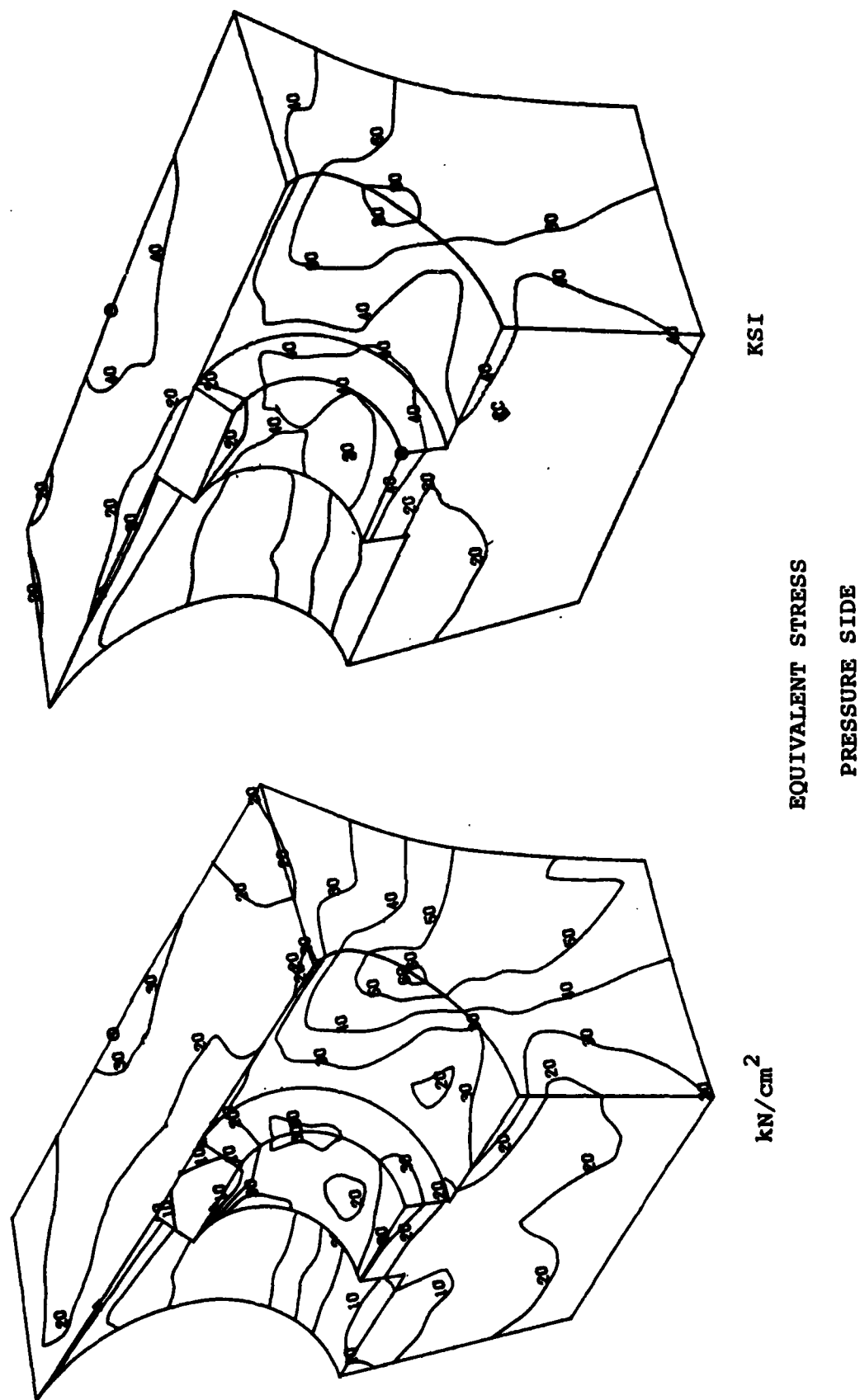
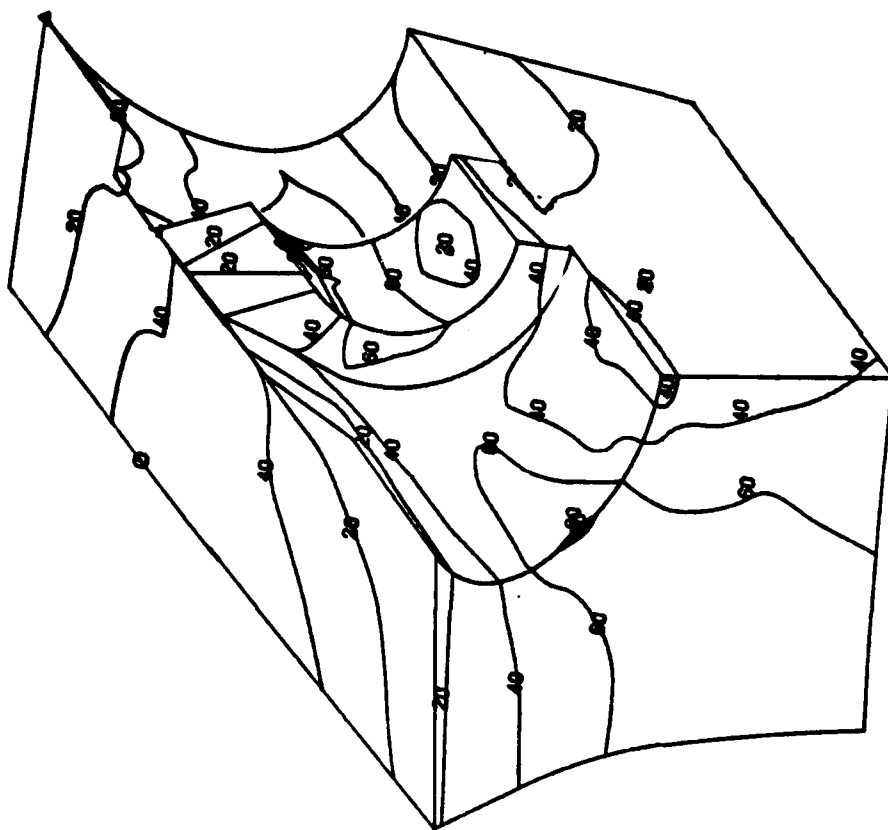


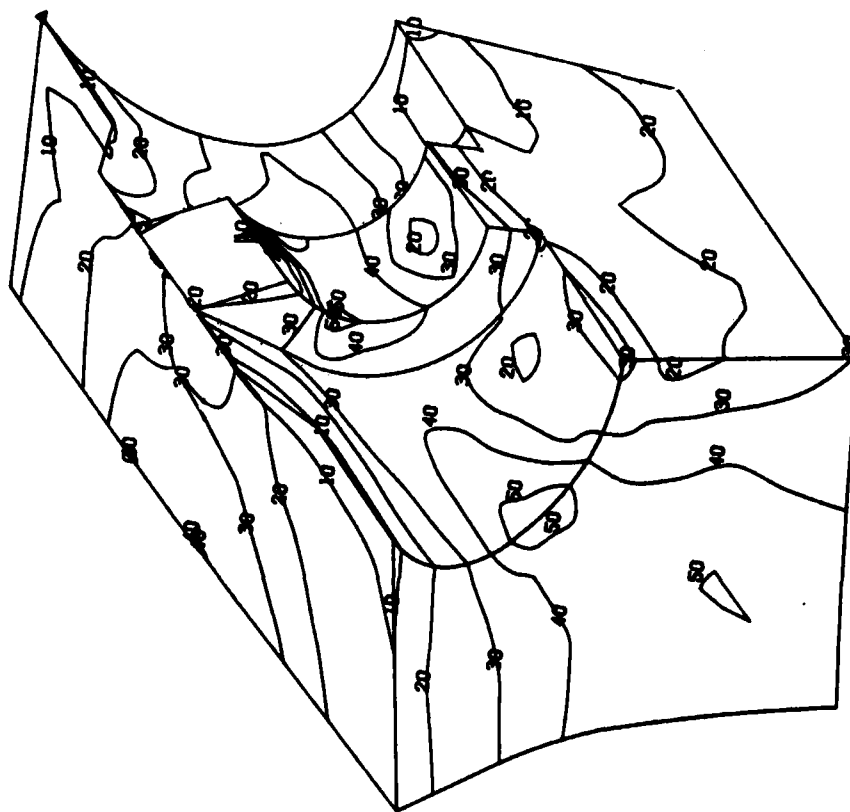
Figure 3-18. Peak Stress During Takeoff at 500 Seconds (Cold Engine).



KSI

EQUIVALENT STRESS

SUCTION SIDE



kN/cm²

21-3640 (22)
3-52

Figure 3-19. Peak Stress During Takeoff at 500 Seconds (Cold Engine).

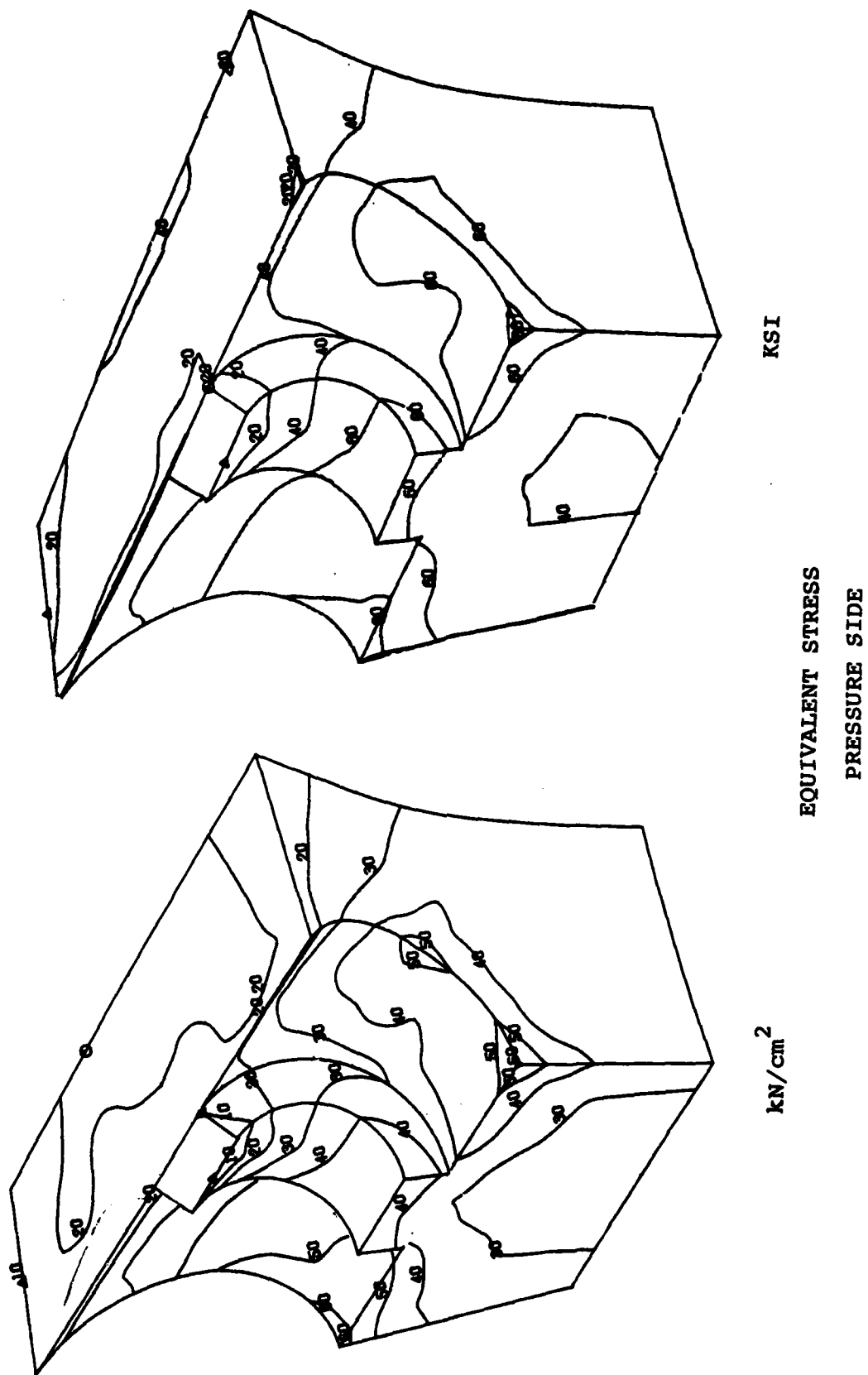
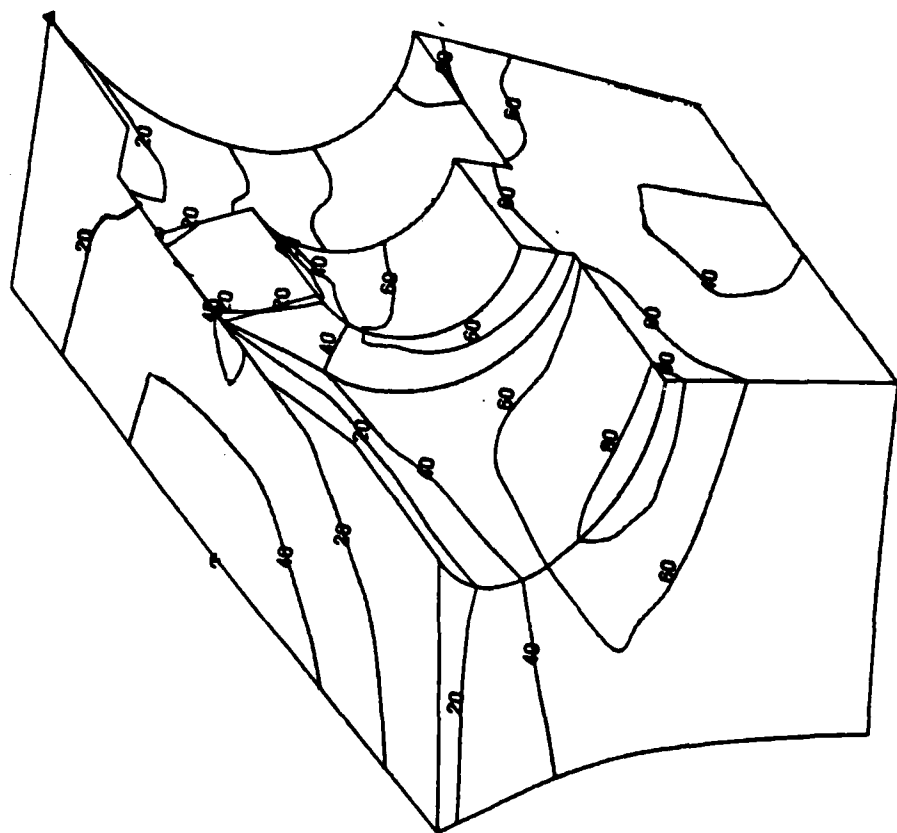


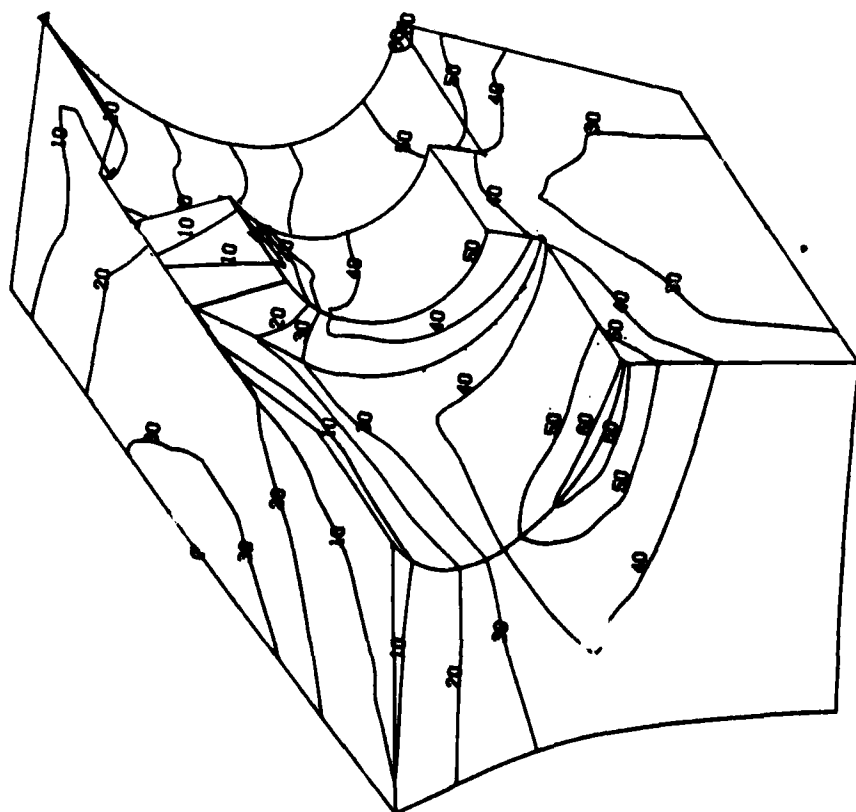
Figure 3-20. Peak Stress During Landing.



KSI

EQUIVALENT STRESS

SUCTION SIDE



KN/cm²

41-3640 (22)
3-54

Figure 3-21. Peak Stress During Landing.

TABLE 3-15. LISTING OF HALF-WHEELS.

<u>Casting S/N</u>	<u>Heat Code</u>	<u>Casting Date</u>
J773	58-KPE	12-14-76
H988	58-JEM	2-9-76
J339	58-JTN	6-15-76
J313	58-JJP	6-22-76
J406	58-KDZ	9-10-76
J840	58-KSM	1-20-77
K039	58-KSE	6-20-77
AT10	58-K=PKB	12-20-78
N651	58-PLB	1-5-79
J845	58-KSE	1-20-77

Prior to removing any specimens, the half-wheels were heat treated at 982-996°C (1800°F-1825°F) for 4 hours, air cooled, and aged at 871°C (1600°F) \pm 25°F for 12 hours, followed by air cooling.

Since the program is concerned with the initiation and propagation of cracks from the rivet holes, specimens were as close as possible to the rim area of the wheel. The wheels were sectioned as shown in Figure 3-22. The LCF specimens were machined tested by Martest, Inc. in Cincinnati, OH. The LCF tests were conducted at 593°C (1100°F) in air at an R ratio of -1.0 under axial strain control at 20 cpm. To contain the crack growth within the region of interest and to allow for negative R ratio testing (i.e., compressive mean stress), a center cracked panel specimen was designed (Figure 3-23). Cyclic crack growth rate tests were performed by Materials Behavior Research Corp. of Cincinnati, OH. Tests were conducted at 593°C (1100°F) in air at 3 R ratios: $R = -1.0, -1.5, \text{ and } 0.0$, under load control at 0.5 Hz. Tensile tests were also conducted at room temperature, 537°C (1000°F) and 593°C (1100°F) in air as part of materials verification. Table 3-16 is a summary of the specimens and test conditions used in the program.

3.6.2 Results of Materials Testing

In order to provide support for the empirical field data, it was decided to generate LCF and crack growth data using standard test specimens taken from actual unmachined wheels without any field service. The following presents the results of the in-lab test program.

3.6.2.1 Tensile Properties

Table 3-16 shows the room temperature tensile results from the casting lot qualification testing done by Howmet prior to shipment of the wheels. The specimens, taken tangentially in the hub, received

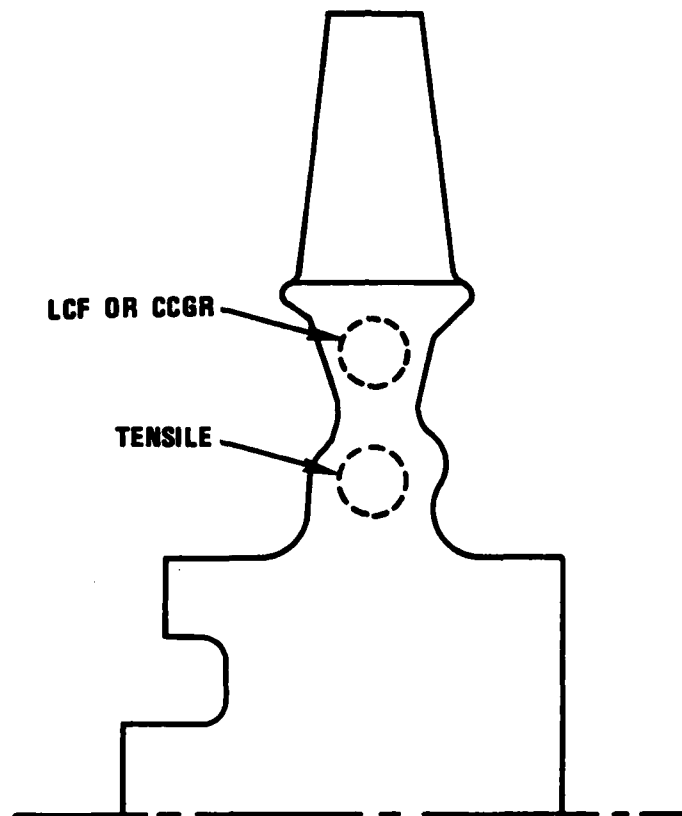
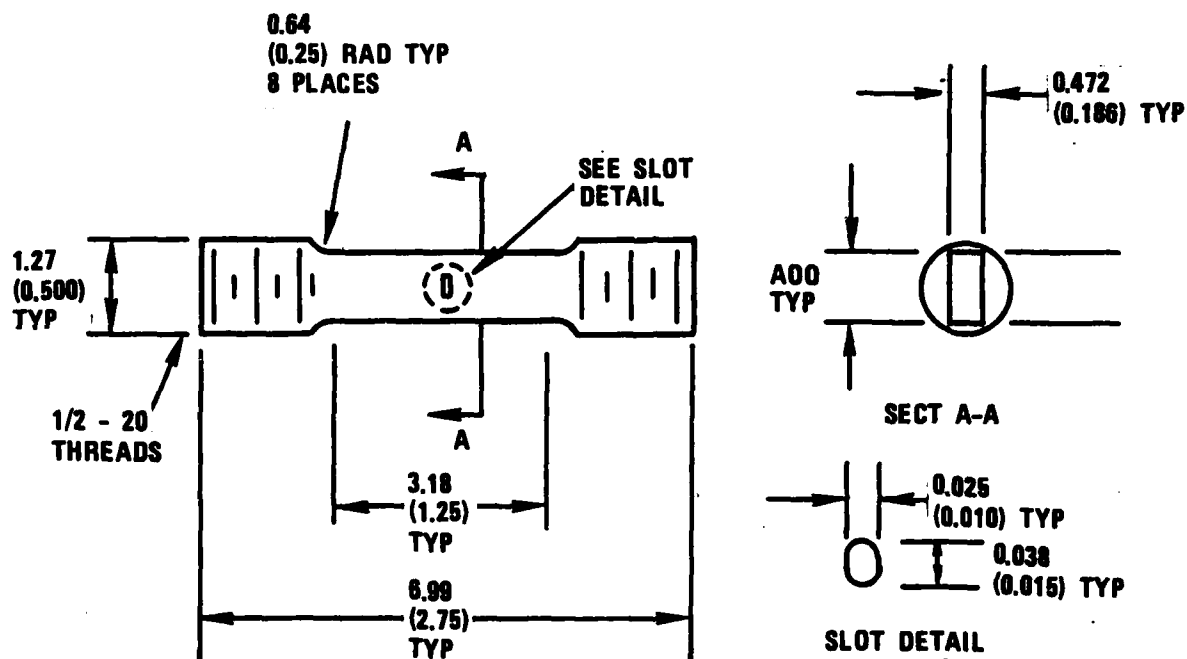


Figure 3-22. Sketch Showing Location of Test Specimens.



- NOTE - RADIUS AND GAGE SECTION TO BLEND SMOOTHLY WITHOUT UNDERCUTS**
- REMOVE ALL BURRS AND SHARP EDGES
 - DIMENSIONS ARE IN CENTIMETERS (INCHES)

Figure 3-23. Small Center Notched Specimen for Compressive CCGR Testing.

TABLE 3-16. ROOM TEMPERATURE TENSILE PROPERTIES (HOWMET).

<u>I.D.</u>	<u>0.2 PERCENT YS</u>	<u>UTS</u>	<u>% EL</u>
	MPa/Ksi	MPa/Ksi	
J773-KPE	710/103	752/109	5.0
H988-JEM	703/102	738/107	4.7
J339-JTN	731/106	779/113	9.4
J313-JTP	710/103	745/108	5.9
J406-KDZ	710/103	752/109	7.5
J840-KSM	710/103	731/106	3.8
J845-KSE	717/104	745/108	5.7
K039-LKL	703/102	779/113	8.5
AT10-PKB	710/103	731/106	2.2
N651-PLB	752/109	793/115	6.2
\bar{x}	710.2/103.0	754.3/109.4	6.0
S_x	14.5/ 2.1	22.1/ 3.2	--
$\bar{x}-3S_x$	671.5/ 97.4	688.8/ 99.9	1.7
EMS52466 Minimum	14/97	696/101	2.0
MDD \bar{x}	704.6/102.2	763.9/110.8	6.2
$\bar{x}-3S_x$	635 / 92.1	647.4/ 93.9	1.5

the 982°C (1800°F) 4-hour heat treatment plus aging after eloxing, but before machining. The results show all the wheels exceeded the specification minima given in EMS52466. Table 3-17 shows the tensile results from the current test program at room temperature, 537°C (1000°F) and 593°C (1100°F). The wheels received the 982°C (1800°F) 4-hour heat treatment before eloxing similar to the actual wheels. These specimens were taken from the area between the rim and the hub as shown in Figure 3-22. The tensile properties as plotted in Figure 3-24 through 3-27 show that the tensile strength of IN 100 is constant from RT up to 537°C (1000°F) with a slight decrease at 38°C (100°F), with a corresponding increase in ductility.

3.6.2.2 LCF Properties

The results of the LCF testing are presented in Table 3-18 and plotted in Figures 3-28 and 3-29. The data was generated for fatigue lives between 10^2 and 5.4×10^4 cycles to failure at total strain ranges between 0.5 percent and 1.2 percent. A runout (1.3×10^5) was encountered at 0.45 percent strain. There is no other LCF data for IN 100 at 593°C (1100°F). Figure 3-30 shows a comparison between 593°C (1100°F) LCF Neuber and the MDD baseline at 24°C (75°F), 427°C (800°F) and 648°C (1200°F). This comparison indicates that the 593°C (1100°F) data is probably typical.

3.6.2.3 Cyclic Crack-Growth Rate

3.6.2.3.1 Data Reduction

The crack length versus number of cycles, a-N data, was analyzed using a 7-point incremental polynomial method as outlined in ASTM E647. The crack length was measured on both sides of the specimen and the average crack length calculated. For the center crack specimens, half the total crack length was used in calculating da/dN and ΔK values. The da/dN and ΔK values were evaluated at the mid-point of the



GARRETT TURBINE ENGINE COMPANY
A DIVISION OF THE GARRETT CORPORATION
PHOENIX, ARIZONA

TABLE 3-17. TENSILE TEST RESULTS (GARRETT)

<u>SPECIMEN I.D. (1)</u>		<u>0.2 PERCENT YS</u>		<u>UTS</u>		<u>% EL</u>	<u>% RA</u>
		cm	in.	cm	in.		
RT	KPE	269.0	105.9	296.9	116.9	6.0	6.3
	JEM	269.5	106.1	310.9	122.4	11.0	7.8
	JTN	269.5	106.1	306.3	120.6	6.6	13.9
	JTP	265.9	104.7	315.7	124.3	10.6	14.3
	KDZ	264.9	104.3	284.5	112.0	10.6	14.3
	KSM	261.4	102.9	283.5	111.6	5.7	7.8
	KSE	269.0	105.9	289.8	114.1	5.0	9.0
	LKL	266.4	104.9	303.0	119.3	9.5	8.6
	PKB	224.3	108.0	289.8	114.1	4.7	6.3
	PLE	269.0	105.9	293.4	293.4	6.9	9.4
	\bar{x}	268.0	105.5	297.4	117.1	7.1	9.6
	S_x	3.5	1.36	11.4	4.5	--	--
	$\bar{x}-3S_x$	257.6	101.4	263.9	103.9	2.69	3.9

(1) Tensile specimens were identified with the 3 letter heat treat code.

YIELD STRENGTH

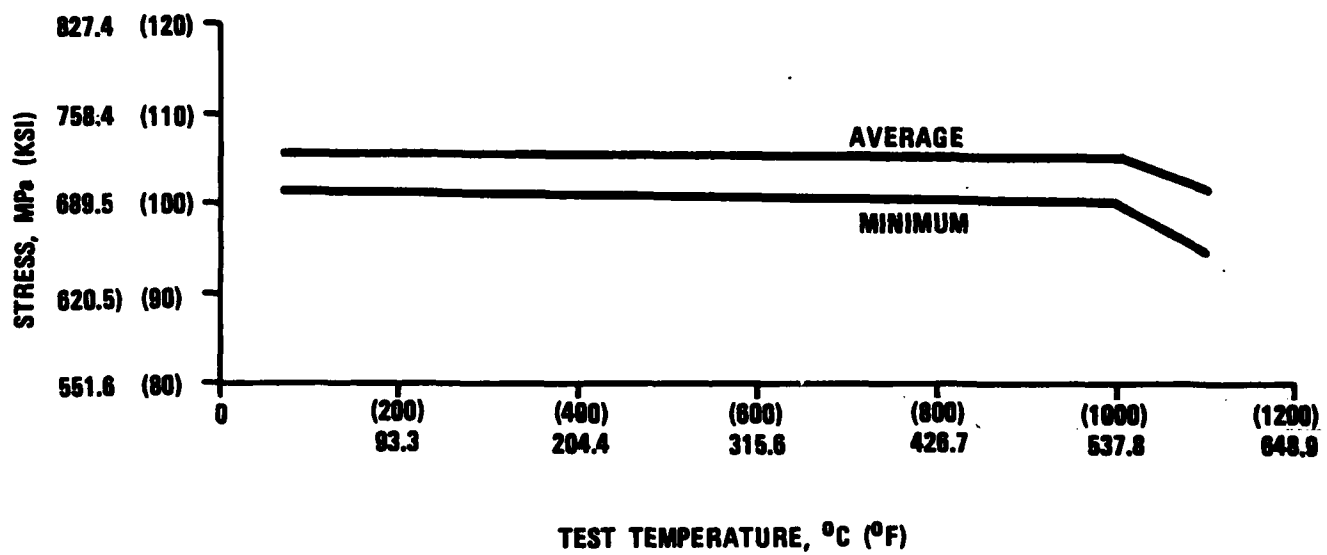


Figure 3-24. Yield Strength of IN-100.

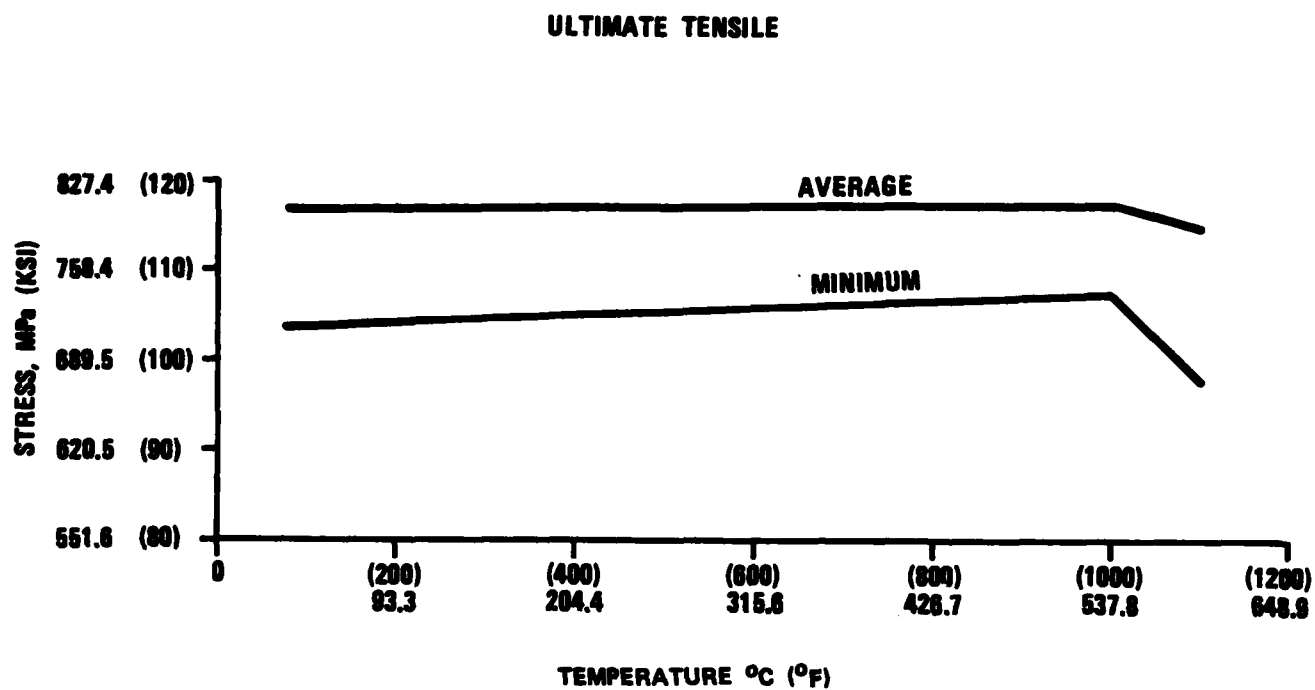


Figure 3-25. Ultimate Tensile Strength of IN-100.

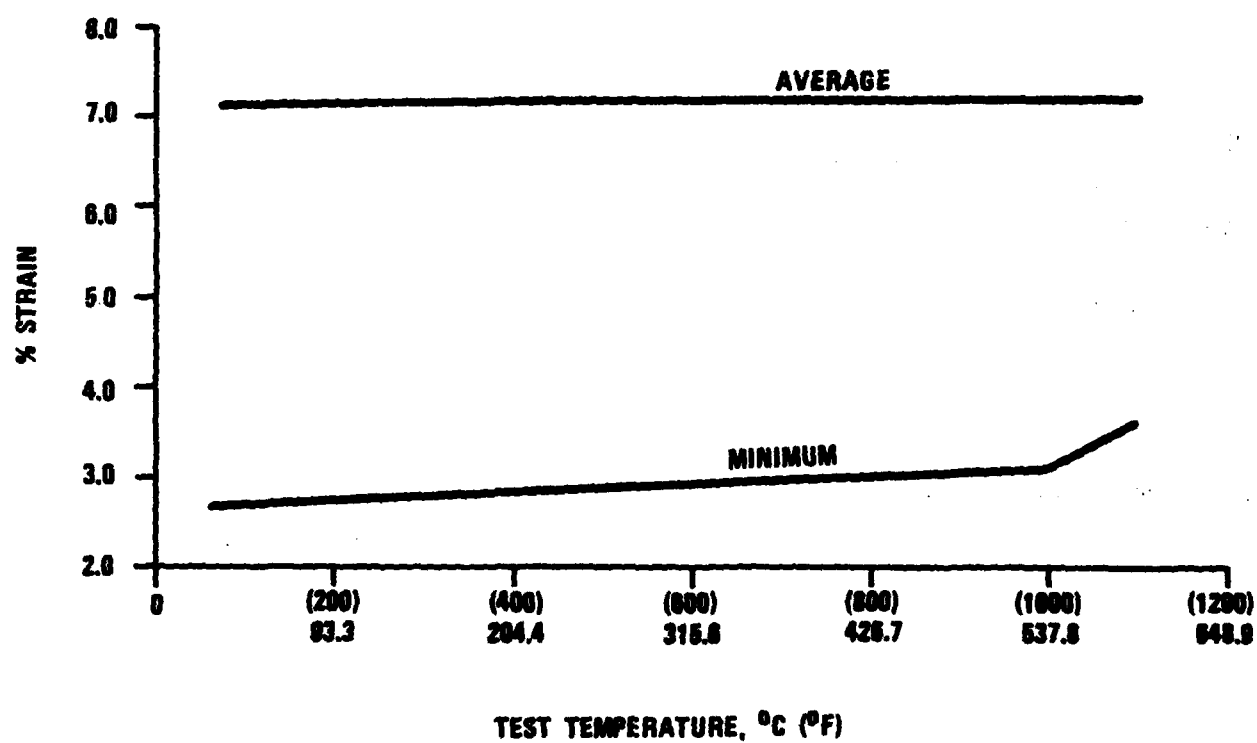


Figure 3-26. Percent Elongation of IN-100.

21-3640(22)
3-64

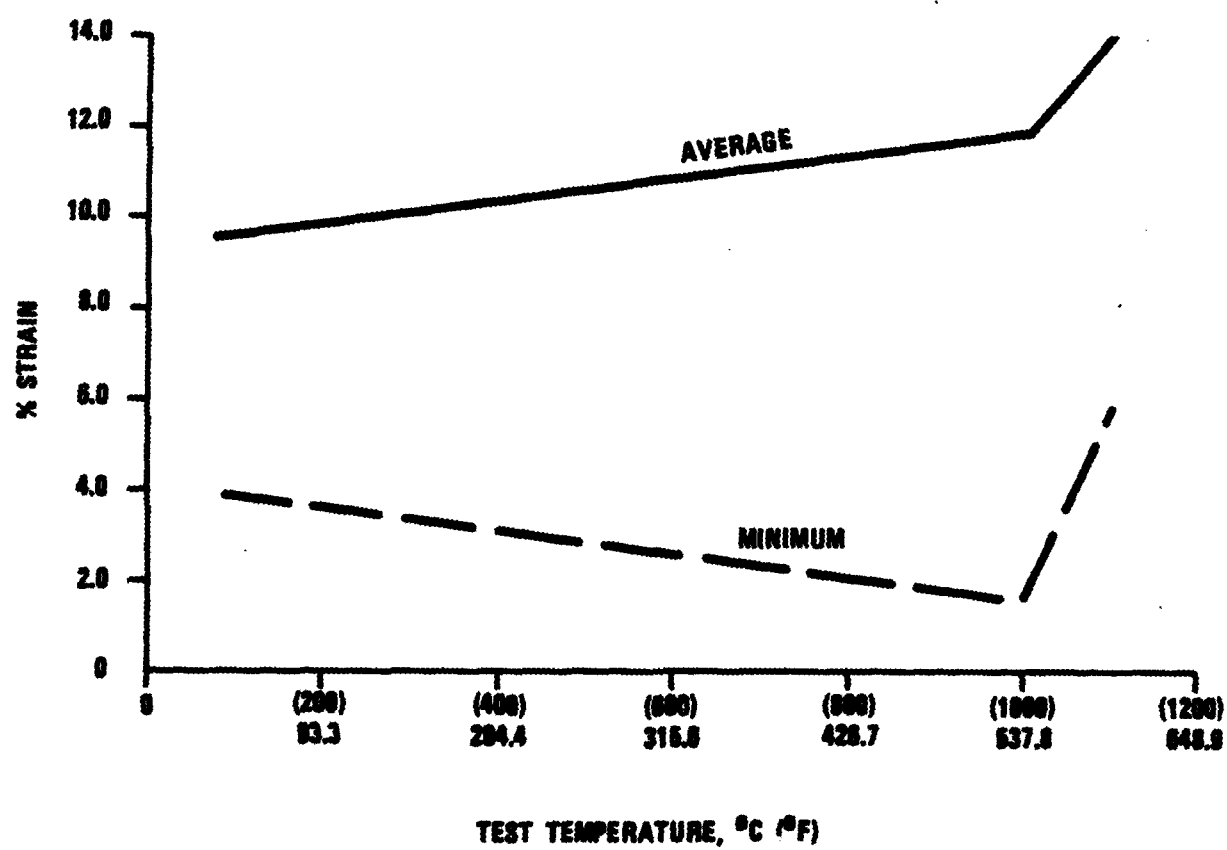


Figure 3-27. Percent Reduction in Area of IN-100, of IN-100.

21-3640(22)
3-55

TABLE 3-18. LCF DATA SUMMARY.

$\sigma = 0.0 \times 10^{-4} \text{ in/in}$
 $\Delta = -$
 Frac. = 20 cps

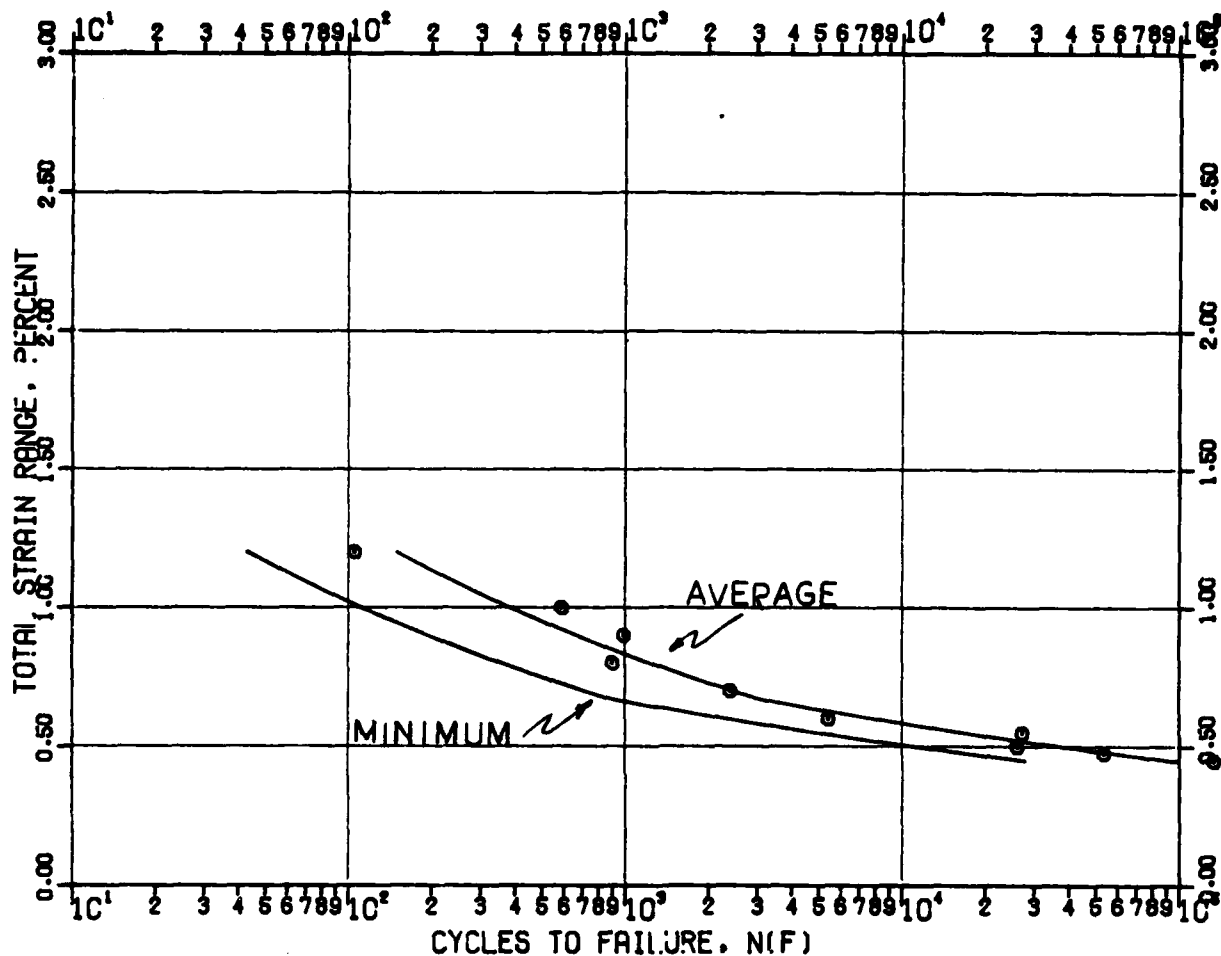
LCF DATA SUMMARY FOR 10-100
 AXIAL STRAIN MEASUREMENT & CONTROL

Engineer: SHIMIZU
 P.E. No: 1000161
 Job No: 1 000-233

Specimen T.A.	Age t	$\Delta \epsilon_p$ At 10/2	$\Delta \epsilon_s$ At 10/2	$\Delta \epsilon_{p/2}$ At 10/2	$\Delta \epsilon_{s/2}$ At 10/2	$\Delta \epsilon_{p/4}$ At 10/2	$\Delta \epsilon_{s/4}$ At 10/2	Test Temp. °F
J70	1.00	0.030	00.0	100.0	0.00	0.00	0.00	1100
J71	0.00	0.775	04.0	100.0	0.00	0.00	0.00	1100
J72	0.00	0.000	04.0	100.0	0.00	0.00	0.00	1100
J73	0.00	0.000	00.0	100.0	0.00	0.00	0.00	1100
J74	0.00	0.000	04.0	100.0	0.00	0.00	0.00	1100
J75	1.00	0.000	00.0	100.0	0.00	0.00	0.00	1100
J76	0.00	0.000	00.0	100.0	0.00	0.00	0.00	1100
J77	0.00	0.000	04.0	100.0	0.00	0.00	0.00	1100
J78	0.00	0.000	00.0	100.0	0.00	0.00	0.00	1100
J79	0.00	0.000	00.0	100.0	0.00	0.00	0.00	1100
J80	0.00	0.000	04.0	100.0	0.00	0.00	0.00	1100
J81	0.00	0.000	00.0	100.0	0.00	0.00	0.00	1100
J82	0.00	0.000	00.0	100.0	0.00	0.00	0.00	1100
J83	0.00	0.000	04.0	100.0	0.00	0.00	0.00	1100
J84	0.00	0.000	00.0	100.0	0.00	0.00	0.00	1100
J85	0.00	0.000	00.0	100.0	0.00	0.00	0.00	1100
J86	0.00	0.000	04.0	100.0	0.00	0.00	0.00	1100
J87	0.00	0.000	00.0	100.0	0.00	0.00	0.00	1100
J88	0.00	0.000	00.0	100.0	0.00	0.00	0.00	1100
J89	0.00	0.000	04.0	100.0	0.00	0.00	0.00	1100
J90	0.00	0.000	00.0	100.0	0.00	0.00	0.00	1100
J91	0.00	0.000	00.0	100.0	0.00	0.00	0.00	1100
J92	0.00	0.000	04.0	100.0	0.00	0.00	0.00	1100
J93	0.00	0.000	00.0	100.0	0.00	0.00	0.00	1100
J94	0.00	0.000	00.0	100.0	0.00	0.00	0.00	1100
J95	0.00	0.000	04.0	100.0	0.00	0.00	0.00	1100
J96	0.00	0.000	00.0	100.0	0.00	0.00	0.00	1100
J97	0.00	0.000	00.0	100.0	0.00	0.00	0.00	1100
J98	0.00	0.000	04.0	100.0	0.00	0.00	0.00	1100
J99	0.00	0.000	00.0	100.0	0.00	0.00	0.00	1100
J100	0.00	0.000	00.0	100.0	0.00	0.00	0.00	1100
J101	0.00	0.000	04.0	100.0	0.00	0.00	0.00	1100
J102	0.00	0.000	00.0	100.0	0.00	0.00	0.00	1100
J103	0.00	0.000	00.0	100.0	0.00	0.00	0.00	1100
J104	0.00	0.000	04.0	100.0	0.00	0.00	0.00	1100
J105	0.00	0.000	00.0	100.0	0.00	0.00	0.00	1100
J106	0.00	0.000	00.0	100.0	0.00	0.00	0.00	1100
J107	0.00	0.000	04.0	100.0	0.00	0.00	0.00	1100
J108	0.00	0.000	00.0	100.0	0.00	0.00	0.00	1100
J109	0.00	0.000	00.0	100.0	0.00	0.00	0.00	1100
J110	0.00	0.000	04.0	100.0	0.00	0.00	0.00	1100
J111	0.00	0.000	00.0	100.0	0.00	0.00	0.00	1100
J112	0.00	0.000	00.0	100.0	0.00	0.00	0.00	1100
J113	0.00	0.000	04.0	100.0	0.00	0.00	0.00	1100
J114	0.00	0.000	00.0	100.0	0.00	0.00	0.00	1100
J115	0.00	0.000	00.0	100.0	0.00	0.00	0.00	1100
J116	0.00	0.000	04.0	100.0	0.00	0.00	0.00	1100
J117	0.00	0.000	00.0	100.0	0.00	0.00	0.00	1100
J118	0.00	0.000	00.0	100.0	0.00	0.00	0.00	1100
J119	0.00	0.000	04.0	100.0	0.00	0.00	0.00	1100
J120	0.00	0.000	00.0	100.0	0.00	0.00	0.00	1100
J121	0.00	0.000	00.0	100.0	0.00	0.00	0.00	1100
J122	0.00	0.000	04.0	100.0	0.00	0.00	0.00	1100
J123	0.00	0.000	00.0	100.0	0.00	0.00	0.00	1100
J124	0.00	0.000	00.0	100.0	0.00	0.00	0.00	1100
J125	0.00	0.000	04.0	100.0	0.00	0.00	0.00	1100
J126	0.00	0.000	00.0	100.0	0.00	0.00	0.00	1100
J127	0.00	0.000	00.0	100.0	0.00	0.00	0.00	1100
J128	0.00	0.000	04.0	100.0	0.00	0.00	0.00	1100
J129	0.00	0.000	00.0	100.0	0.00	0.00	0.00	1100
J130	0.00	0.000	00.0	100.0	0.00	0.00	0.00	1100
J131	0.00	0.000	04.0	100.0	0.00	0.00	0.00	1100
J132	0.00	0.000	00.0	100.0	0.00	0.00	0.00	1100
J133	0.00	0.000	00.0	100.0	0.00	0.00	0.00	1100
J134	0.00	0.000	04.0	100.0	0.00	0.00	0.00	1100
J135	0.00	0.000	00.0	100.0	0.00	0.00	0.00	1100
J136	0.00	0.000	00.0	100.0	0.00	0.00	0.00	1100
J137	0.00	0.000	04.0	100.0	0.00	0.00	0.00	1100
J138	0.00	0.000	00.0	100.0	0.00	0.00	0.00	1100
J139	0.00	0.000	00.0	100.0	0.00	0.00	0.00	1100
J140	0.00	0.000	04.0	100.0	0.00	0.00	0.00	1100
J141	0.00	0.000	00.0	100.0	0.00	0.00	0.00	1100
J142	0.00	0.000	00.0	100.0	0.00	0.00	0.00	1100
J143	0.00	0.000	04.0	100.0	0.00	0.00	0.00	1100
J144	0.00	0.000	00.0	100.0	0.00	0.00	0.00	1100
J145	0.00	0.000	00.0	100.0	0.00	0.00	0.00	1100
J146	0.00	0.000	04.0	100.0	0.00	0.00	0.00	1100
J147	0.00	0.000	00.0	100.0	0.00	0.00	0.00	1100
J148	0.00	0.000	00.0	100.0	0.00	0.00	0.00	1100
J149	0.00	0.000	04.0	100.0	0.00	0.00	0.00	1100
J150	0.00	0.000	00.0	100.0	0.00	0.00	0.00	1100
J151	0.00	0.000	00.0	100.0	0.00	0.00	0.00	1100
J152	0.00	0.000	04.0	100.0	0.00	0.00	0.00	1100
J153	0.00	0.000	00.0	100.0	0.00	0.00	0.00	1100
J154	0.00	0.000	00.0	100.0	0.00	0.00	0.00	1100
J155	0.00	0.000	04.0	100.0	0.00	0.00	0.00	1100
J156	0.00	0.000	00.0	100.0	0.00	0.00	0.00	1100
J157	0.00	0.000	00.0	100.0	0.00	0.00	0.00	1100
J158	0.00	0.000	04.0	100.0	0.00	0.00	0.00	1100
J159	0.00	0.000	00.0	100.0	0.00	0.00	0.00	1100
J160	0.00	0.000	00.0	100.0	0.00	0.00	0.00	1100
J161	0.00	0.000	04.0	100.0	0.00	0.00	0.00	1100
J162	0.00	0.000	00.0	100.0	0.00	0.00	0.00	1100
J163	0.00	0.000	00.0	100.0	0.00	0.00	0.00	1100
J164	0.00	0.000	04.0	100.0	0.00	0.00	0.00	1100
J165	0.00	0.000	00.0	100.0	0.00	0.00	0.00	1100
J166	0.00	0.000	00.0	100.0	0.00	0.00	0.00	1100
J167	0.00	0.000	04.0	100.0	0.00	0.00	0.00	1100
J168	0.00	0.000	00.0	100.0	0.00	0.00	0.00	1100
J169	0.00	0.000	00.0	100.0	0.00	0.00	0.00	1100
J170	0.00	0.000	04.0	100.0	0.00	0.00	0.00	1100
J171	0.00	0.000	00.0	100.0	0.00	0.00	0.00	1100
J172	0.00	0.000	00.0	100.0	0.00	0.00	0.00	1100
J173	0.00	0.000	04.0	100.0	0.00	0.00	0.00	1100
J174	0.00	0.000	00.0	100.0	0.00	0.00	0.00	1100
J175	0.00	0.000	00.0	100.0	0.00	0.00	0.00	1100
J176	0.00	0.000	04.0	100.0	0.00	0.00	0.00	1100
J177	0.00	0.000	00.0	100.0	0.00	0.00	0.00	1100
J178	0.00	0.000	00.0	100.0	0.00	0.00	0.00	1100
J179	0.00	0.000	04.0	100.0	0.00	0.00	0.00	1100
J180	0.00	0.000	00.0	100.0	0.00	0.00	0.00	1100
J181	0.00	0.000	00.0	100.0	0.00	0.00	0.00	1100
J182	0.00	0.000	04.0	100.0	0.00	0.00	0.00	1100
J183	0.00	0.000	00.0	100.0	0.00	0.00	0.00	1100
J184	0.00	0.000	00.0	100.0	0.00	0.00	0.00	1100
J185	0.00	0.000	04.0	100.0	0.00	0.00	0.00	1100
J186	0.00	0.000	00.0	100.0	0.00	0.00	0.00	1100
J187	0.00	0.000	00.0	100.0	0.00	0.00	0.00	1100
J188	0.00	0.000	04.0	100.0	0.00	0.00	0.00	1100
J189	0.00	0.000	00.0	100.0	0.00	0.00	0.00	1100
J190	0.00	0.000	00.0	100.0	0.00	0.00	0.00	1100
J191	0.00	0.000	04.0	100.0	0.00	0.00	0.00	1100
J192	0.00	0.000	00.0	100.0	0.00	0.00	0.00	1100
J193	0.00	0.000	00.0	100.0	0.00	0.00	0.00	1100
J194	0.00	0.000	04.0	100.0	0.00	0.00	0.00	1100
J195	0.00	0.000	00.0	100.0	0.00	0.00	0.00	1100
J196	0.00	0.000	00.0	100.0	0.00	0.00	0.00	1100
J197	0.00	0.000	04.0	100.0	0.00	0.00	0.00	1100
J198	0.00	0.000	00.0	100.0	0.00	0.00	0.00	1100
J199	0.00	0.000	00.0	100.0	0.00	0.00	0.00	1100
J200	0.00	0.000	04.0	100.0	0.00	0.00	0.00	1100
J201	0.00	0.000	00.0	100.0	0.00	0.00	0.00	1100
J202	0.00	0.000	00.0	100.0	0.00	0.00	0.00	1100
J203	0.00	0.000	04.0	100.0	0.00	0.00	0.00	1100
J204	0.00	0.000	00.0	100.0	0.00	0.00	0.00	1100
J205	0.00	0.000	00.0	100.0	0.00	0.00	0.00	1100
J206	0.00	0.000	04.0	100.0	0.00	0.00	0.00	1100
J207	0.00	0.000	00.0	100.0	0.00	0.00	0.00	1100
J208	0.00	0.000	00.0	100.0	0.00	0.00	0.00	1100
J209	0.00	0.000	04.0	100.0	0.00	0.00	0.00	1100
J210	0.00	0.000	00.0	100.0	0.00	0.00	0.00	1100
J211	0.00	0.000	00.0	100.0	0.00	0.00	0.00	1100
J212	0.00							

(a) up shutdown (b) Failed in gaps (c) Failed out of gaps in uniform section (d) Reset at 133,112 cycles, charge - 0000.0 minutes.
 (°F) at test temperature (°F) at termination (°F) at cycle 000

Rev-Test Inc. 7/81



MATHEMATICAL MODEL

$$Y = A0 + A1 \cdot X + A2 \cdot \text{ABS}(X - X0)$$

$$Y_{\text{MIN}} = Y - K \cdot \text{SEE}$$

WHERE $X = \text{ALOG}_{10}(\text{TOTAL STRAIN RANGE, PERCENT})$

$Y = \text{ALOG}_{10}(\text{CYCLES TO FAILURE, } N(F))$

$$A0 = 2.28227$$

$$A1 = -6.93313$$

$$A2 = 1.73555$$

$$X0 = -.174C2$$

$$\text{SEE} = .18045$$

$$K = 3.000$$

$$R = -1.0$$

$$K(T) = 1.0$$

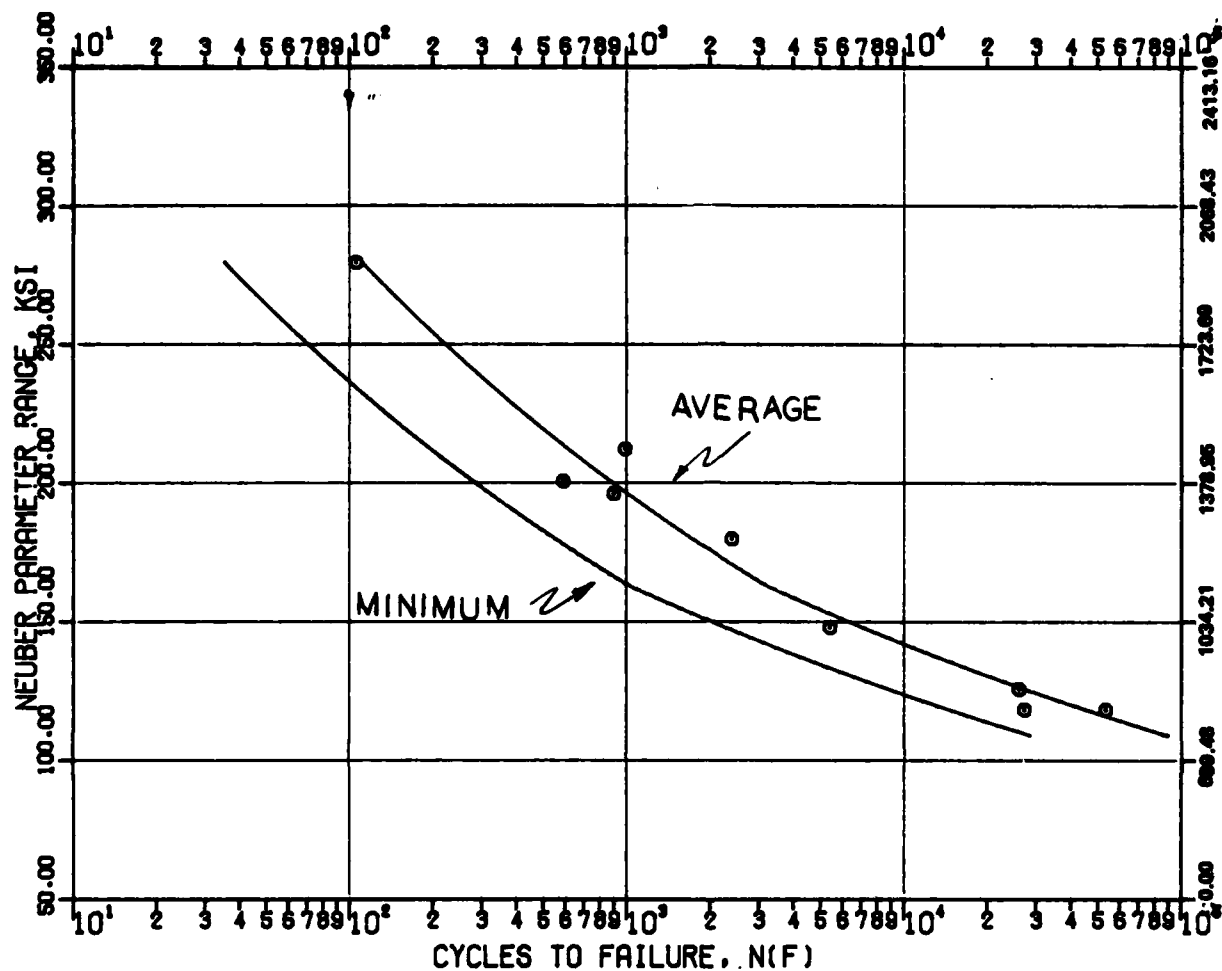
$$\text{FREQUENCY} = 2C \text{ CPM}$$

$$\text{TEMPERATURE} = 1100 \text{ F}$$

$$\text{NUMBER OF DATA POINTS} = 10$$

$$\text{SPECIMEN TYPE} = \text{PAP244001-1}$$

Figure 3-28. Axial Strain Controlled LCF of IN-100.



MATHEMATICAL MODEL

$$Y = AC + A1 \cdot X + A2 \cdot \text{ABS}(X - X0)$$

$$Y_{\text{MIN}} = Y - K \cdot \text{SEE}$$

WHERE $X = \text{ALOG10}(\text{NEUBER PARAMETER RANGE, KSI})$

$Y = \text{ALOG10}(\text{CYCLES TO FAILURE, N(F)})$

$A0 = 19.58481$

$A1 = -7.27022$

$A2 = 1.03905$

$X0 = 2.21219$

$\text{SEE} = .16533$

$K = 3.000$

$R = -1.0$

$K(T) = 1.0$

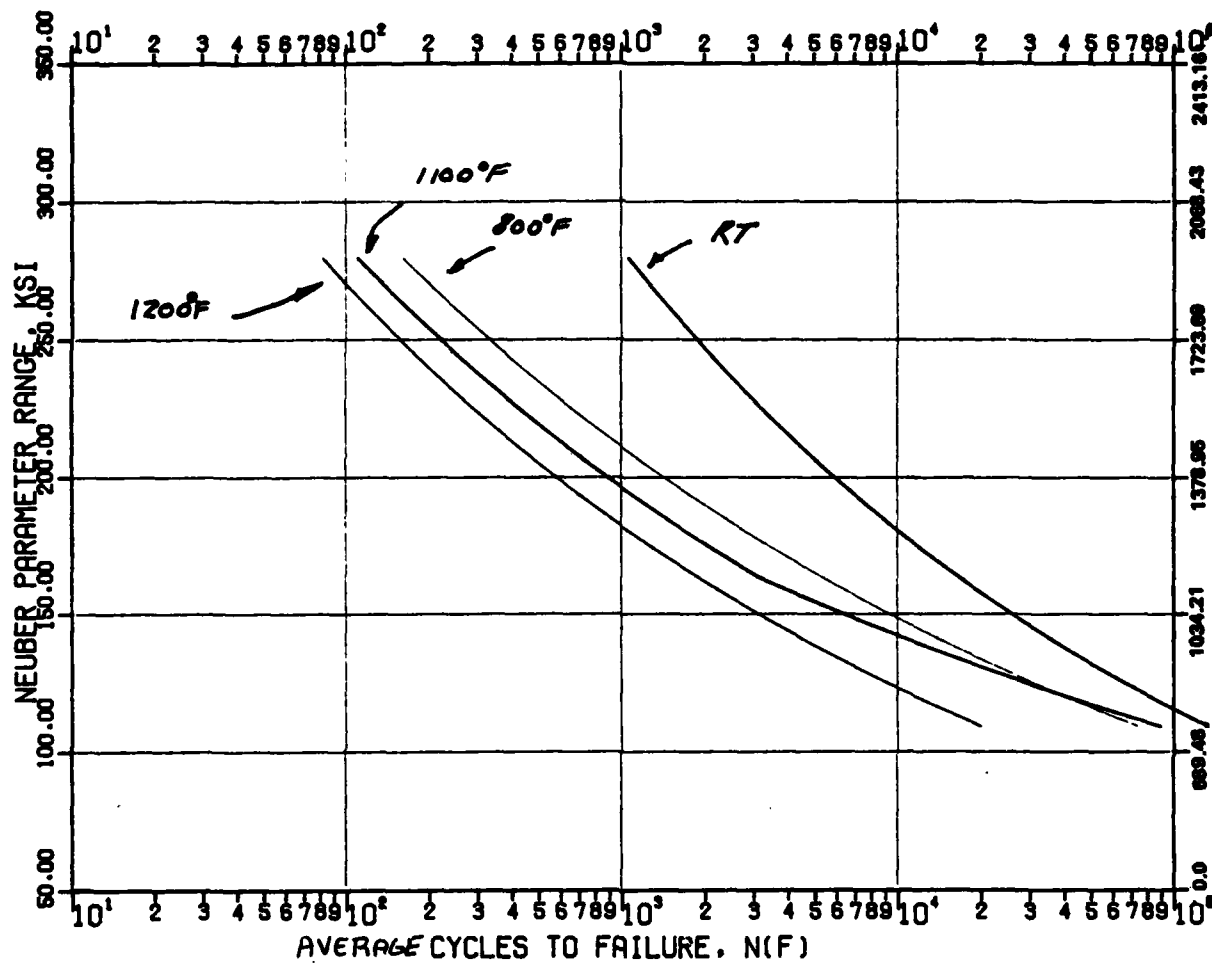
FREQUENCY = 20 CPM

TEMPERATURE = 1100 F

NUMBER OF DATA POINTS = 10

SPECIMEN TYPE = PAP244001-1

Figure 3-29. Axial Strain Controlled LCF of IN-100.



MATHEMATICAL MODEL

$$Y = A_0 + A_1 \cdot X + A_2 \cdot \text{ABS}(X - X_0)$$

$$Y_{\text{MIN}} = Y - K \cdot \text{SEE}$$

WHERE $X = \text{ALOG}_{10}(\text{NEUBER PARAMETER RANGE, KSI})$

$Y = \text{ALOG}_{10}(\text{CYCLES TO FAILURE, } N(F))$

	75°F	800°F	1100°F	1200°F
A_0	18.58638	18.17022	19.58481	16.21023
A_1	-5.13518	-4.52352	-2.21022	-5.84511
A_2	0.0	0.0	1.03905	0.0
X_0	2.2394	2.18281	2.21219	2.09154
S_x	.159143	.125621	.16533	.223764

Figure 3-30. Axial Strain Control LCF of IN-100 at 1100°F Compared to Baseline

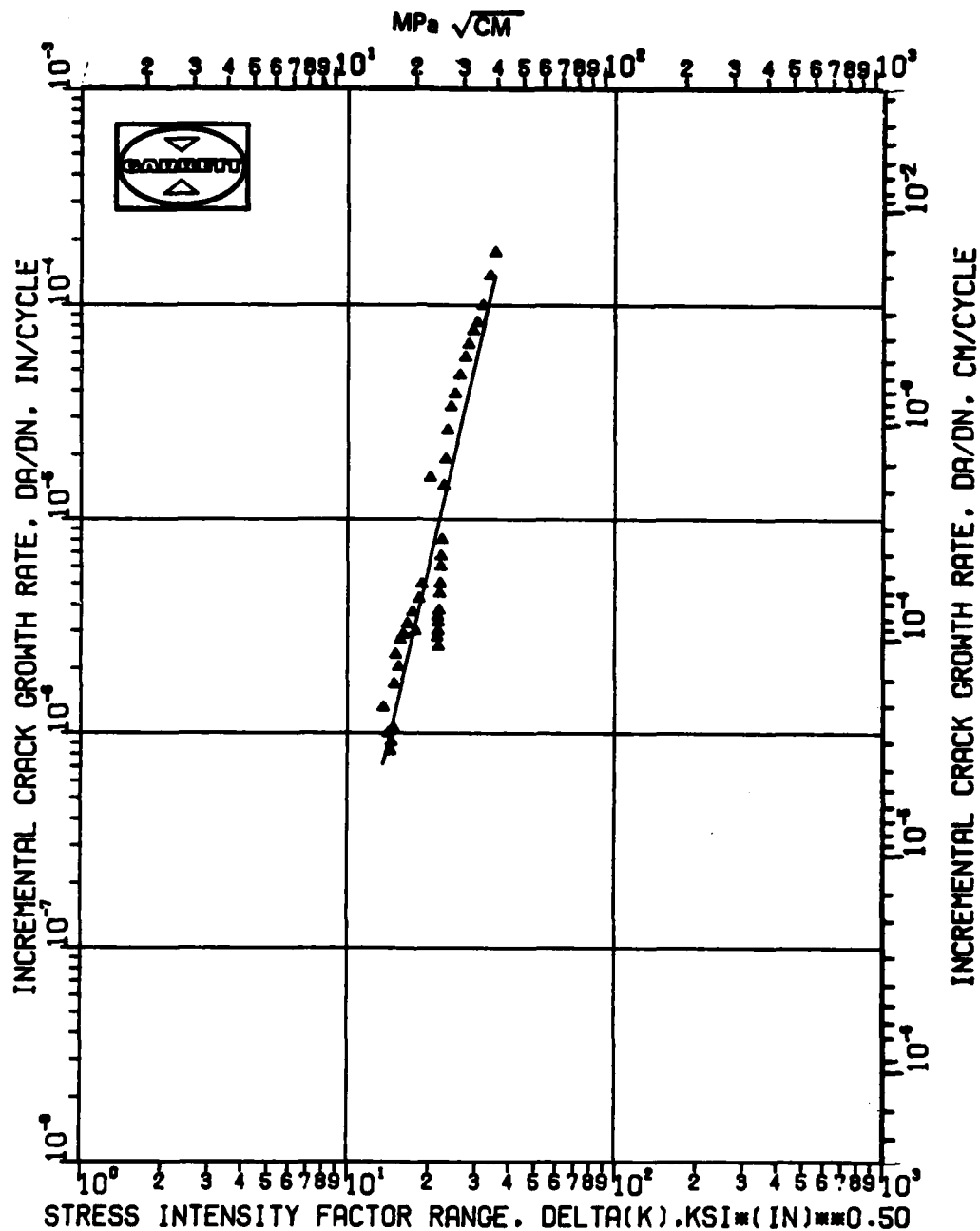
7 data points. A modified sigmoidal fit was used to find the average growth rate for the $R = -1.0$ and $R = 1.5$ data. For the $R = 0.0$ data, a linear technique was used to determine the average growth rate because of the limited data for $R = 0.0$. The curves are plotted in Figures 3-31, 3-32, and 3-33.

3.6.2.3.2 Discussion

The crack-growth rates for the three R ratios are compared in Figure 3-34. The minor differences in the range of crack-growth rates, 10^{-6} to 10^{-4} inch per cycle are within the expected scatter for crack-growth testing which is usually considered a factor of 2 on growth rate. The differences at crack-growth rates below 10^{-7} and above 10^{-4} inches per cycle are due to differences in the curve fitting technique used, and the scatter in the data due to the large grain size of IN 100.

The crack-growth-rate testing did not provide an accurate measurement of the threshold stress intensity K_{TH} or the critical stress intensity, K_Q . Values for K_{TH} and K_Q were assumed in order to provide the asymptotes for the sigmoidal curve fit. As the average line approaches the asymptotes, the degree of curvature is dependent on the amount of data at the low and high-crack-growth rates. Additionally, the linear curve fit is not asymptotic and will give a different indication of the behavior at low and high-crack rates when compared to a sigmoidal curve fit. However, due to insufficient data for $R = 0.0$, a linear curve fit was needed.

Additional scatter came from the crack fronts growing unevenly caused by cracks growing quicker on one surface than on the opposite surface. The alignment on the machines was checked after the first specimen exhibited this behavior and was found to be accurate. The cracks continued to grow unevenly despite efforts to obtain even growth. It is conjectured that the large grain size of IN 100 and the



AVERAGE $\text{LN}(\text{DA/DN}) = A_0 + A_1 \cdot X$

$A_0 = -28.3775$

TEMP = 1100 F

WHERE

$X = \text{LN}(\Delta K)$

$A_1 = 5.4539$

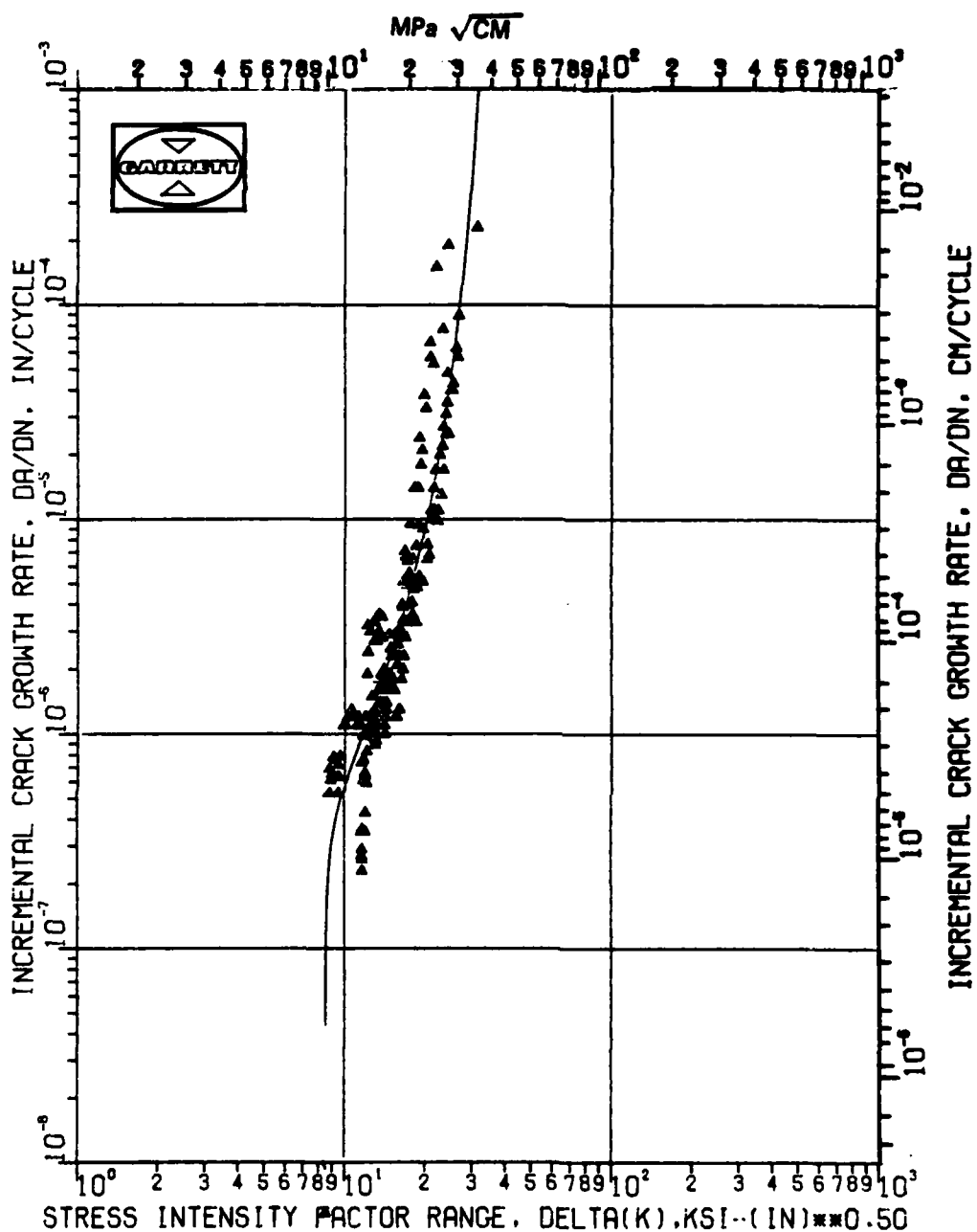
$R = 0.000$

FREQ = 0.50 HZ

SPECIMEN TYPE = PAP244387

NO. OF SPECIMENS = 2

Figure 3-31. Crack Growth Rate Data for IN-100.



AVERAGE $\ln(da/dN) = B + P \ln(X) + Q \ln(Y) + D \ln(Z)$ $B = -11.6072$ $KT = 8.50$ $TEMP = 1100 \text{ F}$
 WHERE $X = \ln(\Delta K / KT)$ $P = -2.1151$ $KC = 40.00$ $R = -1.000$
 $Y = \ln(KC / \Delta K)$ $Q = 0.4147$ $FREQ = 30.00 \text{ HZ}$
 $D = -5.1361$ $SPECIMEN \text{ TYPE} = \text{PAP 244387}$
 $NO. \text{ OF SPECIMENS} = 5$

Figure 3-32. Crack Growth Rate Data for IN-100.

4-A122 982

TPE331/T78 TURBOPROP PROPULSION ENGINE DURABILITY(U)
GARRETT TURBINE ENGINE CO PHOENIX AZ L P WYNN AUG 82
21-3640(22) AFWAL-TR-82-4069 F33615-81-C-5016

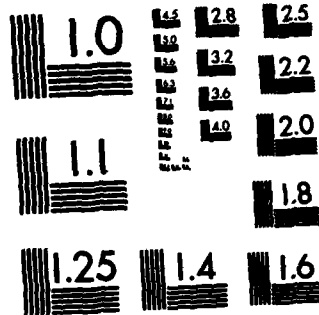
2/2

UNCLASSIFIED

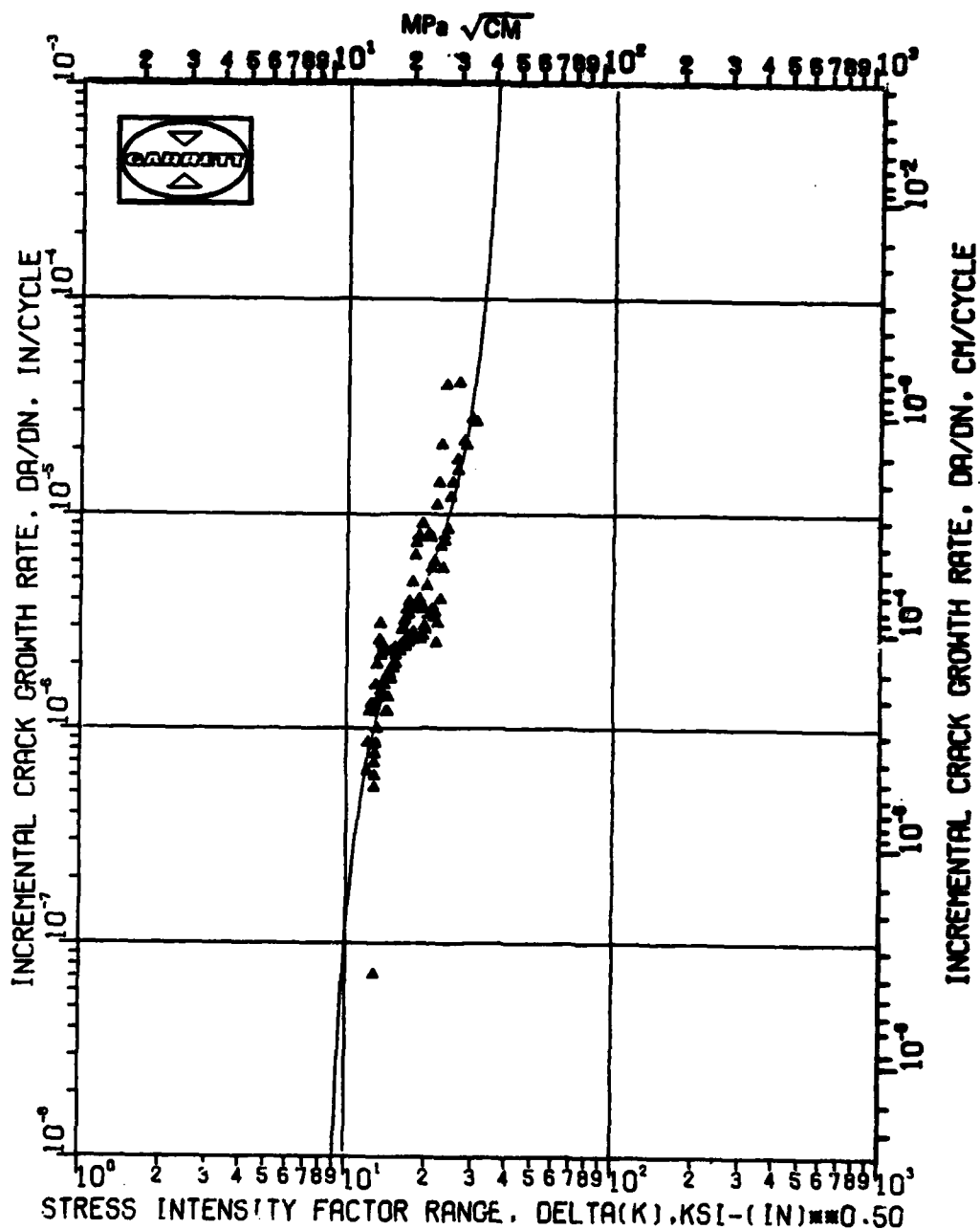
F/G 21/5

NL

END
DATE
FILMED
283
DTIC



MICROCOPY RESOLUTION TEST CHART
NATIONAL BUREAU OF STANDARDS-1963-A



AVERAGE $\ln(da/dN) = B + P \ln(X) + Q \ln(Y)$

WHERE

$X = \ln(\Delta K / K_T)$

$Y = \ln(K_C / \Delta K)$

$B = -8.0845$ $K_T = 8.50$

$P = -5.7902$ $K_C = 40.00$

$Q = 3.1796$

$D = -3.6706$

TEMP = 1100 F

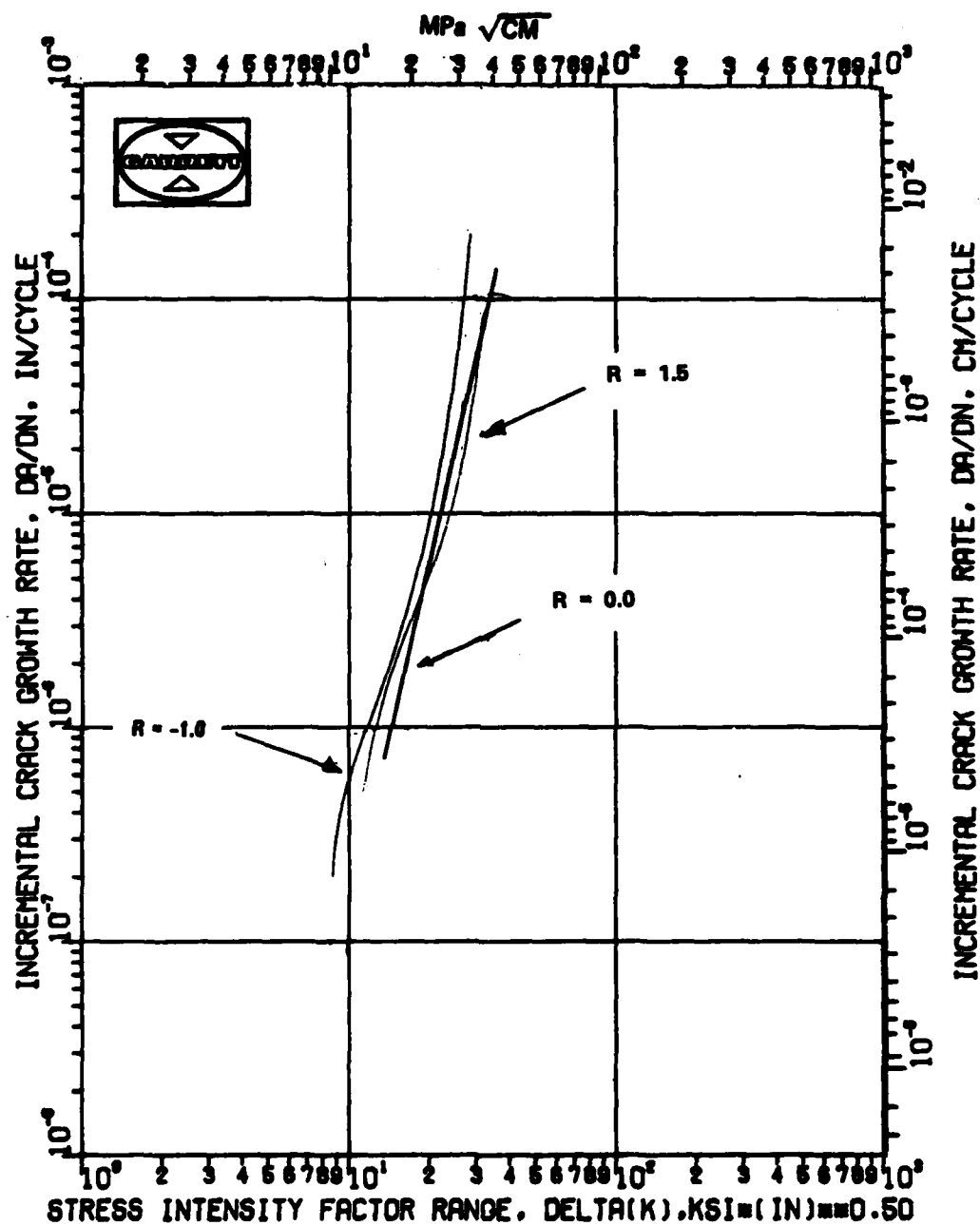
$R = -1.500$

FREQ = 30.00 HZ

SPECIMEN TYPE = PAP 244387

NO. OF SPECIMENS = 3

Figure 3-33. Crack Growth Rate Data for IN-100.



TEMP = 593°C (1100°F)
 R = 0.000, -1.0, -1.5
 FREQ = 0.50 HZ
 SPECIMEN TYPE = PAP244387

Figure 3-34. Crack Growth Rate Data for IN-100.

small size of the specimen caused the uneven growth. Relatively few grains are contained across the width of the specimen. When the crack started at one corner of the notch, it could grow a distance without running into a grain boundary. Once the crack fronts became uneven, the loading becomes uneven and the problem is accentuated. Therefore, the threshold and final failure region of the curve should not be taken as a true threshold or fracture toughness.

3.6.3 Conclusions of Materials Testing

1. Tensile strength is constant over the temperature range of 24°C (75°F) to 593°C (1100°F).
2. Ductility increases slightly with temperature.
3. LCF at 1100°F is consistent with the baseline data at 75°F , 426°C (800°F), and 648°C (1200°F).
4. There was no significant difference between crack growth rates for $R = 0.0$, -1.0 , and -1.5 .
5. The large grain size of IN 100 caused considerable scatter in the crack growth rate.

3.7 Analytical Life Prediction

3.7.1 Crack Propagation Analysis

Fracture mechanics life prediction requires calculation of crack-tip stress intensity factors to quantify both subcritical crack growth and the conditions for unstable fracture in complex geometries under complex loading conditions which lead to high-stress gradients. The "BIGIF" (Boundary-Integral-Equation-Generated-Influence-Functions) codes have been developed and distributed to perform accurately and inexpensively these life predictions for a wide range of two- and three-dimensional elastic and contained plastic stress fields, and crack and structural geometries, given that the elastic stress for the uncracked structure is available from an independent source.

The independent source for these elastic stresses is the three-dimensional stress analysis. This analysis was conducted under this program and uses the Garrett Program IS03DQ.

Three areas of interest have been analyzed. These areas are the forward and aft corner cracks at the bottom of the rivet hole and corner cracks in the small hole that is used as a rivet retainer.

The crack-growth rate analysis has been calculated for the maximum principle stress fields for all three crack locations. The forward-crack growth is shown in Figure 3-35. The aft-crack growth is shown in Figure 3-36, and the rivet-retainer crack growth is shown in Figure 3-37.

The crack depth versus crack length for the forward aft and the rivet-retainer hole crack locations are shown in Figures 3-38 through 3-40. This data was used to correlate crack-aspect ratio from field examination with calculated values.

The stress-intensity factor as a function of crack depth is shown in Figures 3-41 through 3-43 for the same crack locations.

3.7.2 Low-Cycle-Fatigue Prediction

The low-cycle-fatigue prediction for the forward and aft-rivet hole areas are summarized in Table 3-19.

The trends observed in the data indicate that there is a large variation in rivet-hole cracks from slot-to-slot, and from wheel-to-wheel. A slot may have a large crack at the "A" location, and the very next slot may have no crack. There is also no relationship between a crack at location "A" and a crack at any other location for any one slot. The relationship between cracks for any slot that has cracks at more than one location is shown in Figures 3-44 through 3-49.

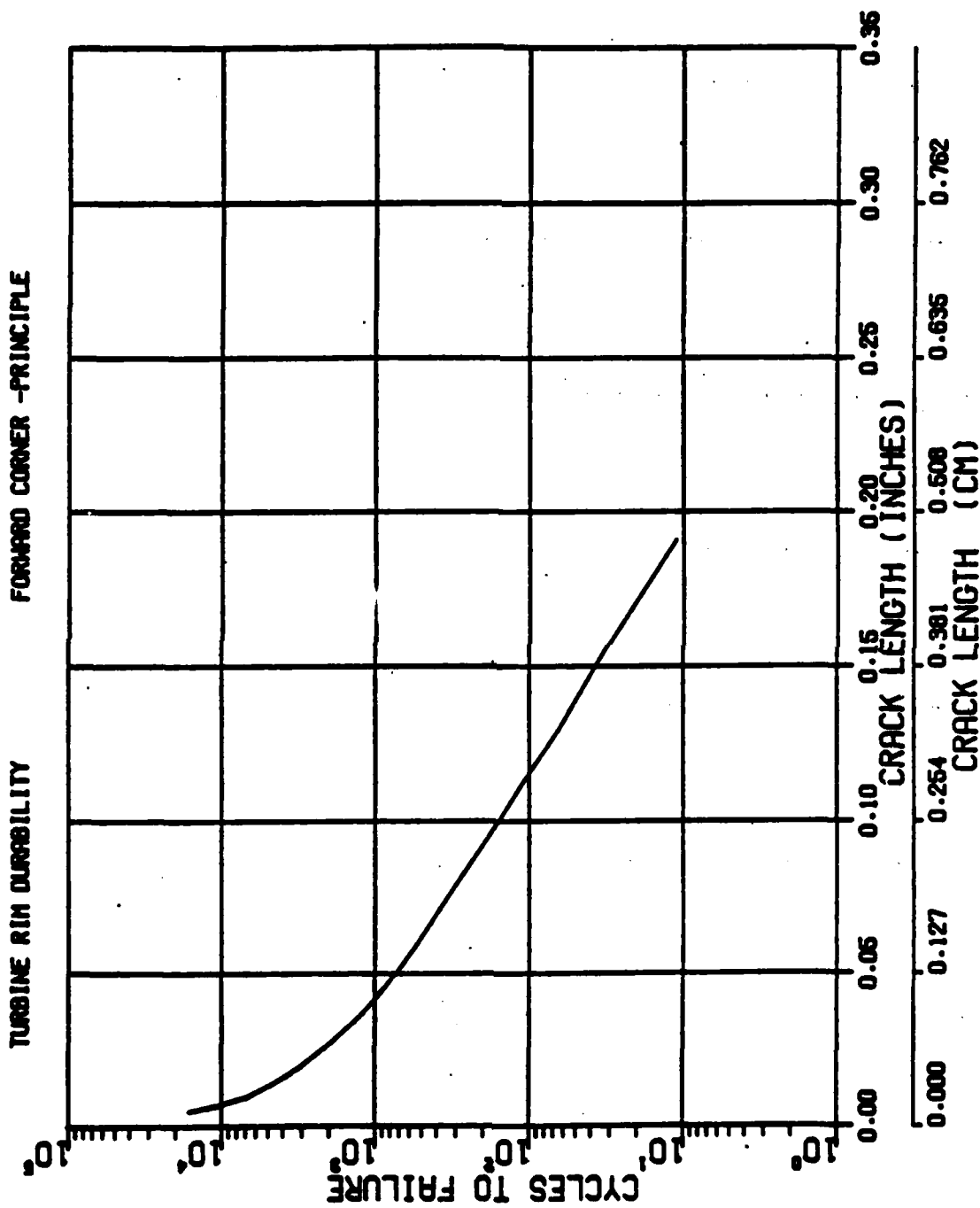


Figure 3-35. Cycles to Failure Versus Crack Length, Turbine Rim Durability, Forward Corner - Principle.

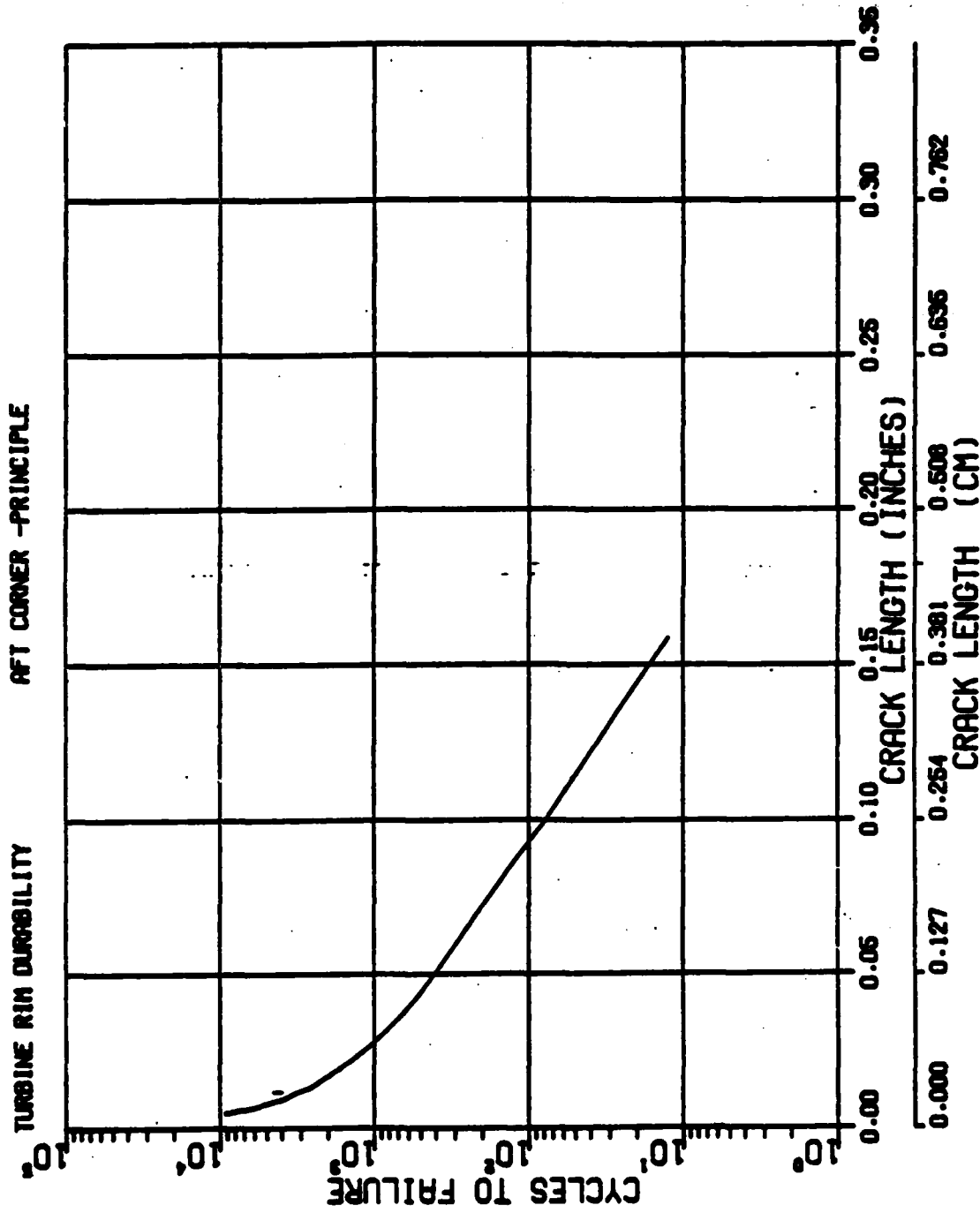


Figure 3-36. Cycles to Failure Versus Crack Length, Turbine Rim Durability, Aft Corner - Principle.

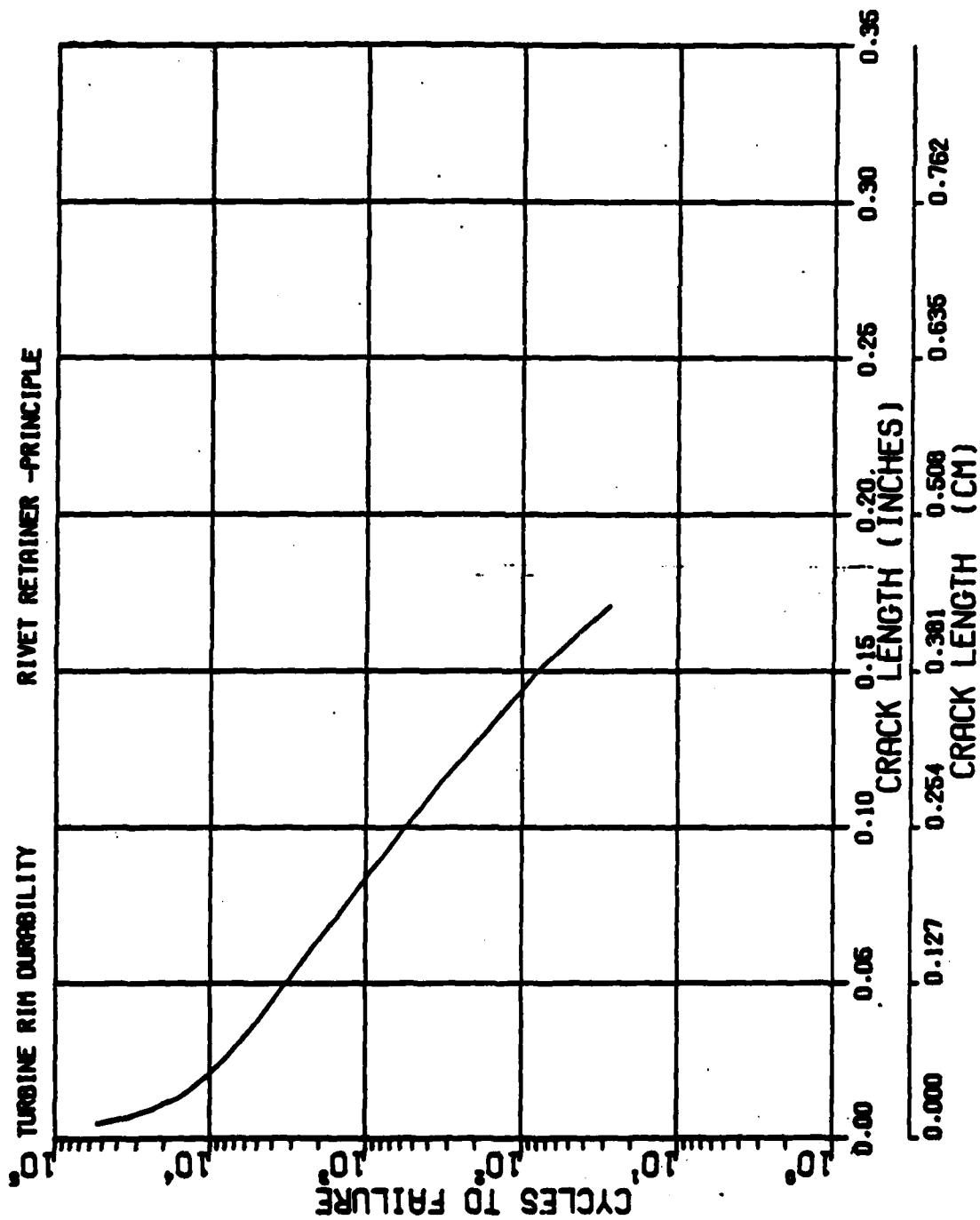


Figure 3-37. Cycles to Failure Versus Crack Length, Turbine Rim Durability, Rivet Retainer - Principle.

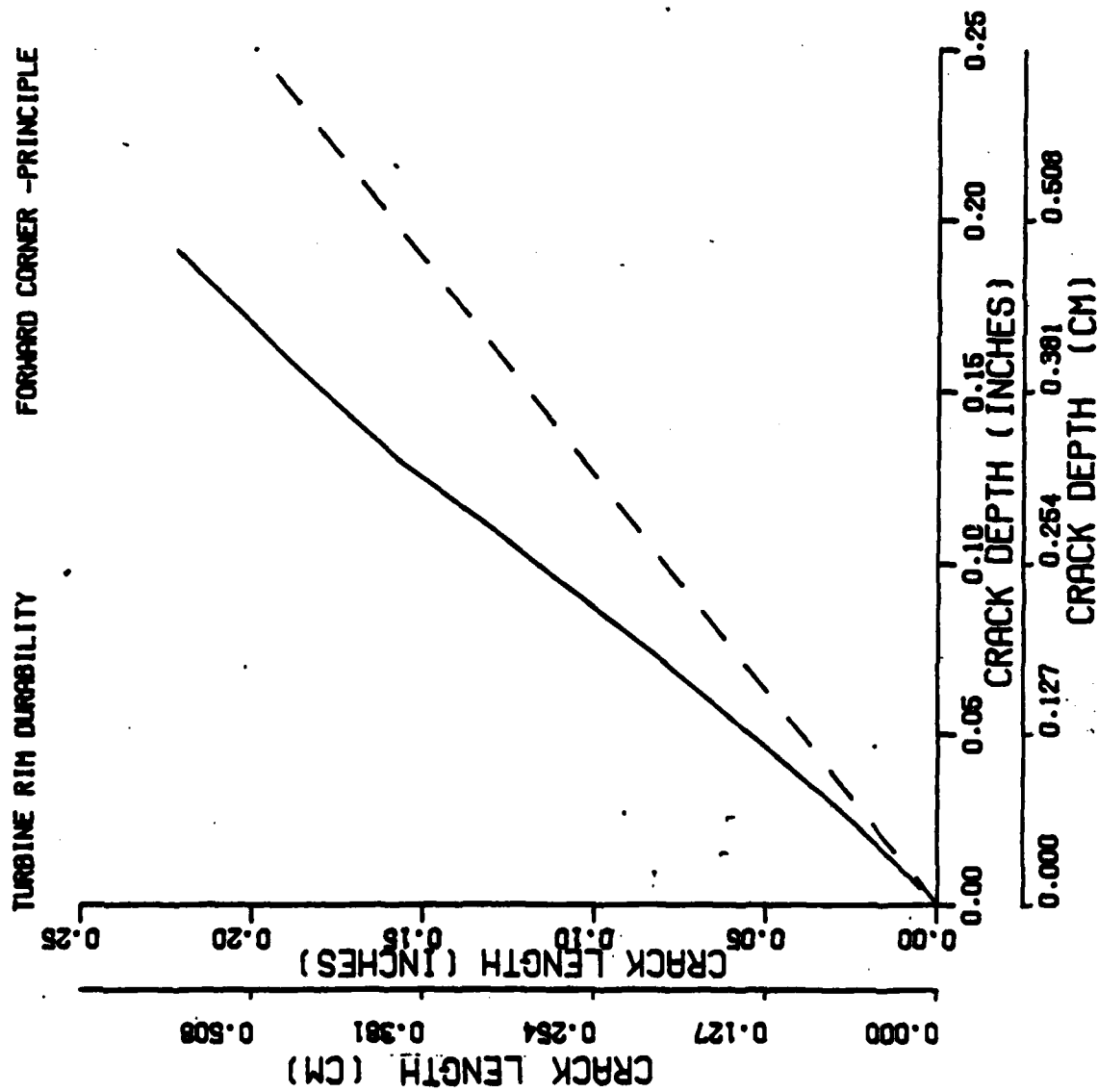


Figure 3-38. Crack Length Versus Crack Depth, Turbine Rim Durability, Forward Corner - Principle.

TURBINE RIM DURABILITY

AFT CORNER - PRINCIPLE

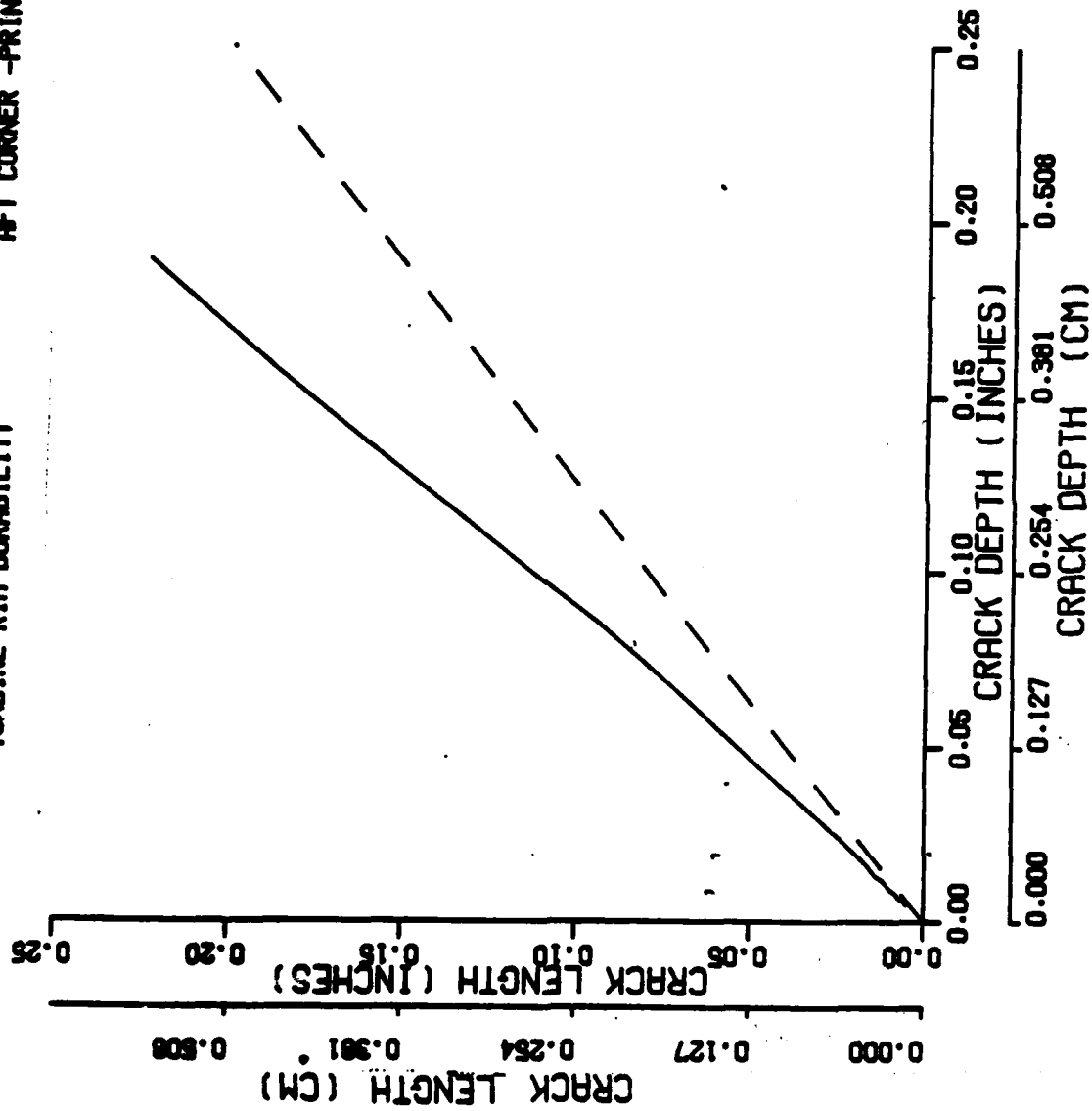


Figure 3-39. Crack Length Versus Crack Depth, Turbine Rim Durability, Aft Corner - Principle.

TURBINE RIM DURABILITY

RIVET RETAINER - PRINCIPLE

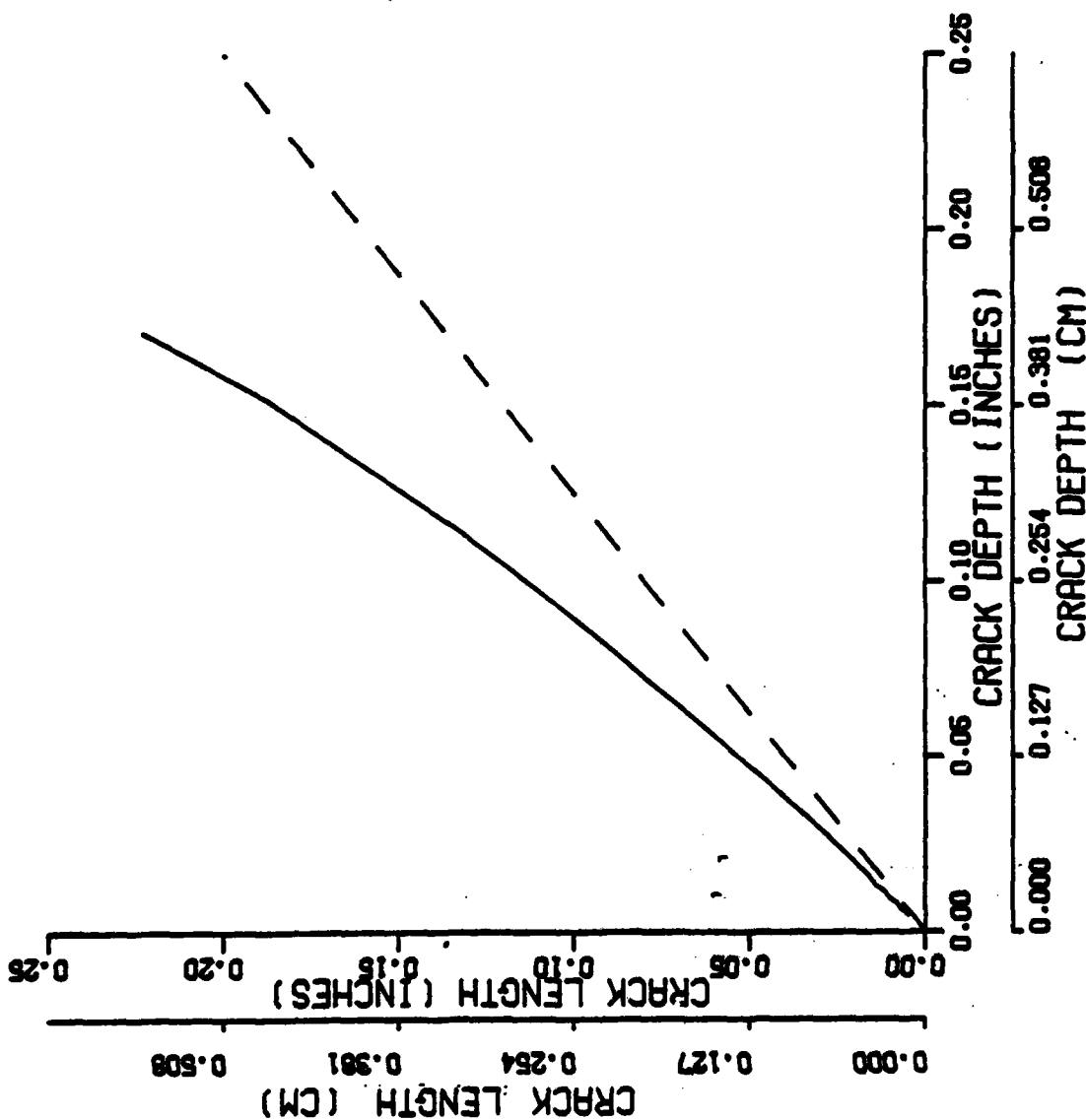


Figure 3-40. Crack Length Versus Crack Depth, Turbine Rim Durability, Rivet Retainer - Principle.

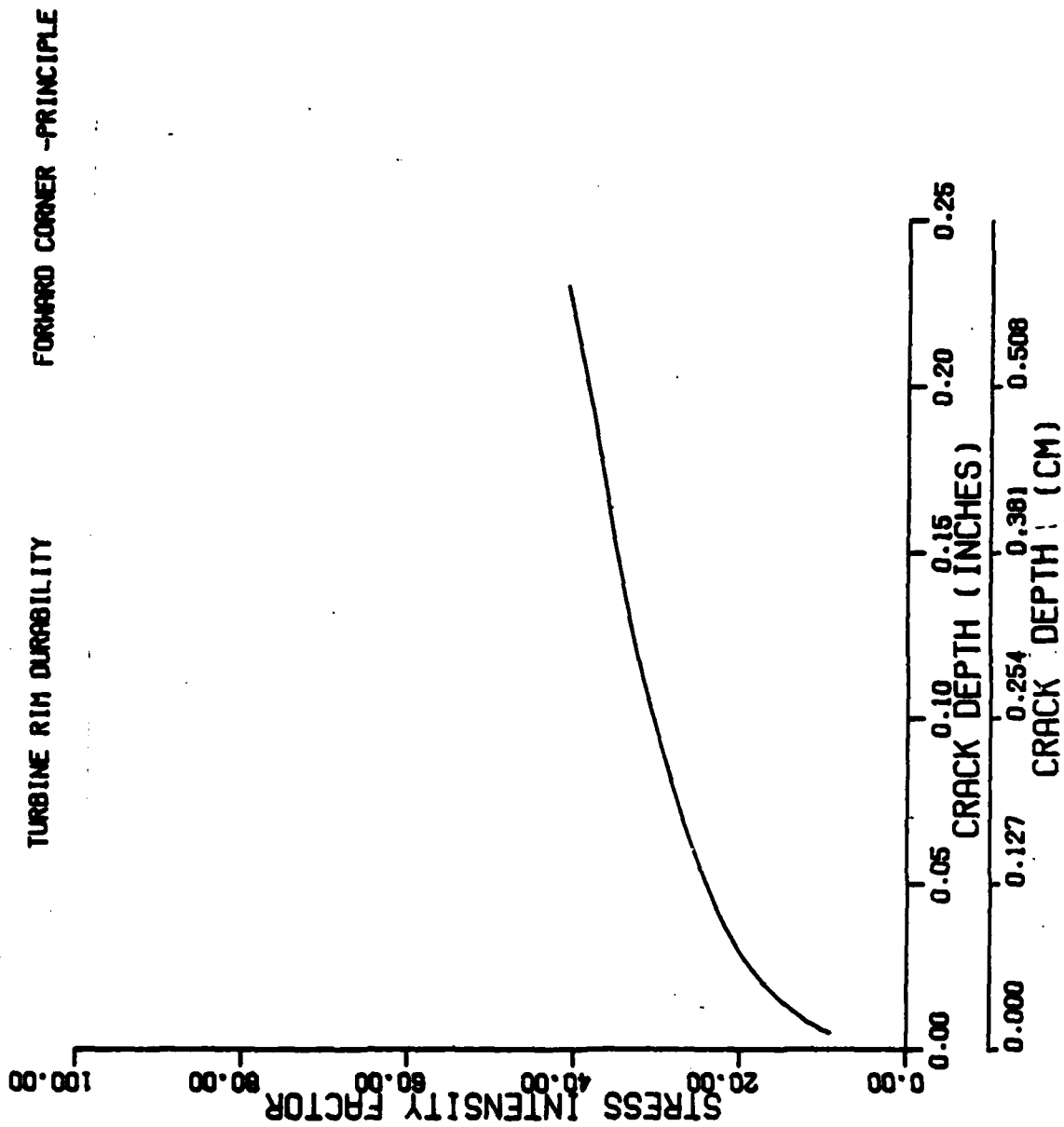


Figure 3-41. Stress Intensity Factor Versus Crack Depth, Turbine Rim Durability, Forward Corner - Principle.

TURBINE RIM DURABILITY

AFT CORNER -PRINCIPLE

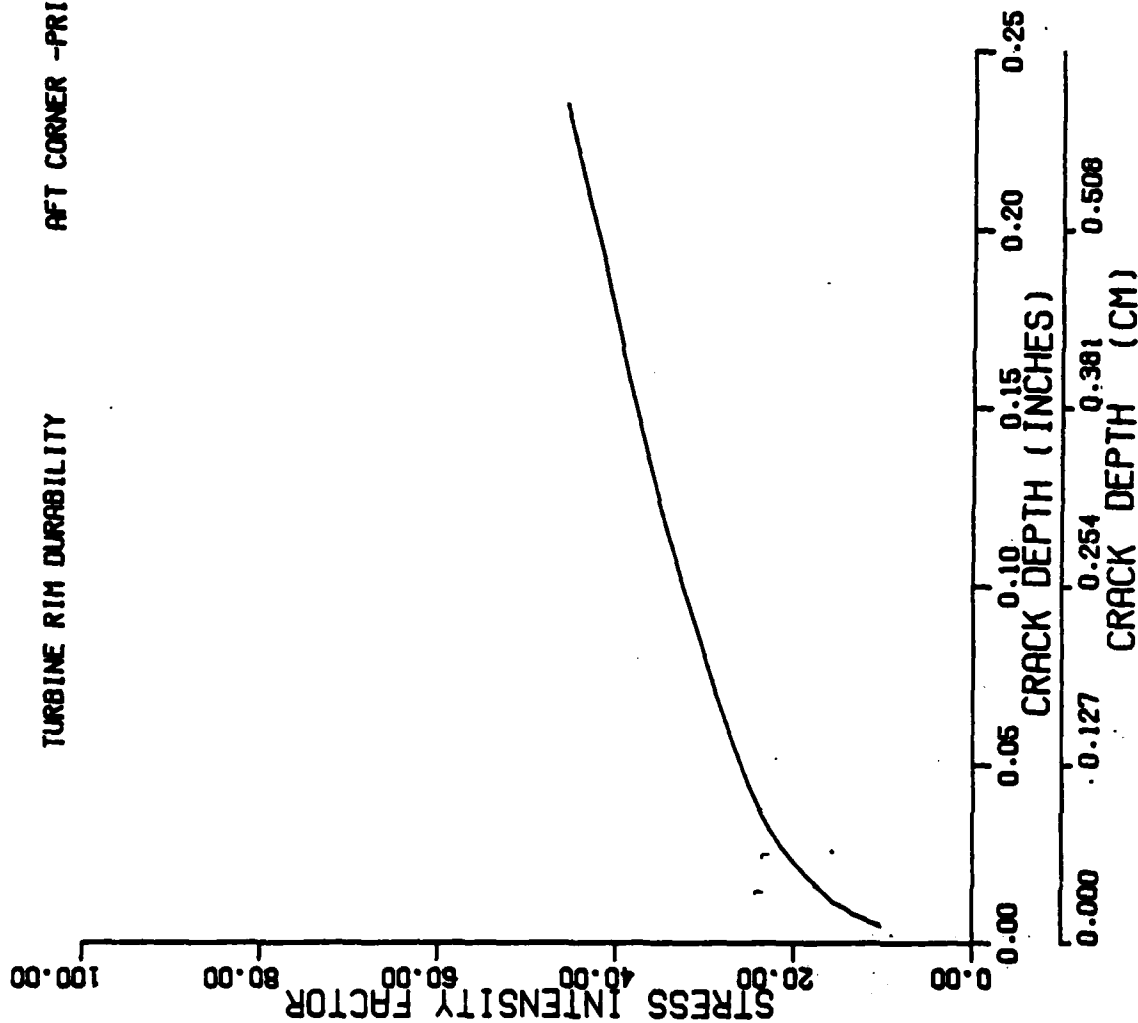


Figure 3-42. Stress Intensity Factor Versus Crack Depth, Turbine Rim Durability, Aft Corner - Principle.

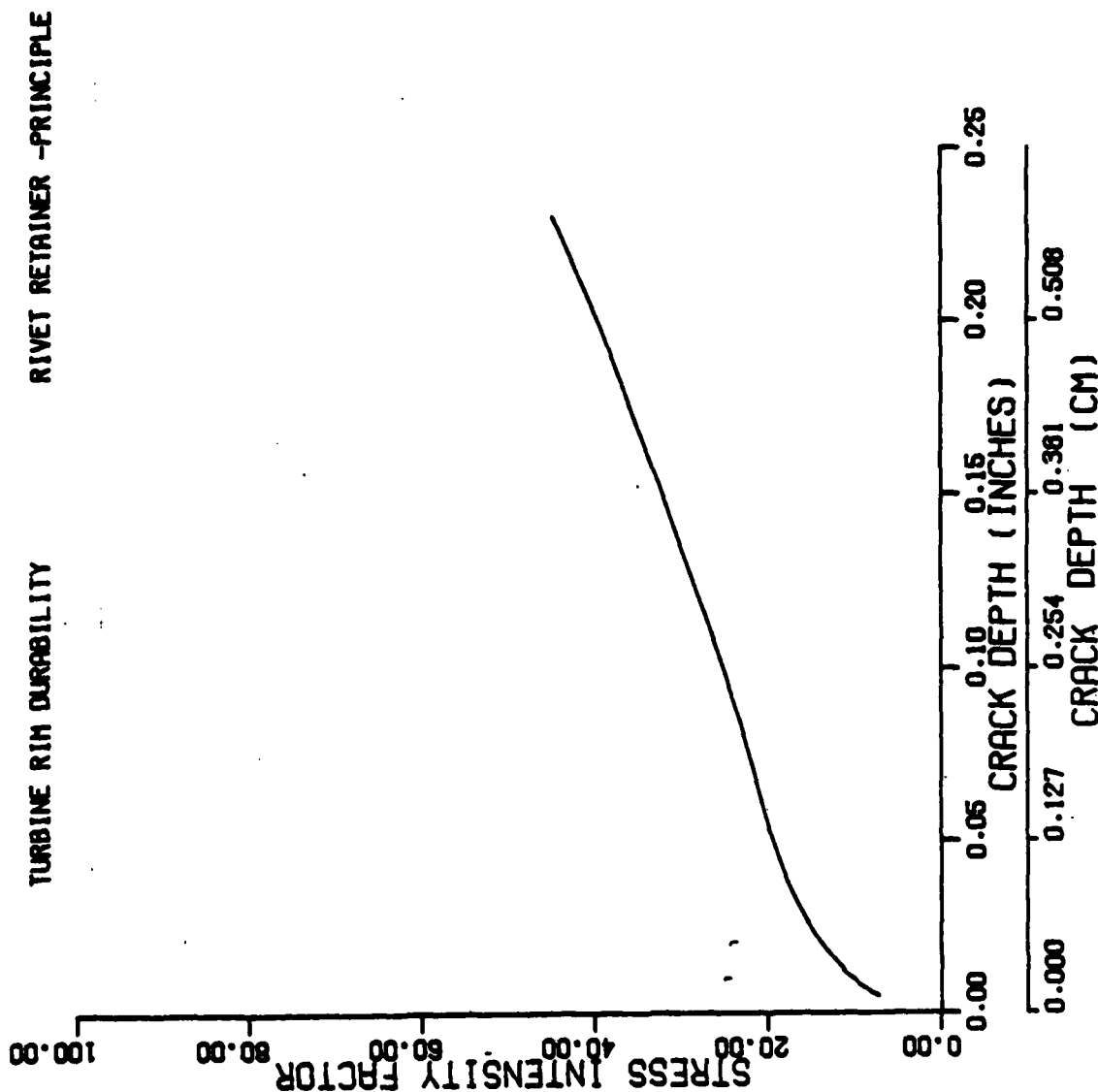


Figure 3-43. Stress Intensity Factor Versus Crack Depth, Turbine Rim Durability, Rivet Retainer - Principle.

TABLE 3-19. LCF LIFE PREDICTION SUMMARY.

	Stress Range Ksi	Cold Start		Stress Range Ksi	Warm Start		Total Life*	
		Min. Life Cycle	Avg. Life Cycle		Min. Life Cycle	Avg. Life Cycle	Min. Cycle	Max. Cycle
"A" Forward Rivet Area	210	205	650	174	535	1700	435	4380
"B" Aft Rivet Area	215	180	570	184	453	1440	372	3740

$$*TOTAL LIFE = \frac{1}{7} \text{ Cold} + \frac{1}{6} \text{ Warm}$$

(1 cold start for every 6 warm starts)

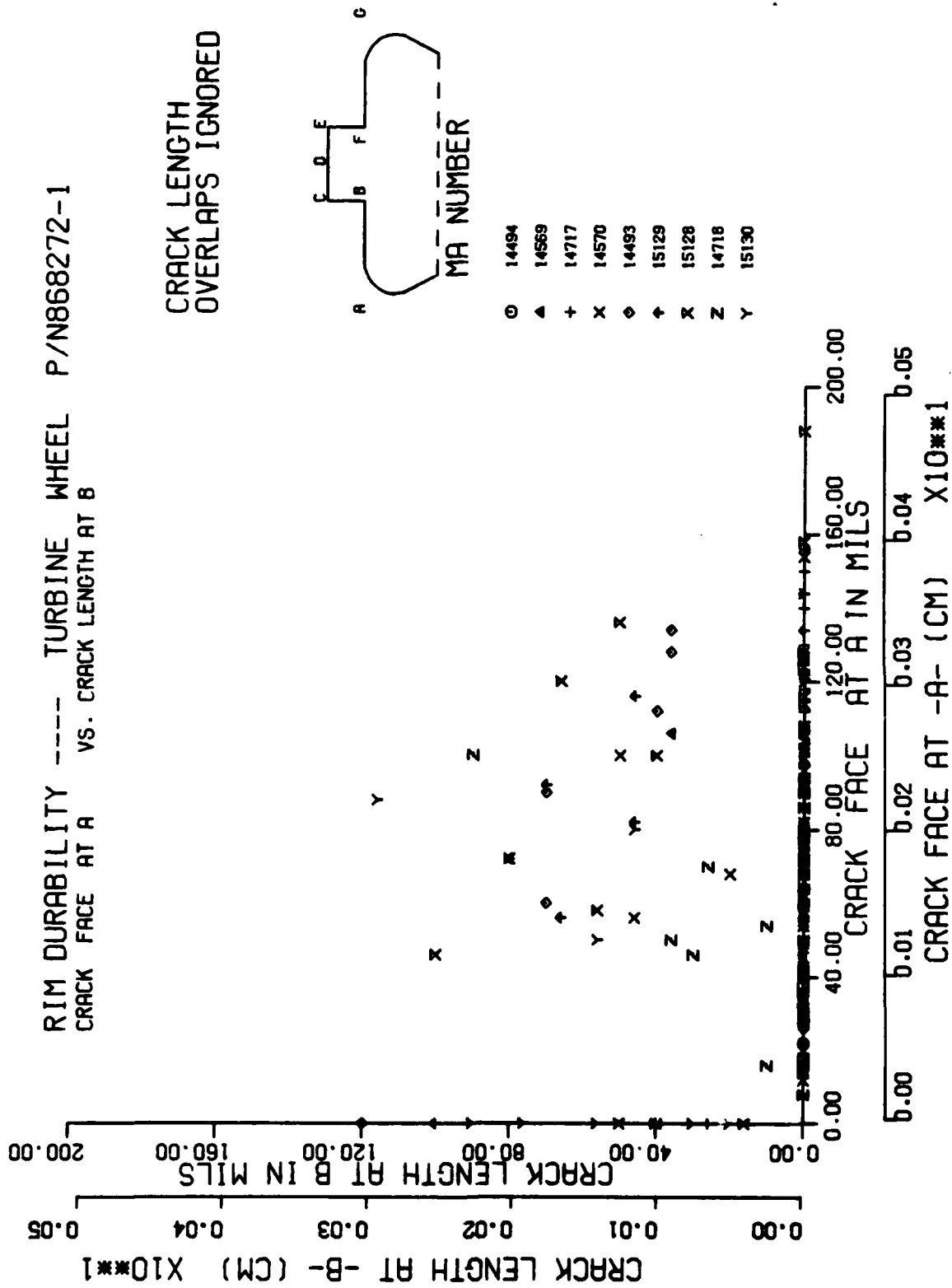
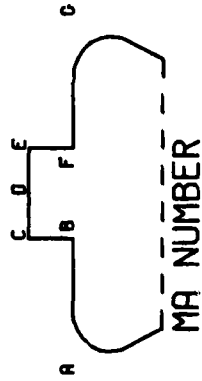


Figure 3-44. Crack Face at A Versus Crack Length at B.

RIM DURABILITY ---- TURBINE WHEEL P/N868272-1
 CRACK FACE AT A VS. CRACK FACE AT C

CRACK LENGTH
 OVERLAPS IGNORED



MA NUMBER	Symbol
14494	O
14569	A
14717	+
14570	X
14493	◇
15129	+
15128	X
14718	Z
15130	Y

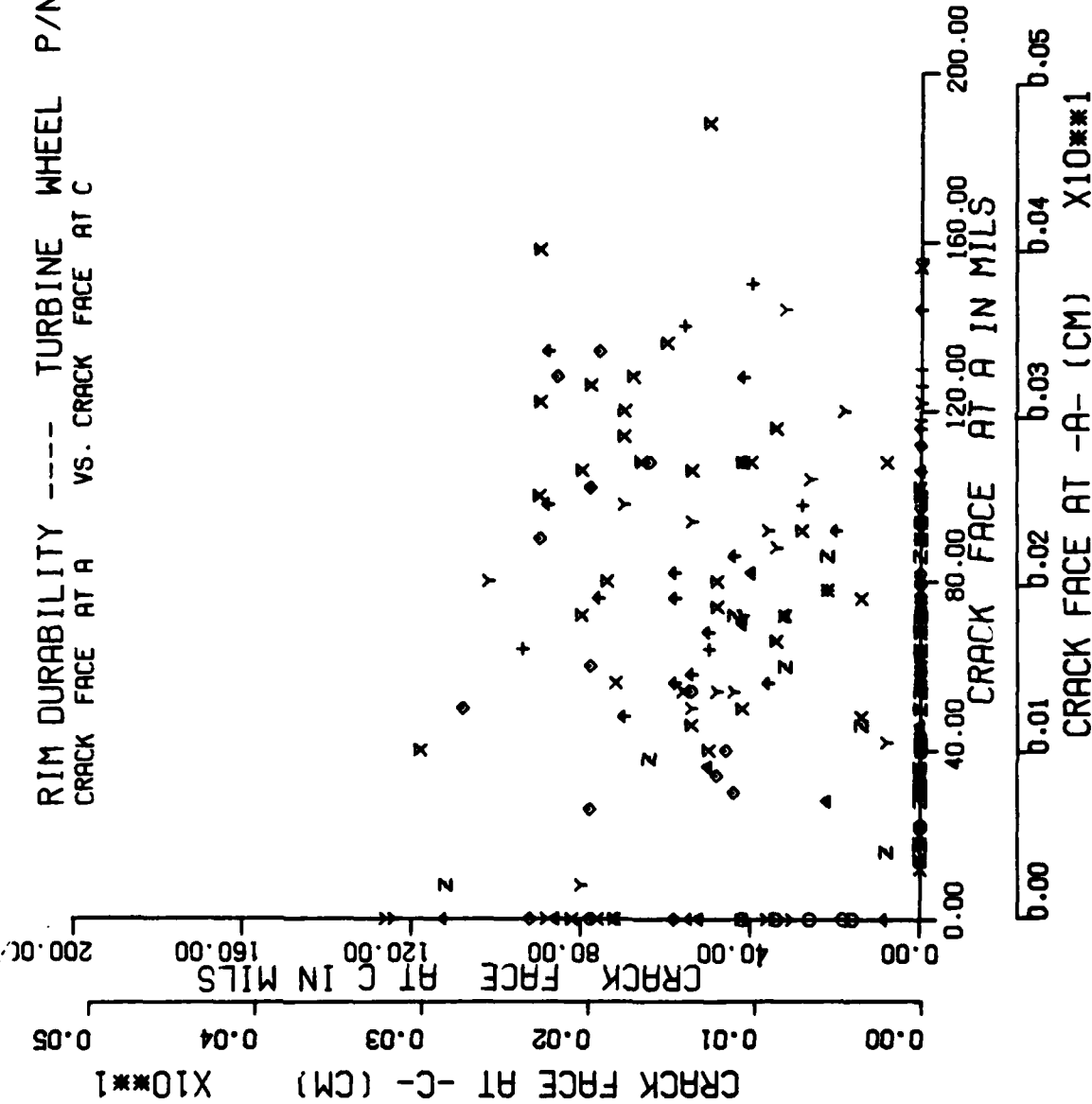


Figure 3-45. Crack Face at A Versus Crack Face at C.

RIM DURABILITY ----- TURBINE WHEEL P/N868272-1
 CRACK FACE AT A VS. CRACK LENGTH AT D

CRACK LENGTH
 OVERLAPS IGNORED

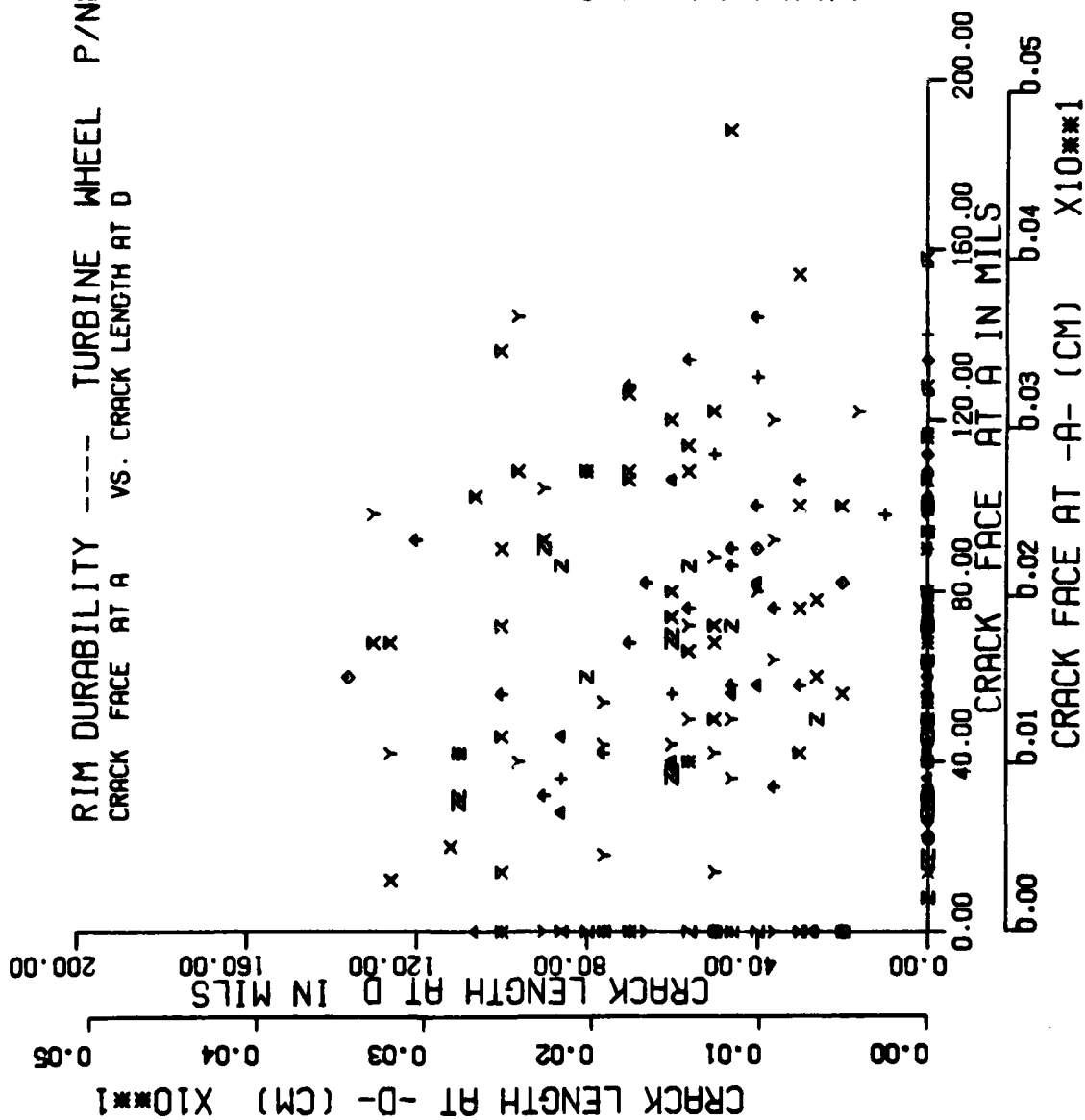


Figure 3-46. Crack Face at A Versus Crack Length at D.

RIM DURABILITY ----- TURBINE WHEEL P/N868272-1
 CRACK FACE AT A VS. CRACK FACE AT C

CRACK LENGTH
 OVERLAPS IGNORED

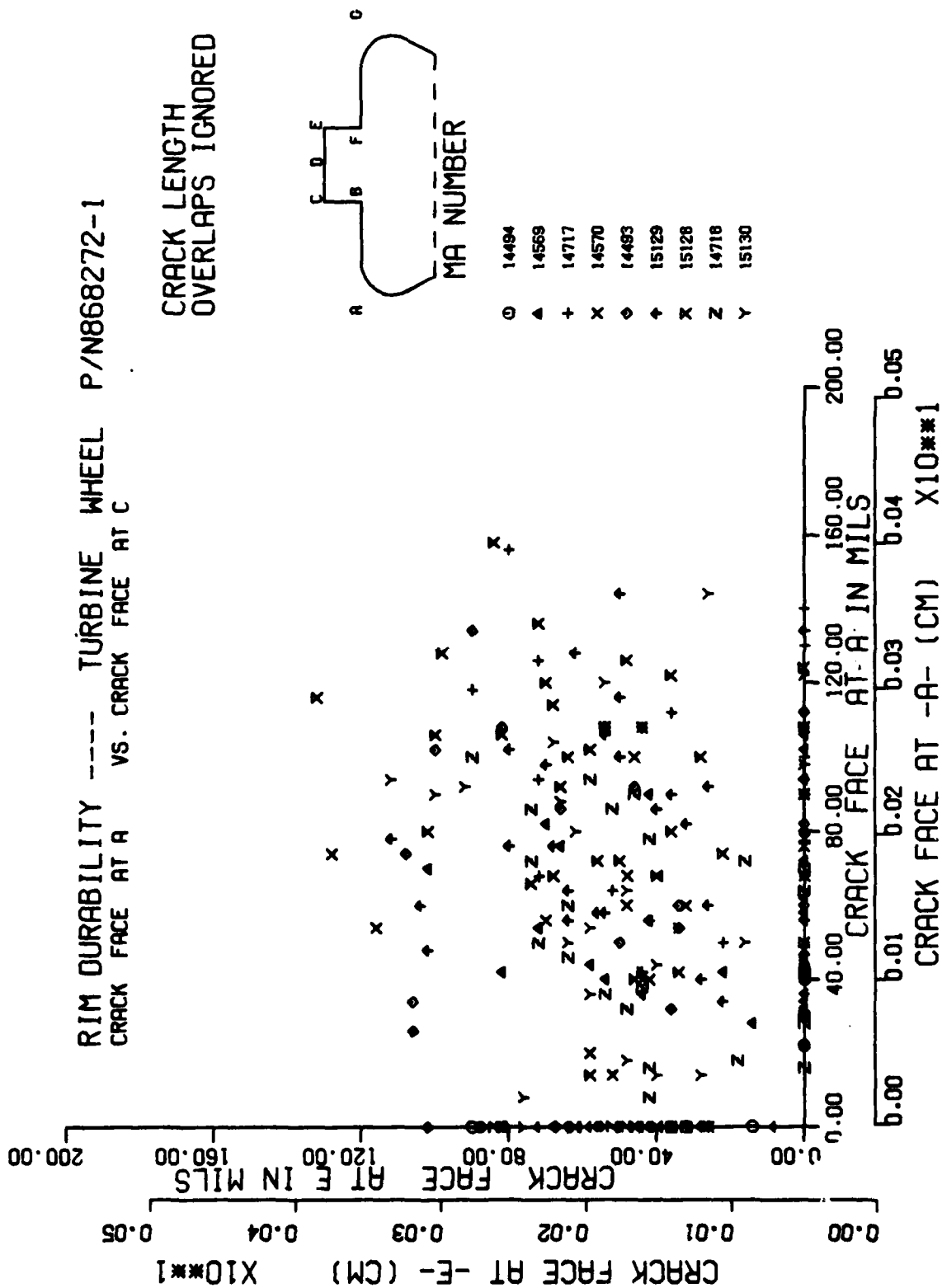


Figure 3-47. Crack Face at A Versus Crack Face at E.

RIM DURABILITY ----- TURBINE WHEEL P/N868272-1
 CRACK FACE AT A VS. CRACK LENGTH AT F

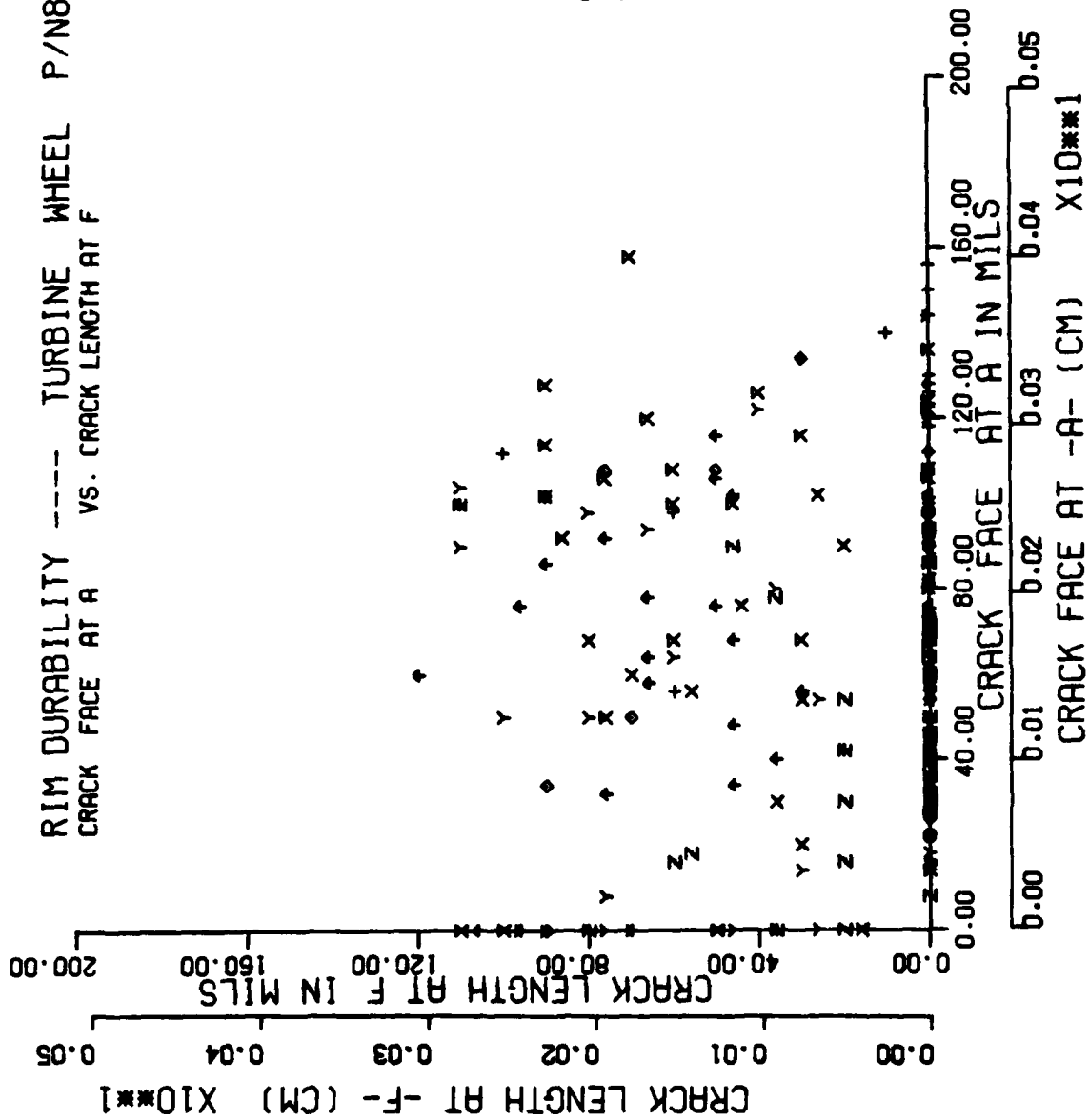


Figure 3-48. Crack Face at A Versus Crack Length at F.

RIM DURABILITY ---- TURBINE WHEEL P/N868272-1
 CRACK FACE AT A VS. CRACK FACE AT G

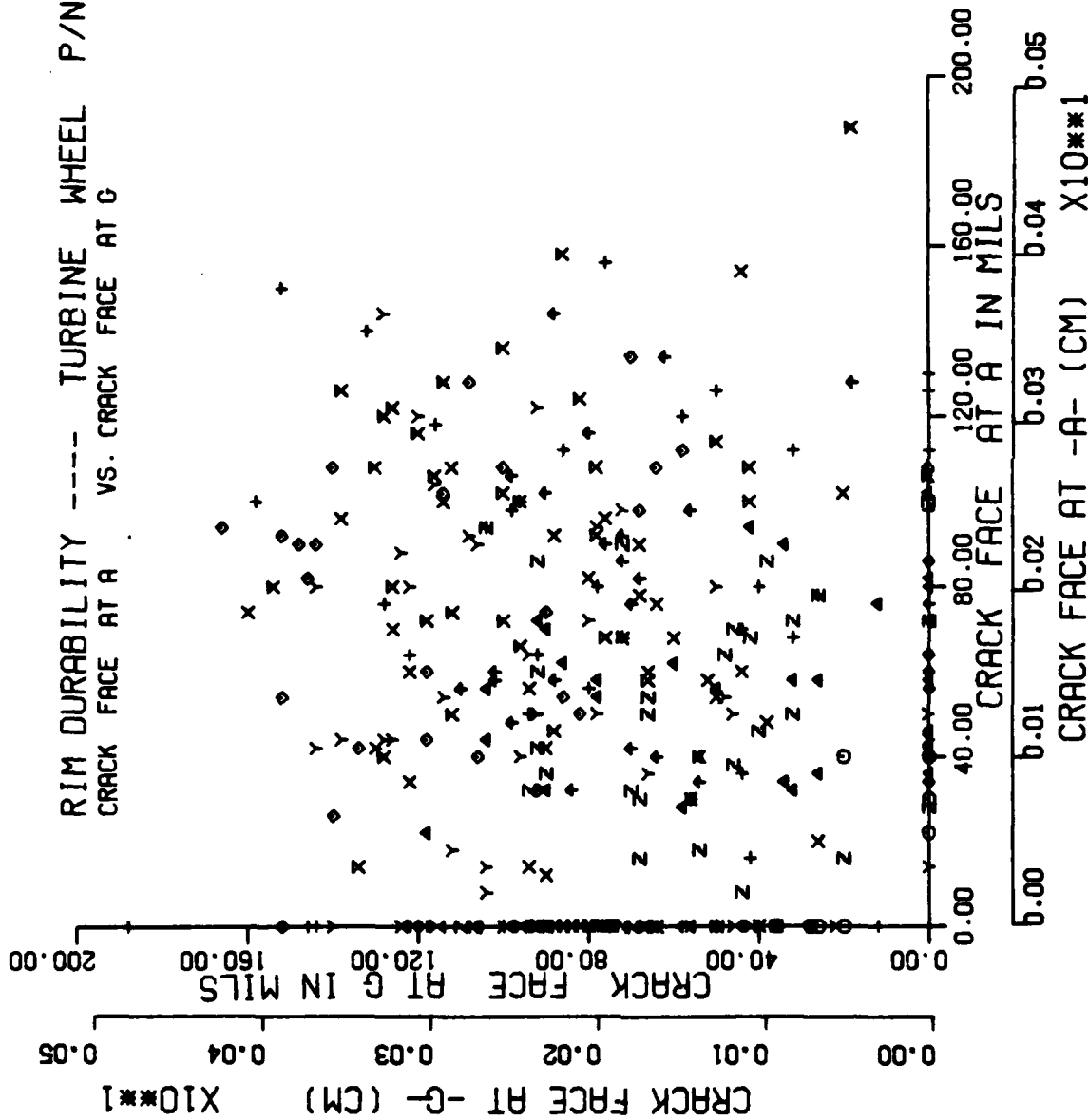


Figure 3-49. Crack Face at A Versus Crack Face at G.

It became obvious that the cracks at the high-stress areas must start at different locations around the peak-stress location due to machining marks and nonhomogenous material weaknesses; therefore, crack depth will show wide variation until the crack has achieved a rather large size.

3.8 Turbine Wheel Crack Characteristics from Field-Service Wheels

For the purpose of comparing the analytically predicted crack sizes and shapes predicted as described in Section 3.8, a program was initiated to examine wheels that were retired from service that had cracks in the rivet-hole area of interest. A total of 14 wheels were examined with cyclic lives ranging from 2400 to 5600 cycles. The data from the examination of these wheels were stored in a data bank so that cross-correlation between different wheels and between different rivet-hole locations could be examined.

For the purpose of identification a diagram of crack locations and directions is shown in Figure 3-50. The raw data is from the data bank reproduced in Appendix D.

For the above stated reasons a series of plots, using only the largest crack on each wheel, was plotted. These are shown in Figures 3-51 through 3-56 for the various correlations. From this correlation it is shown that the larger crack occurs most predominately at the "A" and "G" locations, and the largest cracks at "B" through "F" were always smaller than those at "A" or "G". Also as shown in Figure 3-56, the relationship between "A" and "G" is very close to one-to-one.

The field service wheel crack data was also used to estimate the aspect ratios of the cracks. Again, only the largest crack from each wheel was used to obtain these results. These are shown in Figures 3-57 through 3-62.

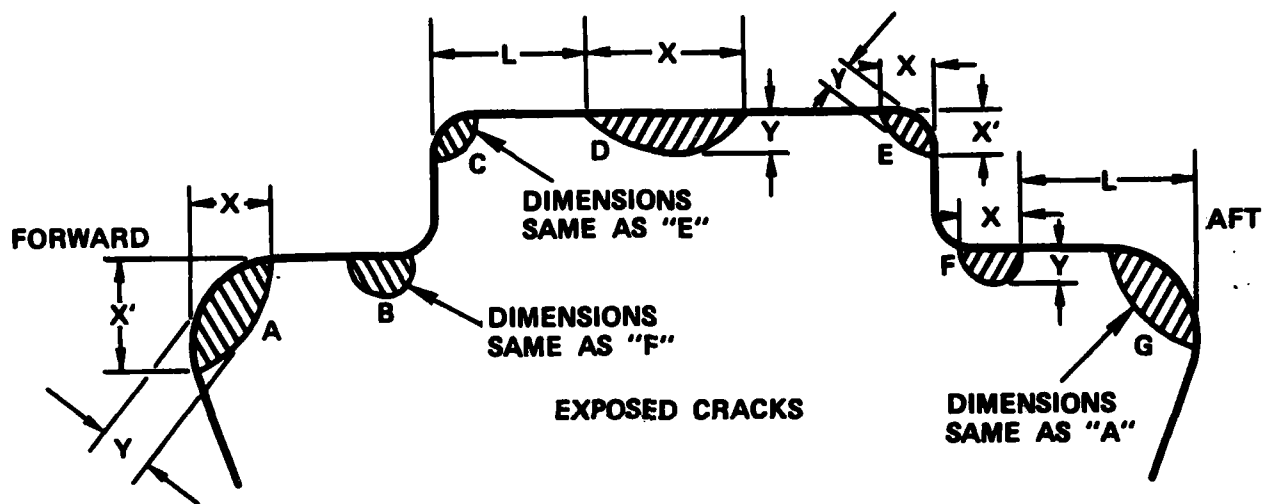
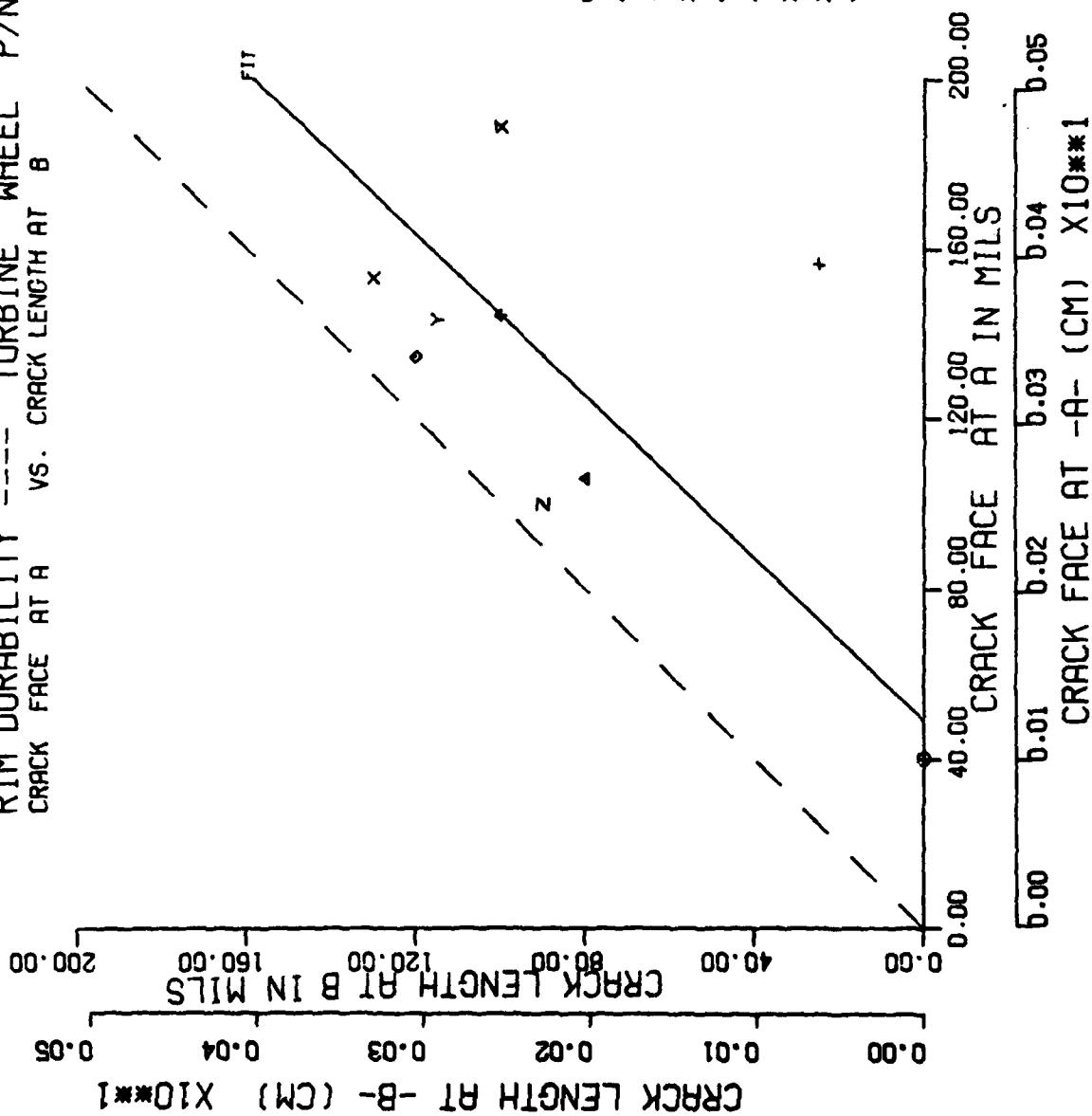
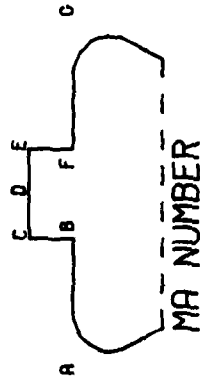


Figure 3-50. Crack Locations and Dimensions.

RIM DURABILITY ---- TURBINE WHEEL P/N868272-1
 CRACK FACE AT A VS. CRACK LENGTH AT B



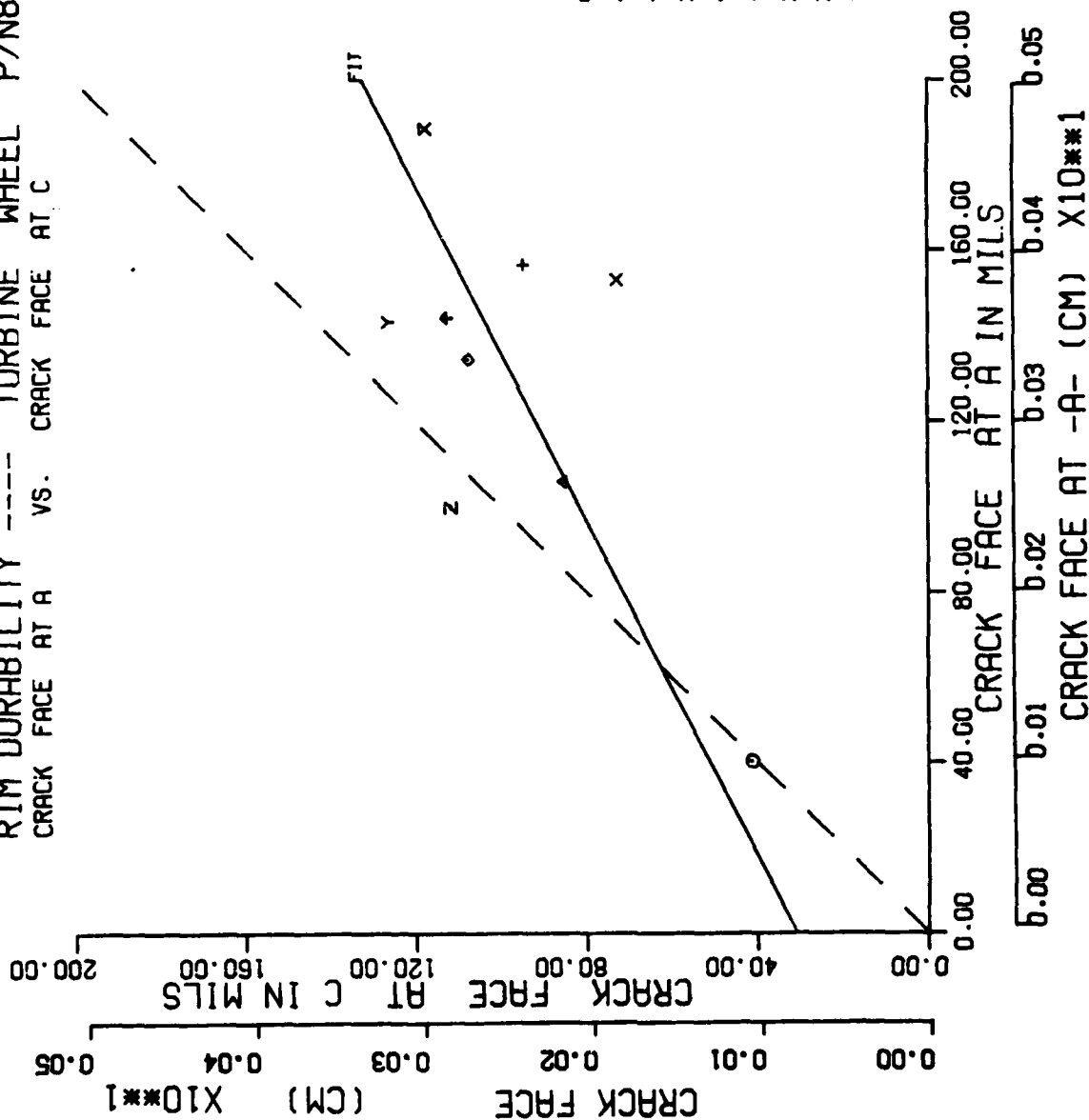
CRACK LENGTH
 OVERLAPS IGNORED
 MAXIMUMS FOR EACH WHEEL



21-3640 (22)
 3-95

Figure 3-51. Crack Face at A Versus Crack Length at B.

RIM DURABILITY --- TURBINE WHEEL P/N868272-1
 CRACK FACE AT A VS. CRACK FACE AT C



CRACK LENGTH
 OVERLAPS IGNORED
 MAXIMUMS FOR EACH WHEEL

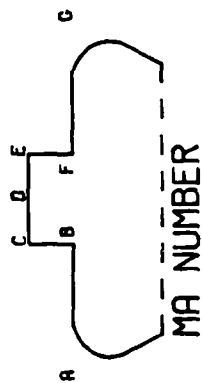
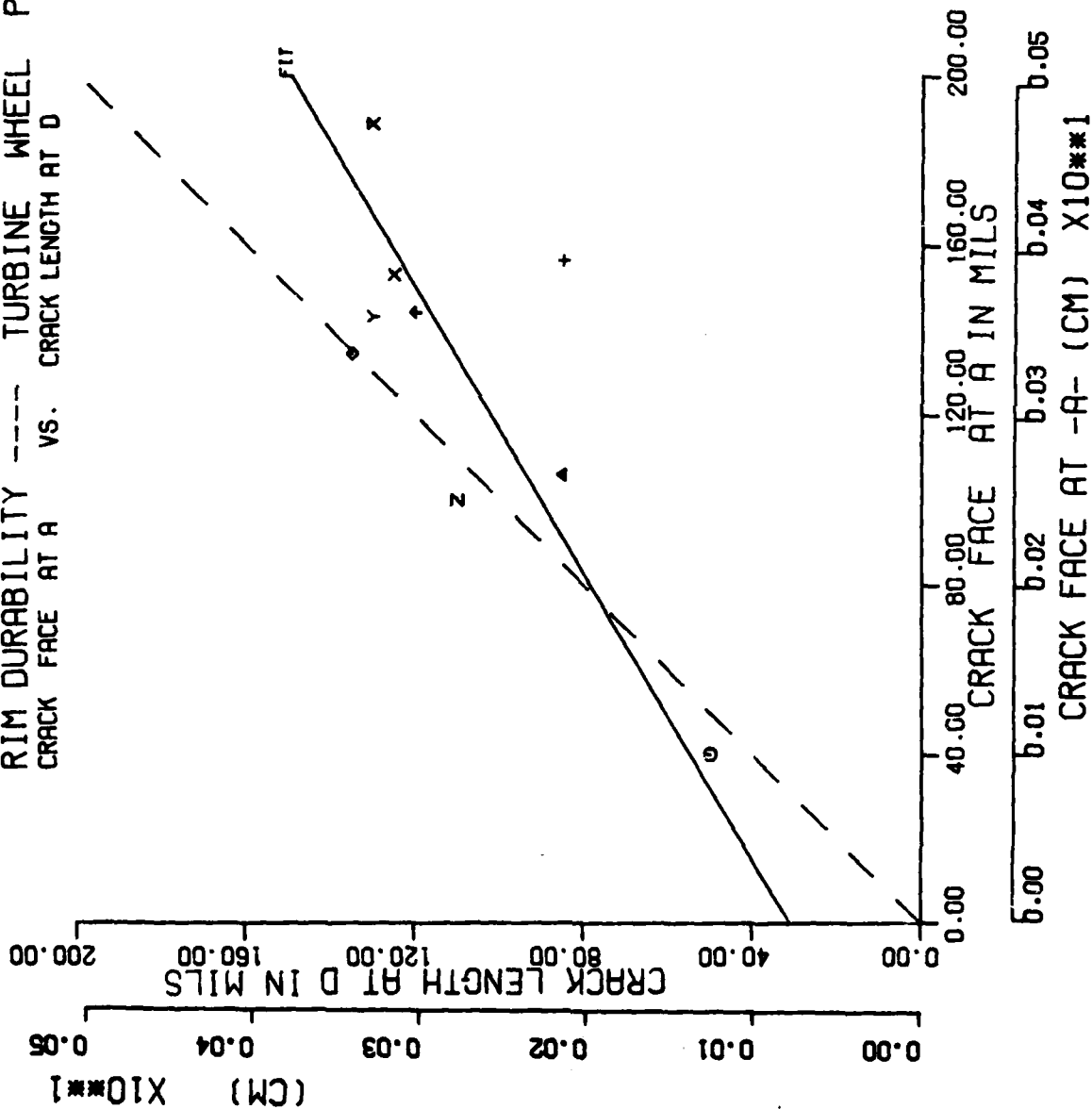


Figure 3-52. Crack Face at A Versus Crack Face at C.

RIM DURABILITY --- TURBINE WHEEL P/N868272-1
 CRACK FACE AT A VS. CRACK LENGTH AT D



CRACK LENGTH
 OVERLAPS IGNORED
 MAXIMUMS FOR EACH WHEEL

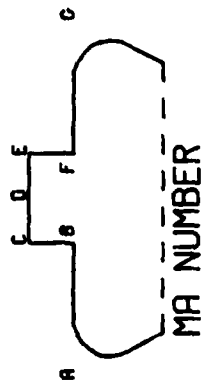


Figure 3-53. Crack Face at A Versus Crack Length at D.

RIM DURABILITY --- TURBINE WHEEL P/N868272-1
 CRACK FACE AT A VS CRACK FACE AT E

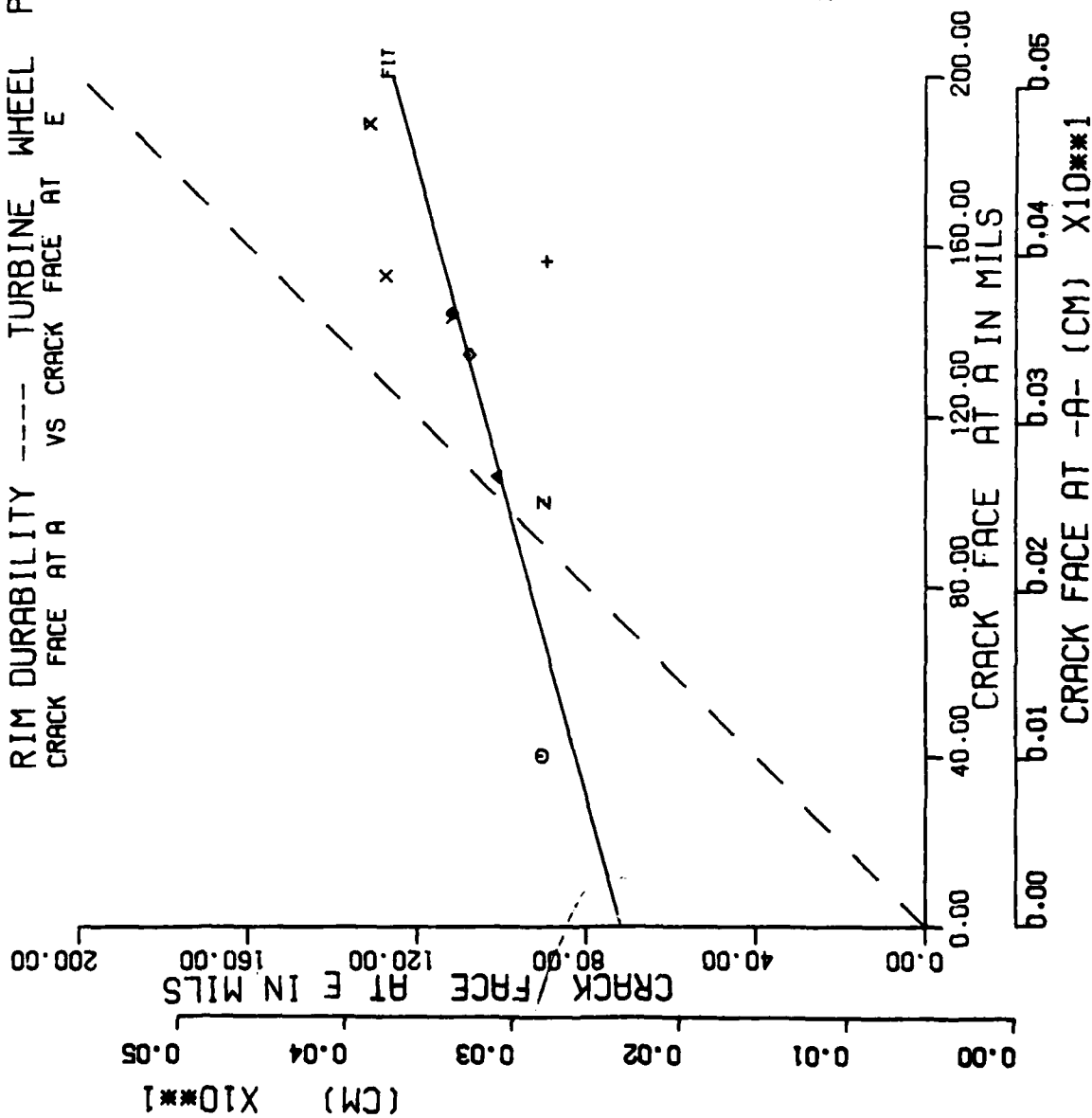
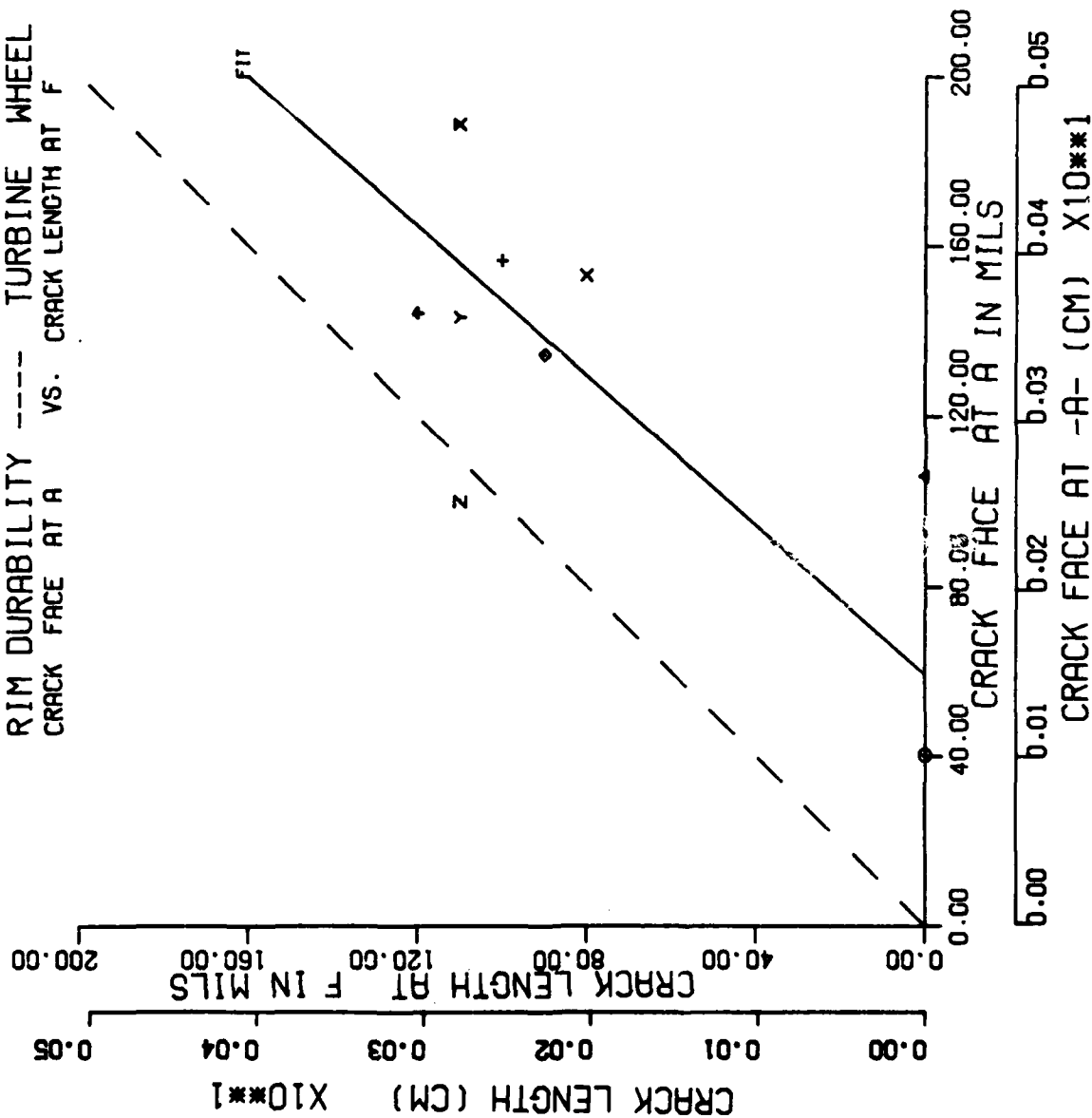
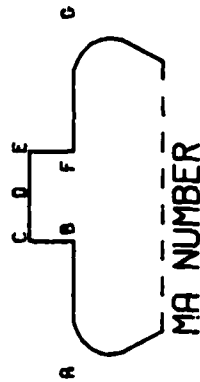


Figure 3-54. Crack Face at A Versus Crack Face at E.

RIM DURABILITY --- TURBINE WHEEL P/N868272-1
 CRACK FACE AT A VS. CRACK LENGTH AT F



CRACK LENGTH
 OVERLAPS IGNORED
 MAXIMUMS FOR EACH WHEEL



14494
 14569
 14717
 14570
 14493
 15129
 15128
 14718
 15130

Figure 3-55. Crack Face at A Versus Crack Length at F.

RIM DURABILITY --- TURBINE WHEEL P/N868272-1
 CRACK FACE AT A VS. CRACK FACE AT G

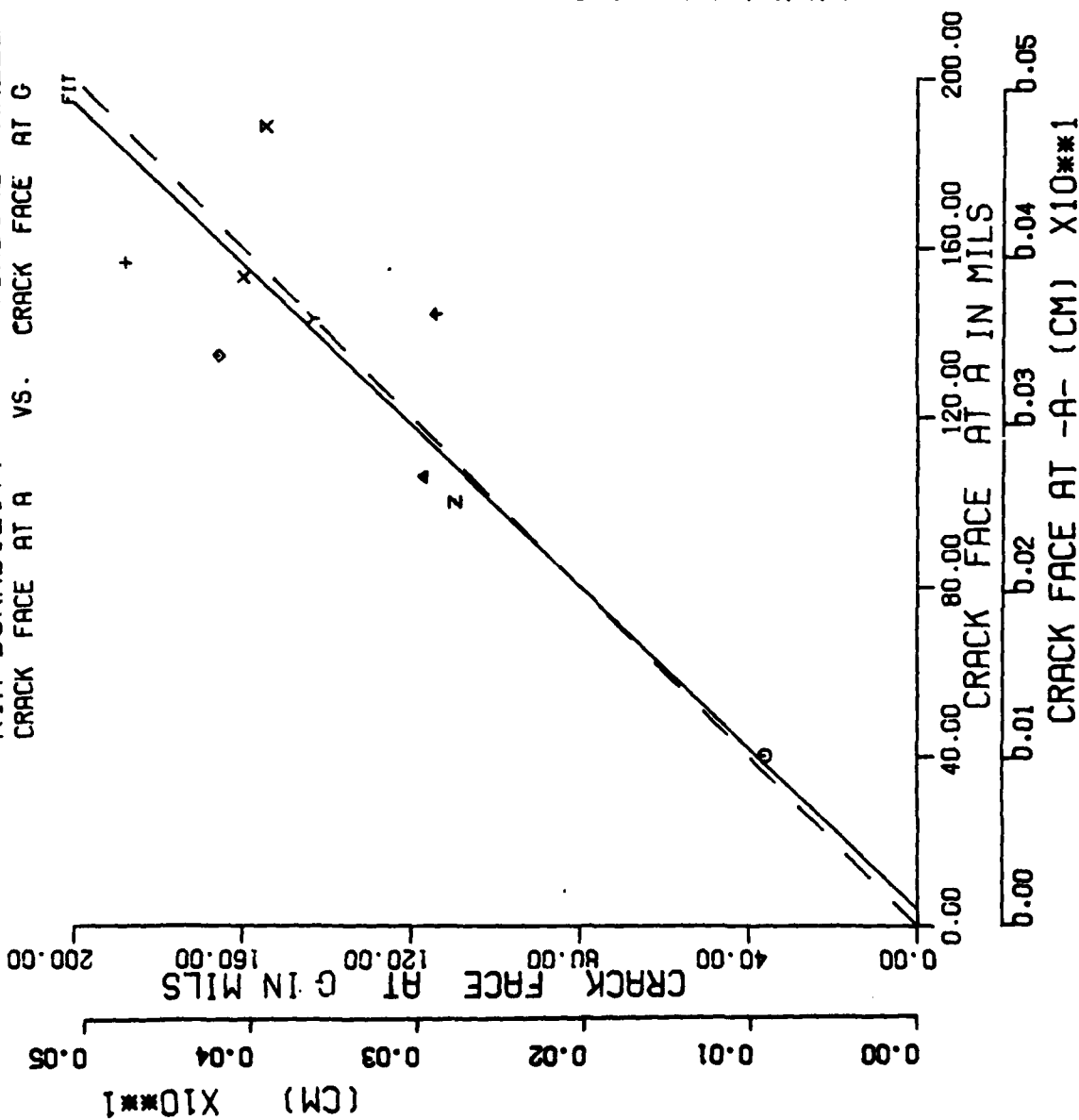
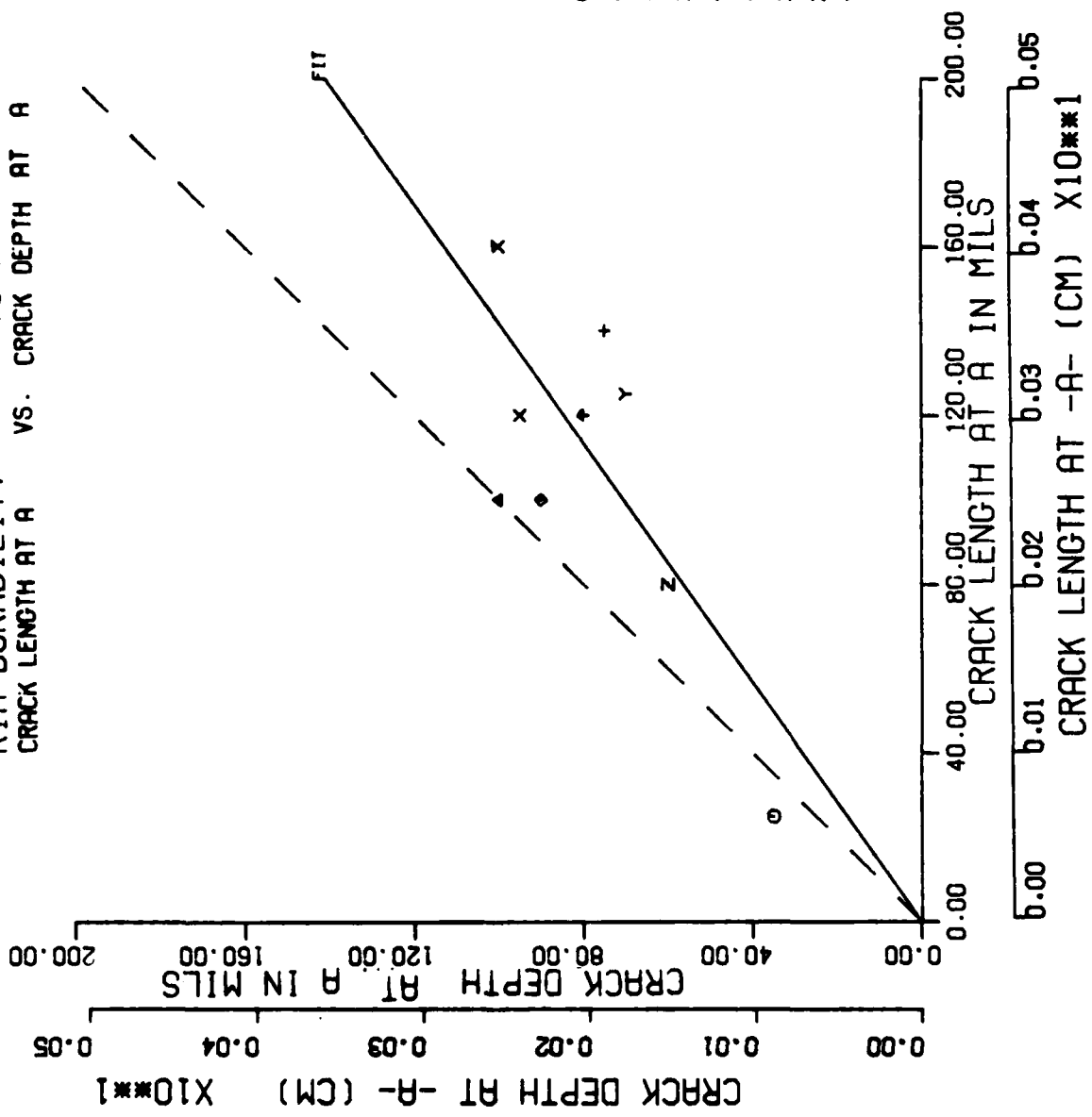
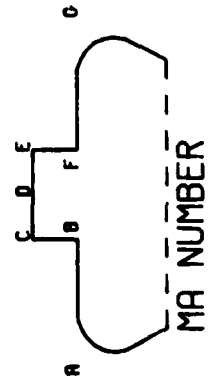


Figure 3-56. Crack Face at A Versus Crack Face at G.

RIM DURABILITY ----- TURBINE WHEEL P/N868272-1
 CRACK LENGTH AT A VS. CRACK DEPTH AT A



CRACK LENGTH
 OVERLAPS IGNORED
 MAXIMUMS FOR EACH WHEEL



- 14494
- ▲ 14569
- +
- x 14717
- ◇ 14570
- † 14493
- x 15129
- z 15128
- y 14718
- 15130

Figure 3-57. Crack Length at A Versus Crack Depth at A.

RIM DURABILITY --- TURBINE WHEEL
 CRACK LENGTH AT B VS. CRACK DEPTH AT B

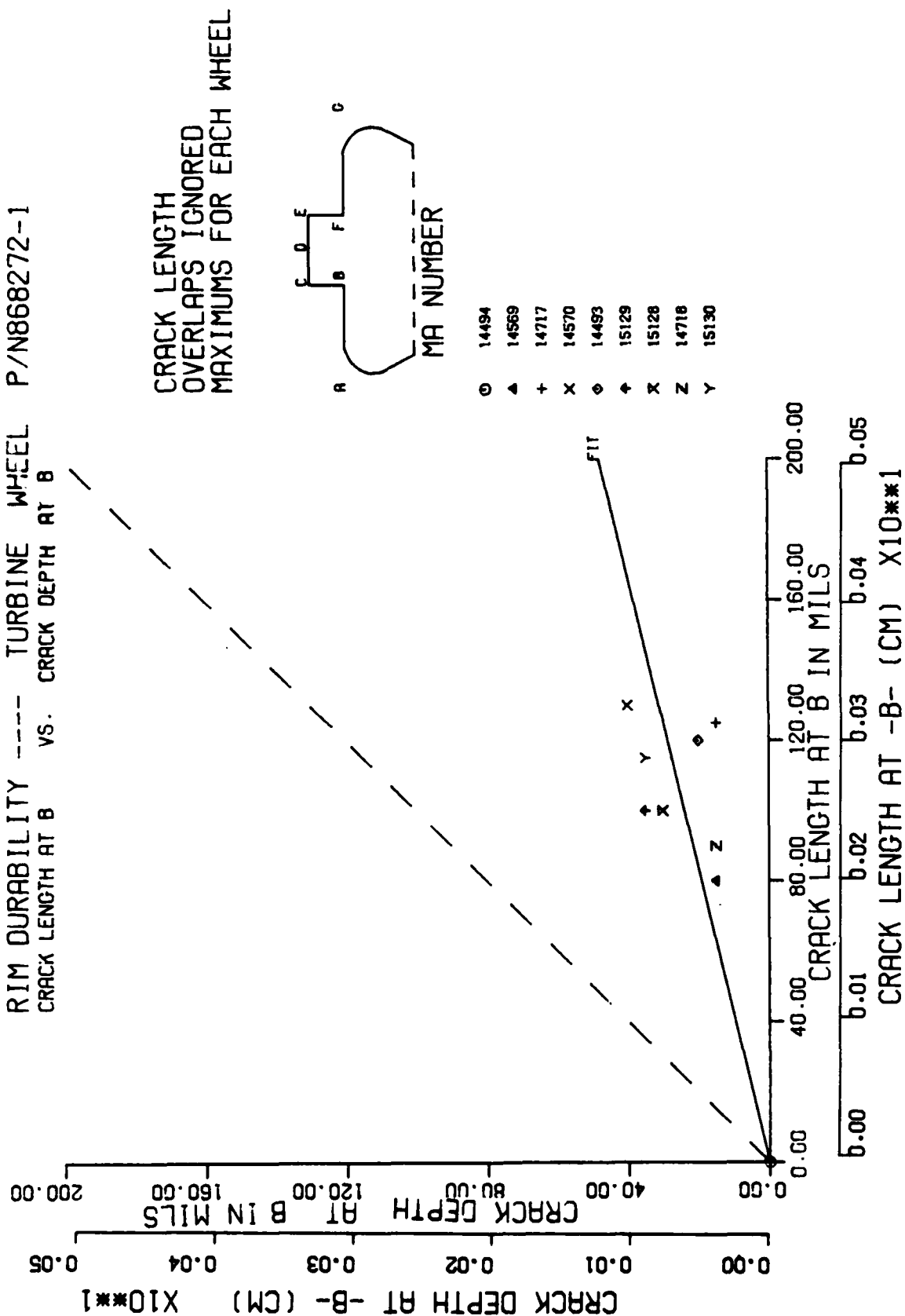


Figure 3-58. Crack Length at B Versus Crack Depth at B.

RIM DURABILITY --- TURBINE WHEEL P/N868272-1
 CRACK LENGTH AT D VS. CRACK DEPTH AT D

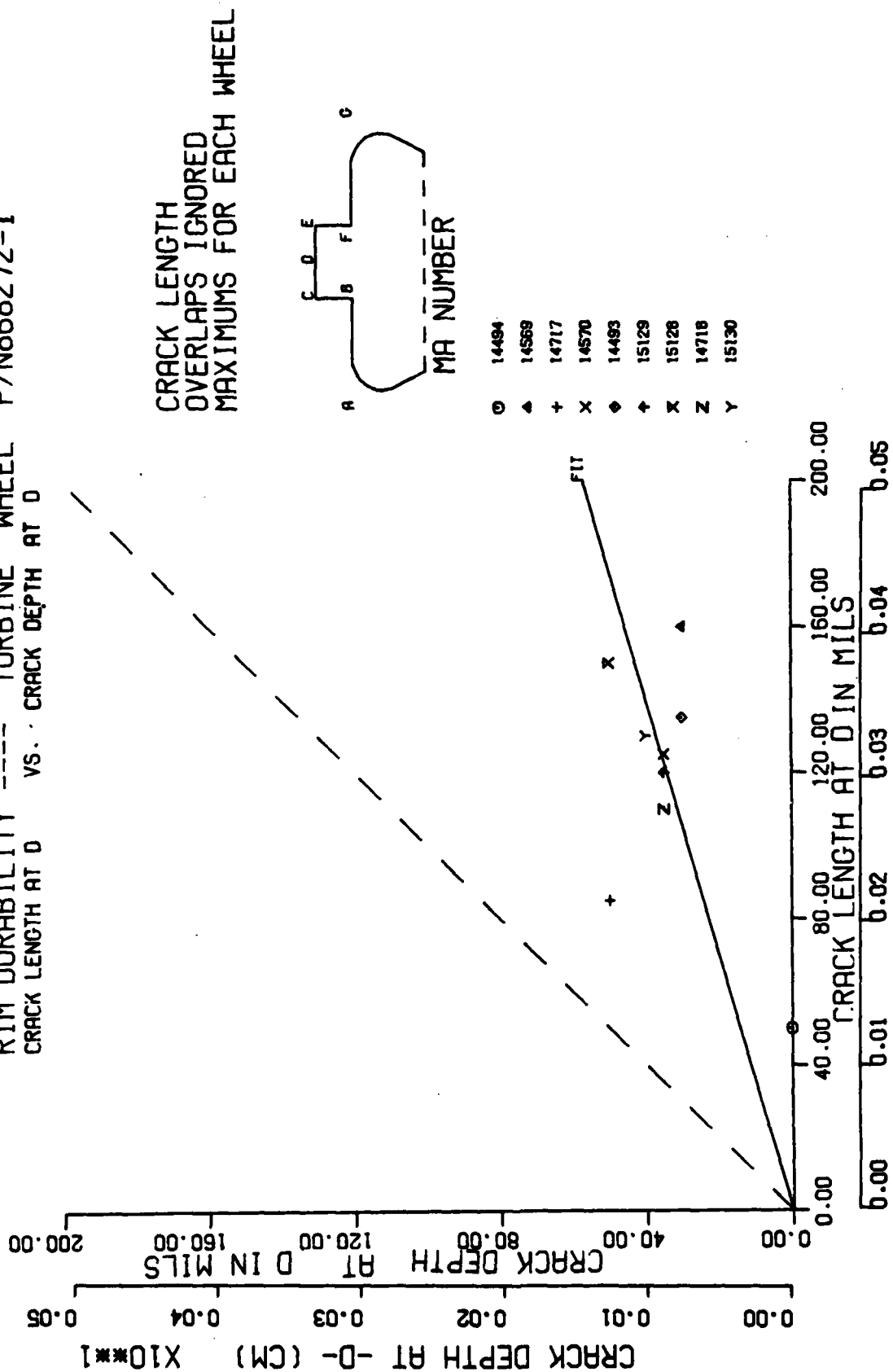


Figure 3-60. Crack Length at D Versus Crack Depth at D.

RIM DURABILITY --- TURBINE WHEEL P/N868272-1
 CRACK LENGTH AT E VS. CRACK DEPTH AT E

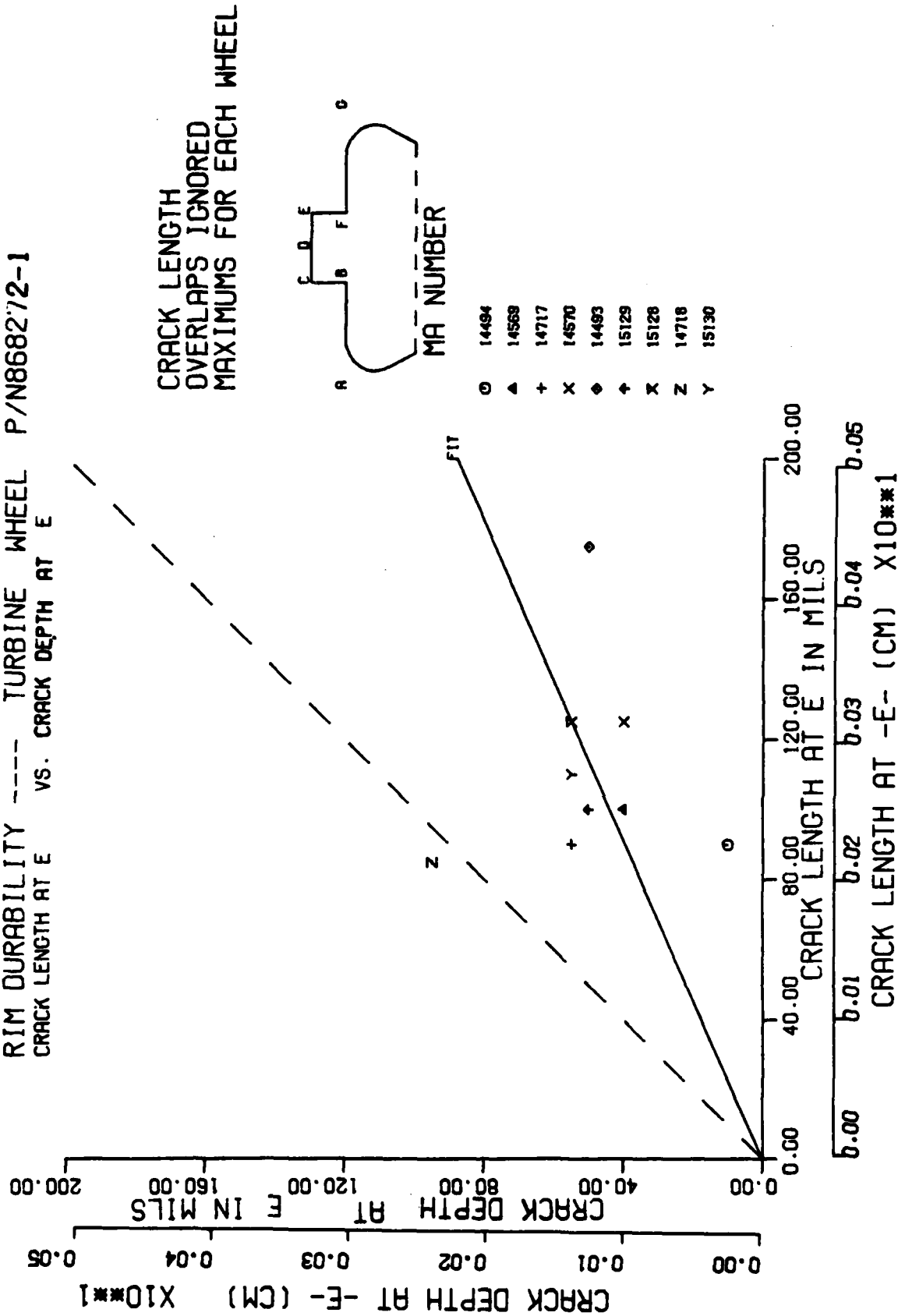
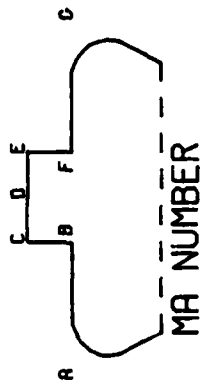


Figure 3-61. Crack Length at E Versus Crack Depth at E.

Graph showing Crack Depth at F-F (CM) versus Crack Length at F in Mils. The Y-axis is labeled "CRACK DEPTH AT F-F (CM) X10**1" and ranges from 0.00 to 0.04. The X-axis is labeled "CRACK LENGTH AT F IN MILS" and ranges from 0.00 to 0.05. A solid line labeled "FIT" represents the linear fit. A dashed line is also shown. Data points are labeled X, Y, Z, and a point marked with a plus sign.

Crack Length at F (Mils)	Crack Depth at F-F (CM) X10**1	Label
0.00	0.00	Origin
~0.018	~0.005	X
~0.022	~0.008	+
~0.028	~0.012	Y
~0.030	~0.013	X
~0.032	~0.015	Z

CRACK LENGTH
OVERLAPS IGNORED
MAXIMUMS FOR EACH WHEEL



Q	14494
A	14569
+	14717
X	14570
D	14493
P	15129
X	15128
Z	14718
Y	15130

CRACK LENGTH AT F (CM) X10***1

3.9 Correlation of Cracked Wheels with Analytical Prediction

The crack locations are shown in Figure 3-63, and the maximum crack for the turbine wheels in the data base as a function of equivalent cycles is shown in Figures 3-64 and 3-65, forward- and aft-rivet holes.

Also shown in Figures 3-64 and 3-65 is the analytical crack propagation as a function of equivalent cycles. The cracks are assumed to propagate from an initial size of 0.030 inch, and the propagation is shown for the minimum, average, and maximum equivalent cycles affecting the 0.030-inch crack.

The same plots are shown in Figures 3-66 and 3-67 with all of the data points presented.

3.9.1 Isolation of Problem Areas in Data Correlation

3.9.1.1 Crack Initiation Determination

Many cracks have been measured on wheels destructively examined for this program. The key problem encountered is the inability to separate crack initiation from crack propagation. Ideally, if the crack-initiation point were known for the cracks examined, a correlation between actual and analytical procedures and limits could be refined to a point of increased confidence in crack-propagation prediction.

Lacking the qualitative information on crack initiation needed for a straight-forward correction of the crack propagation, a number of approaches have been made to statistically determine the initiation cycles and crack size.

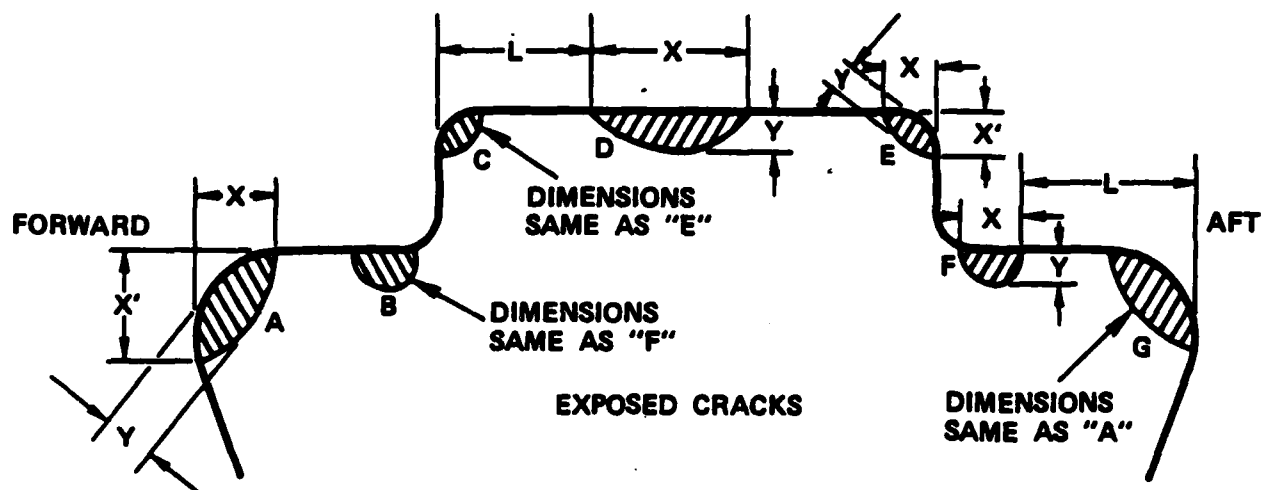
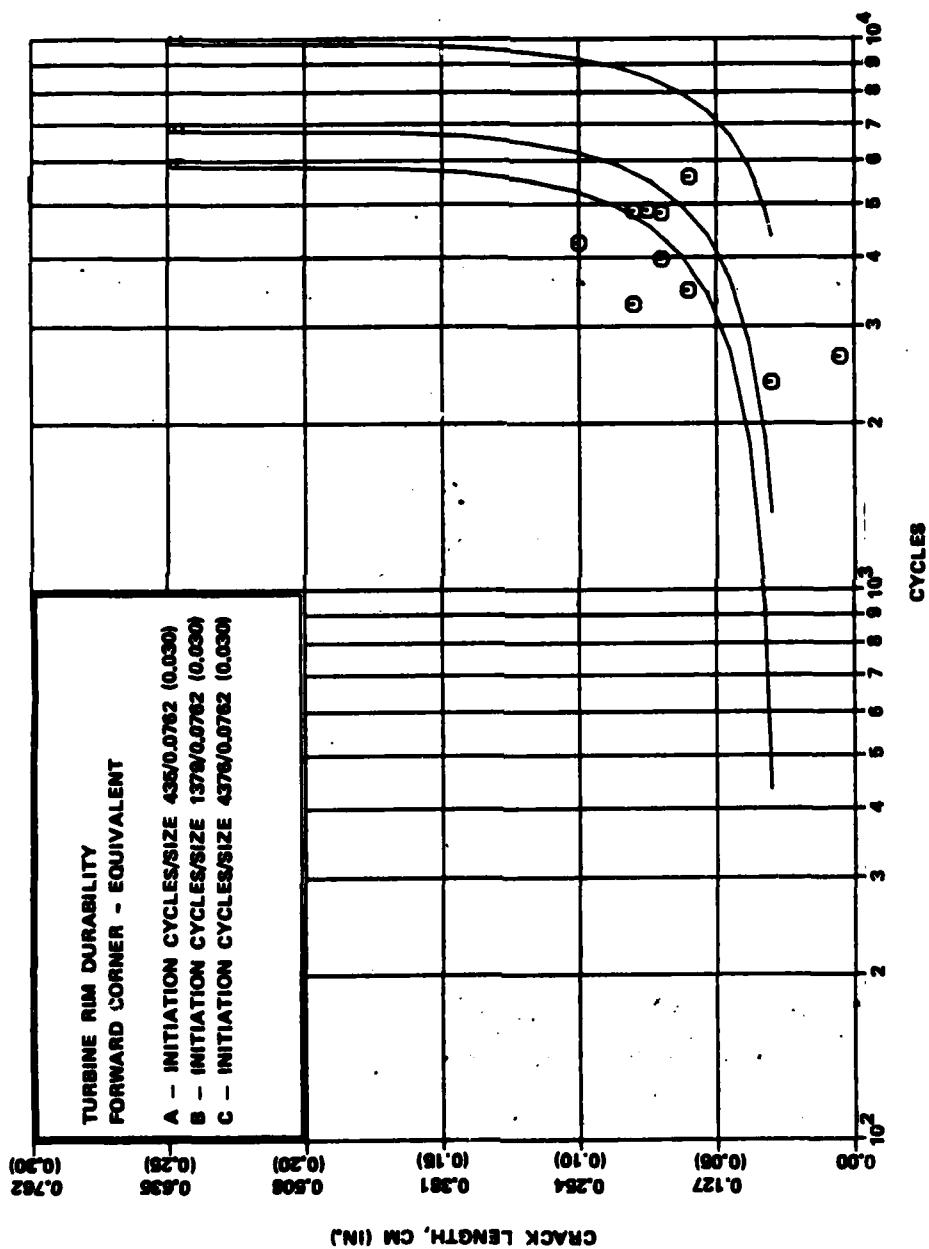


Figure 3-63. Crack Locations and Directions.



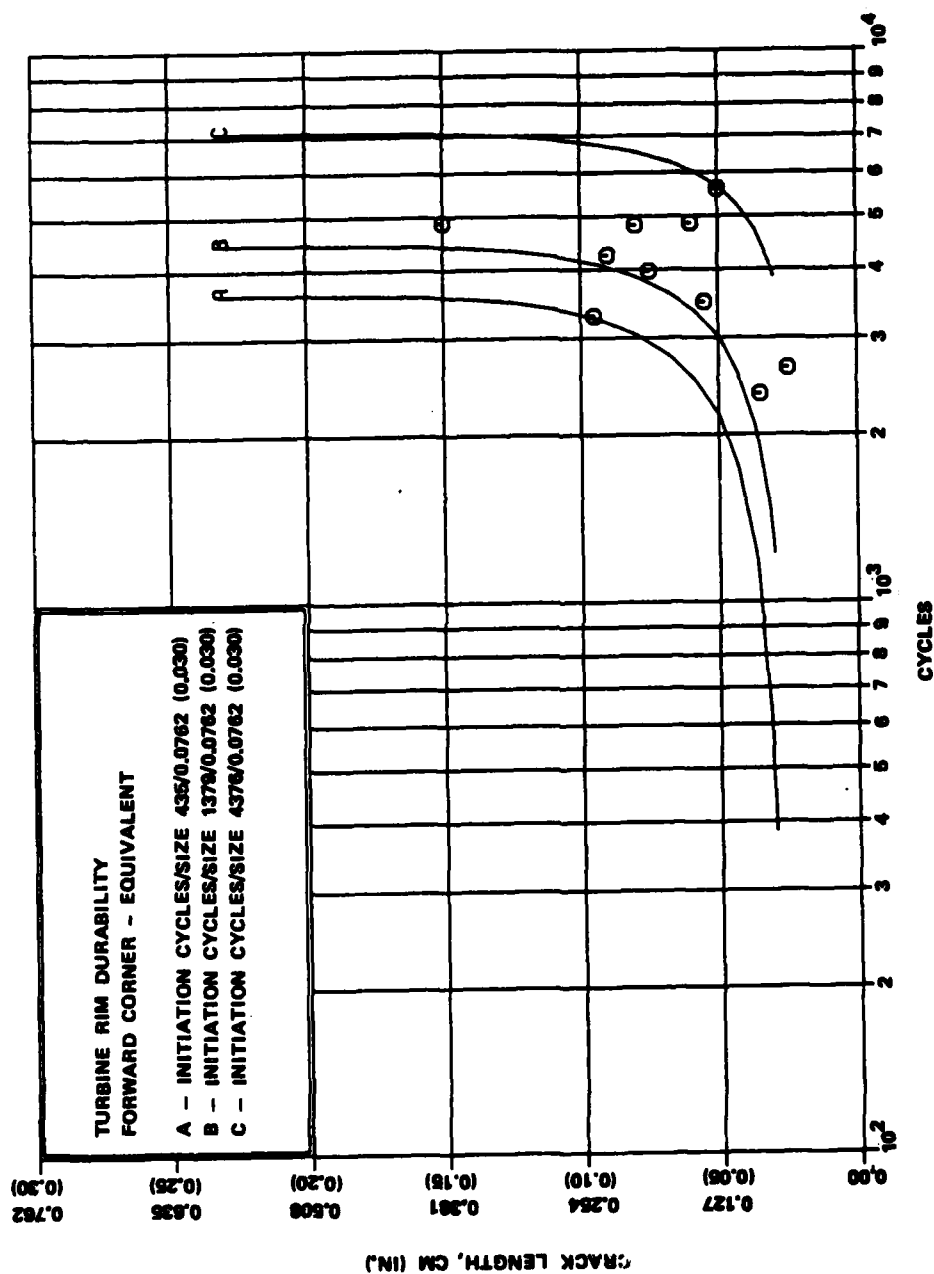


Figure 3-65. Cycles Versus Maximum Crack Aft Corner - Equivalent.

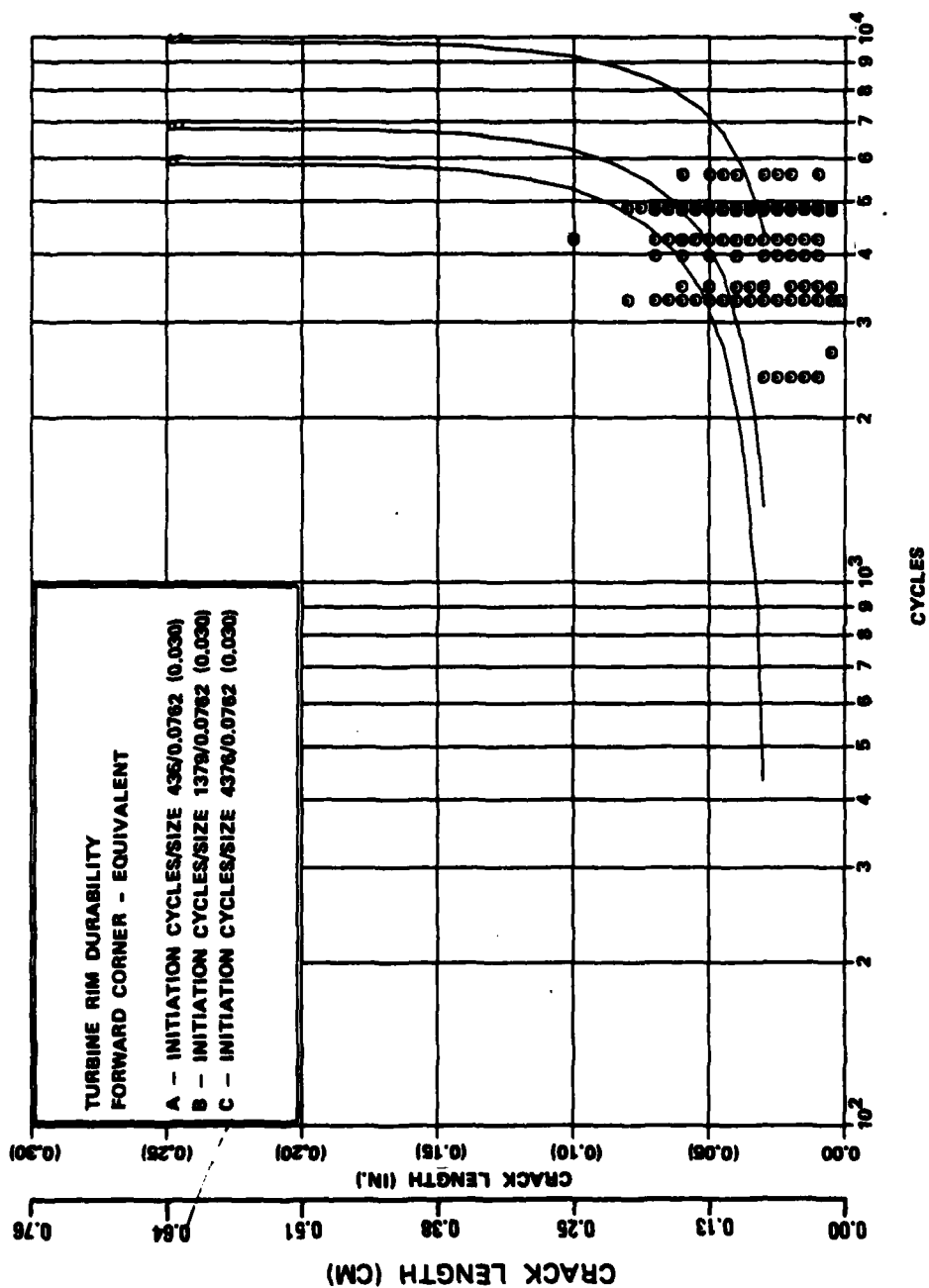


Figure 3-66. Cycles Versus All Cracks Forward Corner - Equivalent.

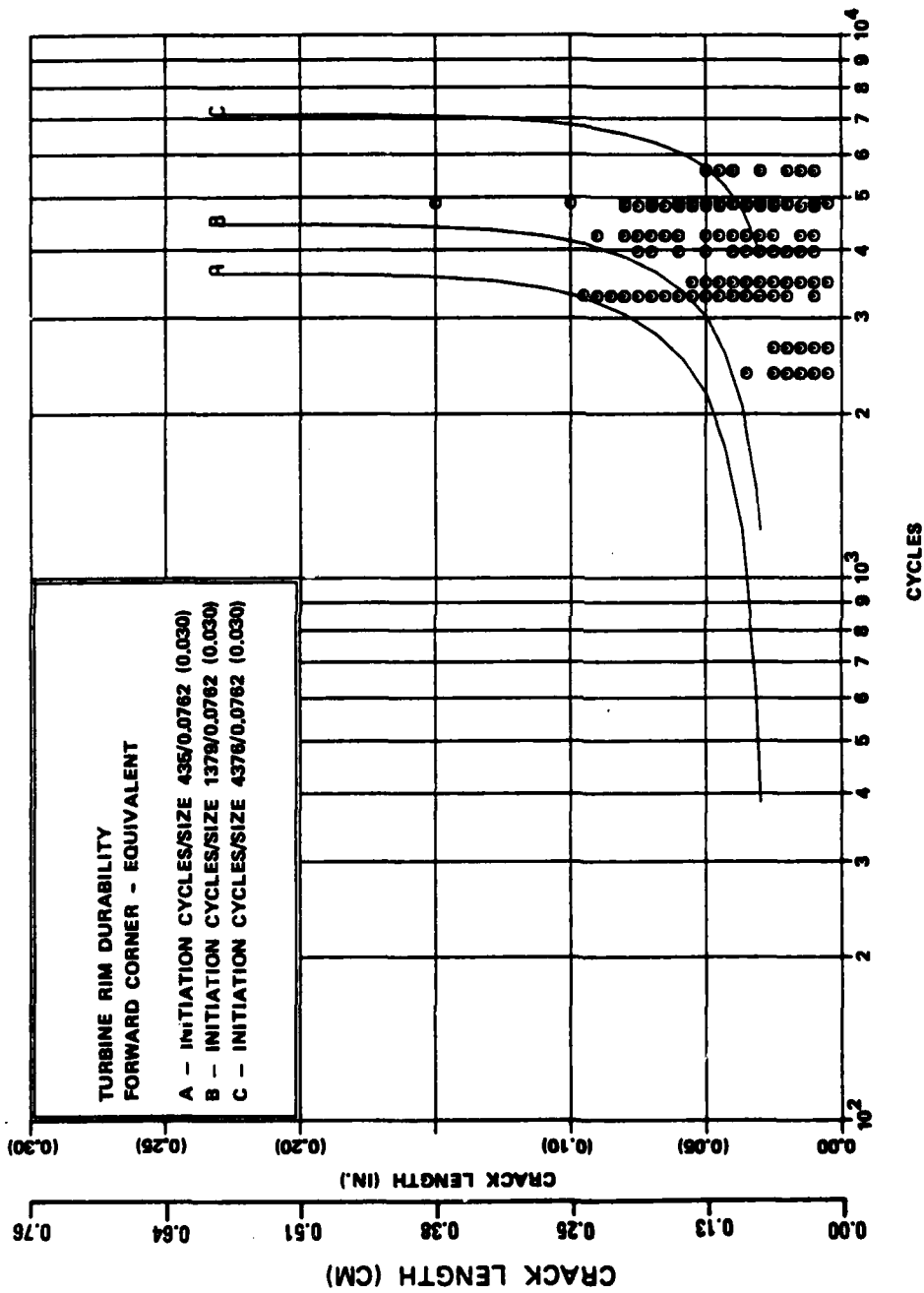


Figure 3-67. Cycles Versus All Cracks Aft Corner - Equivalent.

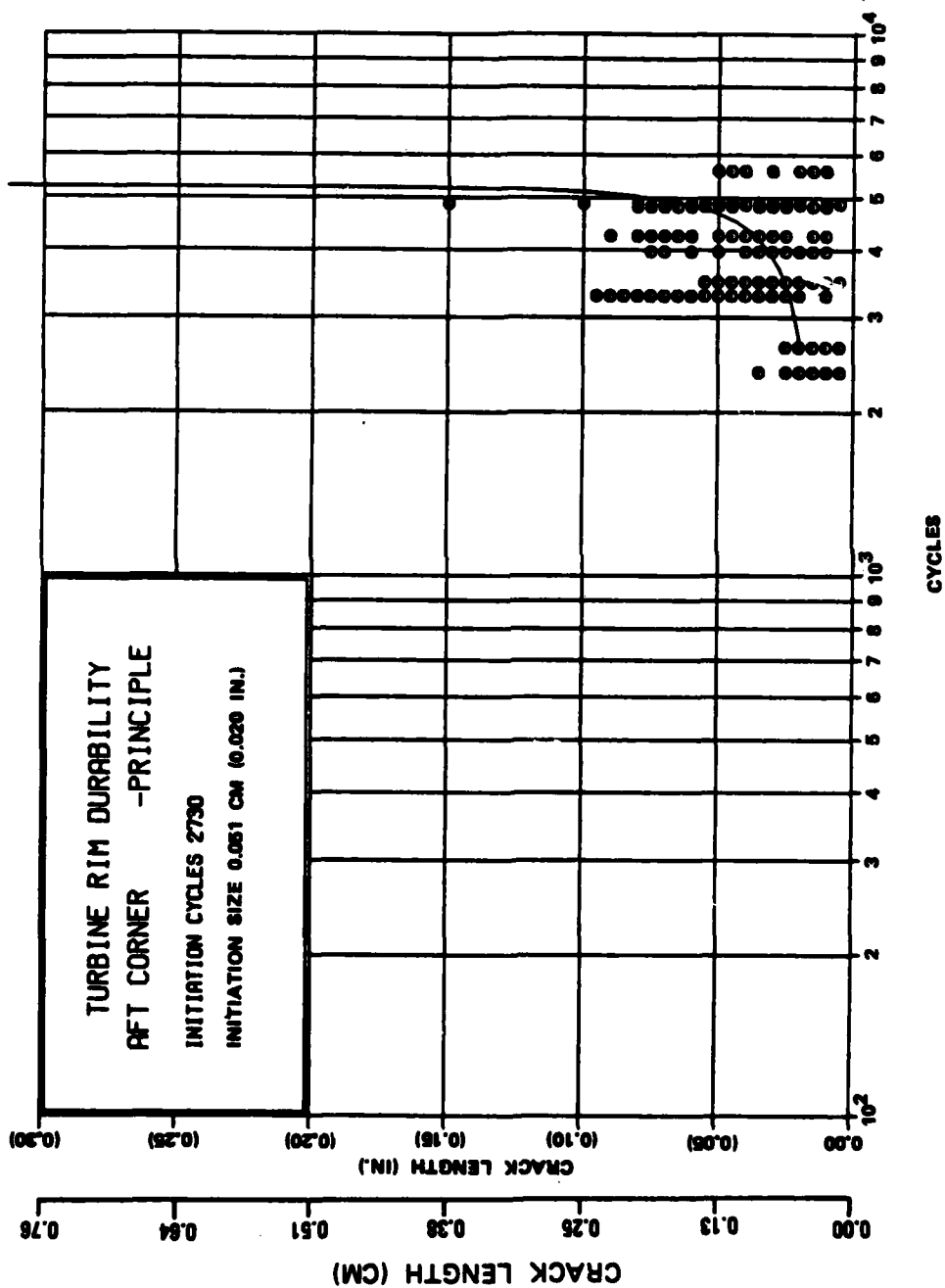


Figure 3-68. Turbine Rim Durability - Aft Corner.

The first approach was to plot the largest of all the cracks on the forward edge of the rivet hole for each wheel, and then to pass the predicted propagation line through these points. A curve with a least squares fit can be passed through the data points with an initial cracks size from 0.0762-0.1016 cm (0.030-0.040 inch). Using an initial crack size of 0.030 inch, the average number of initiation cycles would be 147. Using an initial crack size of 0.1016 cm (0.040 inch) the average number is 1780 cycles. The minimum calculated cycles in initiation, as shown previously, is 430 cycles.

Another approach to back calculate the initiation from the crack data was to pass the propagation line through each crack in the wheels and calculate the number of cycles needed to arrive at that point based upon an initial estimate of crack size and cycles. From this approach it was found that the average initial crack size for the forward rivet hole area (crack location "A") was 0.0508 cm (0.020 inch) with an initiation of 1985 cycles. For the aft rivet hole area (crack location "G"), the crack initiation was 0.0508 cm (0.020 inch) with an initiation of 2730 cycles. For the rivet retainer area (crack location "C"), the crack initiation was 0.0508 cm (0.020) with an initiation of 2186 cycles. These are shown in Figures 3-68, 3-69, and 3-70 for the aft, forward, and rivet retainer areas, respectively. Using this method, it was also possible to estimate the distribution of the cracks as a function of cycles. The maximum, minimum, and average curves are shown in Figures 3-71, 3-72, and 3-73 for the rivet retainer, forwards, and aft areas, respectively.

While these two approaches tend to support the fact that the data does correlate with the prediction, the results are not conclusive.

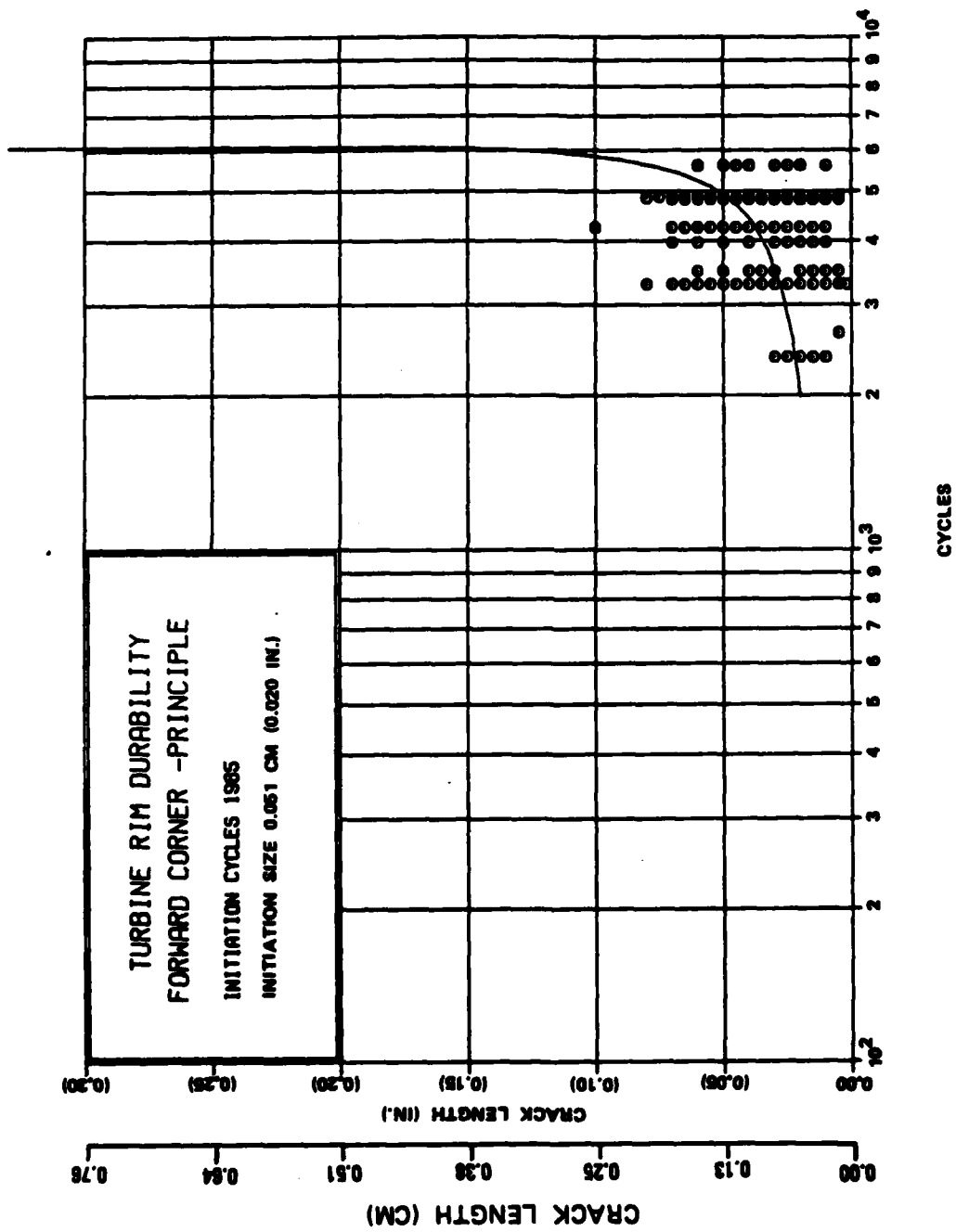


Figure 3-69. Turbine Rim Durability - Forward Corner.

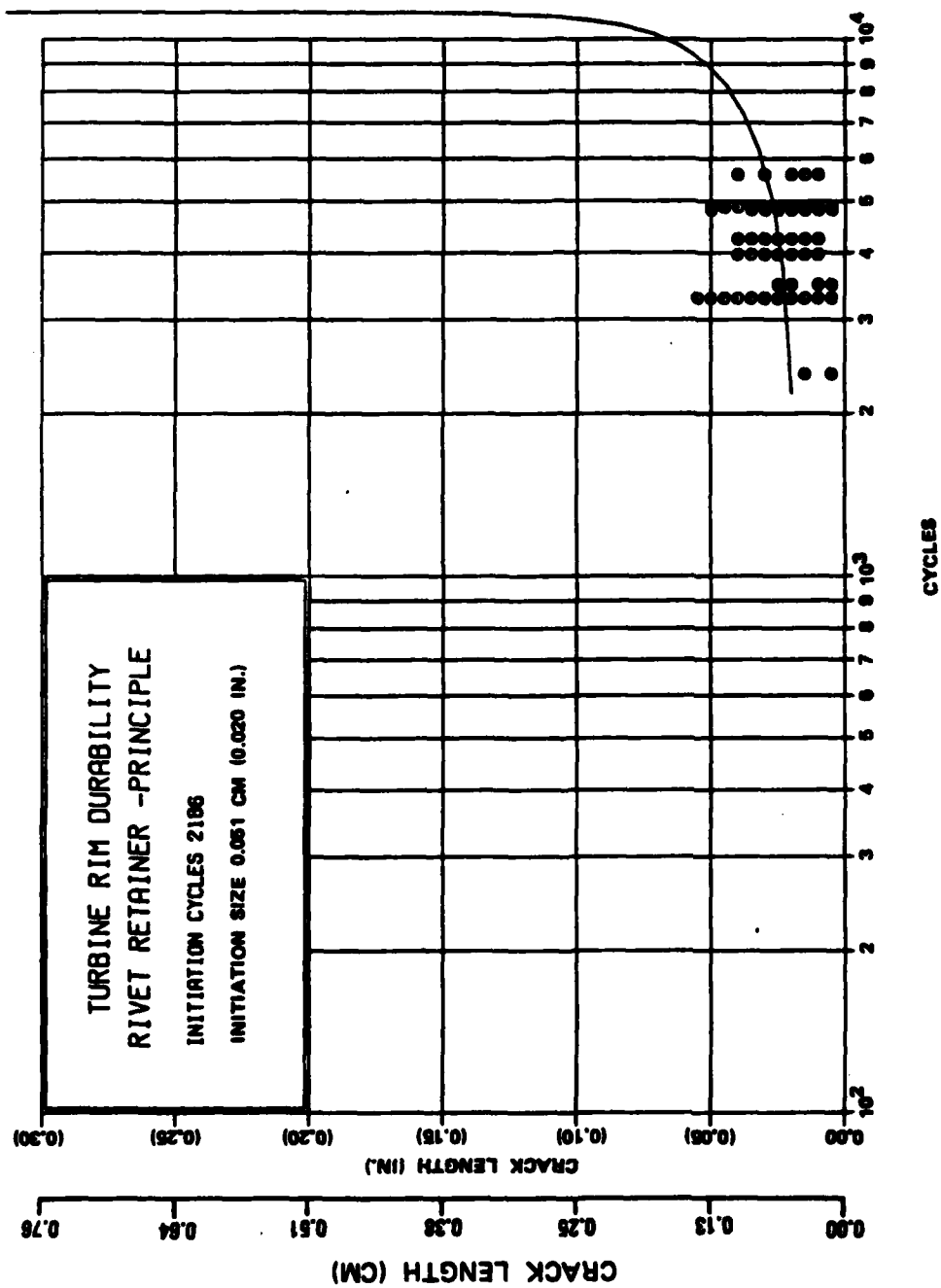


Figure 3-70. Turbine Rim Durability - Rivet Retainer.

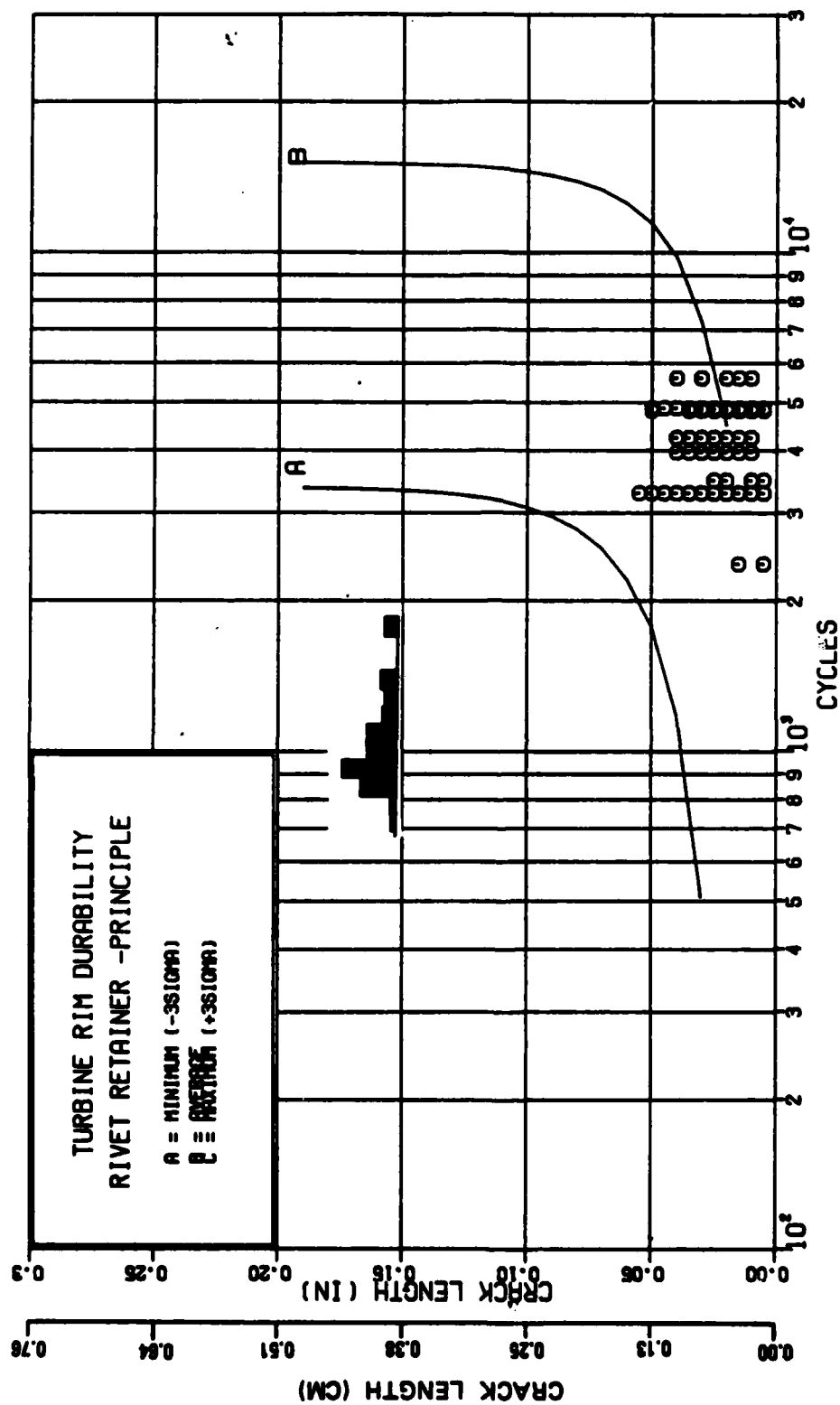


Figure 3-71. Turbine Rim Durability - Rivet Retainer.

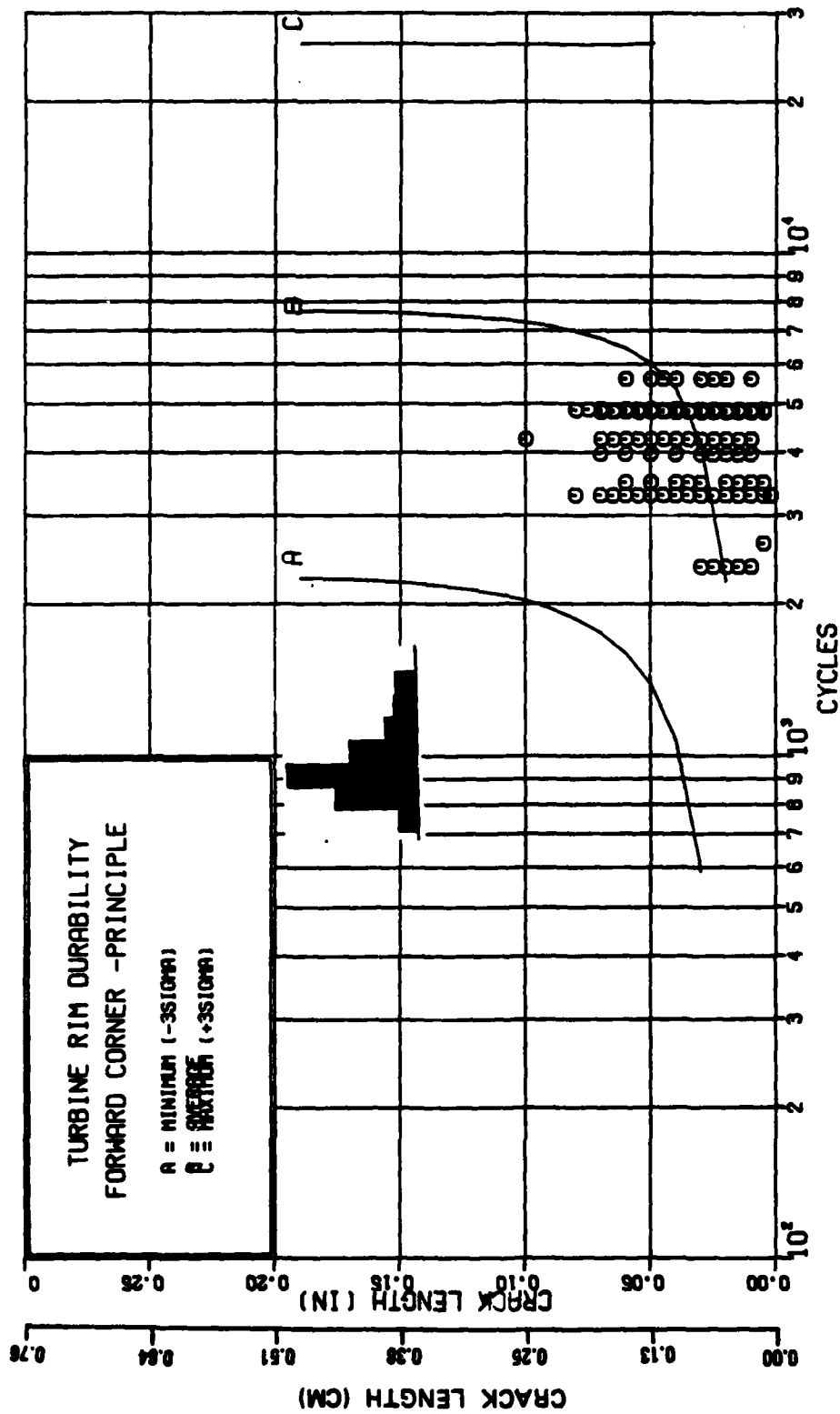


Figure 3-72. Turbine Rim Durability - Forward Corner.

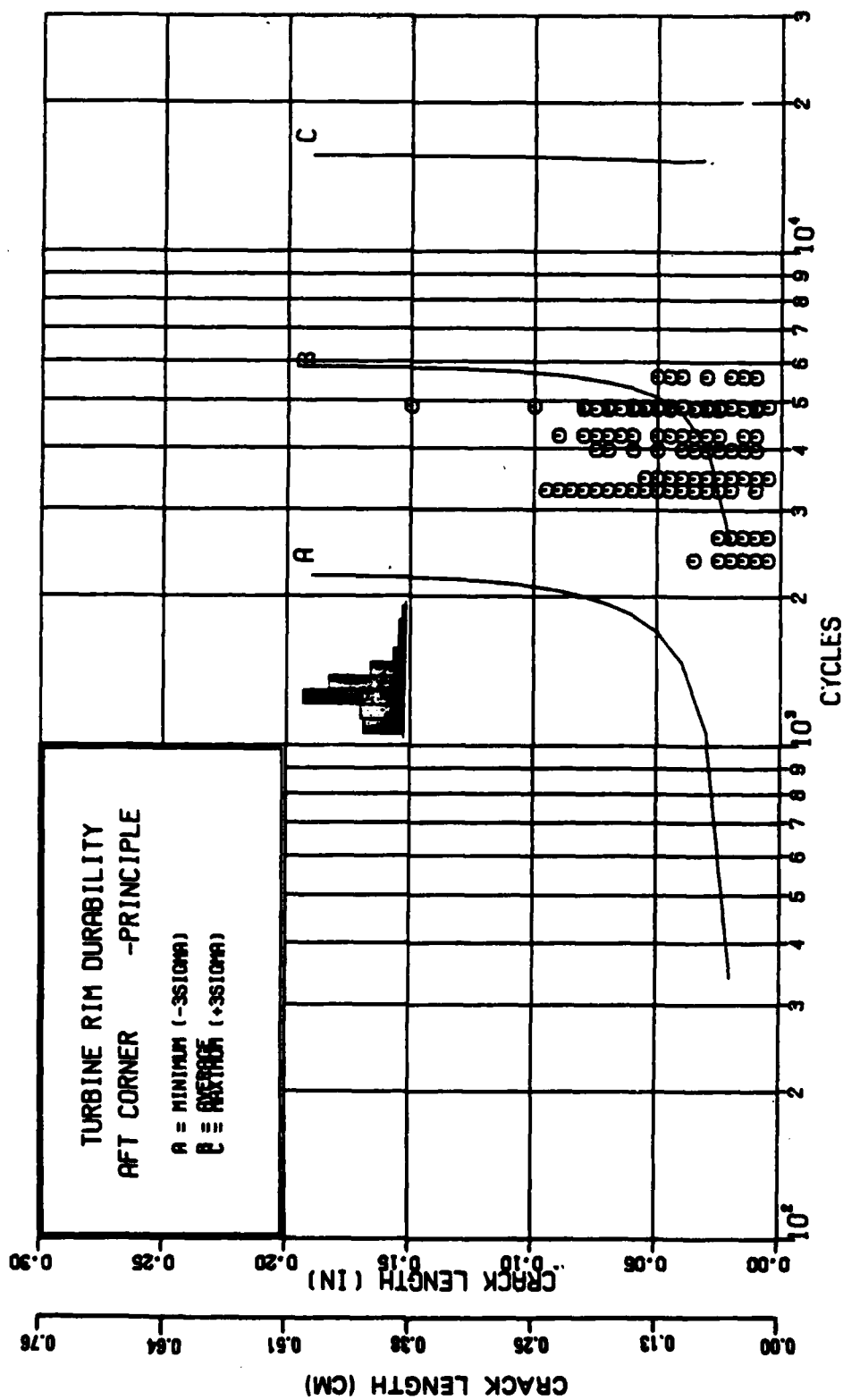


Figure 3-73. Turbine Rim Durability - Aft Corner.

3.10 Whirlpit Test

With the resources allocated for this program, it was not possible to run a heated whirlpit rig test to propagate cracks in wheels retired from service. A room temperature test, however, was devised. It was not possible to run the wheel to a speed that would duplicate the crack-growth rate that was predicted in service. Conditions related to bore stresses and pedestal stresses limited the speed of the test, and if a crack occurred in the pedestal or bore, it would propagate faster than in the rivet hole.

The test was conducted at 52,000 rpm for two wheels to 7500-cycles. The data from these tests is summarized in Table 3-20 and plotted in Figures 3-74 and 3-75. A failure occurred on the first wheel at 6600 cycles due to a pedestal failure. The second wheel was concluded at 7500 cycles with no failure.

The comparison of the predicted crack-growth rate with the results from the whirlpit indicated that the results are within the range of the material properties and tend toward the slower crack-growth rate of that range. The material data curve used for the analysis is shown in Figure 3-76 along with the material curve that would yield the same growth rate as that which was found from the measured data.

TABLE 3-20. CRACK SIZES IN CYCLIC WHIRLPIT TEST.

Wheel No: 4275

Cycles	Crack Size, cm (in.)		
	Slot No. (4)	Slot No. (17)	Slot No. (38)
0	0.0254 (0.010)	0.0635 (0.025)	0.0254 (0.010)
500	0.0381 (0.015)	0.0762 (0.030)	0.0381 (0.015)
1500	0.1016 (0.040)	0.0762 (0.030)	0.0508 (0.020)
2500	0.1016 (0.040)	0.0762 (0.030)	0.0635 (0.025)
4000	0.1016 (0.040)	0.0762 (0.030)	0.0762 (0.030)
5500	0.1016 (0.040)	0.0762 (0.030)	0.0889 (0.035)
7500	0.1016 (0.040)	0.1016 (0.040)	0.0889 (0.035)

Wheel No. 2197

Cycles	Crack Size, cm (in.)		
	Slot No. (13)	Slot No. (23)	Slot No. (28)
0	0.1016 (0.040)	0.1016 (0.040)	0.0762 (0.030)
500	0.1016 (0.040)	0.1016 (0.040)	0.0762 (0.030)
1500	0.1016 (0.040)	0.1016 (0.040)	0.0889 (0.035)
2500	0.1143 (0.045)	0.1016 (0.040)	0.1016 (0.040)
4000	0.127 (0.050)	0.1143 (0.045)	0.1143 (0.045)
5000	0.1397 (0.055)	0.1143 (0.045)	0.1143 (0.045)

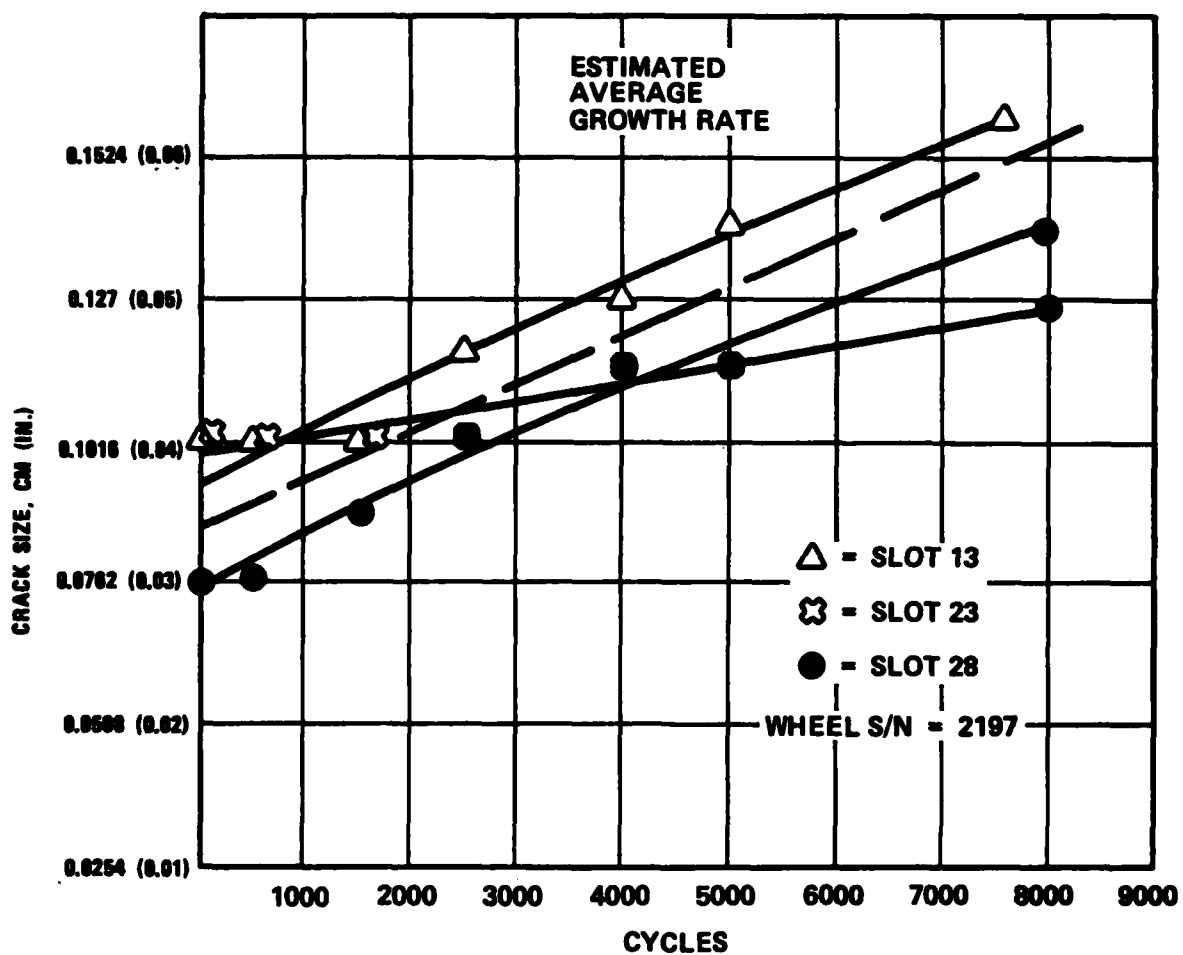


Figure 3-74. Crack Growth Data From Whirlpit Test Wheel 2197.

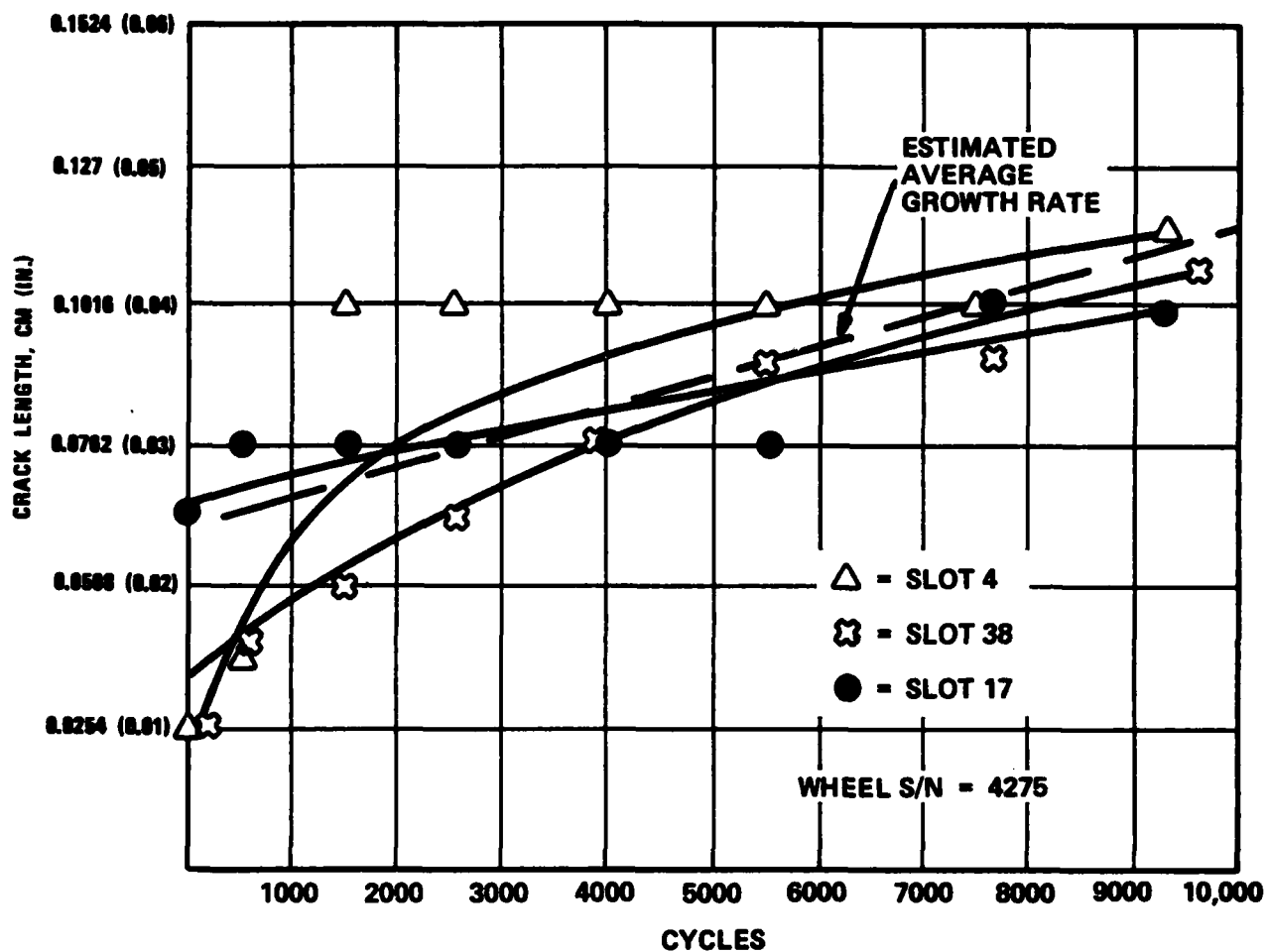


Figure 3-75. Crack Growth Data From Whirlpit Test Wheel 4275.

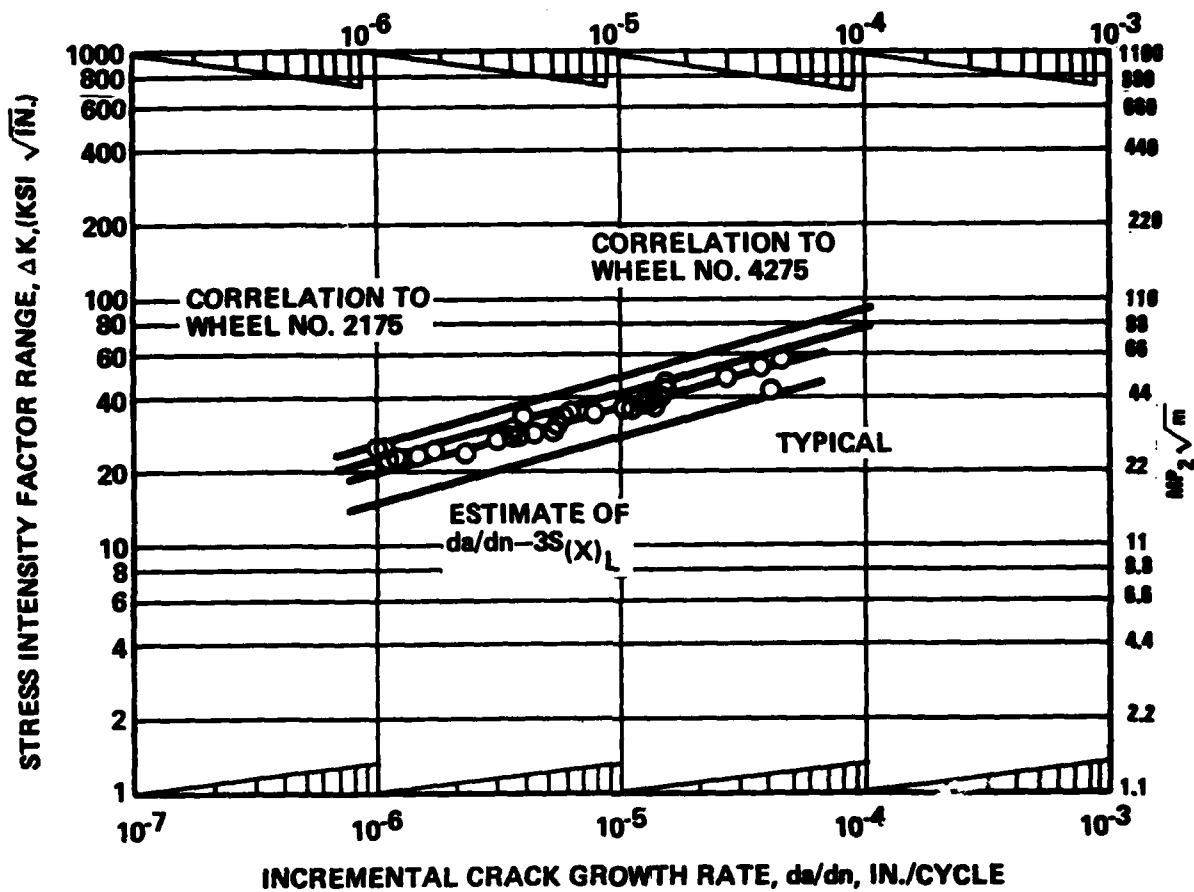


Figure 3-76. Typical Stress Intensity Factor Range Versus Crack Growth Rate for IN-100 Castings at Room Temperature.

APPENDIX A

FLUID BOUNDARY CONDITIONS

MAXIMUM POWER

LOCATION	P _t ABS	P _t Rel	P _{st}	T _t ABS	T _t Rel	T _{st}
OIL SUMP (5)	-	-	16.70	770.0	-	770.0
COMP. INLET (6)	15.27	-	11.62	518.7	-	484.9
COMP. EXIT						
BEFORE DESWIRL (1)	157.6	-	116.9	1140.	-	1021.7
AFTER DESWIRL (7)	157.6	-	152.8	1140.	-	1130.0
1ST STG STATOR IN (9)	-	-	143.61	2299.7	2299.7	2280.5
1ST STG TURB. IN (11)	-	-	98.30	2299.7	2148.4	2101.6
1ST STG TURB EX (34)	-	-	76.94	2056.6	2147.4	2010.1
2ND STG TURB IN (22)	81.23	56.45	50.52	2056.6	1885.6	1836.3
2ND STG TURB EX (27)	44.64	52.08	42.10	1812.8	1881.6	1787.0
3RD STG TURB IN (29)	-	-	21.5	1812.8	1540.9	1517.7
3RD STG TURB EX (33)	-	-	13.7	1452.1	1547.0	1407.5
(17)	157.6	-	157.6	1140.0	-	1140.0

PRESSURES IN PSIA

TEMPERATURES IN °R

NUMBERS IN PARENTHESES REFER TO STATION NUMBERS IN SECONDARY FLOW ANALYSIS. PLEASE SEE APPENDIX B.

FLUID BOUNDARY CONDITIONS

CRUISE

LOCATION	P _t ABS	P _t Rel	P _{st}	T _t ABS	T _t Rel	T _{st}
OIL SUMP (5)	-	-	9.15	745.6	-	770.
COMP. INLET (6)	9.67	-	8.055	502.2	-	480.
COMP EXIT						
BEFORE DESWIRL (1)	99.8	-	74.5	1103.8	-	1060.
AFTER DESWIRL (7)	99.8	-	96.19	1103.8	-	1060.
1ST STG STATOR IN (9)	-	-	90.9	2226.7	2226.7	2251.
1ST STG STATOR EX (11)	-	-	62.2	2226.7	2080.2	2075.
1ST STG TURB EX (34)	-	-	49.4	1991.3	2079.2	1985.
2ND STG TURB IN (22)	51.4	35.74	31.98	1991.3	1825.8	1714.
2ND STG TURB EX (27)	28.26	32.97	26.65	1755.3	1821.9	1766.
3RD STG TURB IN (29)	-	-	13.60	1755.3	1755.	1501
3RD STG TURB EX (33)	-	-	8.65	1406.0	1400.	1392.
)17)	99.8	-	96.19	1103.8	-	1060.

FLUID BOUNDARY CONDITIONS

IDLE

LOCATION	P _t ABS	P _t Rel	P _{st}	T _t ABS	T _t Rel	T _{st}
OIL SUMP (5)	-	-	16.7	-	-	780.0
COMP INLET (6)	-	-	14.5	-	-	572.7
COMP EXIT						
BEFORE DESWIRL (1)	-	-	37.3	-	-	839.7
AFTER DESWIRL (7)	-	-	40.98	-	-	839.7
1ST STG STATOR IN (9)	-	-	39.2	-	-	1787.0
1ST STG STATOR EX (11)	38.8	-	29.1	1777.	-	1777.0
1ST STG TURB EX (34)	25.3	-	24.0	1627.	-	1627.0
2ND STG TURB IN (22)	24.4	-	19.2	1627.	-	1627.0
2ND STG TURB EX (27)	17.1	-	16.3	1512.	-	1512.0
3RD STG TURB IN (29)	16.5	-	15.2	1512.	-	1512.0
3RD STG TURB EX (33)	14.75	-	14.65	1473.	-	1473.0
(17)	-	-	40.98	-	-	839.7

SECOND STAGE ROTOR
AXIAL VELOCITY DISTRIBUTION
R= 2.963"

SUCTION SURFACE		PRESSURE SURFACE	
AXIAL DISTANCE	CRITICAL MACH NUMBER	AXIAL DISTANCE	CRITICAL MACH NUMBER
0.0	0.0	0.0	0.0
.03799	.482	.03799	.388 (.29)
.07598	.509	.07598	.343
.11398	.547	.11398	.341
.151968	.585	.151968	.339
.18996	.619	.18996	.338
.22795	.646	.22795	.346 (.339)
.26594	.665	.26594	.340
.30394	.673	.30344	.344
.34193	.650 (.67)	.34193	.351
.37992	.651 (.67)	.37992	.360
.41791	.673	.41791	.371
.45588	.675	.45588	.381
.49390	.679	.4939	.391
.53189	.683	.53189	.406
.56988	.685	.56988	.406
.60678	.685	.60678	.412
.64599	.683	.64599	.418
.68386	.675	.68386	.425
.72185	.661	.72185	.435
.75984	.655	.75984	.450
.7978	.647	.7978	.478
.8358	.642	.8358	.500
.8738	.640	.8738	.538

Axial Chord = 2.412 cm. (0.9498 in.)

$M_i^* = 0.429$

$M_\phi^* = 0.623$

Critical Velocity 584.55 m/sec (1917.8 ft/sec)

MACH NUMBERS IN PARENTHESES WERE USED TO SMOOTH OUT THE VELOCITY DISTRIBUTIONS

MAXIMUM POWER

SECOND STAGE ROTOR
AXIAL VELOCITY DISTRIBUTION
R= 3.263"

SUCTION SURFACE		PRESSURE SURFACE	
AXIAL DISTANCE	CRITICAL MACH NUMBER	AXIAL DISTANCE	CRITICAL MACH NUMBER
0.0	0	0.0	0.0
.03397	.04	.03397	.212
.06794	.08	.06794	.229
.1019	.12	.1019	.2399
.1359	.16	.1359	.249
.1699	.20	.1699	.258
.2038	.24	.2038	.266
.2378	.28	.2378	.275
.2178	.32	.2178	.284
.3057	.36	.3057	.302
.3396	.40	.3396	.306
.3737	.44	.3737	.328
.4076	.48	.4076	.334
.4416	.52	.4416	.349
.4756	.56	.4756	.378
.4856	.60	.4856	.387
.5435	.64	.5435	.408
.5775	.68	.5775	.430
.6115	.72	.6115	.464
.6454	.76	.6454	.478
.6794	.80	.6794	.503
.7134	.84	.7134	.529
.7813	.92	.7813	.558
.7813	.96	.7813	.592

Axial Chord = 2.157 cm. (0.8493 in.)

$M_i^* = 0.346$

$M_\phi^* = 0.689$

Critical Velocity 586.37 m/sec (1923.8 ft/sec)

MACH NUMBERS IN PARANTHESES WERE USED TO SMOOTH OUT THE VELOCITY DISTRIBUTIONS.

MAXIMUM POWER

TPE 331-3U DURABILITY STUDY
SECOND STAGE ROTOR
AXIAL VELOCITY DISTRIBUTION
R= 3.563"

SUCTION SURFACE		PRESSURE SURFACE	
AXIAL DISTANCE	CRITICAL MACH NUMBER	AXIAL DISTANCE	CRITICAL MACH NUMBER
0.0	0.0	0.0	.30
.02999	(.42)	.02999	.143
.05998	.514	.05998	.188
.08998	.566	.08998	.201
.11997	.601	.11997	.220
.1500	.627	.1500	.235
.1800	.644	.1800	.250
.2099	.655	.2099	.263
.2399	.668	.2399	.277
.2699	.683	.2699	.290
.2999	.701	.2999	.314
.3299	.728	.3299	.321
.3599	.744	.3599	.338
.3899	.761	.3899	.356
.4199	.773	.4199	.377
.4499	.780	.4499	.400
.4799	.781	.4799	.426
.5100	.773	.5100	.454
.5399	.779 (.77)	.5399	.484
.5699	.758	.5699	.516
.5998	.753	.5998	.550
.6300	.750	.6300	.587
.6600	.751	.6600	.625
.6898	.760	.6898	.666
	.75		.75

Axial Chord = 1.904 cm. (0.7498 in.)

$M_i^* = 0.299$

$M_\phi^* = 0.743$

Critical Velocity 588.84 m/sec (1931.9 ft/sec)

MACH NUMBERS IN PARENTHESES WERE USED TO SMOOTH OUT THE VELOCITY DISTRIBUTIONS.

MAXIMUM POWER

TPE 331-3U DURABILITY STUDY
SECOND STAGE ROTOR
AXIAL VELOCITY DISTRIBUTION
R= 3.863

SUCTION SURFACE		PRESSURE SURFACE	
AXIAL DISTANCE	CRITICAL MACH NUMBER	AXIAL DISTANCE	CRITICAL MACH NUMBER
0.0	0.0	0.0	0.0
.05212	.651 (.43)	.02583	.183
.07748	.609 (.53)	.05212	.191
.1033	.645	.07748	.223
.1291	.658	.1033	.2295
.1549	.673	.1291	.244
.1808	.691	.1549	.267
.2066	.709	.1808	.272
.2324	.715 (.735)	.2066	.285
.2583	.751	.2324	.2999
.2841	.770	.2583	.326
.3099	.786	.2841	.345
.3357	.798	.3099	.367
.3616	.806	.3357	.391
.3874	.820 (.806)	.3616	.417
.4132	.806	.3874	.432
.4390	.802	.4132	.464
.4649	.799	.4390	.500
.4907	.803	.4649	.555 (.53)
.5165	.795	.4907	.577
.5423	.795	.5165	.634 (.61)
.5682	.744	.5423	.655 (.68)
.5940	.808	.5682	.708
.6456	.79	.5940	.727
			.79

Axial Chord = 1.640 cm (0.6456 in.)

$M_I^* = 0.300$

$M_{\phi}^* = 0.791$

Critical Velocity = 591.92 m/sec
(1942.0 ft/sec)

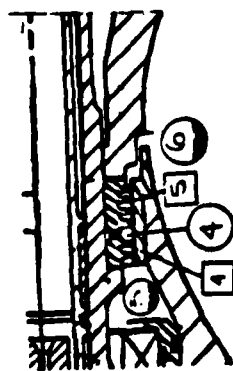
MACH NUMBERS IN PARENTHESES WERE USED TO SMOOTH OUT THE VELOCITY DISTRIBUTIONS.

MAXIMUM POWER

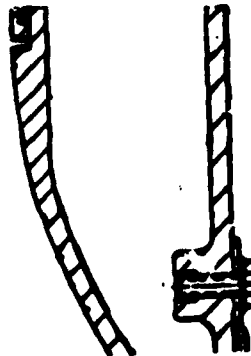
21-3640(22)
Appendix A
A-7

APPENDIX B

SECONDARY FLOW CONDITIONS

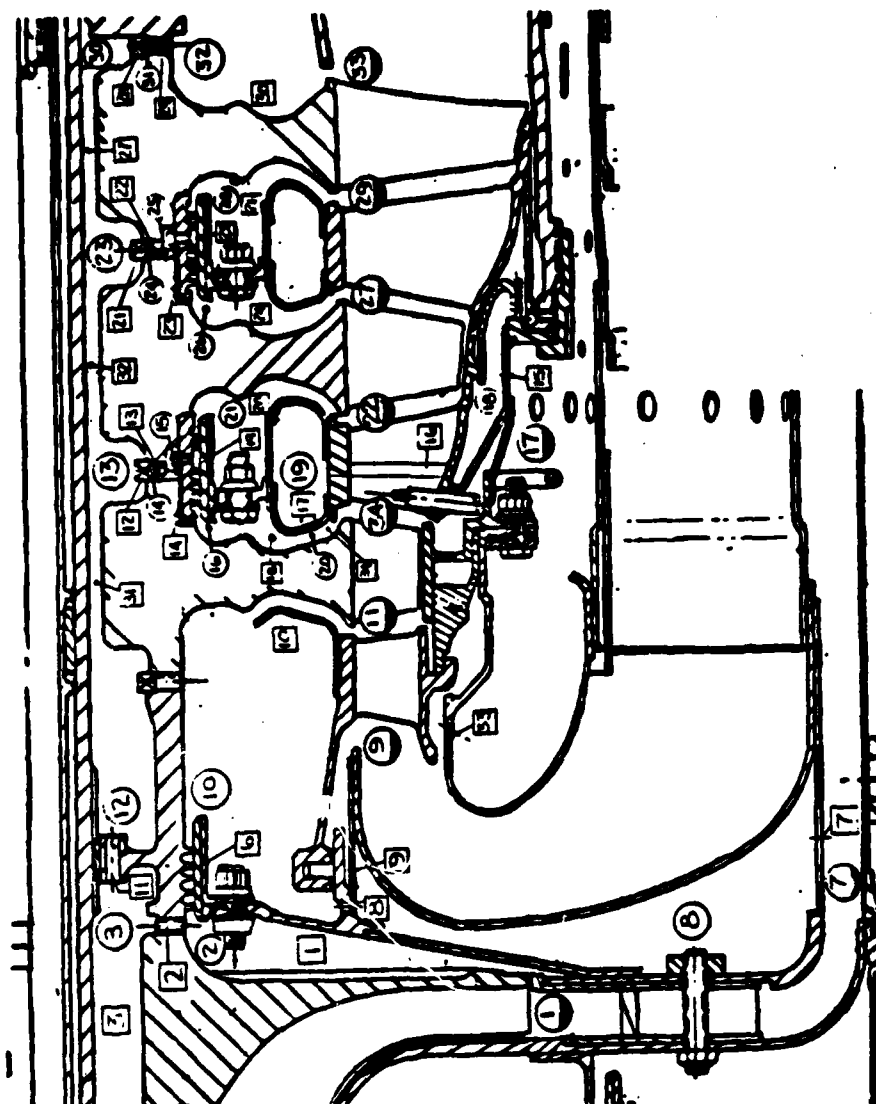


COMPRESSOR
SECTION



- CAVITY
- BOUNDARY CAVITY
- FLOW RESISTANCE

21-3640 (22)
Appendix B
B-1



TPE331-3U Secondary Flow Model.

SECONDARY FLOW PROGRAM INPUT MAX. POWER

RESISTANCE	CODE	FLOW (GPM)	AREA OR PERIM	CLEARANCE (IN)	TOOTH PITCH	NO. OF TEETH
1	4	4.000	*.0000	*.00000	-0.000	1.
2	4	4.000	*.0000	*.00000	-0.000	1.
3	1	.750	.0042	1.00000	-0.000	-0.
4	1	.900	.0119	1.00000	-0.000	-0.
5	2	.715	.0000	.00000	.100	4.
6	2	.700	1.4970	.01000	.125	9.
7	1	.637	.0350	1.00000	-0.000	-0.
8	1	.632	.0334	1.00000	-0.000	-0.
9	1	.632	.5292	1.00000	-0.000	-0.
10	4	4.000	*.0000	*.00000	-0.000	1.
11	1	.750	.1508	1.00000	-0.000	-0.
12	1	.600	.0180	1.00000	-0.000	-0.
13	1	.800	.2197	1.00000	-0.000	-0.
14	1	.800	.1200	1.00000	-0.000	-0.
15	1	.700	.3504	1.00000	-0.000	-0.
16	4	4.000	*.0000	*.00000	-0.000	1.
17	1	.600	.1079	1.00000	-0.000	-0.
18	4	10.000	*.0000	*.00000	-0.000	1.
19	2	.700	1.4970	.01000	.125	4.
20	4	11.000	*.0000	*.00000	-0.000	1.
21	1	.600	.0000	1.00000	-0.000	-0.
22	1	.800	.2197	1.00000	-0.000	-0.
23	1	.800	.1200	1.00000	-0.000	-0.
24	4	11.000	*.0000	*.00000	-0.000	1.
25	2	.700	1.5275	.01000	.125	6.
26	4	11.000	*.0000	*.00000	-0.000	1.
27	1	.900	.5277	1.00000	-0.000	-0.
28	1	.600	.0000	1.00000	-0.000	-0.
29	1	.800	.2197	1.00000	-0.000	-0.
30	-0	-0.000	*.0000	*.00000	-0.000	-0.
31	1	.900	.5277	1.00000	-0.000	-0.
32	1	.900	.5277	1.00000	-0.000	-0.
33	1	.632	.1149	1.00000	-0.000	-0.
34	4	10.000	*.0000	*.00000	-0.000	1.

DELTA-P/P 2 VERSUS CORRECTED FLOW TABLE FOR RESISTANCE 1

DELTA-P/P	COR. FLOW	DELTA-P/P	COR. FLOW	DELTA-P/P	COR. FLOW
.052200	.005540	.091700	.002200	.231400	.010900
.424700	.021400				

DELTA-P/P 2 VERSUS CORRECTED FLOW TABLE FOR RESISTANCE 2

DELTA-P/P	COR. FLOW	DELTA-P/P	COR. FLOW	DELTA-P/P	COR. FLOW
.017200	.001640	.020600	.006550	.026000	.011460
.034910	.016370				

DELTA-P/P 11 VERSUS CORRECTED FLOW TABLE FOR RESISTANCE 10

DELTA-P/P	COR. FLOW	DELTA-P/P	COR. FLOW	DELTA-P/P	COR. FLOW
-.032300	.000600	-.031300	.000900	-.030300	.001200
-.029500	.001500	-.028600	.001700	-.027600	.002000
-.027100	.002300	-.026400	.002600	-.025400	.002900

DELTA-P/P 19 VERSUS CORRECTED FLOW TABLE FOR RESISTANCE 16

DELTA-P/P	COR. FLOW	DELTA-P/P	COR. FLOW	DELTA-P/P	COR. FLOW
.004470	.005200	.044770	.013000	.097490	.018200
.442470	.031200				

DELTA-P/P20 VERSUS CORRECTED FLOW TABLE FOR RESISTANCE 10

DELTA-P/P	COR. FLOW	DELTA-P/P	COR. FLOW	DELTA-P/P	COR. FLOW
-.023500	.003500	-.019800	.007500	-.014500	.011500
-.011300	.019200	-.009700	.019100	-.008800	.022900
-.009300	.026700	-.004000	.030600	-.003000	.034400
-.002100	.038200				

DELTA-P/P22 VERSUS CORRECTED FLOW TABLE FOR RESISTANCE 20

DELTA-P/P	COR. FLOW	DELTA-P/P	COR. FLOW	DELTA-P/P	COR. FLOW
-.030500	.003500	-.026200	.007000	-.021100	.013900
-.019300	.020400	-.015500	.027400	-.019100	.034500
-.014000	.041700	-.013000	.049700	-.012100	.055600
-.011200	.062500	-.010900	.063500		

DELTA-P/P27 VERSUS CORRECTED FLOW TABLE FOR RESISTANCE 24

DELTA-P/P	COR. FLOW	DELTA-P/P	COR. FLOW	DELTA-P/P	COR. FLOW
-.036100	.004000	-.035700	.039000	-.029000	.016100
-.020500	.024700	-.019100	.037100	-.017300	.040200
-.009500	.049200	-.006300	.056200	-.004900	.064300
-.002900	.072300	-.001500	.090300		

DELTA-P/P29 VERSUS CORRECTED FLOW TABLE FOR RESISTANCE 26

DELTA-P/P	COR. FLOW	DELTA-P/P	COR. FLOW	DELTA-P/P	COR. FLOW
-.031400	.001400	-.029800	.002900	-.024900	.009200
-.021900	.009900	-.019500	.011400	-.019100	.014810
-.016700	.017700	-.015500	.020700	-.014500	.023600
-.013700	.026500	-.012900	.029500		

DELTA-P/P34 VERSUS CORRECTED FLOW TABLE FOR RESISTANCE 34

DELTA-P/P	COR. FLOW	DELTA-P/P	COR. FLOW	DELTA-P/P	COR. FLOW
-.007900	.003900	-.001240	.007500	-.000560	.011500
-.000220	.019300	-.000010	.019100	.000120	.022900
.000210	.026700	.000260	.030600	.000290	.030400
.000320	.038200				

THE FLOW RESISTANCES USED IN THE SECONDARY FLOW MODEL AT CRUISE AND IDLE ARE THE SAME AS FOR MAXIMUM POWER EXCEPT THAT SEVERAL CORRECTED FLOW TABLES WERE CHANGED TO PUMPING RESISTANCES AS SHOWN BELOW:

** PUMPING RESISTANCE INPUT **

RESISTANCE	CODE	RADIUS 1 LOCATION	RADIUS 1	RADIUS 2	SLIP FACTOR	SPEED RPM	TEMP. DEG F		
1	7	1.	1.400	4.150	.3600	40060.	1060.	.050	.400
10	7	10.	1.400	2.950	.3750	40060.	1012.	.050	.080
18	7	16.	1.550	2.600	.3750	40060.	1160.	.120	.080
20	7	21.	1.550	2.900	.3750	40060.	1313.	.075	.080
24	7	27.	1.550	2.900	.4000	40060.	1000.	.060	.080
26	7	28.	1.550	2.900	.3750	40060.	1015.	.075	.080
30	7	32.	1.400	2.900	.3750	40060.	848.	.080	.080
34	7	20.	2.600	2.950	.3750	40060.	1160.	.080	.080

CRUISE

** PUMPING RESISTANCE INPUT **

RESISTANCE	CODE	RADIUS 1 LOCATION	RADIUS 1	RADIUS 2	SLIP FACTOR	SPEED RPM	TEMP. DEG F		
1	7	1.	1.400	4.150	.3600	27125.	840.	.050	.400
10	7	10.	1.400	2.950	.3500	27125.	1012.	.050	.080
18	7	16.	1.550	2.600	.3500	27125.	1160.	.120	.080
20	7	21.	1.550	2.900	.3500	27125.	1313.	.075	.080
24	7	27.	1.550	2.900	.3800	27125.	1000.	.060	.080
26	7	28.	1.550	2.900	.3650	27125.	1015.	.075	.080
30	7	32.	1.400	2.900	.3650	27125.	848.	.080	.080
34	7	20.	2.600	2.950	.3500	27125.	1160.	.080	.080

IDLE

BOUNDARY CONDITIONS FOR SECONDARY FLOW

MAX POWER

** AERO INPUT **

CAVITY	PRESSURE	TEMPERATURE
1	116.30000	630.00000
5	16.70000	310.00000
6	11.42000	24.90000
7	152.80000	640.00000
9	143.61000	1820.50000
11	28.30000	1441.60000
17	157.50000	630.00000
22	50.52000	1376.30000
27	42.10000	1327.00000
29	21.42000	1057.70000
33	13.67000	947.50000

CRUISE

** AERO INPUT **

CAVITY	PRESSURE	TEMPERATURE
1	74.54000	600.00000
5	9.15000	310.00000
6	8.05500	20.00000
7	96.19000	600.00000
9	90.90000	1791.00000
11	62.20000	1615.00000
17	96.19000	600.00000
22	31.98000	1354.00000
27	26.65000	1306.00000
29	13.60000	1041.00000
33	8.65000	932.00000
34	49.40000	1525.00000

IDLE

** AERO INPUT **

CAVITY	PRESSURE	TEMPERATURE
1	37.30000	379.70000
5	16.70000	310.00000
6	14.50000	112.70000
7	40.98000	379.70000
9	39.20000	1327.00000
11	29.10000	1317.00000
17	40.98000	379.70000
22	19.20000	1147.00000
27	16.30000	1052.00000
29	15.20000	1052.00000
33	14.55000	1013.00000
34	24.00000	1167.00000

21-3640 (22)

Appendix B

B-5

APPENDIX C

SUMMARY OF HEAT TRANSFER COEFFICIENT RATIOS

PLATFORM

$$\left(\frac{h_1}{h_o}\right) = \left(\frac{N_1}{N_o}\right)^{2.2} \left(\frac{T_1}{T_o}\right)^{0.2}$$

WHERE: N is wheel speed
 T is ITT (Absolute Scale)
 Subscript 1 is transient value
 Subscript 2 is baseline value

RIVET HOLES

$$\left(\frac{h_1}{h_o}\right) = \left(\frac{N_1}{N_o}\right)^{0.25(X+Z+1)} \left(\frac{T_1}{T_o}\right)^{-0.625} \left(\frac{N_1}{N_o}\right)^{0.36X} \left(\frac{T_1}{T_o}\right)^{0.73}$$

WHERE: The first two terms arise from rotation of the rivet hole about the engine centerline and the second two terms arise from varying engine conditions.

Forward face T is Tcd
 Aft Face T is ITT

Engine Speed	<u>VALUES OF Z</u>		<u>VALUES OF X</u>	
	FWD	AFT	FWD	AFT
0 - 96%	1.27	1.29	1.85	1.22
96 - 100%	11.20	9.96	0.98	1.92

SLOTS

$$\left(\frac{h_1}{h_o}\right) = \left(\frac{N_1}{N_o}\right)^{0.3875Z} \left(\frac{T_1}{T_o}\right)^{0.71}$$

WHERE: Z is given above
 Forward Face T is Tcd
 Aft Face T is ITT

DISK FACES

$$\left(\frac{h_1}{h_o}\right) = \left(\frac{N_1}{N_o}\right)^{2.4} \left(\frac{T_1}{T_o}\right)^{-0.4}$$

WHERE: Forward Face T is T_{cd}
Aft Face T is ITT

BORE

$$\left(\frac{h_1}{h_o}\right) = \left(\frac{N_1}{N_o}\right)^{1.94} \left(\frac{T_1}{T_o}\right)^{0.4}$$

WHERE: T is T_{cd}

REIN DURABILITY PROGRAM AFJAL/ML CONTRACT NUMBER F33615-66-C-5027

CRACK LENGTHS FROM RA NUMBER 14717
DIMENSIONS IN MILS (INCHES X 100-00)

HOLE NUMBER	EP	X	Y	L	X	Y	EP	X	Y	L	X	Y	EP	X	Y	L	X	Y	EP	X	Y	L	X	Y
1	30	100	40				0	0	0	30	100	20	30	20	20				30	100	15			
	(127)	(294)	(101)				(0)	(0)	(0)	(127)	(127)	(50)	(76)	(50)	(50)				(0)	(294)	(14)			
2	30	10	30				35	110	35	0	0	0	10	20	10				0	0	3			
	(127)	(23)	(127)				(88)	(279)	(88)	(0)	(0)	(0)	(23)	(50)	(23)				(0)	(0)	(3)			
3	40	110	30				25	125	25	0	0	0	40	60	50				0	3	0			
	(132)	(279)	(127)				(63)	(317)	(63)	(0)	(0)	(0)	(101)	(132)	(127)				(0)	(0)	(0)			
4	30	100	40				45	0	40	0	35	0	0	35	30				0	0	0			
	(127)	(254)	(101)				(114)	(0)	(101)	(0)	(88)	(0)	(0)	(88)	(76)				(0)	(0)	(0)			
5	30	20	15				0	0	0	30	05	25	0	0	0				0	0	0			
	(76)	(50)	(30)				(0)	(0)	(0)	(76)	(213)	(63)	(0)	(0)	(0)				(0)	(0)	(0)			
6	0	0	0				35	125	35	0	0	30	30	0	30				0	0	0			
	(0)	(0)	(0)				(88)	(317)	(88)	(0)	(0)	(76)	(76)	(0)	(76)				(0)	(0)	(0)			
7	40	70	40				30	275	35	0	0	35	40	0	40				0	0	17			
	(101)	(177)	(101)				(76)	(698)	(88)	(0)	(0)	(88)	(101)	(0)	(101)				(0)	(0)	(23)			
8	75	130	60				25	30	25	50	60	25	0	0	25				0	0	0			
	(190)	(330)	(152)				(63)	(76)	(63)	(127)	(203)	(63)	(0)	(0)	(63)				(0)	(0)	(0)			
9	50	40	35				50	130	50	0	0	0	55	0	60				0	0	0			
	(127)	(101)	(88)				(127)	(330)	(127)	(0)	(0)	(0)	(139)	(0)	(152)				(0)	(0)	(0)			
10	60	50	50				10	60	60	0	0	0	0	0	0				0	0	0			
	(152)	(203)	(127)				(25)	(152)	(152)	(0)	(0)	(0)	(0)	(0)	(0)				(0)	(0)	(0)			
11	30	70	20				0	0	0	0	0	0	50	50	50				0	70	25			
	(76)	(177)	(50)				(0)	(0)	(0)	(0)	(0)	(0)	(127)	(127)	(127)				(0)	(177)	(53)			
12	0	0	0				10	125	10	0	15	3	0	20	20				0	0	0			
	(0)	(0)	(0)				(25)	(317)	(25)	(0)	(30)	(0)	(0)	(0)	(50)				(0)	(0)	(3)			
13	50	130	55				40	40	40	0	0	0	0	0	0				10	10	10			
	(127)	(330)	(139)				(101)	(101)	(101)	(0)	(0)	(0)	(0)	(0)	(0)				(20)	(25)	(25)			
14	0	0	0				25	125	30	0	0	25	30	0	30				0	3	0			
	(0)	(0)	(0)				(63)	(317)	(76)	(0)	(0)	(63)	(76)	(0)	(76)				(0)	(0)	(0)			
15	0	0	0				15	125	15	0	0	15	15	0	15				0	3	3			
	(0)	(0)	(0)				(30)	(317)	(30)	(0)	(0)	(30)	(30)	(0)	(30)				(0)	(0)	(3)			
16	40	90	40				20	20	20	0	0	30	50	0	50				40	60	30			
	(101)	(228)	(101)				(50)	(50)	(50)	(0)	(0)	(127)	(127)	(228)	(127)				(101)	(152)	(76)			
17	0	0	0				0	0	0	0	0	0	10	30	10				0	3	0			
	(0)	(0)	(0)				(203)	(63)	(25)	(0)	(0)	(0)	(25)	(76)	(25)				(0)	(3)	(0)			
18	0	0	0				20	125	20	0	0	35	50	0	50				0	0	0			
	(0)	(0)	(0)				(30)	(317)	(50)	(0)	(0)	(88)	(127)	(0)	(127)				(0)	(0)	(0)			
19	0	0	0				30	125	25	0	0	30	45	0	40				0	0	0			
	(0)	(0)	(0)				(76)	(317)	(63)	(0)	(0)	(76)	(114)	(0)	(101)				(0)	(0)	(0)			
20	50	40	45				0	0	0	0	0	0	15	70	15				0	0	0			
	(127)	(203)	(114)				(0)	(0)	(0)	(0)	(0)	(0)	(30)	(177)	(30)				(0)	(0)	(0)			
21	25	20	10				25	125	25	0	0	30	35	0	30				0	0	0			
	(63)	(50)	(25)				(63)	(317)	(63)	(0)	(0)	(76)	(88)	(0)	(76)				(3)	(3)	(3)			
22	0	0	0				0	0	0	0	0	0	20	40	25				0	30	25			
	(0)	(0)	(0)				(0)	(0)	(0)	(0)	(0)	(0)	(50)	(101)	(63)				(0)	(177)	(50)			
23	70	70	60				10	10	20	0	0	20	0	0	0				0	0	0			
	(177)	(177)	(152)				(25)	(25)	(50)	(0)	(0)	(50)	(0)	(0)	(0)				(0)	(3)	(0)			
24	40	70	45				35	110	30	0	0	35	0	0	0				0	0	0			
	(101)	(177)	(114)				(88)	(279)	(76)	(0)	(0)	(88)	(0)	(0)	(0)				(0)	(0)	(0)			
25	40	40	35				0	0	0	10	60	10	0	0	0				0	0	0			
	(101)	(101)	(88)				(25)	(152)	(76)	(0)	(0)	(0)	(0)	(0)	(0)				(0)	(0)	(0)			
26	40	40	30				15	125	20	0	0	15	25	0	30				0	60	20			
	(101)	(101)	(76)				(30)	(317)	(50)	(0)	(0)	(88)	(88)	(0)	(76)				(0)	(152)	(50)			
27	40	120	40				3	0	0	3	3	3	15	70	15				0	0	0			
	(101)	(304)	(101)				(0)	(0)	(0)	(0)	(0)	(0)	(30)	(177)	(30)				(3)	(3)	(0)			
28	0	0	0				25	125	30	0	0	25	30	0	30				0	0	0			
	(0)	(0)	(0)				(63)	(317)	(76)	(0)	(0)	(63)	(76)	(0)	(76)				(0)	(0)	(0)			
29	40	50	45				30	90	30	0	0	15	0	0	0				0	0	0			
	(101)	(127)	(114)				(76)	(228)	(76)	(0)	(0)	(30)	(0)	(0)	(0)				(0)	(0)	(0)			
30	30	60	30				0	0	0	3	3	3	20	70	15				0	0	0			
	(76)	(152)	(76)				(0)	(0)	(0)	(0)	(0)	(0)	(50)	(177)	(30)				(0)	(0)	(0)			
31	0	0	0				5	125	5	0	0	25	25	0	25				0	0	0			
	(0)	(0)	(0)				(12)	(317)	(12)	(0)	(0)	(63)	(63)	(0)	(63)				(0)	(0)	(0)			
32	5	15	5				45	125	10	0	0	40	45	0	45				0	0	0			
	(12)	(30)	(12)				(114)	(317)	(101)	(0)	(0)	(101)	(114)	(0)	(114)				(0)	(0)	(0)			
33	15	120	10				10	125	10	0	0	15	20	0	20				0	0	0			
	(30)	(304)	(25)				(25)	(317)	(25)	(0)	(0)	(30)	(50)	(0)	(50)				(0)	(0)	(0)			
34	40	50	30				30	40	30	0	0	0	15	50	15				0	0	0			
	(101)	(127)	(76)				(76)	(101)	(76)	(0)	(0)	(0)	(30)	(127)	(30)				(0)	(0)	(0)			
35	50	100	40				20	125	20	0	0	15	10	0	10				0	0	0			
	(127)	(254)	(101)				(90)	(317)	(50)	(0)	(0)	(30)	(25)	(0)	(25)				(0)	(0)	(0)			
36	50	120	55				0	0	0	40	40	10	0	0	0				0	0	0			
	(127)	(304)	(139)				(0)	(0)	(0)	(101)	(101)	(25)	(0)	(0)	(0)				(0)	(0)	(0)			
37	55	105	50				0	0	0	0	0	0	40	50	40				0	0	0			
	(139)	(200)	(127)				(0)	(0)	(0)	(0)	(0)	(0)	(101)	(203)	(101)				(0)	(0)	(0)			
38	0	0	0				20	125	20	0	0	30	30	0	30				0	0	0			
	(0)	(0)	(0)				(50)	(317)	(63)	(0)	(0)	(76)	(76)	(0)	(76)				(0)	(0)	(0)			
39	50	50	40				10	125	10	0	0	30	50	0	50				0	75	20			
	(127)	(127)	(101)				(25)	(317)	(25)	(0)	(0)	(76)	(127)	(0)	(127)				(0)	(177)	(50)			
40	70	140	70				0	0	0	0	0	0	40	70	50				0	0	0			
	(177)	(355)	(177)				(0)	(0)	(0)	(0)	(0)	(0)	(101)	(177)	(127)				(0)	(0)	(0)			

CRACK LENGTHS FROM NA NUMBER 19468
DIMENSIONS IN MILS (METERS X 10E-05)

[illegible]

DIN DURABILITY PROGRAM AFH/HL CONTRACT NUMBER F33615-60-C-3027

CRACK LENGTHS FROM RA NUMBER 15193
DIMENSIONS IN MILS (METERS X 10E-03)

HOLE NUMBER	XP	X	Y	L	X	Y	XP	X	Y	L	X	Y	XP	X	Y	L	X	Y	XP	X	Y	L	X	Y
1	0	0	0	0	0	0	0	0	0	0	0	0	0	0	0	0	0	0	0	0	0	0	0	0
2	0	0	0	0	0	0	0	0	0	0	0	0	0	0	0	0	0	0	0	0	0	0	0	0
3	0	0	0	0	0	0	0	0	0	0	0	0	0	0	0	0	0	0	0	0	0	0	0	0
4	0	0	0	0	0	0	0	0	0	0	0	0	0	0	0	0	0	0	0	0	0	0	0	0
5	0	0	0	0	0	0	0	0	0	0	0	0	0	0	0	0	0	0	0	0	0	0	0	0
6	0	0	0	0	0	0	0	0	0	0	0	0	0	0	0	0	0	0	0	0	0	0	0	0
7	0	0	0	0	0	0	0	0	0	0	0	0	0	0	0	0	0	0	0	0	0	0	0	0
8	0	0	0	0	0	0	0	0	0	0	0	0	0	0	0	0	0	0	0	0	0	0	0	0
9	0	0	0	0	0	0	0	0	0	0	0	0	0	0	0	0	0	0	0	0	0	0	0	0
10	0	0	0	0	0	0	0	0	0	0	0	0	0	0	0	0	0	0	0	0	0	0	0	0
11	0	0	0	0	0	0	0	0	0	0	0	0	0	0	0	0	0	0	0	0	0	0	0	0
12	0	0	0	0	0	0	0	0	0	0	0	0	0	0	0	0	0	0	0	0	0	0	0	0
13	0	0	0	0	0	0	0	0	0	0	0	0	0	0	0	0	0	0	0	0	0	0	0	0
14	0	0	0	0	0	0	0	0	0	0	0	0	0	0	0	0	0	0	0	0	0	0	0	0
15	0	0	0	0	0	0	0	0	0	0	0	0	0	0	0	0	0	0	0	0	0	0	0	0
16	0	0	0	0	0	0	0	0	0	0	0	0	0	0	0	0	0	0	0	0	0	0	0	0
17	0	0	0	0	0	0	0	0	0	0	0	0	0	0	0	0	0	0	0	0	0	0	0	0
18	0	0	0	0	0	0	0	0	0	0	0	0	0	0	0	0	0	0	0	0	0	0	0	0
19	0	0	0	0	0	0	0	0	0	0	0	0	0	0	0	0	0	0	0	0	0	0	0	0
20	0	0	0	0	0	0	0	0	0	0	0	0	0	0	0	0	0	0	0	0	0	0	0	0
21	0	0	0	0	0	0	0	0	0	0	0	0	0	0	0	0	0	0	0	0	0	0	0	0
22	0	0	0	0	0	0	0	0	0	0	0	0	0	0	0	0	0	0	0	0	0	0	0	0
23	0	0	0	0	0	0	0	0	0	0	0	0	0	0	0	0	0	0	0	0	0	0	0	0
24	0	0	0	0	0	0	0	0	0	0	0	0	0	0	0	0	0	0	0	0	0	0	0	0
25	0	0	0	0	0	0	0	0	0	0	0	0	0	0	0	0	0	0	0	0	0	0	0	0
26	0	0	0	0	0	0	0	0	0	0	0	0	0	0	0	0	0	0	0	0	0	0	0	0
27	0	0	0	0	0	0	0	0	0	0	0	0	0	0	0	0	0	0	0	0	0	0	0	0
28	0	0	0	0	0	0	0	0	0	0	0	0	0	0	0	0	0	0	0	0	0	0	0	0
29	0	0	0	0	0	0	0	0	0	0	0	0	0	0	0	0	0	0	0	0	0	0	0	0
30	0	0	0	0	0	0	0	0	0	0	0	0	0	0	0	0	0	0	0	0	0	0	0	0
31	0	0	0	0	0	0	0	0	0	0	0	0	0	0	0	0	0	0	0	0	0	0	0	0
32	0	0	0	0	0	0	0	0	0	0	0	0	0	0	0	0	0	0	0	0	0	0	0	0

BEIN DURABILITY PROGRAM AFH/LM CONTRACT NUMBER F33615-80-C-5027

CRACK LENGTHS FROM HA NUMBER 15133
DIMENSIONS IN MILS (INTEGERS X 10E-03)

HOLE NUMBER	X			Y			Z			W			V			U			T		
	1	2	3	4	5	6	7	8	9	10	11	12	13	14	15	16	17	18	19	20	21
1	0	0	0	0	0	0	0	0	0	0	0	0	0	0	0	0	0	0	0	0	0
2	25	70	20	0	0	0	0	0	0	0	0	0	0	0	0	0	0	0	0	0	0
3	0	0	0	0	0	0	0	0	0	0	0	0	0	0	0	0	0	0	0	0	0
4	0	0	0	0	0	0	0	0	0	0	0	0	0	0	0	0	0	0	0	0	0
5	0	0	0	0	0	0	0	0	0	0	0	0	0	0	0	0	0	0	0	0	0
6	60	90	60	0	0	0	0	0	0	0	0	0	0	0	0	0	0	0	0	0	0
7	152	228	152	0	0	0	0	0	0	0	0	0	0	0	0	0	0	0	0	0	0
8	20	100	20	0	0	0	0	0	0	0	0	0	0	0	0	0	0	0	0	0	0
9	30	125	30	0	0	0	0	0	0	0	0	0	0	0	0	0	0	0	0	0	0
10	0	0	0	0	0	0	0	0	0	0	0	0	0	0	0	0	0	0	0	0	0
11	0	0	0	0	0	0	0	0	0	0	0	0	0	0	0	0	0	0	0	0	0
12	60	90	60	0	0	0	0	0	0	0	0	0	0	0	0	0	0	0	0	0	0
13	0	0	0	0	0	0	0	0	0	0	0	0	0	0	0	0	0	0	0	0	0
14	0	0	0	0	0	0	0	0	0	0	0	0	0	0	0	0	0	0	0	0	0
15	0	0	0	0	0	0	0	0	0	0	0	0	0	0	0	0	0	0	0	0	0
16	0	0	0	0	0	0	0	0	0	0	0	0	0	0	0	0	0	0	0	0	0
17	90	120	40	0	0	0	0	0	0	0	0	0	0	0	0	0	0	0	0	0	0
18	127	304	101	0	0	0	0	0	0	0	0	0	0	0	0	0	0	0	0	0	0
19	40	60	50	0	0	0	0	0	0	0	0	0	0	0	0	0	0	0	0	0	0
20	101	152	127	0	0	0	0	0	0	0	0	0	0	0	0	0	0	0	0	0	0
21	0	0	0	0	0	0	0	0	0	0	0	0	0	0	0	0	0	0	0	0	0
22	0	0	0	0	0	0	0	0	0	0	0	0	0	0	0	0	0	0	0	0	0
23	0	0	0	0	0	0	0	0	0	0	0	0	0	0	0	0	0	0	0	0	0
24	0	0	0	0	0	0	0	0	0	0	0	0	0	0	0	0	0	0	0	0	0
25	0	0	0	0	0	0	0	0	0	0	0	0	0	0	0	0	0	0	0	0	0
26	0	0	0	0	0	0	0	0	0	0	0	0	0	0	0	0	0	0	0	0	0
27	10	20	10	0	0	0	0	0	0	0	0	0	0	0	0	0	0	0	0	0	0
28	25	50	25	0	0	0	0	0	0	0	0	0	0	0	0	0	0	0	0	0	0
29	30	50	40	0	0	0	0	0	0	0	0	0	0	0	0	0	0	0	0	0	0
30	127	152	101	0	0	0	0	0	0	0	0	0	0	0	0	0	0	0	0	0	0
31	0	0	0	0	0	0	0	0	0	0	0	0	0	0	0	0	0	0	0	0	0
32	0	0	0	0	0	0	0	0	0	0	0	0	0	0	0	0	0	0	0	0	0
33	0	0	0	0	0	0	0	0	0	0	0	0	0	0	0	0	0	0	0	0	0
34	0	0	0	0	0	0	0	0	0	0	0	0	0	0	0	0	0	0	0	0	0
35	0	0	0	0	0	0	0	0	0	0	0	0	0	0	0	0	0	0	0	0	0
36	0	0	0	0	0	0	0	0	0	0	0	0	0	0	0	0	0	0	0	0	0
37	0	0	0	0	0	0	0	0	0	0	0	0	0	0	0	0	0	0	0	0	0
38	0	0	0	0	0	0	0	0	0	0	0	0	0	0	0	0	0	0	0	0	0
39	0	0	0	0	0	0	0	0	0	0	0	0	0	0	0	0	0	0	0	0	0
40	0	0	0	0	0	0	0	0	0	0	0	0	0	0	0	0	0	0	0	0	0

FIN DURABILITY PROGRAM AFJAL/HL CONTRACT NUMBER F33613-80-C-9027

CRACK LENGTHS FROM HA NUMBER 13131
DIMENSIONS IN MILS (METERS X 10E-05)

MOLE NUMBER	X			Y			Z			W			V			U			T			S			R			Q			P		
	SP	X	Y	L	X	Y	SP	X	Y	L	X	Y	SP	X	Y	L	X	Y	SP	X	Y	L	X	Y	SP	X	Y	L	X	Y			
1	0	0	0	0	0	0	0	0	0	0	0	0	0	0	0	0	0	0	0	0	0	0	0	0	0	0	0	0	0	0			
2	0	0	0	0	0	0	0	0	0	0	0	0	0	0	0	0	0	0	0	0	0	0	0	0	0	0	0	0	0	0			
3	10	50	30	0	0	0	25	90	20	0	0	0	0	0	0	0	0	0	0	0	0	0	0	0	0	0	0	0	0	0			
4	70	120	70	0	0	0	63	229	50	0	0	0	0	0	0	0	0	0	0	0	0	0	0	0	0	0	0	0	0	0			
5	20	20	20	0	0	0	10	40	10	0	0	0	0	0	0	0	0	0	0	0	0	0	0	0	0	0	0	0	0	0			
6	30	10	50	0	0	0	23	101	23	0	0	0	0	0	0	0	0	0	0	0	0	0	0	0	0	0	0	0	0	0			
7	40	50	10	0	0	0	0	0	0	23	30	20	0	0	0	0	0	0	0	0	0	0	0	0	0	0	0	0	0	0			
8	101	127	70	0	0	0	0	0	0	0	0	0	0	0	0	0	0	0	0	0	0	0	0	0	0	0	0	0	0	0			
9	0	0	0	0	0	0	0	0	0	0	0	0	0	0	0	0	0	0	0	0	0	0	0	0	0	0	0	0	0	0			
10	0	0	0	0	0	0	0	0	0	0	0	0	0	0	0	0	0	0	0	0	0	0	0	0	0	0	0	0	0	0			
11	0	0	0	0	0	0	0	0	0	0	0	0	0	0	0	0	0	0	0	0	0	0	0	0	0	0	0	0	0	0			
12	0	0	0	0	0	0	0	0	0	0	0	0	0	0	0	0	0	0	0	0	0	0	0	0	0	0	0	0	0	0			
13	0	0	0	0	0	0	0	0	0	0	0	0	0	0	0	0	0	0	0	0	0	0	0	0	0	0	0	0	0	0			
14	0	0	0	0	0	0	0	0	0	0	0	0	0	0	0	0	0	0	0	0	0	0	0	0	0	0	0	0	0	0			
15	0	0	0	0	0	0	0	0	0	0	0	0	0	0	0	0	0	0	0	0	0	0	0	0	0	0	0	0	0	0			
16	0	0	0	0	0	0	0	0	0	0	0	0	0	0	0	0	0	0	0	0	0	0	0	0	0	0	0	0	0	0			
17	0	0	0	0	0	0	0	0	0	0	0	0	0	0	0	0	0	0	0	0	0	0	0	0	0	0	0	0	0	0			
18	0	0	0	0	0	0	0	0	0	0	0	0	0	0	0	0	0	0	0	0	0	0	0	0	0	0	0	0	0	0			
19	0	0	0	0	0	0	0	0	0	0	0	0	0	0	0	0	0	0	0	0	0	0	0	0	0	0	0	0	0	0			
20	0	0	0	0	0	0	0	0	0	0	0	0	0	0	0	0	0	0	0	0	0	0	0	0	0	0	0	0	0	0			
21	0	0	0	0	0	0	0	0	0	0	0	0	0	0	0	0	0	0	0	0	0	0	0	0	0	0	0	0	0	0			
22	0	0	0	0	0	0	0	0	0	0	0	0	0	0	0	0	0	0	0	0	0	0	0	0	0	0	0	0	0	0			
23	0	0	0	0	0	0	0	0	0	0	0	0	0	0	0	0	0	0	0	0	0	0	0	0	0	0	0	0	0	0			
24	0	0	0	0	0	0	0	0	0	0	0	0	0	0	0	0	0	0	0	0	0	0	0	0	0	0	0	0	0	0			
25	0	0	0	0	0	0	0	0	0	0	0	0	0	0	0	0	0	0	0	0	0	0	0	0	0	0	0	0	0	0			
26	0	0	0	0	0	0	0	0	0	0	0	0	0	0	0	0	0	0	0	0	0	0	0	0	0	0	0	0	0	0			
27	0	0	0	0	0	0	0	0	0	0	0	0	0	0	0	0	0	0	0	0	0	0	0	0	0	0	0	0	0	0			
28	0	0	0	0	0	0	0	0	0	0	0	0	0	0	0	0	0	0	0	0	0	0	0	0	0	0	0	0	0	0			
29	0	0	0	0	0	0	0	0	0	0	0	0	0	0	0	0	0	0	0	0	0	0	0	0	0	0	0	0	0	0			
30	0	0	0	0	0	0	0	0	0	0	0	0	0	0	0	0	0	0	0	0	0	0	0	0	0	0	0	0	0	0			
31	0	0	0	0	0	0	0	0	0	0	0	0	0	0	0	0	0	0	0	0	0	0	0	0	0	0	0	0	0	0			
32	0	0	0	0	0	0	0	0	0	0	0	0	0	0	0	0	0	0	0	0	0	0	0	0	0	0	0	0	0	0			
33	0	0	0	0	0	0	0	0	0	0	0	0	0	0	0	0	0	0	0	0	0	0	0	0	0	0	0	0	0	0			
34	0	0	0	0	0	0	0	0	0	0	0	0	0	0	0	0	0	0	0	0	0	0	0	0	0	0	0	0	0	0			
35	0	0	0	0	0	0	0	0	0	0	0	0	0	0	0	0	0	0	0	0	0	0	0	0	0	0	0	0	0	0			
36	0	0	0	0	0	0	0	0	0	0	0	0	0	0	0	0	0	0	0	0	0	0	0	0	0	0	0	0	0	0			
37	0	0	0	0	0	0	0	0	0	0	0	0	0	0	0	0	0	0	0	0	0	0	0	0	0	0	0	0	0	0			
38	0	0	0	0	0	0	0	0	0	0	0	0	0	0	0	0	0	0	0	0	0	0	0	0	0	0	0	0	0	0			
39	0	0	0	0	0	0	0	0	0	0	0	0	0	0	0	0	0	0	0	0	0	0	0	0	0	0	0	0	0	0			
40	0	0	0	0	0	0	0	0	0	0	0	0	0	0	0	0	0	0	0	0	0	0	0	0	0	0	0	0	0	0			

RIN DURABILITY PROGRAM APVAL/ML CONTRACT NUMBER F33615-60-C-5027

CRACK LENGTHS FROM RA NUMBER 15196
DIMENSIONS IN MILS (METERS X 10E-05)

HOLE	A						B						C						D						E						F					
	HP	L	X	V	HP	L	X	V	HP	L	X	V	HP	L	X	V	HP	L	X	V	HP	L	X	V	HP	L	X	V								
1	05	30	05	80	35	35	30	50	35	45	70	35	25	35	25	0	0	0	55	100	60	0	0	0	0	0	0	0								
2	(155) (127) (241)			(203) (188) (194)			(76) (127) (88)			(114) (177) (88)			(83) (88) (83)			(0) (0) (0)			(241) (355) (152)																	
3	0	0	0	0	0	0	0	0	0	0	0	0	0	0	0	0	0	0	10	60	0															
4	(0) (0) (0)			(0) (0) (0)			(0) (0) (0)			(0) (0) (0)			(0) (0) (0)			(0) (0) (0)			(25) (152) (0)																	
5	25	05	0	0	0	0	0	0	0	55	60	25	25	25	20	110	70	50	75	120	50															
6	(83) (165) (0)			(3) (0) (0)			(0) (0) (0)			(139) (152) (83)			(83) (83) (50)			(279) (177) (76)			(190) (304) (127)																	
7	35	100	30	0	0	0	5	30	0	25	45	15	0	0	0	0	0	0	50	110	40															
8	(88) (254) (76)			(0) (0) (0)			(12) (76) (0)			(83) (114) (38)			(0) (0) (0)			(0) (0) (0)			(127) (279) (101)																	
9	0	0	0	0	0	0	15	15	0	10	100	0	40	80	40	30	55	30	60	55	40															
10	(0) (0) (0)			(0) (0) (0)			(38) (38) (0)			(25) (254) (0)			(101) (203) (101)			(76) (139) (76)			(152) (139) (101)																	
11	0	0	0	0	0	0	0	0	0	0	0	0	0	0	0	0	0	0	40	50	0															
12	(0) (0) (0)			(0) (0) (0)			(0) (0) (0)			(0) (0) (0)			(0) (0) (0)			(0) (0) (0)			(101) (127) (0)																	
13	35	30	15	0	0	0	0	0	0	30	85	25	30	40	30	0	0	0	50	90	30															
14	(88) (76) (38)			(0) (0) (0)			(0) (0) (0)			(76) (125) (83)			(76) (101) (76)			(0) (0) (0)			(127) (228) (76)																	
15	40	105	45	0	0	0	5	30	0	60	85	35	35	40	35	140	25	15	50	120	40															
16	(101) (206) (114)			(0) (0) (0)			(12) (127) (0)			(152) (215) (88)			(88) (101) (0)			(355) (83) (25)			(127) (304) (101)																	
17	0	0	0	0	0	0	25	85	35	0	0	0	0	0	0	0	0	0	0	0	0															
18	(0) (0) (0)			(0) (0) (0)			(83) (103) (88)			(0) (0) (0)			(0) (0) (0)			(0) (0) (0)			(0) (0) (0)																	
19	0	0	0	0	0	0	15	20	20	10	85	45	80	70	60	0	0	0	30	65	20															
20	(0) (0) (0)			(0) (0) (0)			(38) (50) (50)			(25) (215) (101)			(152) (177) (152)			(0) (0) (0)			(76) (165) (50)																	
21	0	0	0	0	0	0	0	0	0	0	0	0	0	0	0	0	0	0	40	65	0															
22	(0) (0) (0)			(0) (0) (0)			(0) (0) (0)			(0) (0) (0)			(0) (0) (0)			(0) (0) (0)			(101) (165) (0)																	
23	45	85	45	55	70	35	0	0	0	35	150	30	0	0	0	0	0	0	30	110	35															
24	(114) (215) (114)			(139) (177) (76)			(0) (0) (0)			(88) (381) (76)			(0) (0) (0)			(0) (0) (0)			(76) (279) (76)																	
25	10	20	0	0	0	0	0	0	0	10	60	10	45	70	45	0	0	0	60	85	40															
26	(25) (50) (0)			(0) (0) (0)			(0) (0) (0)			(25) (152) (25)			(114) (177) (114)			(0) (0) (0)			(152) (215) (101)																	
27	40	80	30	0	0	0	0	0	0	10	150	20	0	0	0	80	95	25	60	110	50															
28	(101) (203) (76)			(0) (0) (0)			(0) (0) (0)			(25) (381) (101)			(0) (0) (0)			(203) (241) (45)			(152) (279) (127)																	
29	0	0	0	0	0	0	0	0	0	25	150	40	0	0	0	100	35	15	55	95	60															
30	(0) (0) (0)			(0) (0) (0)			(0) (0) (0)			(83) (381) (101)			(0) (0) (0)			(254) (88) (76)			(152) (241) (152)																	
31	0	0	0	0	0	0	0	0	0	0	0	0	0	0	0	0	0	0	40	65	0															
32	(0) (0) (0)			(0) (0) (0)			(0) (0) (0)			(0) (0) (0)			(0) (0) (0)			(0) (0) (0)			(101) (165) (0)																	
33	45	85	45	55	70	35	0	0	0	35	150	30	0	0	0	110	45	10	65	100	60															
34	(114) (215) (114)			(139) (177) (76)			(0) (0) (0)			(88) (381) (101)			(0) (0) (0)			(203) (101) (25)			(215) (254) (152)																	
35	70	70	50	70	45	10	0	0	0	40	150	20	0	0	0	0	0	0	90	170	75															
36	(177) (177) (127)			(177) (114) (25)			(0) (0) (0)			(101) (381) (50)			(0) (0) (0)			(0) (0) (0)			(228) (431) (190)																	
37	2	4	0	0	0	0	25	60	0	60	70	0	20	25	0	75	85	0	55	110	0															
38	(0) (0) (0)			(0) (0) (0)			(83) (152) (0)			(152) (177) (0)			(50) (55) (0)			(190) (215) (0)			(139) (279) (0)																	
39	40	90	45	0	0	0	20	25	20	15	70	10	0	0	0	0	0	0	75	140	70															
40	(152) (228) (114)			(0) (0) (0)			(50) (83) (50)			(38) (177) (25)			(0) (0) (0)			(0) (0) (0)			(190) (355) (177)																	
41	15	55	0	0	0	0	0	0	0	35	150	50	0	0	0	110	45	10	60	120	60															
42	(38) (139) (0)			(0) (0) (0)			(0) (0) (0)			(88) (381) (127)			(0) (0) (0)			(279) (114) (25)			(203) (304) (152)																	
43	30	45	25	0	0	0	35	90	30	0	0	0	45	60	50	0	0	0	65	130	60															
44	(76) (165) (83)			(0) (0) (0)			(98) (228) (76)			(0) (0) (0)			(114) (203) (127)			(0) (0) (0)			(165) (330) (152)																	
45	0	0	0	0	0	0	35	40	30	0	0	0	50	110	55	30	60	15	50	90	0															
46	(0) (0) (0)			(0) (0) (0)			(88) (152) (76)			(0) (0) (0)			(127) (279) (139)			(76) (152) (25)			(127) (228) (0)																	
47	30	75	0	0	0	0	35	95	35	0	0	0	45	75	45	100	70	35	80	140	80															
48	(76) (190) (0)			(0) (0) (0)			(88) (241) (88)			(0) (0) (0)			(114) (190) (114)			(254) (177) (99)			(203) (355) (203)																	
49	15	90	20	0	0	0	35	95	40	50	60	25	30	50	35	0	0	0	90	115	75															
50	(38) (228) (50)			(0) (0) (0)			(88) (241) (101)			(127) (152) (83)			(76) (127) (88)			(0) (0) (0)			(203) (292) (190)																	
51	0	0	0	110	55	25	55	100	60	0	0	0	20	40	15	20	85	25	70	90	50															
52	(0) (0) (0)			(279) (139) (55)			(139) (254) (152)			(3) (0) (0)			(50) (101) (38)			(50) (215) (55)			(177) (228) (127)																	
53	55	100	45	0	0	0	50	80	55	70	40	30	60	60	50	100	63	15	90	110	70															
54	(139) (254) (114)			(0) (0) (0)			(127) (203) (139)			(177) (101) (76)			(152) (152) (127)			(254) (152) (38)			(228) (279) (177)																	
55	50	65	40	40	60	25	0	0	0	0	0	0	35	50	55	0	0	0	60	150	60															
56	(127) (165) (101)			(101) (152) (45)			(0) (0) (0)			(0) (0) (0)			(88) (127) (139)			(0) (0) (0)			(152) (381) (152)																	

[illegible]

CRACK LENGTHS FROM RA NUMBER 14900
DIMENSIONS IN MILS (METERS X 100-00)

MCLE NUMBER	AP	X	Y	L	X	Y	AP	X	Y	L	X	Y	AP	X	Y	L	X	Y	AP	X	Y	L	X	Y
1	25	30	25	0	0	0	0	0	0	20	60	10	20	50	20	0	0	0	0	0	0	0	0	0
2	(63)	(76)	(63)	(0)	(0)	(0)	(0)	(0)	(0)	(50)	(132)	(25)	(50)	(127)	(50)	(0)	(0)	(0)	(0)	(0)	(0)	(0)	(0)	(0)
3	15	15	15	0	0	0	0	0	0	0	0	0	0	0	0	0	0	0	0	0	0	0	0	
4	(30)	(30)	(30)	(0)	(0)	(0)	(0)	(0)	(0)	(0)	(0)	(0)	(0)	(0)	(0)	(0)	(0)	(0)	(0)	(0)	(0)	(0)	(0)	
5	35	100	40	140	35	5	0	0	0	0	0	0	0	0	0	0	0	0	0	0	0	0	0	
6	(88)	(254)	(101)	(155)	(30)	(12)	(0)	(0)	(0)	(0)	(0)	(0)	(0)	(0)	(0)	(0)	(0)	(0)	(0)	(0)	(0)	(0)	(0)	
7	0	0	0	0	0	0	0	0	0	0	0	0	0	0	0	0	0	0	0	0	0	0	0	
8	(0)	(0)	(0)	(0)	(0)	(0)	(0)	(0)	(0)	(0)	(132)	(50)	(76)	(152)	(76)	(0)	(0)	(0)	(0)	(0)	(0)	(0)	(0)	
9	130	15	15	0	0	0	0	0	0	0	0	0	0	0	0	0	0	0	0	0	0	0	0	
10	(254)	(30)	(30)	(0)	(0)	(0)	(0)	(0)	(0)	(0)	(0)	(0)	(0)	(0)	(0)	(0)	(0)	(0)	(0)	(0)	(0)	(0)	(0)	
11	10	30	10	0	0	0	0	0	0	0	0	0	0	0	0	0	0	0	0	0	0	0	0	
12	(25)	(76)	(25)	(0)	(0)	(0)	(0)	(0)	(0)	(0)	(0)	(0)	(0)	(0)	(0)	(0)	(0)	(0)	(0)	(0)	(0)	(0)	(0)	
13	0	0	0	0	0	0	0	0	0	20	70	20	0	0	0	0	0	0	0	0	0	0	0	
14	(0)	(0)	(0)	(0)	(0)	(0)	(0)	(0)	(0)	(50)	(177)	(50)	(0)	(0)	(0)	(0)	(0)	(0)	(0)	(0)	(0)	(0)	(0)	
15	30	70	30	0	0	0	0	0	0	0	0	0	0	0	0	0	0	0	0	0	0	0	0	
16	(76)	(177)	(76)	(0)	(0)	(0)	(0)	(0)	(0)	(0)	(0)	(0)	(0)	(0)	(0)	(0)	(0)	(0)	(0)	(0)	(0)	(0)	(0)	
17	10	30	10	0	0	0	0	0	0	0	0	0	0	0	0	0	0	0	0	0	0	0	0	
18	(25)	(76)	(25)	(0)	(0)	(0)	(0)	(0)	(0)	(0)	(0)	(0)	(0)	(0)	(0)	(0)	(0)	(0)	(0)	(0)	(0)	(0)	(0)	
19	0	0	0	0	0	0	0	0	0	0	0	0	0	0	0	0	0	0	0	0	0	0	0	
20	(0)	(0)	(0)	(0)	(0)	(0)	(0)	(0)	(0)	(0)	(0)	(0)	(0)	(0)	(0)	(0)	(0)	(0)	(0)	(0)	(0)	(0)	(0)	
21	45	65	40	0	0	0	0	0	0	0	0	0	0	0	0	0	0	0	0	0	0	0	0	
22	(114)	(165)	(101)	(0)	(0)	(0)	(0)	(0)	(0)	(0)	(0)	(0)	(0)	(0)	(0)	(0)	(0)	(0)	(0)	(0)	(0)	(0)	(0)	
23	20	35	20	0	0	0	0	0	0	0	0	0	0	0	0	0	0	0	0	0	0	0	0	
24	(30)	(88)	(30)	(0)	(0)	(0)	(0)	(0)	(0)	(0)	(0)	(0)	(0)	(0)	(0)	(0)	(0)	(0)	(0)	(0)	(0)	(0)	(0)	
25	25	30	20	0	0	0	0	0	0	0	0	0	0	0	0	0	0	0	0	0	0	0	0	
26	(63)	(127)	(50)	(0)	(0)	(0)	(0)	(0)	(0)	(0)	(0)	(0)	(0)	(0)	(0)	(0)	(0)	(0)	(0)	(0)	(0)	(0)	(0)	
27	30	30	20	0	0	0	0	0	0	0	0	0	0	0	0	0	0	0	0	0	0	0	0	
28	(76)	(76)	(50)	(0)	(0)	(0)	(0)	(0)	(0)	(0)	(0)	(0)	(0)	(0)	(0)	(0)	(0)	(0)	(0)	(0)	(0)	(0)	(0)	
29	30	50	30	0	0	0	0	0	0	0	0	0	0	0	0	0	0	0	0	0	0	0	0	
30	(76)	(127)	(76)	(0)	(0)	(0)	(0)	(0)	(0)	(0)	(0)	(0)	(0)	(0)	(0)	(0)	(0)	(0)	(0)	(0)	(0)	(0)	(0)	
31	45	35	30	0	0	0	0	0	0	0	140	10	0	0	0	0	0	0	0	0	0	0	0	
32	(114)	(88)	(76)	(0)	(0)	(0)	(0)	(0)	(0)	(0)	(0)	(0)	(0)	(0)	(0)	(0)	(0)	(0)	(0)	(0)	(0)	(0)	(0)	
33	15	30	20	0	0	0	0	0	0	0	0	0	0	0	0	0	0	0	0	0	0	0	0	
34	(30)	(76)	(50)	(0)	(0)	(0)	(0)	(0)	(0)	(0)	(0)	(0)	(0)	(0)	(0)	(0)	(0)	(0)	(0)	(0)	(0)	(0)	(0)	
35	40	60	40	0	0	0	0	0	0	0	0	0	0	0	0	0	0	0	0	0	0	0	0	
36	(101)	(203)	(101)	(0)	(0)	(0)	(0)	(0)	(0)	(0)	(0)	(0)	(0)	(0)	(0)	(0)	(0)	(0)	(0)	(0)	(0)	(0)	(0)	
37	10	35	15	0	0	0	0	0	0	0	0	0	0	0	0	0	0	0	0	0	0	0	0	
38	(25)	(88)	(25)	(0)	(0)	(0)	(0)	(0)	(0)	(0)	(0)	(0)	(0)	(0)	(0)	(0)	(0)	(0)	(0)	(0)	(0)	(0)	(0)	
39	15	30	15	0	0	0	0	0	0	0	0	0	0	0	0	0	0	0	0	0	0	0	0	
40	(30)	(76)	(50)	(0)	(0)	(0)	(0)	(0)	(0)	(0)	(0)	(0)	(0)	(0)	(0)	(0)	(0)	(0)	(0)	(0)	(0)	(0)	(0)	
41	40	60	40	0	0	0	0	0	0	0	0	0	0	0	0	0	0	0	0	0	0	0	0	
42	(101)	(203)	(101)	(0)	(0)	(0)	(0)	(0)	(0)	(0)	(0)	(0)	(0)	(0)	(0)	(0)	(0)	(0)	(0)	(0)	(0)	(0)	(0)	
43	10	35	15	0	0	0	0	0	0	0	0	0	0	0	0	0	0	0	0	0	0	0	0	
44	(25)	(88)	(25)	(0)	(0)	(0)	(0)	(0)	(0)	(0)	(0)	(0)	(0)	(0)	(0)	(0)	(0)	(0)	(0)	(0)	(0)	(0)	(0)	
45	15	30	15	0	0	0	0	0	0	0	0	0	0	0	0	0	0	0	0	0	0	0	0	
46	(30)	(76)	(50)	(0)	(0)	(0)	(0)	(0)	(0)	(0)	(0)	(0)	(0)	(0)	(0)	(0)	(0)	(0)	(0)	(0)	(0)	(0)	(0)	
47	40	60	40	0	0	0	0	0	0	0	0	0	0	0	0	0	0	0	0	0	0	0	0	
48	(101)	(203)	(101)	(0)	(0)	(0)	(0)	(0)	(0)	(0)	(0)	(0)	(0)	(0)	(0)	(0)	(0)	(0)	(0)	(0)	(0)	(0)	(0)	
49	10	35	15	0	0	0	0	0	0	0	0	0	0	0	0	0	0	0	0	0	0	0	0	
50	(25)	(88)	(25)	(0)	(0)	(0)	(0)	(0)	(0)	(0)	(0)	(0)	(0)	(0)	(0)	(0)	(0)	(0)	(0)	(0)	(0)	(0)	(0)	
51	15	30	15	0	0	0	0	0	0	0	0	0	0	0	0	0	0	0	0	0	0	0	0	
52	(30)	(76)	(50)	(0)	(0)	(0)	(0)	(0)	(0)	(0)	(0)	(0)	(0)	(0)	(0)	(0)	(0)	(0)	(0)	(0)	(0)	(0)	(0)	
53	40	60	40	0	0	0	0	0	0	0	0	0	0	0	0	0	0	0	0	0	0	0	0	
54	(101)	(203)	(101)	(0)	(0)	(0)	(0)	(0)	(0)	(0)	(0)	(0)	(0)	(0)	(0)	(0)	(0)	(0)	(0)	(0)	(0)	(0)	(0)	
55	10	35	15	0	0	0	0	0	0	0	0	0	0	0	0	0	0	0	0	0	0	0	0	
56	(25)	(88)	(25)	(0)	(0)	(0)	(0)	(0)	(0)	(0)	(0)	(0)	(0)	(0)	(0)	(0)	(0)	(0)	(0)	(0)	(0)	(0)	(0)	
57	15	30	15	0	0	0	0	0	0	0	0	0	0	0	0	0	0	0	0	0	0	0	0	
58	(30)	(76)	(50)	(0)	(0)	(0)	(0)	(0)	(0)	(0)	(0)	(0)	(0)	(0)	(0)	(0)	(0)	(0)	(0)	(0)	(0)	(0)	(0)	
59	40	60	40	0	0	0	0	0	0	0	0	0	0	0	0	0	0	0	0	0	0	0	0	
60	(101)	(203)	(101)	(0)	(0)	(0)	(0)	(0)	(0)	(0)	(0)	(0)	(0)	(0)	(0)	(0)	(0)	(0)	(0)	(0)	(0)	(0)	(0)	

CRACK LENGTHS FROM NA NUMBER 14970
DIMENSIONS IN MILS (METERS X 10E-03)

NUMBER	SP	E	V	L	E	V	SP	E	V	L	E	V	SP	E	V	L	E	V	SP	E	V	L	E	V
1	30	75	0	0	0	0	20	100	0	0	0	0	20	100	0	0	0	0	20	100	0	0	0	0
	(127)	(190)	(0)	(0)	(0)	(0)	(0)	(0)	(0)	(0)	(0)	(0)	(0)	(0)	(0)	(0)	(0)	(0)	(0)	(0)	(0)	(0)	(0)	
1	0	0	0	0	0	0	0	0	0	0	0	0	0	0	0	0	0	0	0	0	0	0	0	
	(0)	(0)	(0)	(0)	(0)	(0)	(0)	(0)	(0)	(0)	(0)	(0)	(0)	(0)	(0)	(0)	(0)	(0)	(0)	(0)	(0)	(0)	(0)	
2	40	65	0	0	0	0	10	10	0	0	0	0	20	30	0	0	0	0	30	40	0	0	0	
	(101)	(165)	(0)	(0)	(0)	(0)	(25)	(25)	(0)	(0)	(0)	(0)	(30)	(76)	(0)	(0)	(0)	(0)	(119)	(100)	(0)	(0)	(0)	
2	0	0	0	0	0	0	0	0	0	0	0	0	25	26	0	0	0	0	0	0	0	0	0	
	(0)	(0)	(0)	(0)	(0)	(0)	(0)	(0)	(0)	(0)	(0)	(0)	(63)	(71)	(20)	(0)	(0)	(0)	(0)	(0)	(0)	(0)	(0)	
3	90	27	0	100	15	7	0	0	0	0	0	0	2	112	20	70	42	40	100	15	7	37	70	39
	(1220)	(66)	(20)	(457)	(18)	(17)	(0)	(0)	(0)	(0)	(0)	(0)	(5)	(204)	(50)	(23)	(106)	(101)	(406)	(38)	(7)	(144)	(100)	(99)
3	0	0	0	0	0	0	0	0	0	0	0	0	0	0	0	0	0	0	0	0	0	0	0	
	(0)	(0)	(0)	(0)	(0)	(0)	(0)	(0)	(0)	(0)	(0)	(0)	(0)	(0)	(0)	(0)	(0)	(0)	(0)	(0)	(0)	(0)	(0)	
4	40	45	0	0	0	0	0	0	0	0	0	0	40	23	0	12	30	12	0	0	0	0	0	0
	(101)	(114)	(0)	(0)	(0)	(0)	(0)	(0)	(0)	(0)	(0)	(0)	(243)	(63)	(0)	(30)	(76)	(30)	(0)	(0)	(0)	(0)	(0)	(0)
5	70	60	40	0	0	0	0	0	0	0	0	0	30	75	0	15	20	0	0	0	0	0	0	0
	(177)	(152)	(101)	(0)	(0)	(0)	(0)	(0)	(0)	(0)	(0)	(0)	(127)	(190)	(0)	(30)	(50)	(0)	(0)	(0)	(0)	(0)	(0)	(0)
6	75	65	30	40	30	7	0	0	0	0	0	0	10	30	0	12	45	17	0	0	0	0	0	0
	(100)	(165)	(127)	(101)	(127)	(7)	(0)	(0)	(0)	(0)	(0)	(0)	(25)	(76)	(0)	(30)	(114)	(43)	(0)	(0)	(0)	(0)	(0)	(0)
6	0	0	0	65	50	18	0	0	0	0	0	0	80	30	12	0	0	0	0	0	0	0	0	0
	(0)	(0)	(0)	(165)	(127)	(45)	(0)	(0)	(0)	(0)	(0)	(0)	(203)	(76)	(30)	(0)	(0)	(0)	(0)	(0)	(0)	(0)	(0)	(0)
7	15	12	10	0	0	0	0	0	0	0	0	0	15	112	15	30	50	0	150	30	0	15	20	0
	(30)	(30)	(25)	(0)	(0)	(0)	(0)	(0)	(0)	(0)	(0)	(0)	(30)	(204)	(30)	(76)	(127)	(0)	(30)	(76)	(7)	(30)	(50)	(20)
8	30	30	0	0	0	0	0	0	0	0	0	0	45	60	20	15	30	30	0	0	0	25	45	15
	(76)	(127)	(0)	(0)	(0)	(0)	(0)	(0)	(0)	(0)	(0)	(0)	(115)	(203)	(50)	(80)	(76)	(76)	(0)	(0)	(0)	(63)	(114)	(38)
8	0	0	0	0	0	0	0	0	0	0	0	0	0	0	0	10	35	15	0	0	0	50	114	40
	(0)	(0)	(0)	(0)	(0)	(0)	(0)	(0)	(0)	(0)	(0)	(0)	(0)	(0)	(0)	(45)	(80)	(30)	(0)	(0)	(0)	(127)	(200)	(101)
10	25	40	0	0	0	0	10	10	0	0	0	0	0	0	0	0	0	0	0	0	15	35	15	15
	(63)	(101)	(0)	(0)	(0)	(0)	(25)	(25)	(0)	(0)	(0)	(0)	(0)	(0)	(0)	(0)	(0)	(0)	(0)	(0)	(0)	(30)	(80)	(30)
11	10	10	0	0	0	0	0	0	0	0	0	0	0	0	0	25	45	25	0	0	0	40	85	35
	(25)	(25)	(0)	(0)	(0)	(0)	(0)	(0)	(0)	(0)	(0)	(0)	(0)	(0)	(0)	(63)	(114)	(63)	(0)	(0)	(0)	(101)	(215)	(80)
12	5	10	5	0	0	0	0	0	0	0	0	0	25	125	25	15	25	30	165	25	0	70	55	50
	(12)	(25)	(12)	(0)	(0)	(0)	(0)	(0)	(0)	(0)	(0)	(0)	(63)	(312)	(63)	(80)	(63)	(76)	(419)	(63)	(7)	(177)	(130)	(127)
13	0	0	0	0	0	0	0	0	0	0	0	0	0	0	0	0	0	0	0	0	0	45	65	0
	(0)	(0)	(0)	(0)	(0)	(0)	(0)	(0)	(0)	(0)	(0)	(0)	(0)	(0)	(0)	(0)	(0)	(0)	(0)	(0)	(0)	(114)	(85)	(0)
13	0	0	0	0	0	0	0	0	0	0	0	0	0	0	0	0	0	0	0	0	10	25	0	0
	(0)	(0)	(0)	(0)	(0)	(0)	(0)	(0)	(0)	(0)	(0)	(0)	(0)	(0)	(0)	(0)	(0)	(0)	(0)	(0)	(25)	(50)	(0)	(0)
14	35	70	35	0	0	0	0	0	0	0	0	0	30	25	5	30	60	35	0	0	0	30	30	0
	(80)	(177)	(80)	(0)	(0)	(0)	(0)	(0)	(0)	(0)	(0)	(0)	(127)	(63)	(12)	(76)	(152)	(80)	(0)	(0)	(0)	(31)	(119)	(76)
15	30	0	0	0	0	0	0	0	0	0	0	0	0	0	0	0	0	0	65	35	15	10	55	20
	(12)	(76)	(0)	(0)	(0)	(0)	(0)	(0)	(0)	(0)	(0)	(0)	(0)	(0)	(0)	(0)	(0)	(0)	(215)	(80)	(10)	(25)	(130)	(80)
16	45	80	35	0	0	0	15	30	10	0	0	0	0	0	0	0	0	0	0	0	35	55	20	0
	(114)	(203)	(80)	(0)	(0)	(0)	(30)	(76)	(25)	(0)	(0)	(0)	(0)	(0)	(0)	(0)	(0)	(0)	(0)	(0)	(0)	(66)	(114)	(90)
17	0	0	0	0	0	0	20	45	20	0	0	0	30	115	25	0	0	0	0	0	0	20	35	15
	(0)	(0)	(0)	(0)	(0)	(0)	(63)	(114)	(50)	(0)	(0)	(0)	(76)	(292)	(63)	(0)	(0)	(0)	(0)	(0)	(0)	(50)	(80)	(38)
18	70	65	55	0	0	0	0	0	0	0	0	0	5	100	30	25	50	40	155	35	15	45	60	0
	(177)	(165)	(130)	(0)	(0)	(0)	(0)	(0)	(0)	(0)	(0)	(0)	(12)	(254)	(76)	(63)	(127)	(101)	(393)	(80)	(39)	(114)	(152)	(0)
19	10	55	0	30	45	10	20	70	25	0	0	0	60	25	12	25	65	45	130	55	24	30	90	50
	(25)	(130)	(0)	(76)	(114)	(25)	(50)	(177)	(63)	(0)	(0)	(0)	(132)	(50)	(30)	(63)	(165)	(114)	(330)	(139)	(63)	(76)	(220)	(127)
19	15	35	15	0	0	0	0	0	0	0	0	0	0	0	0	0	0	0	0	0	0	0	0	0
	(30)	(84)	(30)	(0)	(0)	(0)	(0)	(0)	(0)	(0)	(0)	(0)	(0)	(0)	(0)	(0)	(0)	(0)	(0)	(0)	(0)	(0)	(0)	(0)
20	0	0	0	0	0	0	0	0	0	0	0	0	0	0	0	35	30	0	0	0	0	30	80	0
	(0)	(0)	(0)	(0)	(0)	(0)	(0)	(0)	(0)	(0)	(0)	(0)	(0)	(0)	(0)	(80)	(76)	(0)	(0)	(0)	(0)	(76)	(203)	(0)
21	35	60	25	0	0	0	0	0	0	0	0	0	25	110	20	30	35	30	100	25	10	60	110	45
	(80)	(152)	(63)	(0)	(0)	(0)	(0)	(0)	(0)	(0)	(0)	(0)	(63)	(279)	(50)	(76)	(80)	(76)	(254)	(63)	(25)	(132)	(279)	(114)
22	35	95	25	0	0	0	10	45	17	0	0	0	16	55	16	45	25	0	0	0	20	5	0	0
	(80)	(241)	(63)	(0)	(0)	(0)	(25)	(114)	(43)	(0)	(0)	(0)	(40)	(130)	(40)	(114)	(63)	(0)	(0)	(0)	(50)	(12)	(0)	(0)
23	0	0	0	0	0	0	0	0	0	0	0	0	15	65	0	0	0	0	0	0	70	60	0	0
	(0)	(0)	(0)	(0)	(0)	(0)	(0)	(0)	(0)	(0)	(0)	(0)	(30)	(165)	(0)	(0)	(0)	(0)	(0)	(0)	(177)	(152)	(0)	(0)
24	30	45	25	35	20	0	0	0	0	0	0	0	30	55	0	0	0	0	40	90	10	40	45	0
	(127)	(114)	(63)	(80)	(30)	(7)	(0)	(0)	(0)	(0)	(0)	(0)	(76)	(127)	(3)	(0)	(0)	(0)	(161)	(203)	(25)	(101)	(114)	(0)
25	25	55	25	0	0	0	20	60	25	0	0	0	0	0	0	35	90	0	65	55	0	35	25	20
	(63)	(130)	(63)	(0)	(0)	(0)	(50)	(152)	(63)	(0)	(0)	(0)	(0)	(0)	(0)	(80)	(228)	(0)	(165)	(127)	(0)	(80)	(63)	(50)
26	25	55	25	0	0	0	25	75	25	0	0	0	65	45	25	15	45	20	80	70	20	65	5	0
	(63)	(130)	(63)	(0)	(0)	(0)	(63)	(190)	(63)	(0)	(0)	(0)	(165)	(114)	(63)	(30)	(114)	(50)	(203)	(177)	(50)	(165)	(12)	(0)
27	30	15	0	0	0	0	0	0	0	0	0	0	3	47	10	30	35	35	0	0	0	70	120	50
	(76)	(36)	(0)	(0)	(0)	(0)	(0)	(0)	(0)	(0)	(0)	(0)	(7)	(110)	(25)	(76)	(241)	(80)	(0)	(0)	(0)	(177)	(254)	(127)
28	30	45	20	0	0	0	25	50	25	0	0	0	0	0	0	35	115	25	140	30	14	40	30	30
	(76)	(114)	(50)	(0)	(0)	(0)	(63)	(127)	(63)	(0)	(0)	(0)	(0)	(0)	(0)	(80)	(279)	(63)	(355)	(76)	(10)	(101)	(76)	(76)
29	0	0	0	0	0	0	0	0	0	0	0	0	0	0	0	0	0	0	0	0	25	40	0	0
	(0)	(0)	(0)	(0)	(0)	(0)	(0)	(0)	(0)	(0)	(0)	(0)	(0)	(0)	(0)	(0)	(0)	(0)	(0)	(0)	(0)	(63)	(203)	(0)
29	65	50	40	15	130	40	0	0	0	0	0	0	0	0	0	20	30	20	65	30	0	40	70	0
	(165)	(127)	(161)	(30)	(320)	(101)	(0)	(0)	(0)	(0)	(0)	(0)	(0)	(0)	(0)	(50)	(127)	(50)	(165)	(91)	(10)	(101)	(177)	(0)
30	25	25	0	25	55	15	0	0	0	0	0	0	30	100	15	30	30	15	160	30	15	15	60	0
	(63)	(63)	(0)	(63)	(159)	(39)	(0)	(127)	(76)	(0)	(0)	(0)	(76)	(254)	(80)	(76)	(76)	(80)	(406)	(76)	(10)	(30)	(240)	(0)
30	0	0	0	0	0	0	0	0	0	0	0	0	0	0	0	0	0	0	0	0	0			

DIN DURABILITY PROGRAM AFJAL/ML CONTRACT NUMBER F33615-60-C-5027

CRACK LENGTHS FROM RA NUMBER 14433
DIMENSIONS IN MILS (METERS X 10E-05)

HOLE NUMBER	XP	X	Y	L	X	Y	XP	X	Y	L	X	Y	XP	X	Y	L	X	Y	XP	X	Y	L	X	Y	XP	X	Y	L	X	Y
1	0	0	0	0	0	0	0	0	0	0	0	0	0	0	0	0	0	0	0	0	0	0	0	0	0	0	0	0	0	0
2	0	0	0	0	0	0	0	0	0	0	0	0	0	0	0	0	0	0	0	0	0	0	0	0	0	0	0	0	0	0
3	25	30	20	0	0	0	0	0	0	0	0	0	0	0	0	0	0	0	0	0	0	0	0	0	0	0	0	0	0	0
4	0	0	0	0	0	0	0	0	0	0	0	0	0	0	0	0	0	0	0	0	0	0	0	0	0	0	0	0	0	0
5	0	0	0	0	0	0	0	0	0	0	0	0	0	0	0	0	0	0	0	0	0	0	0	0	0	0	0	0	0	0
6	0	0	0	0	0	0	0	0	0	0	0	0	0	0	0	0	0	0	0	0	0	0	0	0	0	0	0	0	0	0
7	0	0	0	0	0	0	0	0	0	0	0	0	0	0	0	0	0	0	0	0	0	0	0	0	0	0	0	0	0	0
8	0	0	0	0	0	0	0	0	0	0	0	0	0	0	0	0	0	0	0	0	0	0	0	0	0	0	0	0	0	0
9	0	0	0	0	0	0	0	0	0	0	0	0	0	0	0	0	0	0	0	0	0	0	0	0	0	0	0	0	0	0
10	0	0	0	0	0	0	0	0	0	0	0	0	0	0	0	0	0	0	0	0	0	0	0	0	0	0	0	0	0	0
11	0	0	0	0	0	0	0	0	0	0	0	0	0	0	0	0	0	0	0	0	0	0	0	0	0	0	0	0	0	0
12	0	0	0	0	0	0	0	0	0	0	0	0	0	0	0	0	0	0	0	0	0	0	0	0	0	0	0	0	0	0
13	0	0	0	0	0	0	0	0	0	0	0	0	0	0	0	0	0	0	0	0	0	0	0	0	0	0	0	0	0	0
14	0	0	0	0	0	0	0	0	0	0	0	0	0	0	0	0	0	0	0	0	0	0	0	0	0	0	0	0	0	0
15	0	0	0	0	0	0	0	0	0	0	0	0	0	0	0	0	0	0	0	0	0	0	0	0	0	0	0	0	0	0
16	0	0	0	0	0	0	0	0	0	0	0	0	0	0	0	0	0	0	0	0	0	0	0	0	0	0	0	0	0	0
17	0	0	0	0	0	0	0	0	0	0	0	0	0	0	0	0	0	0	0	0	0	0	0	0	0	0	0	0	0	0
18	0	0	0	0	0	0	0	0	0	0	0	0	0	0	0	0	0	0	0	0	0	0	0	0	0	0	0	0	0	0
19	0	0	0	0	0	0	0	0	0	0	0	0	0	0	0	0	0	0	0	0	0	0	0	0	0	0	0	0	0	0
20	0	0	0	0	0	0	0	0	0	0	0	0	0	0	0	0	0	0	0	0	0	0	0	0	0	0	0	0	0	0
21	0	0	0	0	0	0	0	0	0	0	0	0	0	0	0	0	0	0	0	0	0	0	0	0	0	0	0	0	0	0
22	0	0	0	0	0	0	0	0	0	0	0	0	0	0	0	0	0	0	0	0	0	0	0	0	0	0	0	0	0	0
23	0	0	0	0	0	0	0	0	0	0	0	0	0	0	0	0	0	0	0	0	0	0	0	0	0	0	0	0	0	0
24	0	0	0	0	0	0	0	0	0	0	0	0	0	0	0	0	0	0	0	0	0	0	0	0	0	0	0	0	0	0
25	0	0	0	0	0	0	0	0	0	0	0	0	0	0	0	0	0	0	0	0	0	0	0	0	0	0	0	0	0	0
26	0	0	0	0	0	0	0	0	0	0	0	0	0	0	0	0	0	0	0	0	0	0	0	0	0	0	0	0	0	0
27	0	0	0	0	0	0	0	0	0	0	0	0	0	0	0	0	0	0	0	0	0	0	0	0	0	0	0	0	0	0
28	0	0	0	0	0	0	0	0	0	0	0	0	0	0	0	0	0	0	0	0	0	0	0	0	0	0	0	0	0	0
29	0	0	0	0	0	0	0	0	0	0	0	0	0	0	0	0	0	0	0	0	0	0	0	0	0	0	0	0	0	0
30	0	0	0	0	0	0	0	0	0	0	0	0	0	0	0	0	0	0	0	0	0	0	0	0	0	0	0	0	0	0
31	0	0	0	0	0	0	0	0	0	0	0	0	0	0	0	0	0	0	0	0	0	0	0	0	0	0	0	0	0	0
32	0	0	0	0	0	0	0	0	0	0	0	0	0	0	0	0	0	0	0	0	0	0	0	0	0	0	0	0	0	0
33	0	0	0	0	0	0	0	0	0	0	0	0	0	0	0	0	0	0	0	0	0	0	0	0	0	0	0	0	0	0
34	0	0	0	0	0	0	0	0	0	0	0	0	0	0	0	0	0	0	0	0	0	0	0	0	0	0	0	0	0	0
35	0	0	0	0	0	0	0	0	0	0	0	0	0	0	0	0	0	0	0	0	0	0	0	0	0	0	0	0	0	0
36	0	0	0	0	0	0	0	0	0	0	0	0	0	0	0	0	0	0	0	0	0	0	0	0	0	0	0	0	0	0
37	0	0	0	0	0	0	0	0	0	0	0	0	0	0	0	0	0	0	0	0	0	0	0	0	0	0	0	0	0	0
38	0	0	0	0	0	0	0	0	0	0	0	0	0	0	0	0	0	0	0	0	0	0	0	0	0	0	0	0	0	0
39	0	0	0	0	0	0	0	0	0	0	0	0	0	0	0	0	0	0	0	0	0	0	0	0	0	0	0	0	0	0
40	0	0	0	0	0	0	0	0	0	0	0	0	0	0	0	0	0	0	0	0	0	0	0	0	0	0	0	0	0	0

CRACK LENGTHS FROM NA NUMBER 19124
DIMENSIONS IN MILS (INCHES: X 10E-03)

[illegible]

21-1640 (22)

P-11

CRACK LENGTHS FROM RA NUMBER 19128
DIMENSIONS IN MILS (METERS X 100-00)

NUMBER	XP	Y	XP	Y	XP	Y	XP	Y	XP	Y	XP	Y	XP	Y	XP	Y
1	25	75	0	0	0	0	25	40	0	0	25	25	0	0	25	120
2	(62)	(190)	(0)	(0)	(0)	(0)	(53)	(101)	(0)	(0)	(88)	(132)	(0)	(0)	(88)	(132)
3	55	110	0	0	0	0	30	65	30	0	20	30	0	0	50	110
4	(139)	(279)	(127)	(0)	(0)	(0)	(76)	(213)	(76)	(203)	(127)	(50)	(50)	(76)	(132)	(279)
5	45	90	45	0	0	0	30	65	40	0	20	20	15	0	70	60
6	(114)	(228)	(114)	(203)	(101)	(40)	(76)	(213)	(101)	(228)	(130)	(30)	(50)	(50)	(177)	(132)
7	30	50	30	75	55	15	20	0	0	0	150	40	30	20	40	30
8	(76)	(127)	(76)	(190)	(129)	(30)	(50)	(0)	(0)	(0)	(301)	(101)	(76)	(50)	(101)	(68)
9	45	90	45	115	40	15	0	0	0	0	0	0	20	60	25	75
10	(114)	(228)	(114)	(279)	(101)	(25)	(0)	(0)	(0)	(0)	(0)	(0)	(50)	(132)	(63)	(190)
11	130	160	100	0	0	0	35	35	45	15	45	35	35	100	30	0
12	(254)	(406)	(254)	(0)	(0)	(0)	(68)	(88)	(114)	(30)	(114)	(88)	(139)	(254)	(127)	(0)
13	10	10	0	0	0	0	0	0	0	0	100	30	30	30	30	0
14	(25)	(25)	(0)	(0)	(0)	(0)	(0)	(0)	(0)	(0)	(254)	(76)	(76)	(127)	(76)	(0)
15	25	30	25	0	0	0	10	30	10	0	30	30	30	30	40	0
16	(63)	(76)	(50)	(0)	(0)	(0)	(25)	(127)	(25)	(127)	(139)	(76)	(76)	(76)	(101)	(0)
17	30	60	25	0	0	0	0	0	0	0	125	10	30	25	30	0
18	(76)	(132)	(63)	(0)	(0)	(0)	(0)	(0)	(0)	(0)	(317)	(76)	(76)	(63)	(76)	(132)
19	0	0	0	20	15	0	0	0	0	0	0	0	15	60	15	0
20	(0)	(0)	(0)	(30)	(10)	(0)	(0)	(0)	(0)	(0)	(0)	(0)	(30)	(132)	(30)	(0)
21	40	40	0	20	65	10	10	30	0	20	100	30	30	40	0	0
22	(101)	(132)	(0)	(50)	(203)	(25)	(25)	(76)	(0)	(50)	(254)	(76)	(76)	(101)	(0)	(0)
23	15	40	0	0	0	0	0	0	0	0	30	10	30	15	0	0
24	(30)	(101)	(0)	(0)	(0)	(0)	(0)	(0)	(0)	(12)	(75)	(25)	(76)	(34)	(0)	(0)
25	0	0	0	0	0	0	0	0	0	35	75	20	0	0	0	0
26	(0)	(0)	(0)	(3)	(0)	(0)	(0)	(0)	(0)	(88)	(190)	(50)	(0)	(0)	(0)	(0)
27	30	125	30	0	0	0	20	65	25	0	0	0	40	90	0	65
28	(76)	(117)	(76)	(0)	(0)	(0)	(50)	(165)	(63)	(0)	(0)	(0)	(101)	(228)	(0)	(165)
29	40	40	0	0	0	0	40	70	40	65	50	25	40	40	35	0
30	(101)	(132)	(0)	(0)	(0)	(0)	(101)	(177)	(101)	(165)	(127)	(50)	(101)	(101)	(48)	(0)
31	35	35	30	0	0	0	15	30	15	35	55	25	35	65	35	0
32	(68)	(139)	(76)	(0)	(0)	(0)	(30)	(76)	(30)	(88)	(139)	(63)	(88)	(165)	(88)	(0)
33	65	105	60	0	0	0	25	150	0	0	150	35	0	0	0	0
34	(165)	(266)	(132)	(0)	(0)	(0)	(63)	(301)	(0)	(0)	(301)	(88)	(0)	(0)	(0)	(0)
35	0	0	0	0	0	0	40	65	45	0	0	0	35	75	35	0
36	(0)	(0)	(0)	(0)	(0)	(0)	(101)	(165)	(114)	(0)	(0)	(0)	(48)	(190)	(88)	(0)
37	0	0	0	0	0	0	40	60	40	55	55	40	0	0	0	70
38	(0)	(0)	(0)	(0)	(0)	(0)	(101)	(132)	(101)	(139)	(132)	(101)	(0)	(0)	(0)	(177)
39	50	95	55	0	0	0	15	65	15	65	70	25	50	35	0	0
40	(127)	(241)	(139)	(0)	(0)	(0)	(30)	(165)	(30)	(213)	(177)	(63)	(127)	(68)	(0)	(0)
41	0	0	0	0	0	0	0	0	0	0	0	0	0	0	0	0
42	(0)	(0)	(0)	(0)	(0)	(0)	(0)	(0)	(0)	(0)	(0)	(0)	(0)	(0)	(0)	(0)
43	30	35	30	30	100	30	40	35	45	35	100	35	45	35	45	0
44	(76)	(88)	(76)	(76)	(254)	(75)	(101)	(88)	(114)	(88)	(254)	(88)	(114)	(88)	(139)	(190)
45	40	70	40	0	0	0	25	70	25	0	0	0	20	100	30	0
46	(101)	(177)	(101)	(0)	(0)	(0)	(63)	(177)	(63)	(0)	(0)	(0)	(50)	(254)	(76)	(0)
47	65	145	60	0	0	0	40	80	45	0	0	0	45	70	45	100
48	(165)	(368)	(132)	(0)	(0)	(0)	(101)	(203)	(114)	(0)	(0)	(0)	(114)	(177)	(114)	(254)
49	60	105	60	90	65	25	25	65	25	55	60	25	35	60	35	90
50	(152)	(266)	(132)	(223)	(165)	(50)	(63)	(165)	(63)	(139)	(152)	(63)	(88)	(132)	(88)	(228)
51	70	105	50	0	0	0	35	70	35	55	70	0	25	40	25	120
52	(177)	(266)	(127)	(0)	(0)	(0)	(38)	(177)	(48)	(139)	(177)	(0)	(53)	(101)	(63)	(304)
53	0	0	0	0	0	0	30	30	30	20	100	35	20	30	20	0
54	(0)	(0)	(0)	(0)	(0)	(0)	(76)	(76)	(76)	(50)	(254)	(88)	(50)	(76)	(50)	(0)
55	55	100	60	0	0	0	35	60	35	20	55	25	40	55	40	20
56	(139)	(254)	(132)	(0)	(0)	(0)	(68)	(132)	(88)	(50)	(139)	(63)	(101)	(139)	(101)	(50)
57	55	90	55	0	0	0	40	70	40	0	0	0	30	95	45	0
58	(139)	(228)	(139)	(0)	(0)	(0)	(101)	(177)	(101)	(0)	(0)	(0)	(76)	(241)	(114)	(0)
59	60	90	50	0	0	0	30	30	30	30	90	30	20	50	25	20
60	(132)	(228)	(127)	(0)	(0)	(0)	(76)	(76)	(76)	(76)	(203)	(76)	(50)	(127)	(63)	(50)
61	10	50	15	0	0	0	10	40	10	75	50	20	0	0	0	75
62	(25)	(127)	(38)	(0)	(0)	(0)	(25)	(101)	(25)	(190)	(127)	(50)	(0)	(0)	(0)	(190)
63	60	100	65	0	0	0	15	30	15	0	0	0	40	125	40	140
64	(132)	(254)	(165)	(0)	(0)	(0)	(38)	(76)	(38)	(0)	(0)	(0)	(101)	(317)	(101)	(355)
65	60	90	60	0	0	0	25	30	30	25	45	30	0	0	0	0
66	(132)	(228)	(152)	(0)	(0)	(0)	(63)	(76)	(76)	(63)	(241)	(76)	(0)	(0)	(0)	(0)
67	20	35	0	0	0	0	25	115	25	0	0	0	30	35	30	0
68	(50)	(88)	(0)	(0)	(0)	(0)	(53)	(292)	(63)	(0)	(0)	(0)	(76)	(88)	(76)	(0)
69	30	30	40	0	0	0	0	0	0	5	105	20	30	50	30	50
70	(127)	(228)	(101)	(0)	(0)	(0)	(0)	(0)	(0)	(12)	(266)	(50)	(76)	(127)	(76)	(127)
71	40	130	35	110	50	20	40	45	50	25	100	50	45	55	50	0
72	(101)	(139)	(88)	(279)	(127)	(55)	(101)	(114)	(127)	(63)	(254)	(127)	(114)	(139)	(127)	(0)
73	0	0	0	0	0	0	20	30	30	65	70	20	15	20	0	15
74	(0)	(0)	(0)	(0)	(0)	(0)	(50)	(203)	(76)	(165)	(177)	(50)	(30)	(50)	(0)	(25)
75	30	35	35	0	0	0	25	40	25	30	60	30	15	15	10	0
76	(127)	(139)	(30)	(0)	(0)	(0)	(63)	(131)	(63)	(76)	(132)	(76)	(30)	(30)	(22)	(0)
77	55	90	60	0	0	0	35	40	35	45	70	0	55	60	30	65
78	(139)	(228)	(132)	(0)	(0)	(0)	(53)	(101)	(76)	(114)	(177)	(0)	(139)	(132)	(76)	(165)
79	40	70	40	0	0	0	20	20	0	20	40	20	35	35	35	0
80	(152)	(177)	(101)	(0)	(0)	(0)	(50)	(50)	(0)	(50)	(228)	(50)	(68)	(139)	(88)	(139)
81	45	90	0	0	0	0	0	0	0	10	130	50	56	45	50	25
82	(114)	(127)	(0)	(0)	(0)	(0)	(0)	(0)	(0)	(25)	(330)	(127)	(127)	(114)	(127)	(254)

CRACK LENGTHS FROM RA NUMBER 15130
DIMENSIONS IN MILS (PETERS 1 100-09)

NUMBER	CP	X	Y	L	E	V	CP	X	Y	L	E	V	CP	X	Y	L	E	V	CP	X	Y	L	E	V	CP	X	Y	L	E	V	CP	X	Y	L	E	V
1	70	125	75	(177)	(317)	(190)	20	25	0	20	45	20	15	20	0	0	0	0	0	0	0	0	0	0	0	0	0	0	0	0	0	0	0	0	0	0
2	20	40	0	(50)	(101)	(C)	45	75	20	30	25	0	30	25	0	0	0	0	0	0	0	0	0	0	0	0	0	0	0	0	0	0	0	0	0	0
3	20	35	0	(50)	(88)	(0)	10	45	25	25	35	30	0	0	0	0	0	0	0	0	0	0	0	0	0	0	0	0	0	0	0	0	0	0	0	0
3	10	50	10	(23)	(127)	(23)	35	80	35	0	0	0	0	0	0	0	0	0	0	0	0	0	0	0	0	0	0	0	0	0	0	0	0	0	0	0
4	0	0	0	(0)	(0)	(0)	0	0	0	0	0	0	0	0	0	0	0	0	0	0	0	0	0	0	0	0	0	0	0	0	0	0	0	0	0	0
5	0	0	0	(0)	(0)	(0)	0	0	0	0	0	0	0	0	0	0	0	0	0	0	0	0	0	0	0	0	0	0	0	0	0	0	0	0	0	0
6	0	0	0	(0)	(0)	(0)	0	0	0	0	0	0	0	0	0	0	0	0	0	0	0	0	0	0	0	0	0	0	0	0	0	0	0	0	0	0
7	55	70	40	(139)	(177)	(101)	0	0	0	0	0	0	0	0	0	0	0	0	0	0	0	0	0	0	0	0	0	0	0	0	0	0	0	0	0	0
8	10	15	0	(25)	(38)	(0)	0	0	0	0	0	0	0	0	0	0	0	0	0	0	0	0	0	0	0	0	0	0	0	0	0	0	0	0	0	0
9	20	30	20	(50)	(76)	(50)	0	0	0	0	0	0	0	0	0	0	0	0	0	0	0	0	0	0	0	0	0	0	0	0	0	0	0	0	0	0
10	70	60	50	(177)	(152)	(127)	0	0	0	0	0	0	0	0	0	0	0	0	0	0	0	0	0	0	0	0	0	0	0	0	0	0	0	0	0	0
11	35	35	0	(88)	(88)	(0)	0	0	0	0	0	0	0	0	0	0	0	0	0	0	0	0	0	0	0	0	0	0	0	0	0	0	0	0	0	0
12	0	0	0	(0)	(0)	(0)	20	15	0	20	125	20	0	0	0	0	0	0	0	0	0	0	0	0	0	0	0	0	0	0	0	0	0	0	0	0
13	10	40	0	(25)	(101)	(0)	0	0	0	0	0	0	0	0	0	0	0	0	0	0	0	0	0	0	0	0	0	0	0	0	0	0	0	0	0	0
14	10	10	10	(25)	(25)	(25)	0	0	0	0	0	0	0	0	0	0	0	0	0	0	0	0	0	0	0	0	0	0	0	0	0	0	0	0	0	0
15	0	0	0	(0)	(0)	(0)	25	75	20	15	80	25	0	0	0	0	0	0	0	0	0	0	0	0	0	0	0	0	0	0	0	0	0	0	0	0
15	0	0	0	(0)	(0)	(0)	0	0	0	0	0	0	0	0	0	0	0	0	0	0	0	0	0	0	0	0	0	0	0	0	0	0	0	0	0	0
16	10	40	30	(76)	(101)	(76)	0	0	0	0	0	0	0	0	0	0	0	0	0	0	0	0	0	0	0	0	0	0	0	0	0	0	0	0	0	0
17	35	40	0	(88)	(101)	(0)	0	0	0	0	0	0	0	0	0	0	0	0	0	0	0	0	0	0	0	0	0	0	0	0	0	0	0	0	0	0
18	45	65	35	(114)	(165)	(88)	0	0	0	0	0	0	0	0	0	0	0	0	0	0	0	0	0	0	0	0	0	0	0	0	0	0	0	0	0	0
19	30	110	55	(127)	(279)	(139)	0	0	0	0	0	0	0	0	0	0	0	0	0	0	0	0	0	0	0	0	0	0	0	0	0	0	0	0	0	0
19	0	0	0	(0)	(0)	(0)	0	0	0	0	0	0	0	0	0	0	0	0	0	0	0	0	0	0	0	0	0	0	0	0	0	0	0	0	0	0
20	0	0	0	(0)	(0)	(0)	0	0	0	0	0	0	0	0	0	0	0	0	0	0	0	0	0	0	0	0	0	0	0	0	0	0	0	0	0	0
21	55	40	30	(139)	(203)	(127)	0	0	0	0	0	0	0	0	0	0	0	0	0	0	0	0	0	0	0	0	0	0	0	0	0	0	0	0	0	0
22	70	130	75	(177)	(254)	(190)	0	0	0	0	0	0	0	0	0	0	0	0	0	0	0	0	0	0	0	0	0	0	0	0	0	0	0	0	0	0
23	65	85	55	(165)	(203)	(139)	0	0	0	0	0	0	0	0	0	0	0	0	0	0	0	0	0	0	0	0	0	0	0	0	0	0	0	0	0	0
24	0	0	0	(0)	(0)	(0)	125	(228)	(59)	0	0	0	0	0	0	0	0	0	0	0	0	0	0	0	0	0	0	0	0	0	0	0	0	0	0	0
25	0	0	0	(0)	(0)	(0)	0	0	0	0	0	0	0	0	0	0	0	0	0	0	0	0	0	0	0	0	0	0	0	0	0	0	0	0	0	0
26	40	60	40	(131)	(152)	(101)	0	0	0	0	0	0	0	0	0	0	0	0	0	0	0	0	0	0	0	0	0	0	0	0	0	0	0	0	0	0
27	60	65	45	(152)	(165)	(114)	0	0	0	0	0	0	0	0	0	0	0	0	0	0	0	0	0	0	0	0	0	0	0	0	0	0	0	0	0	0
27	20	40	0	(50)	(131)	(0)	0	0	0	0	0	0	0	0	0	0	0	0	0	0	0	0	0	0	0	0	0	0	0	0	0	0	0	0	0	0
28	20	40	20	(50)	(127)	(50)	0	0	0	0	0	0	0	0	0	0	0	0	0	0	0	0	0	0	0	0	0	0	0	0	0	0	0	0	0	0
29	20	40	20	(50)	(101)	(50)	0	0	0	0	0	0	0	0	0	0	0	0	0	0	0	0	0	0	0	0	0	0	0	0	0	0	0	0	0	0
30	45	45	0	(114)	(114)	(0)	0	0	0	0	0	0	0	0	0	0	0	0	0	0	0	0	0	0	0	0	0	0	0	0	0	0	0	0	0	0
31	0	0	0	(0)	(0)	(0)	15	90	15	15	30	0	0	0	0	0	0	0	0	0	0	0	0	0	0	0	0	0	0	0	0	0	0	0	0	0
31	0	0	0	(0)	(0)	(0)	0	0	0	0	0	0	0	0	0	0	0	0	0	0	0	0	0	0	0	0	0	0	0	0	0	0	0	0	0	0
32	0	0	0	(0)	(0)	(0)	0	0	0	0	0	0	0	0	0	0	0	0	0	0	0	0	0	0	0	0	0	0	0	0	0	0	0	0	0	0
32	121	121	0	(0)	(0)	(0)	0	0	0	0	0	0	0	0	0	0	0	0	0	0	0	0	0	0	0	0	0	0	0	0	0	0	0	0	0	0
33	40	30	0	(101)	(76)	(0)	20	55	0	0	0	0	0	0	0	0	0	0	0	0	0	0	0	0	0	0	0	0	0	0	0	0	0	0	0	0
34	25	35	0	(63)	(88)	(0)	0	0	0	0	0	0	0	0	0	0	0	0	0	0	0	0	0	0	0	0	0	0	0	0	0	0	0	0	0	0
35	30	75	30	(76)	(190)	(76)	0	0	0	0	0	0	0	0	0	0	0	0	0	0	0	0	0	0	0	0	0	0	0	0	0	0	0	0	0	0
36	15	40	15	(38)	(121)	(38)	0	0	0	0	0	0	0	0	0	0	0	0	0	0	0	0	0	0	0	0	0	0	0	0	0	0	0	0	0	0
37	50	60	45	(127)	(203)	(114)	0	0	0	0	0	0	0	0	0	0	0	0	0	0	0	0	0	0	0	0	0	0	0	0	0	0	0	0	0	0
38	40	70	45	(131)	(177)	(114)	0	0	0	0	0	0	0	0	0	0	0	0	0	0	0	0	0	0	0	0	0	0	0	0	0	0	0	0		

RIN DURABILITY PROGRAM AFJAL/ML CONTRACT NUMBER F33615-60-C-9027

CRACK LENGTHS FROM 4A NUMBER 14719
DIMENSIONS IN MILS (PETERS X 10E-03)

MOLE NUMBER	A			B			C			D			E			F			G		
	AP	BP	CP	AP	BP	CP	AP	BP	CP	AP	BP	CP	AP	BP	CP	AP	BP	CP	AP	BP	CP
1	0	0	0	0	0	0	0	0	0	75	45	13	25	30	25	3	3	7	30	40	20
2	0	0	0	0	0	0	0	0	0	190	114	33	63	76	63	3	3	7	76	101	50
3	0	0	0	0	0	0	0	0	0	0	0	0	0	0	0	3	3	7	0	0	0
4	10	60	20	0	0	0	20	25	20	15	80	25	20	60	0	3	3	0	45	60	3
5	25	152	50	0	0	0	50	63	50	34	203	63	50	152	63	6	3	7	114	203	0
6	20	22	10	0	0	0	0	0	0	0	0	0	0	0	0	0	0	0	0	0	0
7	50	50	25	0	0	0	0	0	0	0	0	0	0	0	0	0	0	0	0	0	0
8	50	20	20	0	10	5	0	0	0	0	0	0	22	65	20	13	20	12	25	60	30
9	127	50	50	0	25	12	0	0	0	50	80	35	55	165	50	25	50	25	63	152	76
10	0	0	0	0	0	0	0	0	0	0	0	0	35	30	40	3	3	7	20	70	30
11	0	0	0	0	0	0	0	0	0	127	203	84	86	76	161	4	3	7	50	177	76
12	30	65	25	0	3	0	0	0	0	45	45	20	0	15	10	3	0	7	0	0	0
13	76	165	63	0	3	7	0	0	0	114	114	50	0	38	25	4	3	7	0	0	0
14	10	15	5	0	0	0	0	0	0	0	0	0	10	15	0	35	55	20	20	50	20
15	25	38	12	0	0	0	0	0	0	0	0	0	25	38	6	46	134	77	50	127	50
16	40	80	0	0	0	0	0	0	0	30	90	22	22	40	22	23	45	12	30	35	35
17	101	203	0	0	0	0	0	0	0	76	229	55	55	101	55	6	50	30	76	165	84
18	0	0	0	0	0	0	0	0	0	45	50	0	0	0	0	3	0	7	55	110	40
19	0	0	0	0	0	0	0	0	0	114	127	0	0	0	0	4	3	7	139	279	101
20	50	40	0	0	0	0	0	0	0	0	0	0	20	55	0	0	0	0	25	100	15
21	127	203	0	0	0	0	0	0	0	0	0	0	50	134	0	0	0	0	63	254	38
22	60	50	30	65	40	10	0	0	0	0	0	0	0	85	30	30	110	12	0	0	0
23	152	203	127	165	229	25	0	0	0	0	0	0	76	215	76	0	0	0	0	0	0
24	40	50	0	8	3	3	0	0	0	0	0	0	0	0	0	0	0	0	40	25	20
25	101	127	0	0	0	0	0	0	0	0	0	0	0	0	0	0	0	0	131	63	50
26	30	35	0	20	30	15	10	10	10	0	0	0	20	60	20	3	3	7	20	35	20
27	76	88	0	50	76	25	25	25	25	0	0	0	50	152	50	6	3	7	50	88	50
28	20	45	0	0	0	0	0	0	0	70	25	0	40	70	35	3	35	10	20	25	0
29	50	114	0	0	0	0	10	20	0	177	63	0	101	177	88	6	3	7	50	63	20
30	127	177	101	0	0	0	25	30	0	101	139	50	63	177	63	0	0	0	114	203	114
31	30	40	0	25	35	15	0	0	0	0	0	0	20	70	20	0	0	0	35	55	30
32	76	101	0	63	89	25	0	0	0	3	3	0	50	177	50	6	3	7	88	139	76
33	0	0	0	0	0	0	0	0	0	25	55	15	0	0	0	0	0	0	45	100	35
34	0	0	0	0	0	0	0	0	0	63	139	39	0	0	0	0	0	0	114	254	68
35	0	0	0	0	0	0	0	0	0	0	0	0	0	0	0	0	0	0	20	30	15
36	0	0	0	80	40	15	0	0	0	0	0	0	0	0	0	0	0	0	50	76	36
37	0	0	0	203	101	39	0	0	0	0	0	0	0	0	0	0	0	0	30	65	30
38	0	0	0	0	0	0	0	0	0	3	55	20	30	55	25	25	20	10	76	215	76
39	0	0	0	0	0	0	0	0	0	12	215	50	76	139	63	6	3	7	45	45	45
40	0	0	0	0	0	0	0	0	0	60	40	20	25	40	30	0	0	0	45	45	45
41	0	0	0	0	0	0	0	0	0	132	101	50	63	101	76	0	0	0	114	215	114
42	0	0	0	0	0	0	0	0	0	65	30	10	0	0	0	4	50	14	40	80	35
43	35	60	35	60	25	15	0	0	0	163	76	23	0	0	0	0	0	0	101	203	84
44	88	152	88	152	63	39	0	0	0	114	152	50	0	0	0	0	0	0	12	45	20
45	0	0	0	0	0	0	0	0	0	70	55	20	29	20	25	0	0	0	25	114	50
46	0	0	0	0	0	0	0	0	0	177	139	50	63	50	63	0	0	0	76	177	101
47	0	0	0	0	0	0	0	0	0	25	85	20	25	45	25	3	0	0	15	35	15
48	50	70	50	3	0	0	0	0	0	63	215	50	63	114	63	6	3	7	38	88	16
49	127	177	127	0	0	0	0	0	0	25	110	35	40	25	40	0	0	0	35	60	30
50	20	25	25	0	0	0	0	0	0	63	279	88	101	63	101	0	0	0	58	152	76
51	50	63	63	0	0	0	0	0	0	70	75	5	10	30	10	15	80	7	30	40	0
52	0	0	0	0	0	0	0	0	0	76	190	12	25	76	25	139	203	0	76	101	0
53	0	0	0	0	0	0	0	0	0	25	105	30	15	40	15	45	35	4	15	20	0
54	127	152	0	0	0	0	63	266	76	0	0	0	38	101	38	114	88	12	38	50	0
55	15	40	10	0	0	0	0	0	0	20	110	20	0	0	0	25	20	0	35	45	30
56	38	101	25	0	0	0	0	0	0	50	279	50	0	0	0	139	50	0	35	215	76
57	0	0	0	0	0	0	0	0	0	127	70	12	63	203	63	6	3	7	0	0	0
58	0	0	0	0	0	0	0	0	0	0	0	0	15	40	15	153	20	5	12	50	12
59	12	38	0	88	25	12	0	0	0	0	0	0	38	101	38	254	50	12	12	50	12
60	10	30	10	0	0	0	0	0	0	0	0	0	15	45	15	3	3	7	50	80	40
61	25	76	25	0	0	0	0	0	0	0	0	0	38	114	38	6	3	7	127	203	101
62	0	0	0	0	0	0	0	0	0	50	20	10	95	45	46	65	40	20	35	60	0
63	0	0	0	0	0	0	0	0	0	127	70	25	241	114	101	165	203	50	84	152	0
64	15	25	10	0	0	0	0	0	0	15	110	20	0	0	0	25	20	5	30	60	20
65	38	63	25	0	0	0	0	0	0	38	279	50	0	0	0	165	50	12	76	152	50
66	5	15	5	0	0	0	5	5	5	0	0	0	0	0	0	70	60	25	30	60	35
67	12	38	12	0	0	0	12	12	12	0	0	0	0	0	0	177	152	63	76	152	88
68	30	60	0	0	0	0	0	0	0	60	60	15	20	35	20	3	0	0	10	40	0
69	76	152	63	0	0	0	0	0	0	152	152										